A framework for evaluating forest ecological vulnerability in tropical deforestation fronts from the assessment of forest degradation in a landscape approach : Case studies from Brazil and Vietnam

Clément Bourgoin

agreenium
l'institut agronomique, vétérinaire & forestier de France

AgroParisTech

NNT : 2019IAVF0027

THESE DE DOCTORAT

préparée à l'Institut des sciences et industries du vivant et de l'environnement (AgroParisTech)

pour obtenir le grade de

Docteur de l'Institut agronomique vétérinaire et forestier de France

Spécialité : Géographie

École doctorale n°581
Agriculture, alimentation, biologie, environnement et santé (ABIES)

par

Clément BOURGOIN

A framework for evaluating forest ecological vulnerability in tropical deforestation fronts from the assessment of forest degradation in a landscape approach: Case studies from Brazil and Vietnam

Directeur de thèse : Valéry GOND
Co-directeur de la thèse : Lilian BLANC

Thèse présentée et soutenue à Montpellier, le 18.12.2019 :

Composition du jury :

Mme Sandra LUQUE, Directeur de Recherche, IRSTEA Montpellier	Présidente
M. Frédéric GOSSELIN, ICPEF (HDR), IRSTEA Nogent-sur-Vernisson	Rapporteur
M. Frédéric ACHARD, Chercheur, JRC Italie	Rapporteur
Mme Aurélie SHAPIRO, Chercheur, WWF Berlin	Examinatrice
M. Maxime REJOU-MECHAIN, Chargé de Recherche, IRD Montpellier	Examinateur
Mme Laurence MOY, Professeur des Universités, Université de Rennes-2 Rennes	Examinatrice
M. Yves LAUMONIER, Chercheur, CIRAD Indonésie	Examinateur
M. Valéry GOND, Chercheur, CIRAD Montpellier	Directeur de thèse

CIRAD UPR 105 – Forets et Sociétés
Campus international de Baillarguet
34398 Montpellier cedex 5

A framework for evaluating forest ecological vulnerability in tropical deforestation fronts from the assessment of forest degradation in a landscape approach:

Case studies from Brazil and Vietnam

Clément Bourgoin

Supervised by Valéry Gond, Lilian Blanc, Louis Reymondin, Peter Läderach and Johan Oszwald

A thesis presented for the degree of Doctor at

AgroParisTech

Content

List of Figures

List of Tables

Abstract

The conservation of tropical forest cover is a key to ensuring sustainable provision of multiple ecosystem services. However, increasing demography, demand for agricultural products and changes in land uses are affecting forest sustainability through degradation processes. A first step to tailor effective forest management is to identify most vulnerable forests and to characterize their drivers. The objective of this thesis is to develop a multidimensional approach to assess forest degradation and the relations with the broader dynamics of land use/cover towards the evaluation of forest ecological vulnerability. The thesis was applied in Paragominas (Brazil) and Di Linh (Vietnam) where large-scale deforestation driven by commercial agriculture shaped the landscape into land use mosaics with increasing degradation pressures. In Paragominas, degradation is linked with selective logging and fire implying changes in forest structure. We estimated the potential of multisource remote sensing to map forest aboveground biomass from large-scale field assessment of carbon stock and investigated the consequences of degradation history on forest structures. We found that canopy textures correlated with forest structure variability and could be used as proxies to characterize degraded forests using very high resolution images. Based on environmental, geographical factors and landscape structure metrics, we demonstrated that 80% of forest degradation was mainly driven by accessibility, geomorphology, fire occurrence and fragmentation. The drivers of degradation acted together and in sequence. The combination of current forest state, landscape dynamics and information on degradation drivers would be at the basis of ecological vulnerability assessment. In Di Linh, degradation is driven by encroachment of coffee-based agriculture. Field inventory of the different forest types and other landscape elements combined with Sentinel-2 images allowed to map with high precision the current land cover. We constructed trajectories of landscape structure dynamics from which we characterized the expansion of the agricultural frontier and highlighted heterogeneous agricultural encroachment on forested areas. We also identified degradation and fragmentation trajectories that affect forest cover at different rates and intensity. Combined, these indicators pinpointed hotspots of forest ecological vulnerability. Through the developed remote sensing approaches and indicators at forest and landscape scales, we provided a holistic diagnosis of forests in human-modified landscapes This thesis aims to pave the way for tailored and prioritized management of degraded forests at the landscape scale.

Keywords : Ecological vulnerability, agricultural expansion, forest degradation, remote sensing

Résumé

La conservation du couvert forestier tropical est essentielle pour assurer la fourniture durable de services écosystémiques. Cependant, l'accroissement de la démographie, la demande de produits agricoles et les changements dans l'utilisation des terres affectent leur durabilité. L'objectif de cette thèse est de développer une approche multidimensionnelle pour évaluer la dégradation des forêts et les relations avec la dynamique de l'utilisation des terres afin d'estimer leur vulnérabilité. La thèse a été appliquée à Paragominas (Brésil) et Di Linh (Vietnam), où la déforestation due à l'agriculture commerciale a façonné le paysage en mosaïques d'utilisation des terres. A Paragominas, la dégradation est liée à l'exploitation sélective du bois et au feu impliquant des changements dans la structure forestière. Nous avons estimé le potentiel de la télédétection multisource pour cartographier la biomasse forestière aérienne à partir de données de stock de carbone et avons étudié les conséquences de la dégradation sur les structures forestières. Nous avons constaté que les textures de la canopée étaient corrélées à la variabilité de la structure forestière et pouvaient être utilisés comme indicateurs pour caractériser les forêts dégradées grâce aux images à très haute résolution. En nous basant sur des facteurs environnementaux, géographiques et de structure du paysage, nous avons démontré que 80 % de la dégradation était principalement due à l'accessibilité, la géomorphologie, la fréquence des incendies et à la fragmentation et que ces facteurs agissaient en séquence. A Di Linh, la dégradation est due à l'empiètement de la culture de café. L'inventaire sur le terrain des différents types de forêts et d'autres éléments, combiné aux images Sentinel-2, a permis de cartographier avec une grande précision la couverture du sol actuelle. Nous avons construit des trajectoires de dynamique paysagère afin de caractériser l'expansion de la frontière agricole et mis en évidence l'empiétement agricole sur les zones forestières. Nous avons identifié des trajectoires de dégradation et de fragmentation qui affectent le couvert forestier à différentes intensités. Ensemble, ces indicateurs ont mis en évidence des points chauds de vulnérabilité. Grâce aux approches et aux indicateurs de télédétection développés à l'échelle de la forêt et du paysage, nous avons fourni un diagnostic holistique des forêts dans les paysages modifiés par l'homme. Cette thèse vise à ouvrir la voie à une gestion adaptée et prioritaire des forêts dégradées à l'échelle du paysage.

Mots-clés : Vulnérabilité écologique, expansion agricole, dégradation des forêts, télédétection

Résumé substantiel

La conservation du couvert forestier tropical est essentielle pour assurer la fourniture durable de services écosystémiques. Dans les paysages anthropisés, la conservation des forêts doit également être conciliée avec la productivité agricole. Toutefois, l'accroissement de la démographie, la demande de produits agricoles et les changements dans l'utilisation des terres affectent la durabilité des forêts à travers des dynamiques de degradation complexes. Une première étape pour adapter la gestion efficace des forêts par les décideurs locaux consiste à identifier les forêts les plus vulnérables et à caractériser ce qui la génère. L'objectif de cette thèse est de développer une approche multidimensionnelle utilisant la télédétection et autres analyses spatiales pour évaluer la dégradation des forêts et les relations avec la dynamique de l'utilisation des terres afin d'estimer la vulnérabilité écologique des forêts.

L'examen des méthodes existantes illustre le manque de compréhension et de quantification des conséquences de la degradation à long terme sur la structure des forêts. Il met également en évidence les compromis à faire entre résolution, précision, superficie couverte, coût et fréquence pour cartographier les structures forestières dégradées et la biomasse forestière à travers des gradients de perturbations anthropiques. Par conséquent, un objectif de cette these est de mieux caractériser le large éventail de structures résultant de la dégradation via des approches de télédétection multidimensionnelle.

De plus, la degradation forestière est majoritairement étudiée dans des approches centrées sur le peuplement forestier et non sur des approches holistiques ou paysagères. Cela limite considérablement la compréhension des effets de cascade des facteurs directs et indirects de la dégradation et des influences des changements d'utilisation et de couverture des sols sur l'état du couvert forestier. Par consequent, nous avons peu de connaissances sur les moteurs de la degradation liés aux dynamiques complexes des changements d'utilisation des terres et des decisions de gestion des territoires sous-jacentes. Dans cette these, nous insistons sur le fait que la dégradation des forêts doit être analysée dans le cadre d'une approche paysagère afin de i) saisir les interactions entre les forêts et la dynamique plus large de l'utilisation de la couverture des sols qui rend compte des pratiques agricoles et des consequences de la gestion territoriale et ii) de caractériser les facteurs directs et indirects de la dégradation des forêts.

Enfin, il n'existe pas de méthodes ou de cadre conceptuel visant à caractériser la vulnérabilité du couvert forestier aux impacts anthropiques. L'évaluation de la vulnérabilité écologique des forêts permet d'intégrer différents indicateurs à l'échelle de la forêt et du paysage afin d'informer sur la

localisation des forêts les plus vulnérables et ainsi de hierarchiser les priorités de gestion des forêts dégradées en envisageant par exemple la conservation ou la restoration forestière.

Dans le chapitre 2 de la thèse, nous avons évalué le potentiel des sources de télédétection optique (Landsat, MODIS) et radar (ALOS-1 PALSAR), Sentinel-1) pour la modélisation et la cartographie de la biomasse forestière dans la commune de Paragominas (Brésil). Nous avons extrait un large éventail d'indices de végétation et de texture et les avons combinés avec des données de biomasse recueillies in situ au sein d'un modèle de régression pour prédire la biomasse des forêts à une résolution de 20m. Le modèle a expliqué 28% de la variance avec une erreur quadratique moyenne de 97,1 Mg-ha-1. Nous avons identifié les indicateurs les plus robustes ayant le plus grand pouvoir explicatif. La cartographie de la biomasses révèle que 87% des forêts restantes dans la commune de Paragominas sont dégradées, avec des activités d'exploitation forestière illégale et des impacts sur les lisières. Nous avons validé cette carte avec des inventaires terrain renseignant sur la structure forestière le long d'un gradient de dégradation.

Dans le chapitre 3, nous avons évalué comment l'analyse de la texture de la canopée pouvait saisir les complexités de la structure forestière résultants de différentes histoires de dégradation des forêts. Nous avons utilisé un drone léger pour cartographier 739 ha de forêts dégradées à Paragominas et 33 ans d'images d'archive issues de Landsat pour reconstituer l'historique de la dégradation par la détection des perturbations dues à l'exploitation forestière et aux incendies. Des analyses de texture de la canopée ont été utilisées pour évaluer la structure de la canopée forestière et pour établir une typologie reliant l'historique de la dégradation et l'état actuel. Les mesures de texture permettent de saisir le grain du couvert, l'hétérogénéité et gradients d'ouverture et sont en lien avec la variabilité de la structure forestière (r^2 : 0,58). Nous montrons que des structures forestières similaires partagent une histoire commune de dégradation et peuvent être discriminées grâce aux mesures de texture de la canopée (précision : 55%).

Dans le chapitre 4, nous avons identifié les facteurs directs et indirects de la dégradation des forêts en utilisant une approche paysagère qui permet d'aller au-delà de la détection directe des perturbations forestières. Nous utilisons des méthodes de regression et de clustering afin de cartographier les facteurs de dégradation des forêts primaires à partir d'un large ensemble de facteurs environnementaux et géographiques, et de mesures de la structure du paysage dérivées de la classification de l'utilisation/couverture des terres. Les modèles ont révélé qu'à l'échelle du paysage, l'accessibilité, la géomorphologie, la fréquence des incendies et la fragmentation ont été les principaux facteurs indirects et directs de dégradation (80% de la variance expliquée). Nous avons clairement montré que les facteurs directs et indirects de la degradation forestière ont agi ensemble et en

séquence révélant une utilisation différente des terres et donc des pratiques de gestion du couvert forestier différentes. Dans la partie centrale de la municipalité, les forêts sont dégradées en raison de la surexploitation passée du bois, qui a été indirectement renforcée par l'accessibilité aux parcelles forestières et au marché, et plus récemment en raison des conflits liés à l'expansion agricole et aux boucles de rétroaction négatives générées par la fragmentation. Dans les mosaïques de paysages plus complexes, les forêts sont dégradées en raison du résultat conjoint entre une degradation historique liée à la colonisation de cet espace et de facteurs plus recents tel que l'utilisation du feu dans les pratiques agricoles qui, s'il n'est pas maitrisé et controlé, peut impacter la structure des forêts. Ce phénomène est amplifié par le niveau élévé de fragmentation du paysage ainsi que des évenements de sécheresse de plus en plus intenses et longs. Connaitre et cartographier les facteurs de la degradation forestière à l'échelle du paysage permet d'engager des politiques de gestion du couvert adaptées.

Dans le chapitre 5, nous avons élaboré un cadre méthodologique rigoureux pour évaluer la vulnérabilité des forêts aux impacts anthropiques. Nous avons présenté une méthode novatrice qui intègre la cartographie actuelle des mosaïques de paysages avec les trajectoires de 45 ans de structures de paysages en utilisant des images Sentinel-2 et Landsat. Nous avons extrait des indicateurs d'exposition à l'expansion des terres cultivées, de sensibilité liée à la dégradation et à la fragmentation des forêts, et la capacité d'adaptation des forêts fondée sur la composition du paysage dans le district de Di Linh (Vietnam). Nous avons cartographié les mosaïques forestières-agricoles actuelles avec une grande précision pour évaluer l'intensification du paysage (indice kappa = 0,78). Nous avons également cartographié l'expansion de la frontière agricole et a mis en évidence l'empiètement hétérogène de l'agriculture sur les zones forestières (indice kappa = 0,72-0,93). Enfin, nous avons identifié des trajectoires de dégradation et de fragmentation qui ont affecté le couvert forestier à des rythmes et des intensités différents. Combinés, ces indicateurs ont mis en évidence les points chauds de la vulnérabilité des forêts. Cette étude a fourni des réponses et des leviers de gestion adaptés pour pour les décideurs locaux afin de donner la priorité aux actions visant à prévenir la dégradation future des forêts.

Enfin, nous présentons dans cette these une synthèse qui vise à discuter des méthodes les plus adaptées pour caractériser l'état du couver forestier resultant de la degradation et d'insister sur la pertinence de l'approche paysagère pour l'analyse des moteurs de la degradation conjointement avec la dynamique de changement d'occupation du sol. Ainsi, cette these vise à poser un cadre d'analyse de la vulnérabilité des forêts dans le but de guider la gestion future des forêts tropicales dans les paysages modifiés par l'homme où les enjeux environnementaux liés à la gestion du couvert sont majeurs.

Acknowledgements

J’ai pensé à la redaction de cette partie de remerciement dès mon premier jour de these, m’efforçant de mémoriser chaque personne ou institut qui ont contribué à son aboutissement. Je vais essayer ici de restituer au mieux cet exercice de mémorisation de 3 ans où j’ai eu l’opportunité de rencontrer des personnes exceptionnelles sur 3 continents et de partager des experiences humaines, culturelles et professionnelles assez incroyables.

Partons de la fin ou dirais-je du sprint final où on est tout essouflé et fatigué, merci aux (nombreux) membres du jury de these qui malgré les grèves et autres complications logistiques ont assuré leurs rôles d’évaluateur de ce travail: Sandra Luque, Laurence Moy, Maxime Réjou-Méchain, Yves Laumonier, Frédéric Achard, Frédéric Gosselin et Aurélie Shapiro.

Le plus gros des remerciements, je les dois à mon équipe choc d’encadrants/directeurs. Il y a tout d’abord le duo génial Valéry et Lilian qui jour après jour m’ont porté pour arriver à la fin de cette aventure. Que de discussions, de questionnements et de soutien (comme pendant le deuil du premier drone, rip) toujours dans une bonne humeur si agréable, que cela soit à baillarguet, dans un combi, au Pic Saint Loup, autour d’un verre/pizza ou sur le terrain… Je remercie mes encadrants du CIAT, Louis et Peter qui malgré la distance et autres difficultés m’ont aidé à intégrer un autre site d’étude et donc à compléxifier de façon positive le sujet pour aboutir à ce cadre d’analyse dont on est tous fier. Je ne remercierai jamais assez Johan pour toute l’aide qu’il m’a apporté, toujours entre deux blagues ou deux ACP dont il a le secret. J’ai hâte de faire du terrain au Canada avec toi. Enfin, mon cortège de personnes qui ont aussi passé un temps fou avec moi: Julie (la turbo compresseur/serveur de l’équipe), Hélène (la pro de l’analyse discriminate), Jacques Hugues & Chloé, Guillaume (R master), Jean-Stéphane, Renan (R master n°2), Solen, Trong (meilleur copilote de honda wave, malgré les ouragans), Pablo, Damien aux idées débordantes et Plinio le grand chef.

Merci aussi à toutes les personnes qui m’ont aidé sur le terrain, je pense notamment à René, aux dirigeants de la CIKEL (et aux ouvriers queridos), aux membres du DP Amazonie, aux collègues vietnamiens du CIAT et aux fermiers qui savent réparer les motos à coups de machette.

Ce qui était aussi génial et qui dynamisait les printemps et étés suffocants, c’était d’encadrer et/ou d’être encadré chaque année par des supers stagiaires, doctorants et postdoc. Alors là j’espère ne pas oublier quelqu’un : Giacomo, Andes, Amah, Elodie, Ophélie, Pierro, François, Begum, Sarah, Flo, Mario, Ali, Regis, Camille, ToinonmaisOui, Etienne, Gael, Malou, Fanny, Justine, Théo, Jimmy, Emna, Audrey, Gabriel, Thomas, Uday, Loic etc etc..

Merci aussi à l'unité F&S du CIRAD et au CIAT-Asie pour son accueil et son aide. A Daphné/deepl/Claire pour les traductions. Au CIRAD et à ABIES pour toutes les formations auxquelles j'ai pu participer.

Enfin et on va s'arrêter là, merci à tous mes amis pour leur soutien : Mael, Julien, Alejandro, Kevin, Nicolas, Geoffrey, Audrey, Catherine, Marie, Louis, Le, Nhiem, Than, Donatien, Arnaud, Marcel, Brice, Lucia, Armando, Tiffany, Erik, Mao, Kien, Trung, Lisette etc. Pendant toute cette aventure, merci à ma famille (pas besoin de citer, ils se reconnaîtront), cette thèse est aussi la vôtre. De ses étoiles, j'embrasse mon cousin Arnaud.

Chapter 1 - General introduction

Painting of the forest transition curve adapted from Mather and Needle (1998), by Giacomo Fedele

1.1 Background

Tropical forests located between the Tropics of Cancer and Capricorn have historically covered about 12 percent of Earth's land area and now only make up less than 5 percent (Hansen et al. 2013). Yet, tropical forests are considered as the most diverse and complex biomes on Earth exerting major influences on weather patterns, freshwater, natural disasters, biodiversity, food and human heath from local to global scales (Thompson et al. 2009). Tropical forests house approximately two third of the planet's terrestrial biodiversity (Gardner et al. 2009) and provide many ecosystem services (ES) which are essential to human well-being (MEA 2005). Tropical rainforests in particular (e.g. evergreen and semi-evergreen forest) play major roles in global climate regulation acting as carbon sinks, in water cycle regulation, protection of ecosystems from soil erosion, and provision of many goods (timber and non timber products) directly used by humans (Brandon 2014).

Tropical deforestation and forest degradation reduce or halt the flows of ecosystem goods and services (Seymour and Busch 2016). Collectively these two processes amount to the second largest source of anthropogenic emissions of carbon dioxide after fossil fuel combustion (Van Der Werf et al. 2009). They impact local to regional climate (Pielke 2005; Kalnay and Cai 2003), biodiversity (Barlow et al. 2016), soil degradation and livelihood (Lambin et al. 2001; Song et al. 2018). However, changes in land use and land cover provide essential provisioning services to humans (e.g. food, fiber and fresh-water).

Most of worldwide forest loss (2.3 million square kilometers) from 2000 to 2012 was located in Brazil, Democratic Republic of the Congo and South East Asia (mainly Indonesia), though opposite trends of deforestation rates between countries are recorded (Hansen et al. 2013; Lewis et al. 2015)(Fig 1.1). The main driver of global forest loss in the tropics can be attributed to deforestation through permanent land use change for commodity production (Curtis et al. 2018).

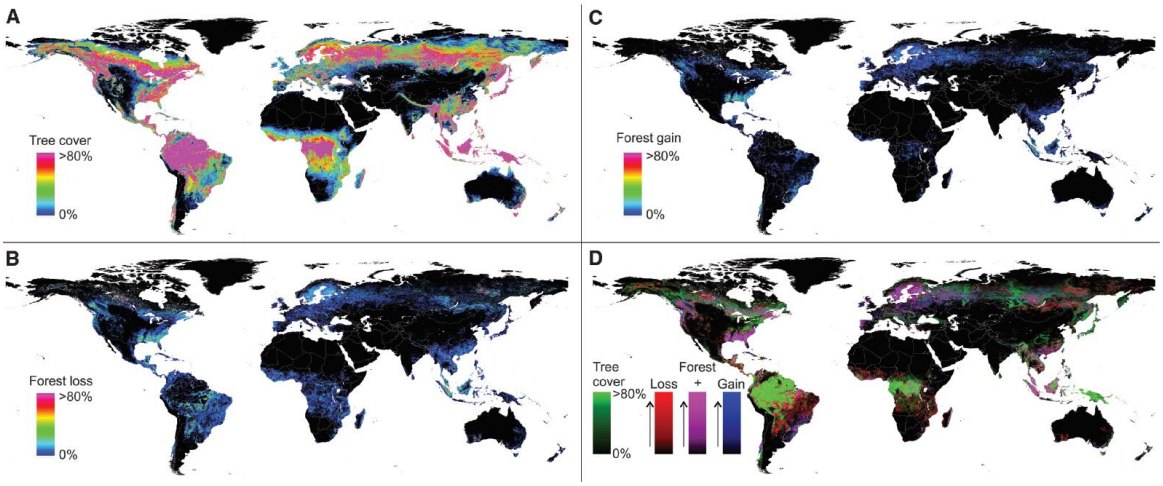

Figure 1.1 (A) Tree cover, (B) forest loss, (C) forest gain and (D) color composite of tree cover in green, forest loss in red, forest gain in blue and forest loss and gain in magenta, from Hansen et al. (2013)

Compared with deforestation, information on the rates, locations and drivers of forest degradation vary widely as do the estimates for carbon emissions. In 2000, it was assessed that tropical forest degradation ranged from 350 to 500 millions hectares (20-30% of tropical forest cover)(International Tropical Timber Organization 2002). Forest degradation accounts for 25% (Pearson et al. 2017) to 68.9% (Baccini et al. 2017) of overall tropical forest carbon losses, and accounts for at least 15% of total carbon emissions from land-cover and land-use changes in the tropics (Houghton 2013)(Fig 1.2).

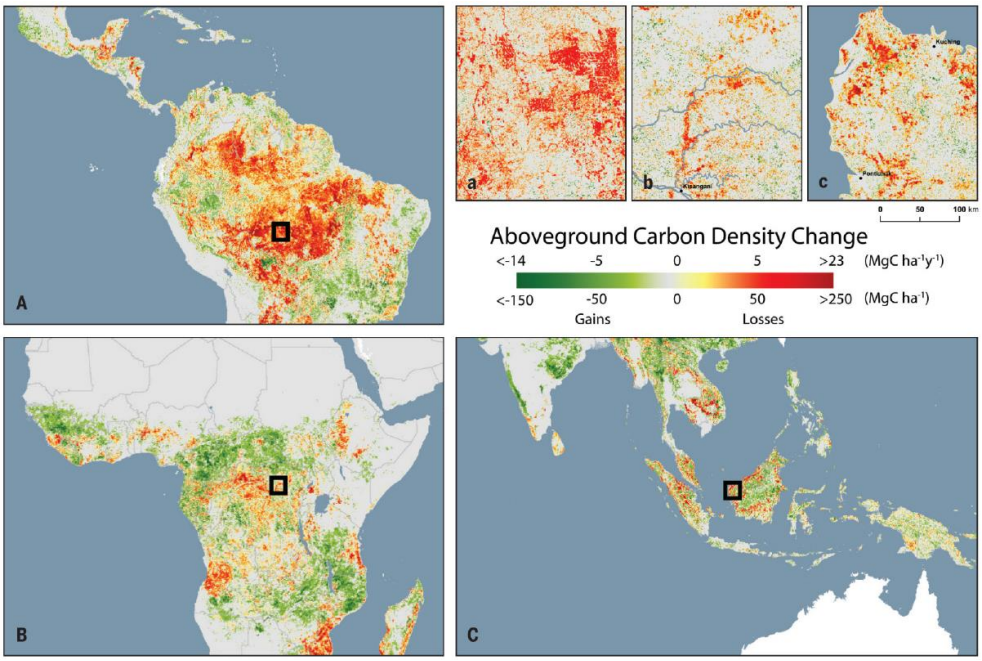

Figure 1.2 Geography of carbon density change (gains, losses and no change) from 2003 to 2014, from Baccini et al. (2017)

Deforestation and forest degradation shaped landscapes into a patchwork of forest, agricultural lands and other uses. Most remaining tropical forests experienced anthropogenic effects of logging and other resource extraction, wildfire and defaunation and keep experiencing increasing pressures from degradation and fragmentation dynamics (Malhi et al. 2014). Intact forests declined by 18% between 2007 and 2013, particularly in old pioneer fronts of Southeast Asia, Africa and Latin America (Tyukavina et al. 2016). Historical land/forest-use-associated drivers (i.e. degradation, fragmentation and agricultural expansion) determine the large range of heterogeneous status and configuration of current forest landscapes. Future forest landscapes will thus be shaped by both ongoing pressures and management responses (Malhi et al. 2014)(Fig 1.3).

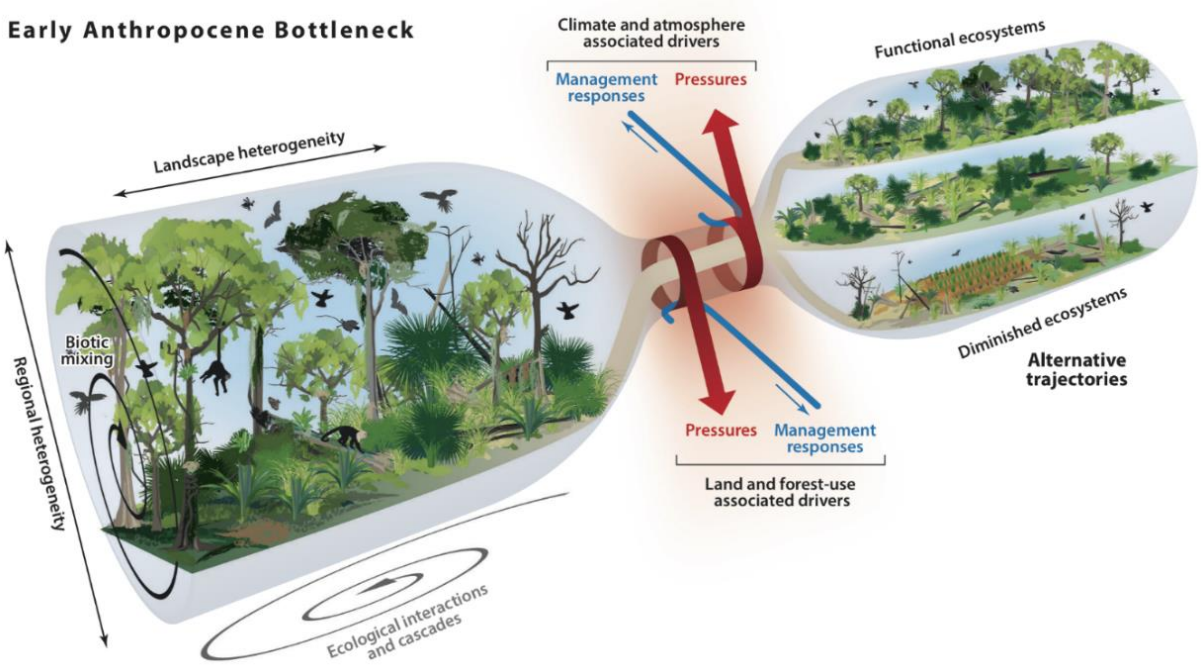

Figure 1.3 The future of tropical forests are determined by the severity and duration of the Anthropocene bottleneck influenced by the current forest state, ongoing pressures and management responses, from (Malhi et al. 2014)

Considering the importance of the extent and dynamics of forest degradation and their major consequences on the provision of forest ecosystem goods and services, there is an urgent need to better understand the heteregenous status of remaining forests and the pressures they are facing in order to plan management interventions to avoid and mitigate these pressures. However, fostering multiple transitions towards the improved management or restoration of forests within multifunctional landscapes and avoiding severe bottlenecks of degradation is only possible if there is a complete understanding of the vulnerability of forest cover to agricultural expansion and degradation.

Despite the potential of spatial analyses using remote sensing to monitor forests and land use/cover, the implementation of ecological vulnerability assessment based on the characterization of the status of remnant forests and the exogenous forces or pressures that affect forest cover is still rare (Malhi et al. 2014; Mitchell et al. 2017; Melito et al. 2018). Forest degradation is a complex multi-aspect phenomenon which makes the mapping of forest degradation indicators a challenge within the remote sensing community (Herold et al. 2011). There is a particular need to analyze forest degradation at the landscape scale in order to interconnect degradation and land use/cover change dynamics towards a better understanding of forest vulnerability. Such a spatially explicit assessment can inform decision makers on identifing the most vulnerable forests in order to prioritize tailored interventions through the direct reduction of exposition factors or through forest management and land use planning.

1.2 Key concepts linking forest degradation with broader landscape dynamics to assess forest vulnerability

1.2.1 Forest degradation

While deforestation refers to a rapid conversion of land use, forest degradation describes a change in forest quality while remaining classified as forest. The difficulty in tackling forest degradation lie in the definition of this change and on the construction of indicators to capture it.

Deforestation is globally recognized as being the strict conversion of forest to other land uses (Achard et al. 2014). However, this definition remains reliant on the definition of forest itself, which varies in terms of tree size, area, and canopy density, while also depending on the perception and management objectives of each country or community (Chazdon et al. 2016; Sasaki and Putz 2009a; Putz and Redford 2010a). Nevertheless, the consensus on defining deforestation and the parallel development of remote sensing allowed the development of efficient methods to pinpoint and monitor deforestation at a large scale (Achard et al. 2007). Deforestation alert systems (Hansen et al. 2010; P. Potapov et al. 2019) are good example of this as they provide key near-real time information to decision makers for direct impact at the field (Leisher et al. 2013; Reymondin et al. 2012; Finer et al. 2018) and institution levels (« PRODES — Coordenação-Geral de Observação da Terra »). Latest developments are focusing on refining data spatial resolution towards more precise and accurate detection and on improving more frequent data acquisition thanks to the coupling of radar and optical images (Reiche et al. 2015; 2018; Bouvet et al. 2018).

By comparison, there is little agreement on the definition of forest degradation, making it more difficult to measure and monitor (Thompson et al. 2013; Putz and Redford 2010; Simula 2009; Bustamante et al. 2016). A degraded forest is the result of a process of degradation which negatively affects the structural and functional characteristics of that forest. Degradation triggers a reduction in the forest capacity to produce ecosystem services (e.g. carbon storage, wood products, soil protection, regulation of water supply and climate)(Vásquez-Grandón et al. 2018). Beyond this theoretical concept, there are more than 50 definitions of degraded forest and forest degradation (Lund 2009) that currently do not allow a practical understanding of the spatial and temporal complexities of degradation (Sasaki and Putz 2009; Putz and Redford 2010; Simula 2009). This lack of coherence in the definition of forest degradation is explained by several difficulties linked with the complexity of the phenomenon (Thompson et al. 2013a).

Forest degradation is a temporal process of disturbances accumulation

Degradation is often assimilated with human-made disturbances such as selective logging and understory fires (Matricardi et al. 2010; Asner et al. 2009; Souza et al. 2005). Each disturbance event affects the status of the forest by damaging the canopy and the internal structure without triggering any changes in land use (Putz and Redford 2010b; Herold et al. 2011). The damages in the forest structure depend on the type and intensity of the disturbance and can vary from limited gaps in the canopy from reduced impact logging to larger opening following unsustainable logging up to large scale destruction of the structure following fire (Rappaport et al. 2018). Repetitive unsustainable logging events weakens the forest structure triggering increasing tree mortality and drying effects, which will increase forest structure flammability (Morton et al. 2011). At the forest stand scale, degradation is therefore a multidimensional process within which the accumulation in space and time of disturbances are key factors for explaining the resulting degraded forest structure (Chazdon et al. 2016; Malhi et al. 2014). Moreover, the recovery (i.e. vegetation regrowth) in between disturbances is another crucial parameter that needs to be taken into account in forest degradation evaluation. The partial opening of the canopy further to selective logging or to forest fires is a transient problem that is difficult to detect as vegetation returns to these clearings at different rates depending on the state of the soil and the surrounding vegetation (Piponiot et al. 2016). At a larger scale (e.g. landscape to regional scales), degradation is driven by other parameters such as the increase of drought on edge areas (Briant et al. 2010), infrastructure development (Laurance et al. 2009) or fragmentation (Broadbent et al. 2008).

Forest degradation and loss of resilience

From an ecological point of view, degraded forests are forests that have lost their resilience capacity, i.e. capacity to return to their stable pre-disturbance state (Holling 1973; Gunderson 2000; Folke et al. 2004). Forests can naturally cope with “small impact disturbances” (storms, climate variability, pest and diseases, etc) and still retain their basic function and structure but intense and frequent disturbances can shift forest ecosystems into a state from which transitions back to the stable state are unlikely or can only occur after a long period of time (Thompson et al. 2009; Ghazoul et al. 2015). This definition calls for an understanding of two major concepts, the state of reference and the ecological threshold beyond which a forest is considered as degraded (Ghazoul and Chazdon 2017). A reference state or baseline may be used in the evaluation of degradation. It must be taken from forests located within the same edaphoclimatic zone and biome type (i.e. similar biophysical characteristics) with no sign of previous human-made disturbances (Tucker et al. 2008) which in practice is difficult to prove due to data limitation (Morales-Barquero et al. 2014). The ecological threshold or tipping point

is the instance where forest composition, structure and function are radically altered considering the reference and stable state. In practice, this boundary could be defined using a combination of ecological indicators (Thompson et al. 2013a) but remains at this time an unsolved limitation (Vásquez-Grandón et al. 2018).

Forest degradation and the influence of perceptions

Perceptions of forest degradation vary according to each individual and their own understanding of the degradation process. Some authors consider tropical forests to be degraded once the forest has been logged once (Foley 2005) whereas others consider it only when the forest has been heavily burned and logged several times (Souza et al. 2005b). There are currently two main opposing visions: the conservationist vision claims that any human presence or activity in a forest ecosystem are signs of degradation while the vision shared by users of forest resources following sustainable forest management practices claim that forest production is not a degradation. This antagonism is amplified by the fact that the term degradation is often perceived in a pejorative way by some actors, which can complicate its study (Sasaki and Putz 2009b).

Considering the different complexities linked with forest degradation raised previously, we stress the importance of characterizing the disturbances at the origin of degradation and identifying conserved forest. The adopted definition of degradation is the following:

> Forest degradation (process) is the accumulation in time and space of human-made disturbances operating at forest stand (direct disturbances such as logging and fire) and larger scales (indirect drivers), which affect the states of the forest by partially destroying the canopy and internal structure without triggering any changes in land use (Fig 1.4). Degraded forests (state) are therefore the consequence of complex degradation and recovery processes which radically differ in terms of structure and ecological functioning from a conserved forest i.e. reference state (no sign of recent historical disturbances).

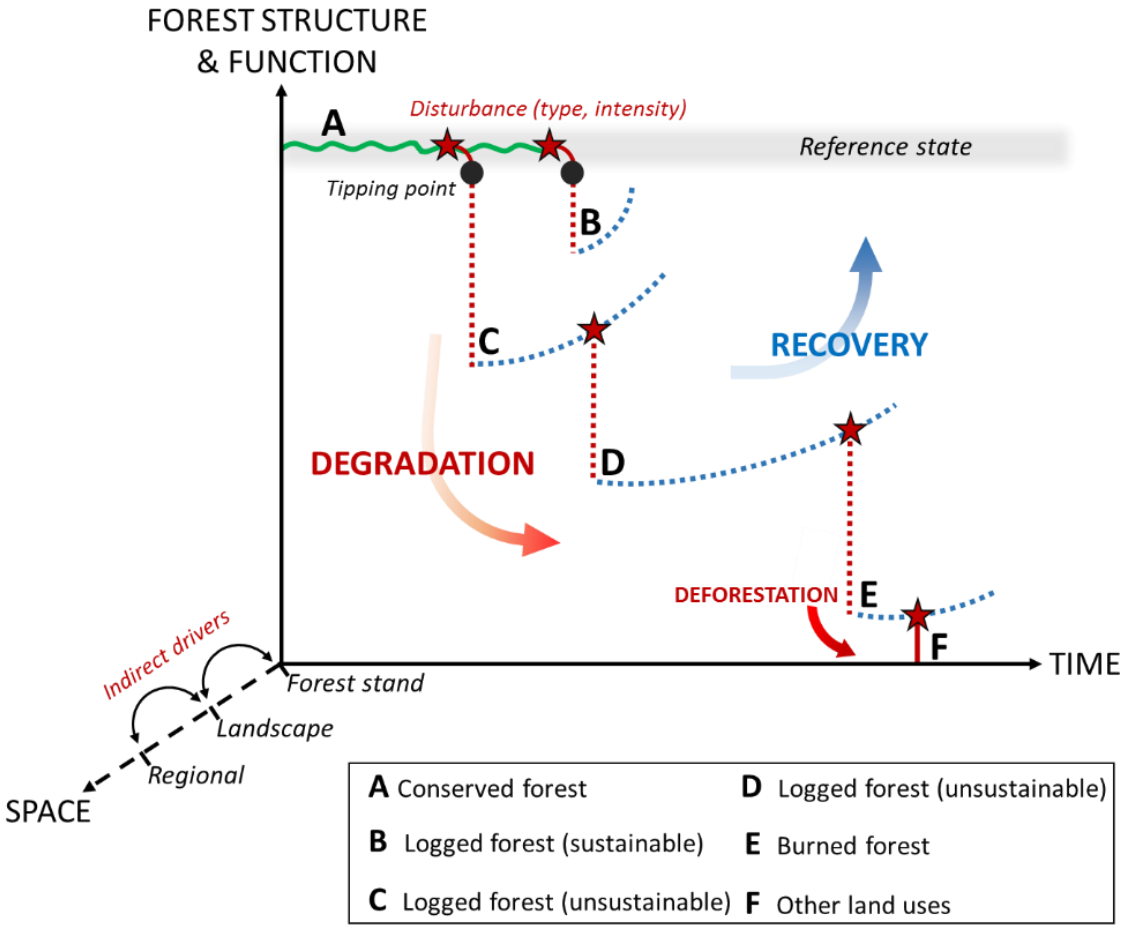

Figure 1.4 Adopted framework of simplified degradation and recovery trajectories at the forest stand scale where an accumulation of different direct drivers (disturbances) such as logging and fire trigger a rapid change in the forest structure and function. Dashed lines represents various degradation and recovery conditions depending on the respective disturbance type and intensity and environment/ecological conditions. The time between the stages A to F can also vary depending a multitude of factors. The cascade of indirect drivers operating at the landscape and regional scale are not shown in detail here.

1.2.2 Landscape approach of land use and land cover change dynamics to analyze forest degradation

Among other natural resource management and environmental issues, tropical forest and its degradation can be analyzed using the social-ecological system (SES) approach built upon the dynamical and reciprocal interactions that exist between human systems and forest ecosystems (Ostrom 2009). Humans not only benefit from forest ecosystems but impact and shape their capacity to generate services (Folke et al. 2005). SES approaches allows for the dissection of complex cause-effects relationships involving multiscale influences and feedbacks. In a SES approach, forest

degradation analysis cannot be restricted to only forest ecosystems but needs to encompass broader scales and be linked with land use and cover change dynamics.

Land use and land cover changes (LULCC) are the result of the close interaction between human activities and their environment (Turner et al. 1995; Lambin et al. 2001; Foley 2005). Analyzing LULCC offer a better understanding of how decisions at the local scale affect land use change and how global drivers can influence these decisions (Lambin and Meyfroidt 2010; Turner et al. 2007; Geist and Lambin 2002). More generally, understanding the drivers, trends and impacts of LULCC on social and natural processes helps to reveal how changes in the land system affect the functioning of the socio-ecological system as a whole (Verburg et al. 2015). Land use change is influenced by driving forces involving the complex interaction of biophysical environments, socioeconomic activities, and cultural contexts in time and space. Global drivers relate to economic (e.g. market prices and capital flows) and biophysical factors and processes, access to technology and policies. Local drivers relate to farmer choices and practices but also on farming systems including demographic, social and cultural factors (Lambin et al. 2003). As a growing number of drivers at multiple spatial scales influence land use and land cover, and as these drivers interact in chain-linked or nested ways, they produce dissimilar land cover/use outcomes (Fig 1.5).

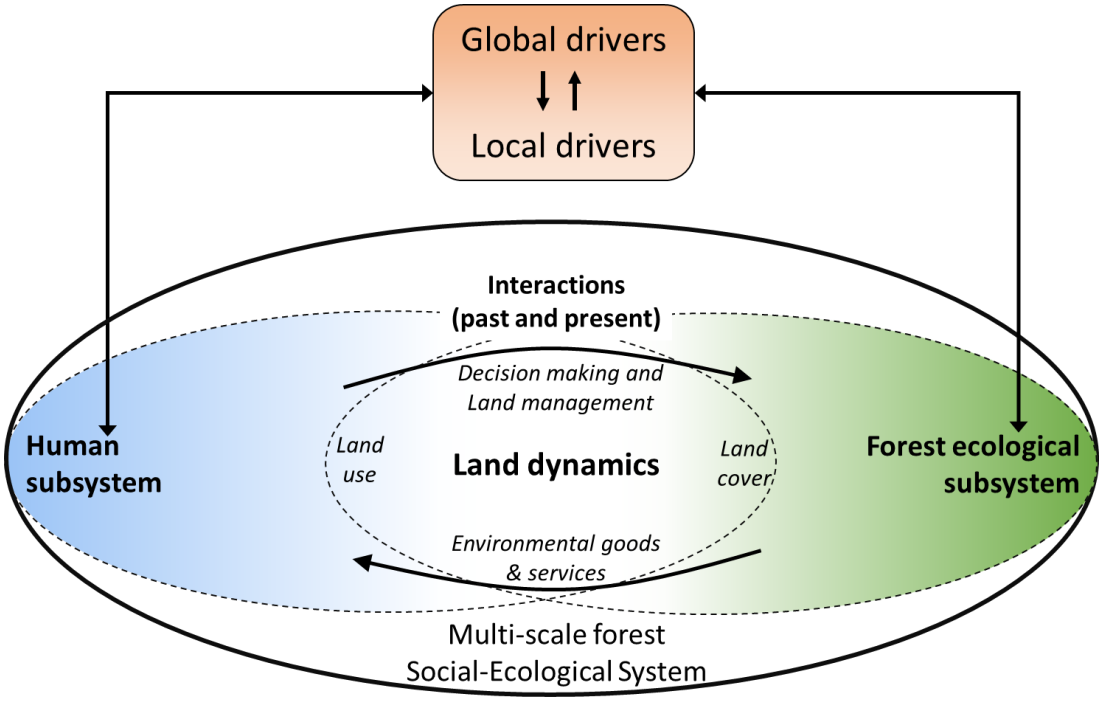

Figure 1.5 Multi-scale forest social-ecological system where land dynamics are at the intersection between human and forest ecological subsystems and under the influence of a cascade of global and local drivers, adapted from Turner et al. (2007), Virapongse et al. (2016) and Gardner et al. (2013).

Characterizing forest social-ecological system throughout the interconnection of forest within land use and land cover dynamics are challenges closely linked with the landscape approach objectives. Integrated landscape approach aims at solving environmental, social and economic issues in unison within a geographical area composed by a variety of competing land uses and multiple stakeholders (Reed et al. 2016; Opdam et al. 2018). Landscape approaches show potential as a framework for balancing and finding trade-offs between conservation of natural resources and development i.e. improve social capital (enhance community income, employment opportunities) while reducing land degradation (Sayer et al. 2013). However, the implementation and evaluation progress of such approaches are still under development, mainly due to the difficulty in engaging diverse stakeholders (Reed et al. 2017; 2019).

In a spatially explicit approach, landscapes are the scale at which people and nature mesh and interact. The composition and configuration of a landscape both profoundly affect and are affected by human activities (Wu 2013). Landscape approach provides a supplementary level of understanding on LULCC as its scale encompasses spatial patterns that reveal the underlying social, environmental and ecological processes (Wu 2007; Messerli et al. 2009; Hett et al. 2012). Assessing drivers of change usually consists of interpretation of human–environmental interactions through the translation of land cover into land use information at the pixel scale. However, LULCC triggers changes at a larger scale where the spatial distribution and configuration of land use and cover types are key information for interpreting dynamics and underlying drivers (Messerli et al. 2009). Complex landscape mosaics resulting from long-term LULCC can be characterized using landscape approaches (Oszwald et al. 2011).

Spatial heterogeneity is a key concept for characterizing landscape mosaics. Spatial heterogeneity can refer to the quantification of the variation of a process in space. This general definition of functional heterogeneity can be applied to individuals, species, biological processes or other ecological variables (Fahrig et al. 2011; Katayama et al. 2014). Spatial heterogeneity can also refer to its structural dimension and becomes a measurable property of a considered landscape. Based on this concepts of structural heterogeneity, many methods allow quantifying the structure and spatial patterns of the landscape defined as the combination of landscape composition and configuration (O'Neill et al. 1997; 1999). This structural approach of spatial heterogeneity was adopted in this thesis in order to disentangle landscape structure dynamics i.e. the analysis of spatial structures or spatial arrangement of the landscape elements in relation to others (Burel and Baudry 1999). Spatial heterogeneity is based on two components: the diversity of landscape elements (composition) and the complexity of their spatial relationships (configuration). The heterogeneity of composition increases with an increase in

the number of land cover types. The configuration heterogeneity increases with an increase in the complexity of the spatial organization of these land covers (Fig 1.6).

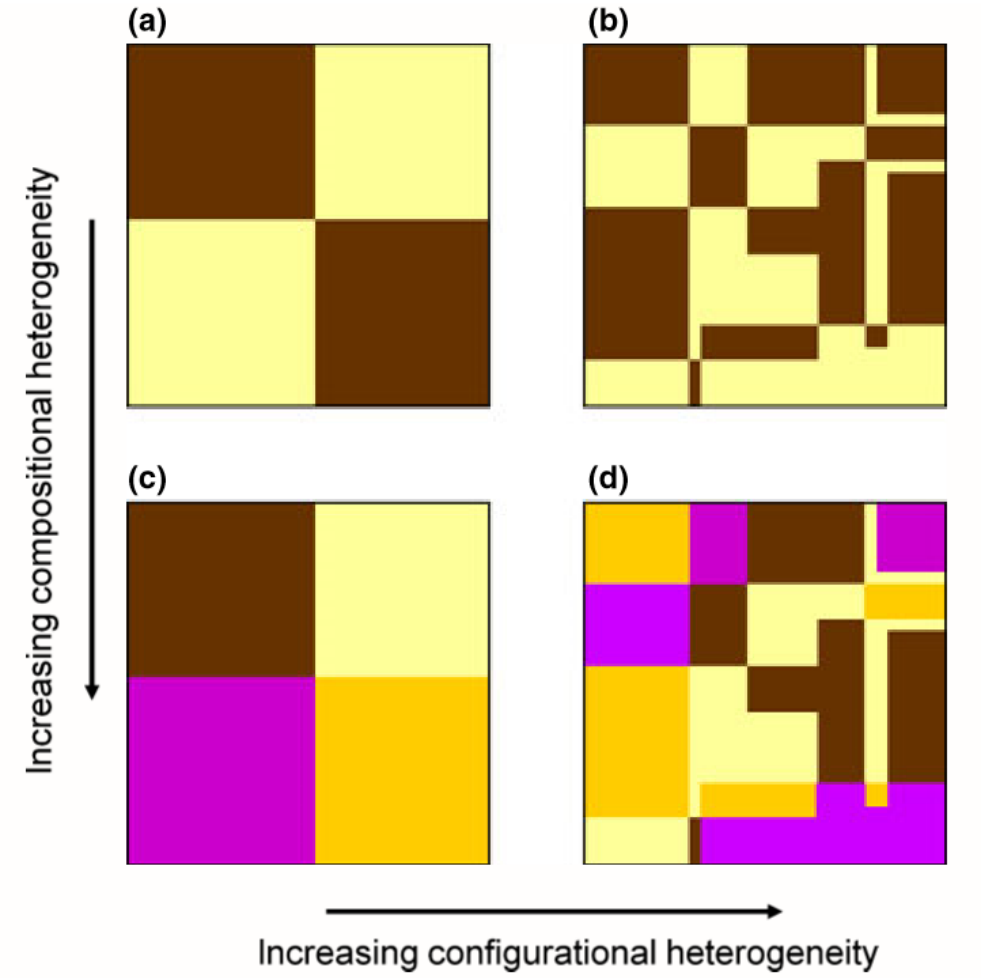

Figure 1.6 Two components of spatial heterogeneity: composition and configuration, extracted from Fahrig et al. 2011.

Spatial heterogeneity can be described through the concepts of fragmentation and connectivity. Fragmentation is the transformation of a large area of habitat into a greater or lesser number of fragments of varying sizes, whose total area is smaller than that of the original habitat and which are more or less isolated from each other (Fig 1.7). Spatial connectivity is defined by the fact that two patches of same land cover type are adjacent or joined in space.

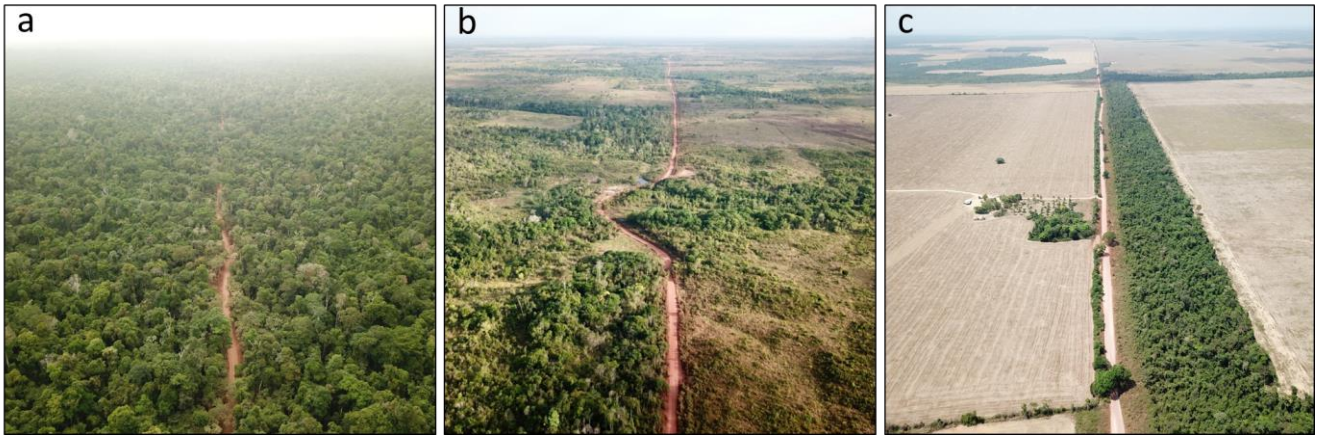

Figure 1.7 The a,b,c photos represent an increasing degree of fragmentation of forest landscape (Paragominas landscapes, September 2017)

The notion of scale in landscape approach is essential, as it will have a direct impact on the LULCC process that need to be characterized in both space and time dimensions (Burel and Baudry 1999). Here, the spatial scale refers to the resolution of the map and to the extent within which the different metrics related to fragmentation, connectivity and heterogeneity will be computed while temporal scale refers to the gap of time between the dates of the analysis.

To conclude, forest cover is integrated within a mosaic of land use and cover types in constant mutual interaction. As highlighted above, there is a need to combine social-ecological system, land dynamics science and the quantitative aspect of landscape approaches for better characterizing forest degradation:

Forest degradation must be analyzed within a landscape approach in order to i) capture human-environment interactions occurring between forests and the broader land use and land cover dynamic and ii) to characterize the direct and indirect drivers of forest degradation. A landscape is a geographical area of varying extent characterized by specific structure (i.e. composition and configuration of landscape units or land cover types) which transcribes specific LULCC history, human practices and governance.

1.2.3 Ecological vulnerability of degraded forests to agricultural expansion

Analyzing forest degradation and its drivers (interacting factors and feedback loops between human and forest ecological systems) at the landscape level are key elements for better understanding and characterizing the vulnerability of forest cover within human-modified landscapes. The concept of vulnerability directly emerges from the social-ecological system framework as it focuses on the consequences of mutual interactions between exogenous and endogenous processes. Forest resilience is often compared with vulnerability but these two concepts are very different. Resilience refers to the capacity of a system to anticipate, absorb or recover from the effects of perturbations and other stressors, and to ensure the preservation, restoration or improvement of its structure and functions (Holling 1973; Folke et al. 2004). Resilience and vulnerability are both related to understanding the response of systems to change and share common elements but resilience is not the flip side of vulnerability (Adger 2006). While resilience focuses on the preservation of a system within a stable state, vulnerability refers to the propensity or predisposition a system to be adversely transformed. Moreover, resilience is an internal property of the system and does not include exposure to perturbations (Gallopín 2006). Vulnerability is better adapted to multidimensional degradation processes. In the context of old deforestation fronts where historical and current processes of forest degradation are active, the concept of vulnerability of forest cover is a fundamental concept for prioritizing sustainable forest and landscape management and reduce degradation risks.

Originally formalized for climate change and the agricultural sector by the Intergovernmental Panel on Climate Change (IPCC), the vulnerability framework makes it possible to assess the key determinants of system responses to external stress and pressures (Marshall et al. 2010; Parker et al. 2019). Vulnerability assessments provide guidance on how to target interventions and to support decision making processes (Adger 2006). Adapted from the IPCC definition, vulnerability is the degree to which a forest ecosystem is susceptible to, or unable to cope with, adverse effects of human-triggered impacts such as land use and land cover change and forest degradation (McCarthy 2001). Vulnerability is commonly defined as the combination of three main components where exposure relates to the magnitude of stress undergone by a system (exogenous processes) ; sensitivity refers to the degree to which the stress may affect the system, and the adaptive capacity is the system's ability to respond to the stress (endogenous processes)(McCarthy 2001). This definition is widely used in the literature to

describe human-environment interactions and the resulting pressure and response options in the framework of socio-ecological systems (Thiault et al. 2018; Morel et al. 2019)(Fig 1.8).

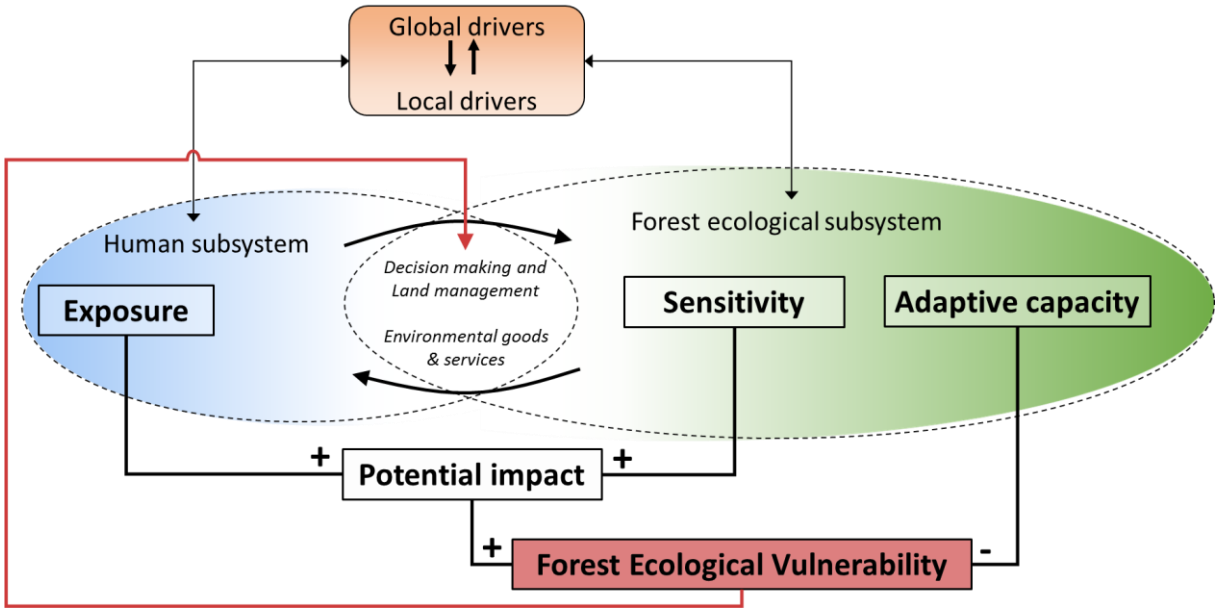

Figure 1.8 Conceptual framework of forest ecological vulnerability as the combination of exposure (exogenous), sensitivity and adaptive capacity (endogenous), modified from Gallopín (2006) and Thiault et al. (2018). Vulnerability assessment has a direct link with decision-making and management to reduce exposure risks and enhance adaptive capacity.

1.3 Litterature review of forest degradation and landscape approach towards the assessment of forest ecological vulnerability

1.3.1 Characterizing structures resulting from forest degradation using remote sensing

In human-dominated landscapes such as old deforestation fronts, the distinction between forested and deforested lands traditionally used to map the state of the forest does not reflect the reality of the situation. A whole gradient exists for these forests, spanning from well conserved to severely degraded. Due to the complexity of the forest degradation concept, a wide range of remote sensing methods exist in the literature and can be generally grouped into two main approaches: direct and indirect (Herold et al. 2011). These methods vary in terms of remote sensing sources (satellite and airborne optical, Synthetic Aperture Radar (SAR), Light Detection And Ranging (LiDAR) or fusion), timescales (punctual to long time-series) and spatial coverage (local to pantropical)(Frolking et al. 2009; Herold et al. 2011; Hirschmugl et al. 2017; Mitchell et al. 2017)(Fig 1.9).

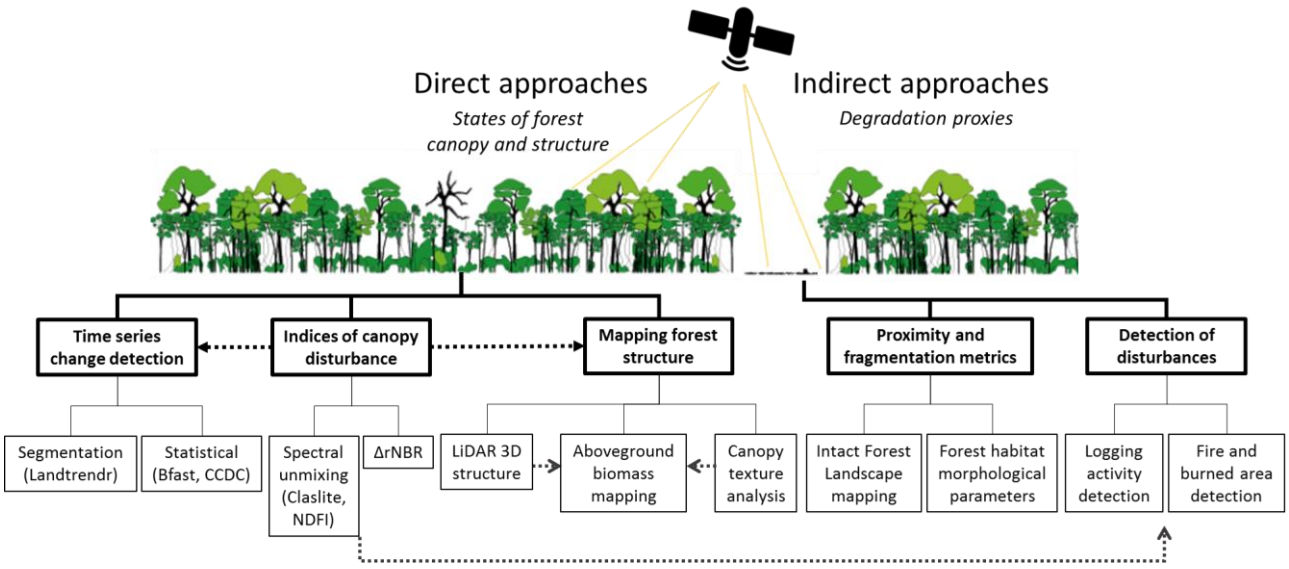

Figure 1.9 Direct and indirect approaches to characterize forest degradation/degraded forest using remote sensing and non exhaustive list of related methods

Indirect approach

Indirect approaches focus on the spatial distribution and evolution of human infrastructure and on the identification of forest disturbances along time. They are usually used as proxies for assessing potentially degraded forest areas. Indirect methods are thus useful for large area mapping and may serve as a guide to identify hotspots of degradation.

Proximity metrics such as distance to roads, agricultural activity or infrastructure but also size and connectivity of forest patches are used for delineating hinterland forests and map intact forest landscapes (Tyukavina et al. 2016; Potapov et al. 2017; Tyukavina et al. 2017). Fragmentation of forest habitat could also be a proxy of degradation (Broadbent et al. 2008). For instance, Shapiro et al. (2016) demonstrated that forest biomass was significantly different within different fragmentation classes constructed on the basis of forest habitat morphological parameters (geometry and connectivity).

The detection of logging roads, skid trails and log decks using moderate resolution optical and SAR provide proxy indicators of selective logging activity (Asner et al. 2002; Lei et al. 2018; Hethcoat et al. 2019). For instance, Bourbier et al. (2013) developped semi-automatic algorithm to extract road network and canopy gaps using Landsat imagery.

The detection of fire using MODIS Fire product (Justice et al. 2002; Giglio 2015) allows near-real time monitoring of forest and land fires but the coarse resolution of the data and the relatively high uncertainty of detection may be limiting. Other methods decided to focus on mapping the resulting burned vegetation and develop indicators of forest fire scars using Landsat images (Silva et al. 2018) or using multisource remote sensing such as Sentinel-1/2 (Verhegghen et al. 2016) or Landsat/Sentinel-2 (Roy et al. 2019).

Direct approach

Direct approaches focus on assessing the damage of forest canopy and forest structure generated by human-made disturbances. To capture these subtle changes, the use of common vegetation indices such as the NDVI (Normalized Difference Vegetation Index) from optical data is not sufficient due to saturation effects in forests with abundant undergrowth (Gond et al. 2013). In addition, degradation is a phenomenon only visible at a very fine scale and therefore cannot be detected correctly if the spatial resolution of the data is too coarse.

At the sub-pixel scale, degraded forests are mixed fractions of photosynthetic vegetation, non-photosynthetic vegetation, and bare soil. Spectral unmixing analysis (SMA) distinguishs these three

fractions and is recognized as the most effective method to assess the degradation of forest canopy using optical images (Asner et al. 2009b; Souza, Jr et al. 2013; Tritsch et al. 2016). However, SMA requires the selection of calibration values named pure spectral endmembers, which can be limiting when not available or when the data has to be selected manually. To overcome these limitations, Langner et al. (2018) developed a method using the differences of the Landsat-based normalized burn ratio (NBR) index to monitor the disturbance in forest canopy closure with no additional input of calibration data. These vegetation indices can be directly used as continuous variables to assess forest canopy disturbance or as inputs for classifying degraded forest.

The partial opening of the canopy further to selective logging or to forest fires is a transient problem that is difficult to detect through single image remote sensing analysis. Vegetation returns to these clearings at different rates depending on the state of the soil and the surrounding vegetation and, in just a few months, the opening in the canopy may no longer be detectable by satellite imagery (Mitchell et al. 2017). A temporal approach is therefore essential in order to analyze forest and degradation dynamics. It requires dense time series (several images per year, usually from Landsat archive), relevant vegetation indices and an efficient change detection algorithm that takes advantage of the seasonal and/or long-term trends in the data. A large range of methods exist in the literature (Zhu 2017). Break detection For Additive Seasonal Trends (BFAST)(Verbesselt et al. 2010) is a pixel approach that consists of modelling the expected variation in vegetation indices over a monitoring time and detecting breaking points where the indices deviate significantly from the models (DeVries et al. 2015a; DeVries et al. 2015b). The Landsat-based Detection of Trends in Disturbance and Recovery (LandTrendr) extracts spectral change trajectories using annual Landsat time series and applies time segmentation to identify slow processes (e. g. regeneration) and abrupt changes (e. g. harvesting)(Kennedy et al. 2010; Cohen et al. 2018). The Continuous Change Detection and Classification algorithm (CCDC, (Zhu and Woodcock 2014)) flags land cover change by differentiating the predicted and observed Landsat data and was applied at the sub-pixel scale to characterize degradation (magnitude of change, time of recovery…) using unmixing indices (Bullock et al. 2018). These three approaches are the most commonly utilized in the study of forest degradation but all face several difficulties. Firstly, the time series capture seasonal changes (natural variation), noise linked due to data quality or preprocessing inconsistencies and actual degradation trend that needs to be extracted and quantified. The detection of degradation is therefore a major challenge and is amplified by other constraints linked with the resolution of the data which is often too coarse compared with the small-scale impacts caused by degradation (Zhu 2017). Secondly, the density of the data used is restricted by cloud cover, which causes large gaps in the time series especially in tropical regions and thus affect the efficiency of the change detection algorithm (Fig 1.10).

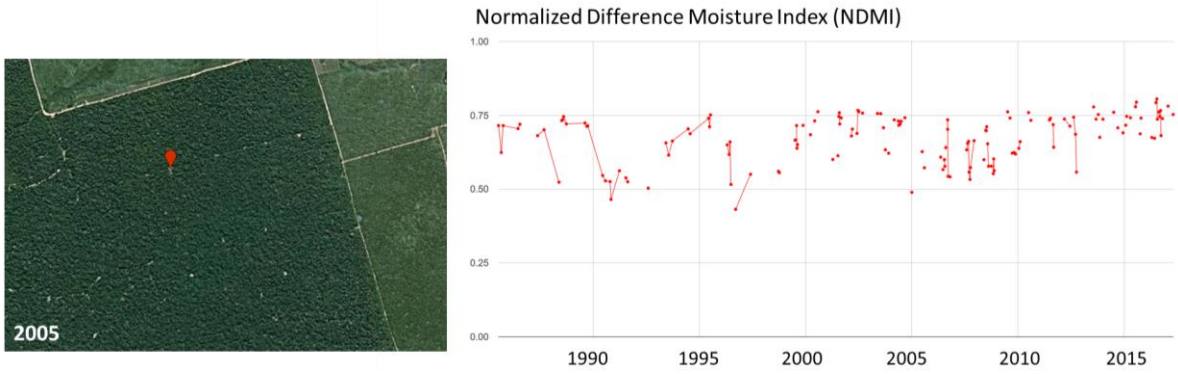

Figure 1.10 Example of the trajectory of the Normalized Difference Moisture Index (NDMI) extracted from surface reflectance Landsat data (from 1985 to 2018) over a logged forest in 2005 in Paragominas municipality. Limitations of time series change detection approach for this case are: the detection of degradation trend is mixed with noise and natural vegetation variation, large gaps in the time series (before 2000) prevent the algorithm to train over historical period (pre-disturbance) and the scale of the degradation is too small to be detected using remote sensing time series.

Thirdly, field validation of time series detection approach is a complicated and difficult task due to historical data availability. It often involves collection of reference observation using Google Earth but leads to bias and misinterpretation of disturbances (Bullock et al. 2018).

To overcome these limitations, another direct approach consists of analyzing the structure and the aboveground biomass of the forest that result from long-term degradation history. Airborne Light Detection and Ranging (LiDAR) is the most adopted remote sensing source to retrieve three-dimensional forest structural parameters and estimate aboveground biomass (AGB) stocks and changes (Asner et al. 2012; Meyer et al. 2013). LiDAR has specifically been used to assess aboveground carbon density within a gradient of degraded Amazonian forest types (Longo et al. 2016) and informs on long term consequences of different degradation trajectories on forest structure (Rappaport et al. 2018). LiDAR is also used as ground inventory data for the calibration and validation of multisource remote sensing upscaling approaches to map regional aboveground biomass across gradients of degradation (Asner et al. 2018; Meyer et al. 2019). However, airborne LiDAR data are often difficult to access (acquisition cost) and to replicate in both time and space (Silva et al. 2017). Radar images provide promising alternatives to LiDAR for estimating degraded forest AGB but remains in development (Englhart et al. 2011; Mitchard et al. 2011).

Canopy texture analysis using Very High Spatial Resolution (VHSR) images inform on the distribution of dominant tree crowns defining the forest canopy, which provides important indirect indicators of three-dimensional forest structure (Bastin et al. 2015; Meyer et al. 2018). The spatial distribution of trees, the shapes and dimensions of their crowns and characteristics of the inter-crown gaps define

the forest canopy grain and can be assessed through canopy texture analysis (Couteron et al. 2005). Many studies demonstrated the potential of texture methods (i.e. the spatial dependencies of grey-level pixels) to characterize VHSR canopy images (Couteron et al., 2005; Frazer et al., 2005; Haralick et al., 1973). Among them, the Fourier transform textural ordination (FOTO) method has been used in a variety of tropical forests and mangrove ecosystems to characterize gradients of canopy grain, canopy heterogeneity and crown size distribution (Barbier et al. 2010; Bastin et al. 2014; Couteron et al. 2005; Ploton et al. 2012; Proisy et al. 2007; Singh et al. 2014). Case studies have shown that FOTO indices can correlate with forest structural parameters along gradients of natural variation (Couteron et al. 2005) of degradation (Singh et al. 2014) or in landscapes mixing both (Bastin et al. 2014). As such, they can enable the assessment of AGB at large scale with reasonable predictive error (Bastin et al. 2014; Pargal et al. 2017; P. Ploton et al. 2017; Ploton et al. 2012; Proisy et al. 2007).

Methods that aim to map forest structure are closely related with the adopted definition of forest degradation. However, the review of existing methods illustrates the lack in understanding and quantification of the consequences of long-term degradation on forest structure and canopy texture. It also highlights trade-offs that need to be made between resolution, accuracy, area covered, cost and frequency to map degraded forest structures and forest biomass across anthropogenic disturbance gradients. Consequently, one objective of this thesis is to better characterize the large range of structures resulting from degradation through multidimensional approach.

1.3.2 Land use characterization and landscape temporal dynamics for vulnerability assessment

Most approaches used to characterize forest degradation are uniquely focused at the forest patch scale and the overall dynamics of land use and cover change is not taken into consideration. A need exists to broaden the understanding of forest degradation dynamics and drivers towards a more integrative and holistic approach. In other words, analyzing forest and its degradation in a landscape approach consists of considering and characterizing the interconnections between forest cover state and the different land use processes at multiple scales (Melito et al. 2018). The analysis of the ecological vulnerability of forest cover is only possible at the landscape scale where the intrinsic state of the forest is documented and the dynamics of land use change are decoded, thus requiring analyzes of land use and cover changes and landscape dynamics.

Remote sensing imagery provides great potential for characterizing and monitoring land cover and the elements of landscape matrices across spatial and temporal scales. Images with high and very high spatial resolutions provide greater spatial detail and precise information (Wulder et al. 2004). However, the low temporal resolution of such data does not enable monitoring vegetation dynamics and assess land cover changes at large scale. In contrast, satellite time series offers great opportunities for this purpose. MODIS and Landsat optical time series have been used extensively for land cover classification since the 1970s. Land cover derived from MODIS has low local accuracy for mapping complex landscape mosaics due to the maximum spatial resolution of 250 m. The Landsat constellation has an 8-day revisit time but has a higher spatial resolution (30 m) than MODIS. The Sentinel-2 satellite has even higher capacities, with a five-day revisit time and a 10 m spatial resolution (Drusch et al. 2012). The accessibility (free and open source) of Landsat and Sentinel images has had substantial impact on Earth observation studies, especially on vegetation mapping purposes and operational applications (Zhu et al. 2019).

The proliferation of remote sensing sources (optical, radar and fusion) and the unprecedented combination of spectral, spatial and temporal resolutions constitute a large volume of data that remains a significant challenge for the automated mapping of tropical lands. In parallel, machine learning techniques such as Random Forest emerged to face this difficulty and are now recognized as commonly utilized tools for land cover classification thanks to their a robustness and capacity to handle a large number of input data and variables (even those that are highly correlated)(Breiman 2001; Pal and Mather 2005).

A large range of remote sensing approaches have been developed to identify cropping systems and practices (Inglada et al. 2016; Bégué et al. 2018; Picoli et al. 2018) but also to discriminate natural vegetation such as forests and their different successional stages (Piazza et al. 2016; Sothe et al. 2017). However, the identification of land cover classes in forest–agriculture mosaics distributed along vegetation gradients remains a challenge and often results in misclassification. Extensive fieldwork combined with multispectral remote sensing images and pixel-based approach classifier was preferred in this thesis for mapping these complex mosaics. Although object based image analysis (OBIA) presents many advantages over per pixel methods including a more precise delineation of landscape elements with similar textural and spectral properties, the pixel-based approach does not require user-inputs making it more robust for long-term land cover reconstruction using time series.

Based on multiple land cover classifications, landscape structure dynamics (i.e. composition of land cover/uses elements and the configuration of the elements within a given space) are key in understanding the complexity of forest-agricultural mosaics and reconstructing land use and land cover change history. This approach is already well referenced and some authors have highlighted its robustness for the analysis of spatial patterns of land use dynamics at the landscape scale and its ability to supply further information on human-environment processes (Wu 2007; Messerli et al. 2009). Some authors also demonstrated the relevance of landscape structure metrics in the characterization of agricultural frontiers dominated by fragmentation dynamics (Oszwald et al. 2011; Wang et al. 2014; Hargis et al. 1998). Furthermore, the availability of time series of remote sensing images opens up a wide range of perspectives to characterize agricultural frontiers through historical trajectories of landscape change (Lausch and Herzog 2002; Ernoult et al. 2006). In that sense, Oszwald et al. (2011) used multivariate statistics to reconstruct landscape trajectories defined as the changes in landscape structures among a group of observations entities. These trajectories informed on the relative changes in both composition and configuration reflecting landscape homogenization or fragmentation for a set of farms experiencing different deforestation history (Grimaldi et al. 2014; Lavelle et al. 2016). However, this approach was not generalized to study the landscape structure dynamics over a whole territory.

To this date, there are no methods or conceptual framework that aim to characterize the ecological vulnerability of forest cover to anthropogenic impacts. Assessing forest ecological vulnerability is an opportunity to integrate different indicators at the forest and landscape scales in order to spatially inform on the location of the most vulnerable forests. Moreover, most forest degradation analyses are strictly focused on the forest patch scale. This greatly limits the understanding of the cascading effects of direct and indirect drivers of degradation and influences of land use and cover changes and landscape structure on the status of forest cover.

1.4 Research questions and objectives

This research is guided by the question "*how does forest degradation and the changes in land use and cover change affect the ecological vulnerability of forest cover in human-modified landscapes?*". Central to this research are the interactions between forests and human and their dynamics in a context of old deforestation fronts.

The global scientific objective is to develop a multidimensional approach using remote sensing to assess forest degradation and the relations between the broader dynamics of land use/cover and landscape changes towards the evaluation of the ecological vulnerability of forest cover. The global operational objective is to develop a holistic diagnosis of forests based on spatial indicators of forest cover state, forest degradation drivers and on the identification of most vulnerable forests in order to provide actionable knowledge to decision makers for tailored and prioritized management of forest at the landscape scale.

The main research question (RQ) was split into four sub-questions (Fig 1.11):

RQ1 *How to assess the state of forest cover across gradients of human-induced degradation using multisource remote sensing?*

> Hypothesis: Multisource remote sensing provide relevant indicators in modelling and mapping aboveground biomass of degraded forests.

RQ2 *How to quantify long-term changes in forest structures from degradation?*

> Hypothesis: Canopy texture analysis and derived metrics from UAV to satellite sources correlate with 3D forest structure parameters within a large range of degraded forest types.

RQ3 *How to identify and disentangle cascading effects of forest degradation drivers at the landscape scale?*

> Hypothesis: A landscape approach is necessary to capture the influence of changes in composition (land use and land cover) and configuration onto the status of forest cover.

RQ4 *How to characterize the ecological vulnerability of forest cover?*

> Hypothesis: A landscape approach combining indicators of forest cover state, drivers of forest degradation and landscape structure dynamics are keys to assess sensitivity, exposure and adaptive capacity components of ecological vulnerability.

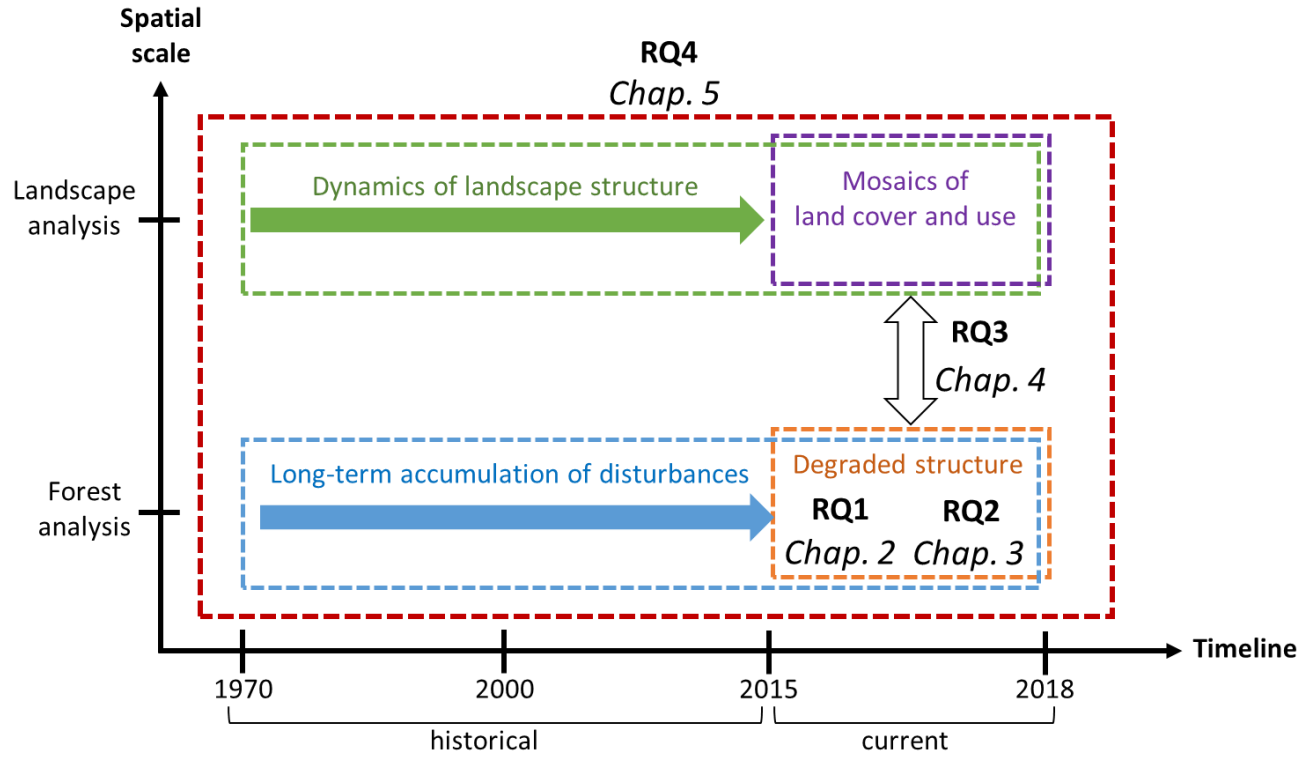

Figure 1.11 Overview of the thesis structure with the sub-research questions and respective chapters located according forest and landscape scales of analysis and current and historical timelines

1.5 Study sites: human-dominated tropical landscapes in deforestation fronts

The study sites for this research were located in two old deforestation fronts in the Brazilian Amazon and in the Central Highlands of Vietnam (Fig 1.12). Both sites are human-dominated landscapes where humid-tropical forests (state and configuration) are the result of complex colonization and land use change dynamics. These forests are currently threatened by agricultural expansion and related forest degradation risks.

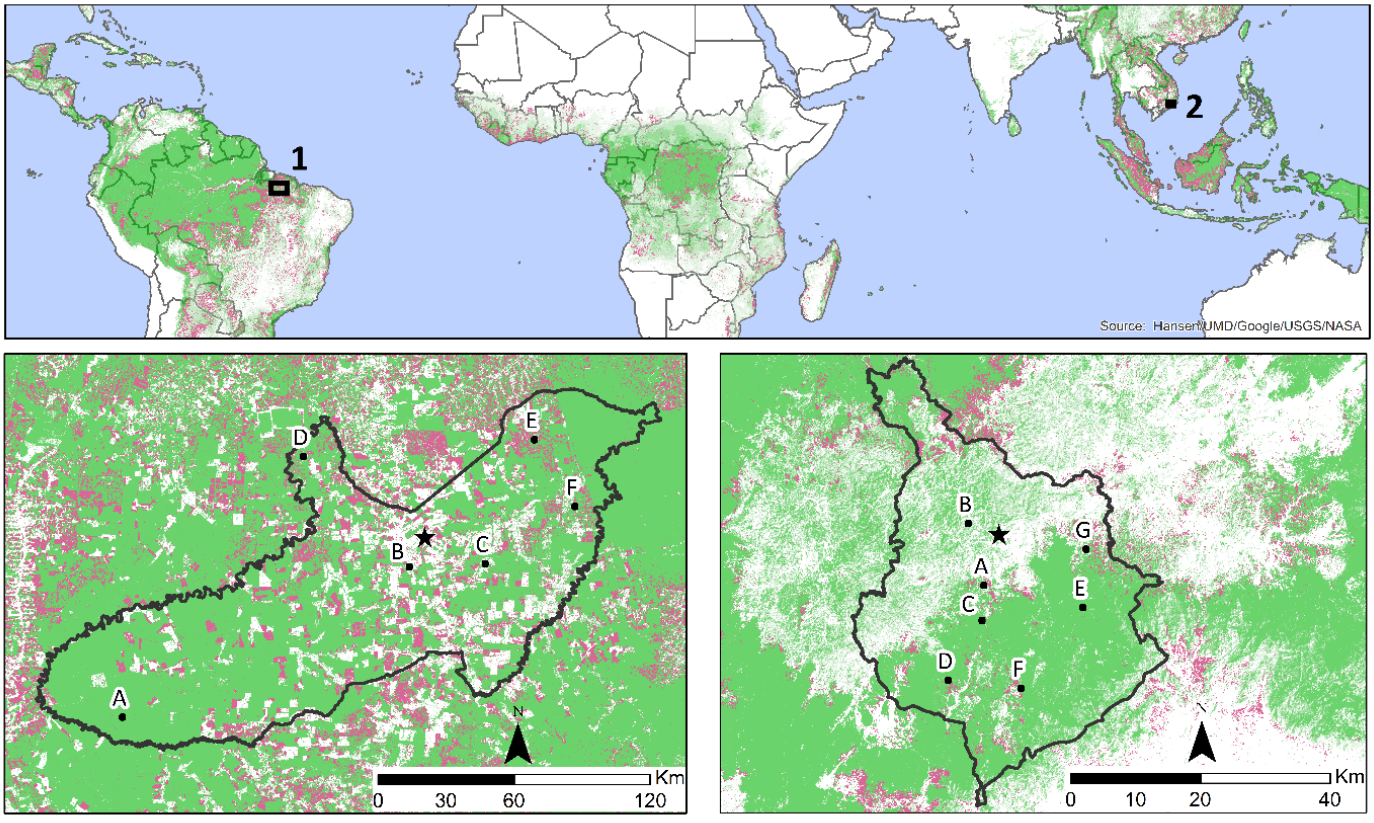

Figure 1.12 Study sites located in human-dominated tropical landscapes of deforestation fronts. Green shows tree cover in 2000 and pink forest cover loss from 2000 to 2014, source: (Hansen et al. 2010). Landscape mosaics numbered by letters are presented in figures 1.15 and 14. The star represents the location of the main city.

1.5.1 Paragominas municipality, state of Pará, Brazilian Amazon

Geographical conditions

The municipality of Paragominas (19,342 km²) is located within the Brazilian deforestation front in the northeastern part of the State of Pará (Fig 1.12). The climate is tropical with an average annual temperature of 26.3°C and a mean relative humidity of 81%. Average annual rainfall recorded at Paragominas station between 1992 and 2010 was 1,693 mm (Andrade 2011). Eighty-three percent of the annual precipitation falls in the rainy season from December to May. From June to November, mean monthly rainfall is less than 100 mm/month. Landforms consist of plateaus at an elevation of 160–190 m above sea level, separated by valleys up to several kilometers wide. The most prevalent soils are Ferralsols, clayey on the plateaus and sandy in the valleys (Laurent et al. 2017).

Historical colonization processes

Colonization began in 1965 with the construction of the BR-010 road connecting Brasilia to Belém coupled with the rapid conversion of forest to pasture for cattle ranching mainly located in the valleys and lowlands. The boom in the logging industry started from the 1980s which saw the installation of 350 sawmills along the main road, therefore accelerating the overexploitation of forest resources. In the 2000s, deforestation in the high and fertile lands marked the boom of the grain agro-industry through large-scale soybean and maize cultivation. In 2007, the municipality was red-listed by the federal government as one of the most deforested Amazonian municipalities (Viana et al. 2016)(Fig 1.13). The consequences were an immediate loss of access to credit and market for any commodities. In response, Paragominas became the first “green municipality” in the country in 2008 in order to end illegal deforestation, to tend to zero net deforestation by 2014, and to promote alternative production systems and reforestation (Piketty et al. 2015). These colonization processes mainly occurred in the central part of the municipality. The eastern part of the municipality is delimited by an indigenous reserve (protected area). Since 2000 the western region has been owned by the private forestry company CIKEL Brazil Verde Madeiras Ltda. Smallholder dominated areas can be found in the east and north part of the municipality. These areas were colonized at different time through government incentive migration (Yanai et al. 2017). Besides subsistence agriculture (mainly cassava), farmers practice small-scale cattle breeding and the cultivation of pepper and açai (Laurent et al. 2017).

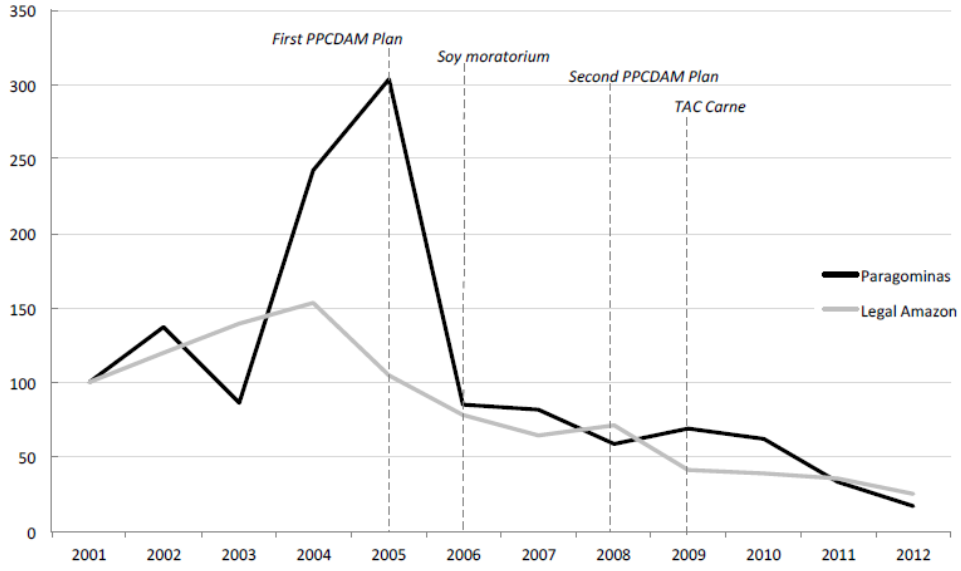

Figure 1.13 Annual deforestation index in Paragominas and the Legal Amazon since 2001 (2001: base 100). Source: Adapted from PRODES data.

Landscape elements and configuration

A range of interconnected elements can be found within Paragominas landscapes linked through degradation, deforestation, regrowth and conversion or intensification dynamics (Fig 1.14). Conserved forest is degraded due to repetitive selective logging, which can be amplified by fire. The regrowth from these states to conserved forest is long and uncertain. Deforestation is the conversion of a degraded forest (logged or logged and burned) to pasture or for cash crop agriculture (soybean, maize). When pastures are not well managed, wooden vegetation can invade the land. The pasture can be abandoned and turn into a juquiera (e.g. fallow) characterized by a mix of grass and shrub vegetation which may evolve into a young secondary forest or the pasture can be cleared using fire. Pasture (wooden or clean), juquiera and young secondary forests can be converted to cash crop agriculture in areas where the soil is fertile and suitable (high plateaus). Pastures can also be converted into tree plantation (teak, eucalyptus or parika) if the land is not productive or if it is sold to private companies.

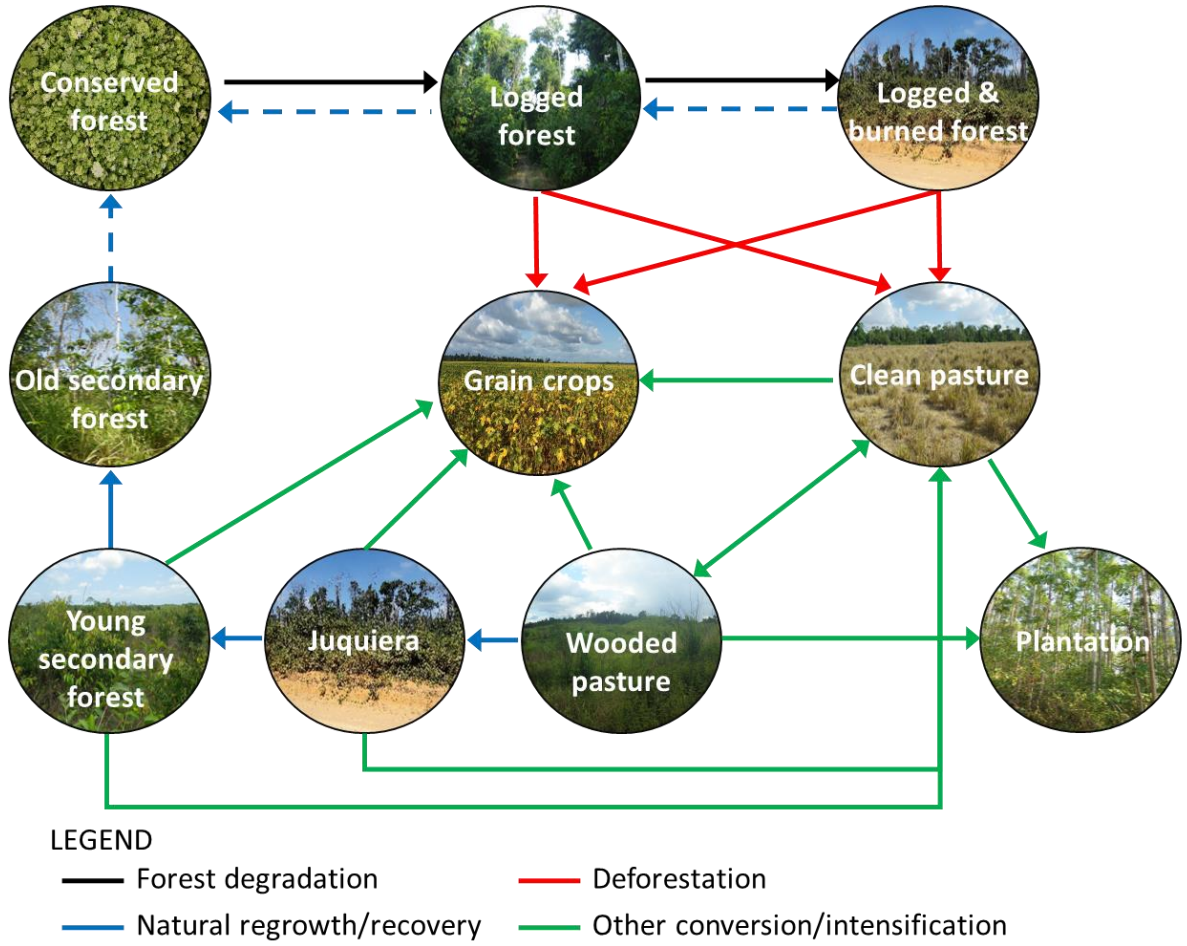

Figure 1.14 Systemic model of landscape elements dynamics in Paragominas in 2018 (non-exhaustive). Dashed arrows reflect less probable dynamics.

Paragominas is composed by a large diversity of landscape mosaics (Fig 1.15). Mosaic A is dominated by conserved forest. Mosaic B located in the central part of the municipality is dedicated to large-scale cash crop agriculture (here soybean) with some isolated patches of remnant forests. The central part is also a patchwork of large pastureland and forest (Mosaic C). Mosaics D, E and F are more diverse and complicated landscapes as they are composed by degraded forest (logged and burned), secondary forests at different ages, juquiera, small-scale agriculture (cassava, pepper) and wooded pasture.

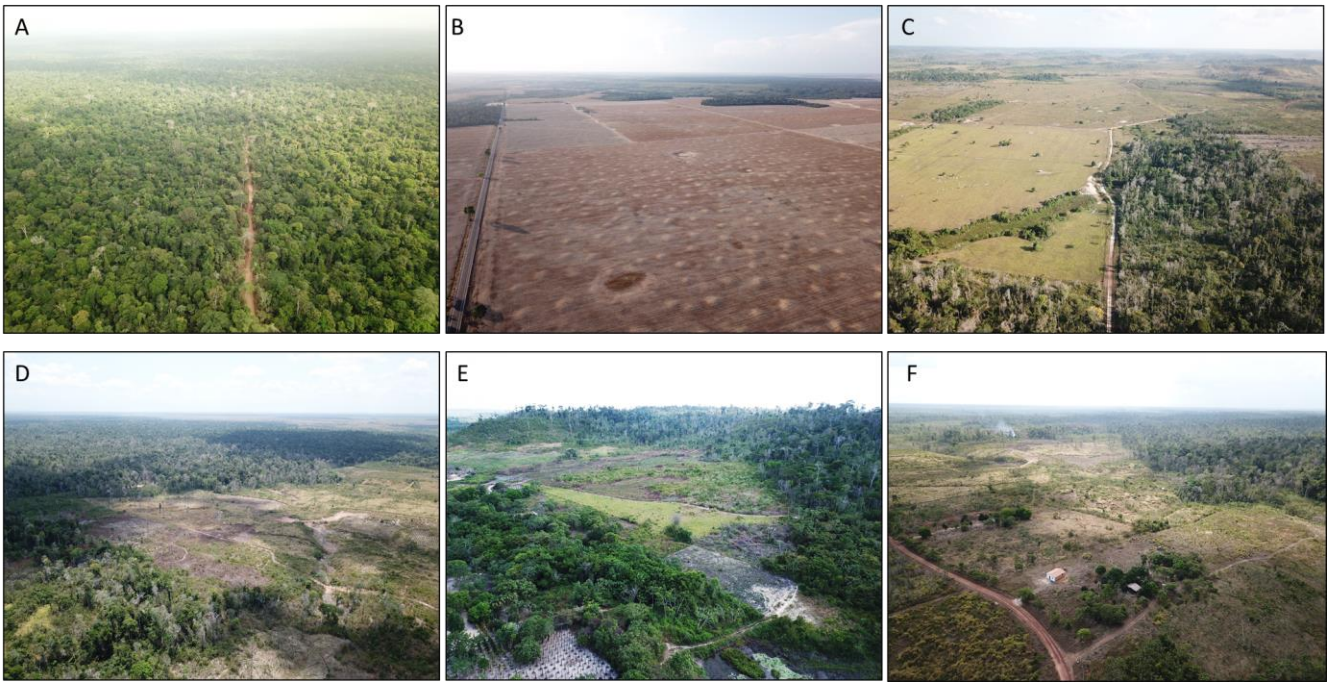

Figure 1.15 Diversity of landscape mosaics and land uses in Paragominas municipality (2017). See figure 1.12 for the location of landscape mosaics within the municipality.

1.5.2 Di Linh district, Lam Dong province, Central Highlands of Vietnam

Geographical conditions

The district of Di Linh is located in Lam Dong province of the Central Highlands in Vietnam (Fig 1.12). The district has a tropical monsoon climate with varying altitude and, two distinct seasons: the rainy season from May to November and the dry season from December to April. The average temperature ranges from 18 - 25°C. Average rainfall is 1,750 - 3,150 mm / year and average humidity is 85 - 87%. The average sunshine per year is 1,890 - 2,500 hours. Soil in Lam Dong province is generally of high quality and suitable for agriculture (coffee, tea and vegetables). Lam Dong has a relatively varied terrain (from 0 to 1860m) mainly consisting of mountains and plateaus but also some flat small valleys.

Historical colonization processes

French colonialists founded the town of Di Linh in 1899 as an administrative post located along the road connecting Ho Chi Minh City (Saigon) to Da Lat. The rapid development of the infrastructure network in the early 20th century marked the beginning of the agricultural colonization (rice cultivation and vegetables) associated with a flow of immigrants for administrative development. The two Indochina wars (1945 - 1954; 1955 - 1975) triggered an acceleration in the transformation of Di Linh territory through increased flows of migrants and settlements from the lowlands. This influx of migrants enabled the continuous development of coffee and tea as cash crops. Starting in 1975, the government implemented several housing and agricultural policies as incentives for migrants to settle in the vicinity of Di Linh city, to clear land and cultivate food crops in the valley and cash crops in higher lands (Déry 2000). The state-sponsored migration and the resettlement of ethnic minority groups relying on slash and burn agriculture on the forest margins were accompanied by the coffee boom of the 1980s (Trædal and Vedeld 2017; Meyfroidt et al. 2013). In the mid-1990s, Lam Dong became the second largest coffee producing province in Vietnam (Ha and Shively 2008). From 1990 - 2000, the government kept encouraging the expansion of agricultural land (mainly coffee) to meet the community needs (Fig 1.16). From 2001 - 2010, deforestation rates declined thanks to law enforcement and improved forest management and protection and reduced market demand. Since 2006, market demand has again increased leading to further expansion of the coffee. This large-scale coffee production has been identified as one of the main drivers of deforestation and degradation and is responsible for triggering other environmental problems such as increased drought and soil erosion (Meyfroidt et al. 2013; Grosjean et al. 2016). In order to reduce these risks, Lam Dong province was the subject of a pilot study for incentive programs for environmental conservation and restoration (Thuy 2013). The district was also the subject of forest restoration programs with afforestation of khasi pine (Pinus kesiya) for watershed protection and the conversion of poor forest land (low productivity) into commercial plantations (higher wood yields)(Dien et al. 2013). Despite these efforts, active deforestation fronts are still present in the Central Highlands (Meyfroidt and Lambin 2008), and even though degradation caused by logging and human triggered fire have been drastically reduced since the 1990s, they remain present along the agricultural frontier (Dien et al. 2013; Vogelmann et al. 2017).

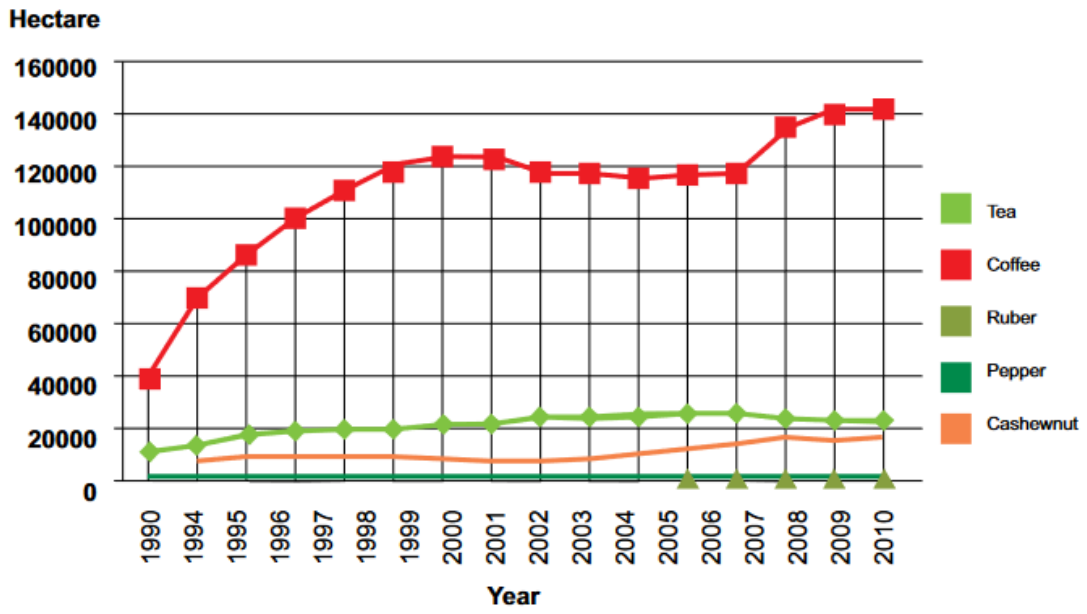

Figure 1.16 Area (ha) of perennial crops in Lam Dong province, from 1990 – 2010 (source: Land use, forest cover change and historical GHG emission (USAID LEAF), Lam Dong province, 2013)

Landscape elements and configuration

Conserved broadleaf forest with no signs of recent human-induced disturbance is usually classified into three density types, respectively high (200-300 m3/ha), medium (100-200 m3/ha) and low density (< 100 $m^3.ha^{-1}$) and can be explained by natural or anthropogenic impacts (Fig 1.17). Low-density forest is degraded due to selective logging and fire and can be colonized by bamboo vegetation. Degraded or "poor" (low density) forest is converted into coffee but can also be enriched through plantation of pine forest for protection of the forest edge. It can also be converted into pine forest for production (wood for construction or transformation into processed goods). To a lesser extent, degraded forest is converted into maize or banana plantation. Natural pine forest is isolated in the dynamic as strictly protected with rare conversion into coffee. Rainfed and irrigated rice fields are not involved in the agricultural expansion dynamic. Finally, natural bushes are experiencing recent conversion into agricultural land (maize or banana plantation) and into pine forest for timber production.

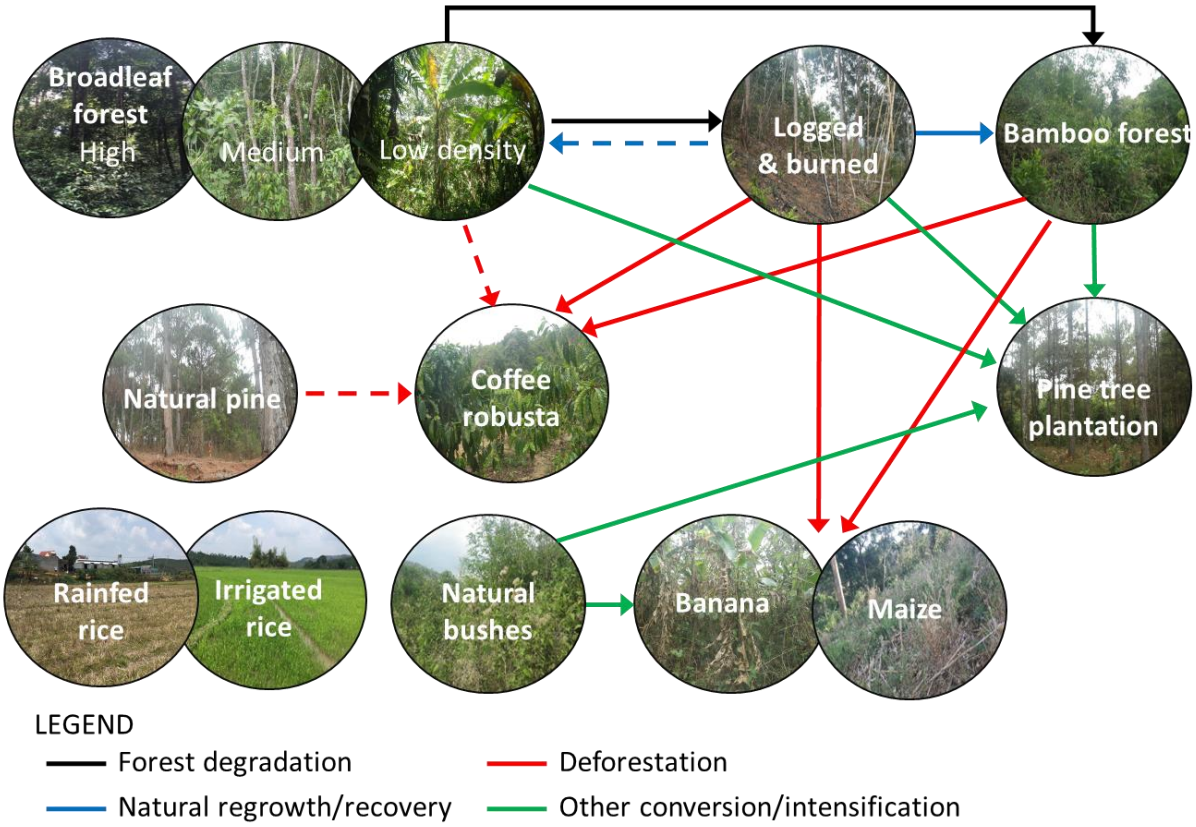

Figure 1.17 Systemic model of landscape elements dynamics in Di Linh in 2018 (non-exhaustive). Dashed arrows reflect less probable dynamics.

Di Linh district is characterized by very different landscapes between the north and south (Fig 1.18). The north is marked by large scale coffee plantation (mosaic B) and rainfed paddy rice associated with coffee at the beginning of slopes and pine forest in higher elevation (mosaic A). Mosaic C shows a gradient of old to younger coffee plantation following the elevation and mixed broadleaf and pine forest. This can be explained by natural alternation between both types or by a replantation of pine forest following deforestation in order to protect forest edge from further encroachment and soil erosion. Mosaic D shows a typical topographic gradient where rainfed rice is located at the bottom, coffee plantation positioned on the slope and degraded and fragmented forest patches due to slow encroachment of coffee over forest area through selective logging and fire. Mosaic E is located at a higher elevation and mainly shows different states of forest cover mixed with coffee and maize. Mosaic F shows a highly heterogeneous landscape of coffee at different ages, natural bush and degraded forest. Mosaic G shows interconnected coffee and pine plantation for production purposes (cycle of growth/harvest of 25 years).

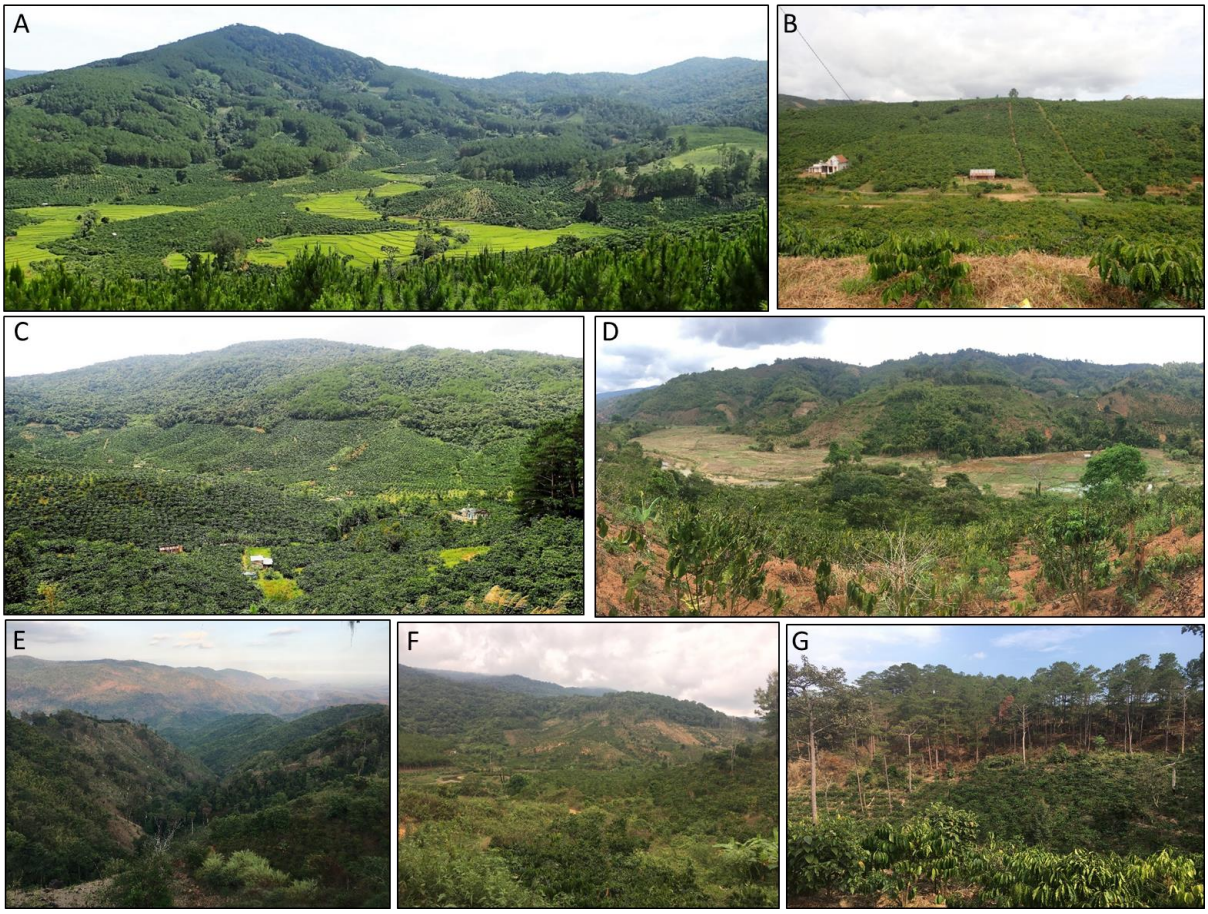

Figure 1.18 Diversity of landscape mosaics and land uses in Di Linh district (2018). See figure 1.12 for the location of landscape mosaics within the district.

1.6 Thesis structure

This PhD thesis is organized in six chapters. Between the general introduction (Chapter 1) and the conclusion (Chapter 6), the Chapters 2, 3, 4 and 5 reproduce the scientific papers (published or submitted) that address the different sub-research questions (RQ1 to RQ4).

In Chapter 2, we assess the potential of multisource remote sensing and derived indicators to model and map the aboveground biomass (AGB) of forest across gradients of degradation in Paragominas. The model is calibrated and validated with field inventory data from the Sustainable Amazon Network. In addition, we identify a five class-typology of degraded forest types from the field and use it to validate the AGB map.

In Chapter 3, we explore the use of 2D canopy texture metrics to retrieve the structure of degraded forests resulting from various degradation histories in Paragominas. We map 40 forest plots using UAV and use photogrammetry method to generate independent canopy height models and high-resolution images. We investigate how the different gradients of texture captured by Fourrier-based textural ordination and lacunarity correlate with canopy structure. We finally discuss how long-term accumulation of disturbances varying in type and frequency have affected current forest structure and how it can be measured using canopy texture analysis.

In Chapter 4, we explore the different cascades of direct and indirect drivers of forest degradation in Paragominas. Based on collected field data, we map forest-agricultural mosaics and apply a landscape quantitative approach to derive landscape structure indicators. Additionally, we collect direct driver (fire occurrence) and indirect drivers (environmental and geographical factors). Linear regression models are then used to identify most significant dirvers of degradation and we analyze the spatial distribution of these drivers using clustering methods. The discussion focuses on the sequential interaction of forest degradation drivers at the landscape scale and identifies different forest management options.

In Chapter 5, we develop a rigorous methodological framework to assess forest ecological vulnerability in Di Linh. We use remote sensing to characterize forest landscape dynamics in spatial and temporal dimensions integrating current landscape mosaic mapping with 45 years of landscape structure trajectories. We adapt the definition of vulnerability by the IPCC to derive indicators of forest sensitivity, exposure and adaptive capacity. Combined, these indicators pinpoint hotspots of forest vulnerability.

Chapter 2 - The Potential of Multisource Remote Sensing for Mapping the Biomass of a Degraded Amazonian Forest

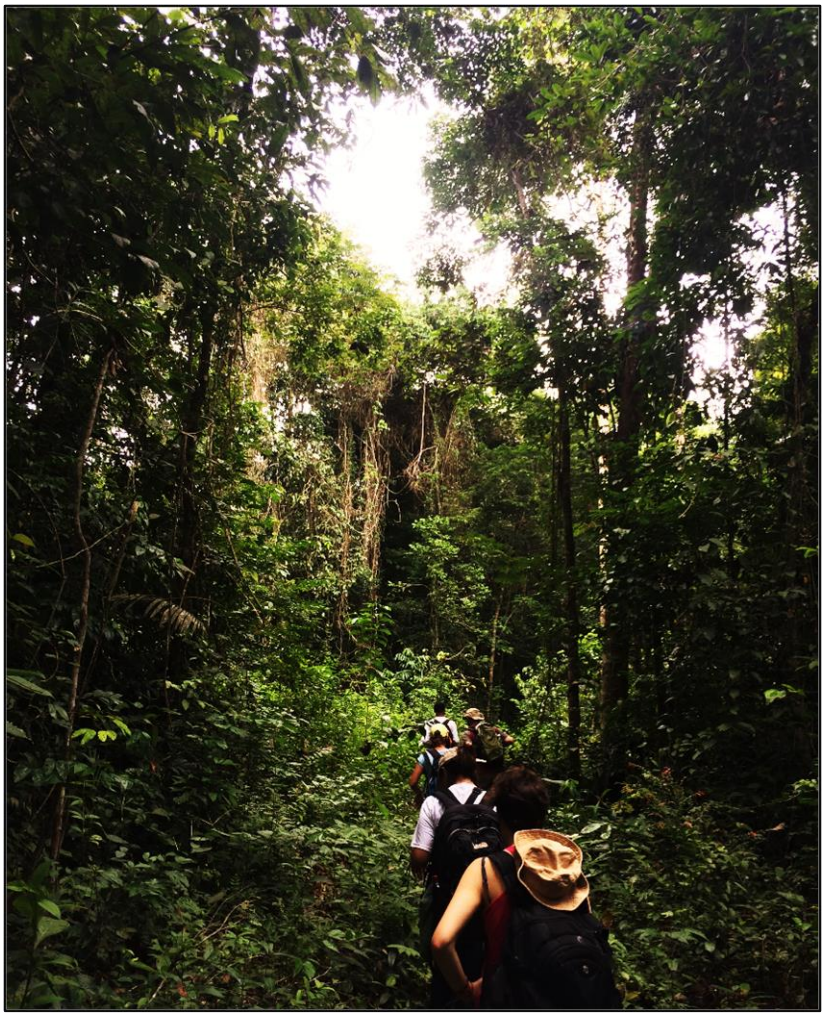

A transect through a selectively logged forest of Paragominas municipality to observe and document the different vegetation strata and the canopy structure (picture by Clément Bourgoin)

Reproduced from the article:

Bourgoin, C.; Blanc, L.; Bailly, J.-S.; Cornu, G.; Berenguer, E.; Oszwald, J.; Tritsch, I.; Laurent, F.; Hasan, A.F.; Sist, P.; Gond, V. (2018) The Potential of Multisource Remote Sensing for Mapping the Biomass of a Degraded Amazonian Forest. *Forests* **2018**, *9*, 303. https://doi.org/10.3390/f9060303

The Potential of Multisource Remote Sensing for Mapping the Biomass of a Degraded Amazonian Forest

Bourgoin C.[1,2,*], Blanc L. [1,2], Bailly JS. [3,4], Cornu G. [1,2], Berenguer E. [5,6], Oszwald J. [7], Tritsch I. [8], Laurent F. [9], Hasan AF. [9], Sist P. [1,2] and Gond V. [1,2]

1 CIRAD, Forêts et Sociétés, Montpellier, France
2 Forêts et Sociétés, University Montpellier, CIRAD, Montpellier, France
3 LISAH, University Montpellier, INRA, IRD, Montpellier SupAgro, Montpellier 34398, France
4 Department SIAFEE AgroParisTech, Paris, France
5 Environmental Change Institute, University of Oxford, Oxford, UK
6 Lancaster Environment Centre, Lancaster University, Lancaster, UK
7 UMR CNRS LETG 6554, Université de Rennes 2, Rennes, France
8 UMR 7227, Université Sorbonne Nouvelle, Paris 3, Paris, France
9 UMR CNRS ESO (Espaces et Sociétés), Le Mans Université, Le Mans, France

Abstract

In the agricultural frontiers of Brazil, the distinction between forested and deforested lands traditionally used to map the state of the Amazon does not reflect the reality of the forest situation. A whole gradient exists for these forests, spanning from well conserved to severely degraded. For decision makers, there is an urgent need to better characterize the status of the forest resource at the regional scale. Until now, few studies have been carried out on the potential of multisource, freely accessible remote sensing for modelling and mapping degraded forest structural parameters such as aboveground biomass (AGB). The aim of this article is to address that gap and to evaluate the potential of optical (Landsat, MODIS) and radar (ALOS-1 PALSAR, Sentinel-1) remote sensing sources in modelling and mapping forest AGB in the old pioneer front of Paragominas municipality (Para state). We derived a wide range of vegetation and textural indices and combined them with in situ collected AGB data into a random forest regression model to predict AGB at a resolution of 20 m. The model explained 28% of the variance with a root mean square error of 97.1 $Mg \cdot ha^{-1}$ and captured all spatial variability. We identified Landsat spectral unmixing and mid-infrared indicators to be the most robust indicators with the highest explanatory power. AGB mapping reveals that 87% of forest is degraded, with illegal logging activities, impacted forest edges and other spatial distribution of AGB that are not captured with pantropical datasets. We validated this map with a field-based forest degradation typology built on canopy height and structure observations. We conclude that the modelling framework developed here combined with high-resolution vegetation status indicators can help improve the management of degraded forests at the regional scale.

Keywords Forest degradation, Multisource remote sensing, Modelling aboveground biomass, Random forest, Brazilian Amazon

2.1 Introduction

Deforestation and forest degradation are major sources of greenhouse gas emissions (Houghton 2013; Simula and Mansur 2011), contributing to forest carbon losses (Baccini et al. 2017), global climate change, affecting biodiversity (Barlow et al. 2016) and the entire forest ecosystem. While deforestation refers to the rapid conversion from forest to non-forest areas, degradation implies changes in the forest structure with no change in land use (Thompson et al. 2013; Putz and Redford 2010). In Amazonia, over the last decades, deforestation and forest degradation have shaped the rural landscape, resulting in a complex mosaic of fragmented forests associated with agricultural lands (Lamb et al. 2005). A total area of 766,448.5 km^2 was cleared in 2015 (« PRODES — Coordenação-Geral de Observação da Terra »), representing 20% of Amazonia (Hansen et al. 2010; Fearnside 2005).

Since 2005, deforestation in Brazil has drastically decreased thanks to coercive measures taken by the Brazilian government associated with private initiatives (soy and beef moratoria), among other factors (D. Nepstad et al. 2009). However, these measures are not effective for reducing forest degradation (« DEGRAD — Coordenação-Geral de Observação da Terra »; « Florestas do Brasil em Resumo 2013 »). Most of the remaining forested lands are degraded due to the accumulation over time and space of severe degradation processes mainly triggered by anthropogenic impacts through unsustainable logging practices, fire, shifting cultivation and charcoal production (Asner et al. 2005; Souza et al. 2013).

Reducing forest degradation is a major challenge given the rapid need to reduce carbon emissions to the atmosphere, conserve biodiversity, limit soil erosion and regulate the water cycle (Thompson et al. 2009). Forest monitoring based on the forest/non-forest approach used to quantify deforestation is not relevant for providing information on the forest status (Potapov et al. 2017; Bernier et al. 2016). The biomass value of a forest is a relevant indicator to quantify the intensity of degradation (Berenguer et al. 2014). Forest biomass mapping is therefore a critical step to reach the challenge (Bustamante et al. 2016b).

At the pantropical scale, two maps of biomass density that present the spatial distribution of the biomass of all forest types at a moderate resolution (Saatchi et al. 2011; Baccini et al. 2012) have been used as baselines for the tropical belt. More recently, a harmonized reference aboveground biomass (AGB) map has been released that significantly improves the estimation and local distribution of AGB using the combination of in-situ collected data, remote sensing and regional biomass maps (Avitabile et al. 2016).

At the local scale, most of the approaches integrate field-collected data with Light Detection and Ranging (LIDAR) to scale up forest biomass natural distribution, which normally requires spatial interpolation of in-situ biomass (Malhi et al. 2006). LIDAR can map the forest canopy in three dimensions and can retrieve accurate forest biomass through forest canopy height and structure (Asner et al. 2012; Asner 2009; Asner and Mascaro 2014; Fayad et al. 2017; Mascaro et al. 2011). It is also sensitive to the carbon density of the different types of degraded forests, from logging at a low impact to forest stands burned multiple times (Longo et al. 2016). Satellite LIDAR has been used in validating AGB maps (Baccini et al. 2008), calibrating local regressions between in situ AGB data and metrics derived from LIDAR footprints and extrapolating using different remote sensing sources (Fayad et al. 2017; Fayad et al. 2014). However, most airborne and satellite LIDAR datasets are often difficult to access (acquisition cost) and to replicate in both time and space (Hirschmugl et al. 2017).

At the meso-scale (regional), many studies demonstrated the potential of optical and radar remote sensing-derived indicators to characterize degraded forests (Herold et al. 2011). The study of degraded forests requires the analysis of vertical and horizontal disturbances within the forest structure (Thompson et al. 2013; Hirschmugl et al. 2017; Rappaport et al. 2018; Achard et al. 2014; Lambin 1999). Optical images can provide information on the photosynthetic activity and moisture of the forest canopy (Gond et al. 2013). Spectral unmixing approaches are recognized to be the most effective method to assess the status of degraded forests using the percentage of active vegetation, dead vegetation and bare soil at the pixel scale (Souza et al. 2013; Asner et al. 2009; Tritsch et al. 2016). Radar images are sensitive to the texture of the impacted forest canopy (Joshi et al. 2015). Canopy texture-derived indicators based on co-occurrence matrices use the variance of the signal in a given window to spatially quantify the distribution of tree crowns structure (Kuplich et al. 2005; Luckman et al. 1997; Haralick et al. 1973). Estimating the biomass from the radar data generally concerns wavelengths up to the meter (band P or L) with signal saturation thresholds around 200 $Mg.ha^{-1}$ of AGB (Morel et al. 2011; Mitchard et al. 2011; Englhart et al. 2011).

This review of recent remote sensing methods illustrates the trade-off that needs to be made between resolution, accuracy, area covered, cost and frequency to map forest biomass. It also highlights the fact that there is remarkably little information at the regional scale on the potential of open access optical and radar remote sensing to model and map the aboveground biomass of degraded forests. Most of the approaches tend to capture the local variation of AGB following environmental variables, i.e., climate, topography and natural forest dynamic gradients, but do not particularly capture the distribution along anthropogenic disturbance gradients (Longo et al. 2016).

In this sense, there is a need to better understand how remotely sensed indicators perform with AGB modelling at the regional scale in order to provide relevant information to decision makers on the state of the resource of remnants forest.

In order to answer this need, this paper aims (i) to assess the potential of multisource, multi-indicator and open access remote sensing in modelling and mapping aboveground biomass of degraded forests, (ii) to quantify the spatial distribution of degraded forest biomass in comparison with the pantropical AGB map, and (iii) to evaluate the relevance of this regional forest AGB mapping at the stand scale.

This quantification is highly informative for forested land use planning and policy makers. Many South American governments and global NGOs are seeking more accurate and definitive information about the scale of degradation so they can propose policies and actions to ameliorate and reduce the level of degradation (« Imazon – Instituto do Homem e Meio Ambiente da Amazônia »).

2.2 Materials and Methods

2.2.1 Study Area

The study was carried out in the municipality of Paragominas, located in the northeastern part of the State of Para, Brazil, and covering an area of 19,342 km^2 with a population size of 108,547 (« IBGE, Paragominas »). The municipality was founded in 1965 along the BR-010 road connecting Brasilia to Belém (Fig 2.1). The colonization process led to a large conversion of lands into pasture, with cattle ranching becoming the dominant land use. The municipality went through a succession of different economical models that have drastically shaped the landscape (Piketty et al. 2015). The boom in the logging industry started from the 1980s, where most of the timber was transformed in the 350 sawmills located along the main road. Deforestation and forest degradation were accentuated with the grain agribusiness boom in the 2000s (soybean and maize cultivation) and charcoal production. In 2007, the municipality was red-listed by the federal government as one of the most deforested Amazonian municipalities. The consequences were an immediate loss of access to credit and market for any commodities. Many charcoal plants and illegal sawmills were shut down. In response to this governmental ban, Paragominas became the first “green municipality” in the country in 2008 in order to end illegal deforestation, to tend to zero net deforestation by 2014, and to promote alternative production systems and reforestation. Land management was also improved through the Rural Environmental Registry (Viana et al. 2016).

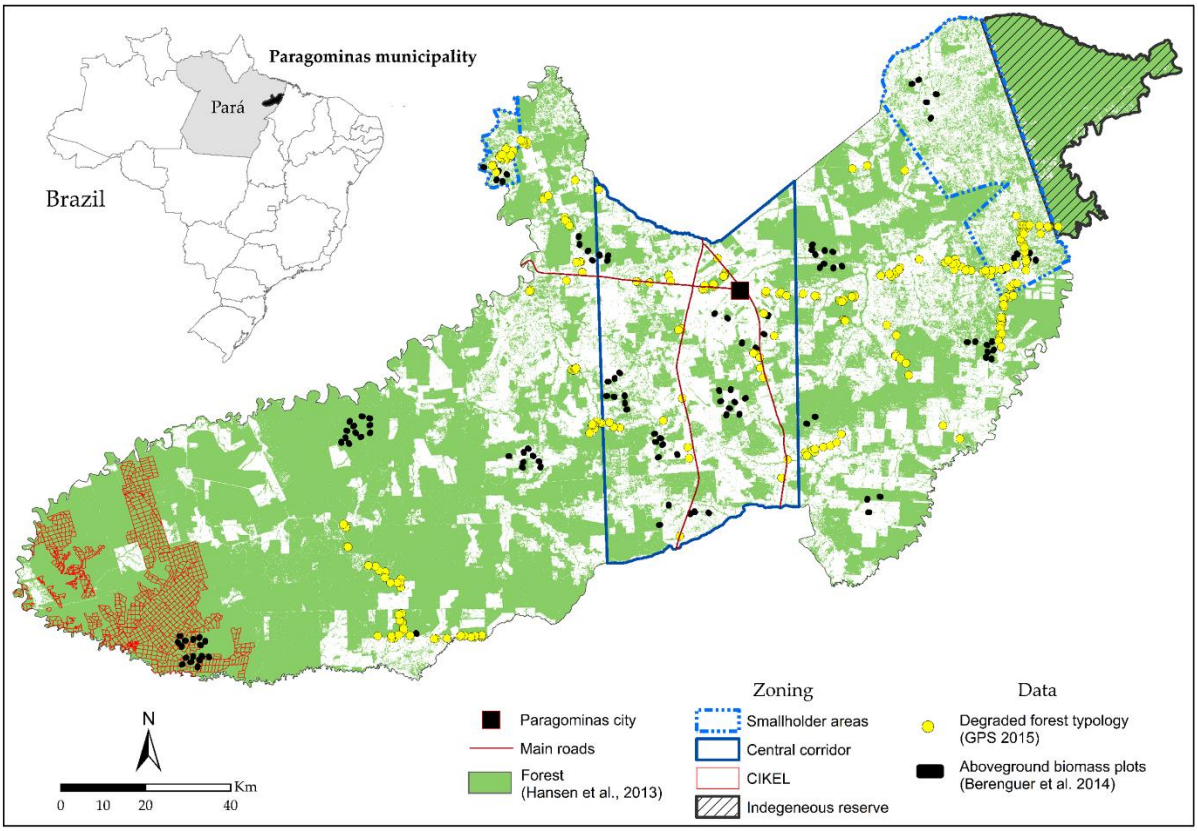

Figure 2.1 Map of Paragominas municipality in the northeastern part of the State of Para with the location of the biomass-collected plots, the degraded forest typology and the main zoning areas (extracted from (Hansen et al. 2010)).

2.2.2 In Situ AGB Collection

Aboveground biomass data were collected during the dry seasons in 2009 and 2010 by teams from the Sustainable Amazon Network (Rede Sustentavel Amazonia—RAS) (Berenguer et al. 2014; Gardner et al. 2012; Gardner et al. 2013). In total, 18 study sites were randomly selected in the municipality of Paragominas. For each site, plots of 250 m by 20 m were designed, resulting in a total of 121 plots. Each plot represents a homogeneous type of forest, classified into four types: undisturbed forest, logged forest, logged forest and burned and secondary forest. Aboveground biomass was estimated using Chave's allometric equations (Chave et al. 2005) and was based on the measurements and identification of all live trees, palms and lianas (≥10 cm DBH). The results of this study showed significant differences in biomass for each type of forest (Table 1). We chose a threshold of 286 $Mg \cdot ha^{-1}$ to distinguish between degraded and sustainably managed or conserved forests. Mazzei et al. (2010) showed that undisturbed forests store on average 409.8 $Mg \cdot ha^{-1}$ in the Cikel Fazenda, located in the western part of the municipality (Fig 2.1). The mean AGB total lost under reduced-impact logging operations is 94.5 $Mg \cdot ha^{-1}$, which represents around 23% of biomass lost (Mazzei et al. 2010a). The

threshold is thus the percentage of biomass lost applied to the undisturbed primary forest biomass identified by RAS.

The aboveground vegetation that corresponds to the largest carbon storage compartment is very sensitive to the type of disturbance, with about a 40% of difference in ABG between mature forests and secondary forests. We used the RAS AGB dataset in shapefile format to calibrate the Random Forest model presented in Section 2.2.4.

Table 2.1 AGB collection data in the municipality of Paragominas (see Berenguer et al. 2014).

Forest Type	Mean AGB ($Mg \cdot ha^{-1}$)	Standard Deviation ($Mg \cdot ha^{-1}$)	No. of Plots
Undisturbed primary forest	371.8	96.9	13
Logged primary forest	229.5	79.2	44
Logged and burnt primary forest	145.8	73.4	44
Young secondary forest	1.1	0.5	2
Intermediate secondary forest	57.6	38.3	12
Old secondary forest	92.2	58.4	5
Abandoned plantation	54.1	/	1

2.2.3 Remote Sensing Multisource Data: Image Acquisition, Pre-Processing and Biophysical Indicators Variables Extraction

We used 38 indicators derived from passive (MODIS, Landsat-8) and active (ALOS-1, Sentinel-1) remote sensing sources. These indicators are correlated with different vegetation parameters such as photosynthesis activity and vegetation structure. All the satellite images used in this study are freely available and span the globe.

MODIS

To quantify forest canopy health and temporal dynamics, we used the enhanced vegetation index (EVI) from the MODIS sensor. EVI was extracted from the '16-Day L3 Global 250m product (MOD13Q1 c5)' from January 2001 to December 2014. EVI is directly related to photosynthetic activity (Huete et al. 2002). It does not saturate quickly for high values of chlorophyll activity and provides improved sensitivity for high biomass areas such as tropical forests (Gond et al. 2013). The 16-day composite was built by choosing within the 16 daily acquisitions the two pixels with the highest value of NDVI

(Normalized Difference Vegetation Index). Of these two values, the pixel with the smallest viewing angle was chosen in order to minimize the residual angle (Huete et al. 2002). A quality filter was then applied to the composite to remove clouds and reduce atmospheric contamination [38]. We extracted three indicators from this dataset: the mean and the standard deviation calculated for the whole time series based on annual average EVI and the pooled variance which is the weighted sum of annual variance based on the number of values available for each pixel for each year (giving more weight to the pixels that were not under cloud coverage during the 16 days × 14-year period).

$$\text{Pooled variance} = \frac{\sum_{i=1}^{14} Variance(i) \times available\ values(i)}{\sum_{i=1}^{14} available\ values(i) - 14} \quad (1)$$

These three indicators provide global information on the stability of the forest canopy photosynthetic activity.

Landsat 8

We used three Landsat 8 images taken during the dry season of 2014, at 30 m resolution. We acquired the surface reflectance data with the pre-processing already performed with the algorithm developed by the NASA Goddard Space Flight Center (GSFC). We used 5 spectral bands (blue, green, red, near-infrared and short-wave infrared) and we derived 13 indicators using the Orfeo toolbox (« Orfeo ToolBox – Orfeo ToolBox is not a black box »). We used the Carnegie Landsat Analysis System-lite (Claslite) to derive the Photosynthetic Vegetation (PV), Non Photosynthetic Vegetation (NPV) and Bare Soil indexes (Asner et al. 2009b).

ALOS-1 PALSAR

We downloaded seven images ALOS-1 PALSAR (L-band) taken in 2010 from the JAXA (Japan Aerospace Agency, http://www.eorc.jaxa.jp/ALOS/en/index.htm) platform. These images have 25-m spatial resolution (“ALOS-1 mosaic 25 m” product) and are dual-polarized (HH and HV). The incidence angle varies between 35° (near range) to 42° (far range). The images were correctly geo-referenced, so we only processed the conversion from digital raw number (DN) to gamma and sigma following these two equations (Mermoz et al. 2014; Shimada et al. 2014):

$$\text{gamma [dB]} = 10 \times log10(DN^2) - 83 \quad (2)$$

$$\text{sigma [dB]} = 10 \times log10(DN^2) - 83 + 10 \times log10(cos\theta) \quad (3)$$

We tested these two indicators, expecting a strong correlation between backscatter coefficients and aboveground biomass (Englhart and al. 2011).

Sentinel-1

We acquired one image Sentinel-1 (C-band, dual polarization VV/VH, descending pass direction) taken in May 2015, at 10-m resolution and in Interferometric Wide (IW) swath mode. We performed the pre-processing using the free software Sentinel Toolbox, which allows the derivation of backscatter coefficients and processing of the range Doppler terrain corrections using the 3 arc-seconds SRTM Digital Elevation Model. We derived 9 indicators from the grey level co-occurrence matrix (GLCM) that are based on the statistical relationship between the values of the pixels within a 9 × 9 pixels window (Ploton et al. 2017). These indicators are relevant to quantify forest canopy texture (Champion et al. 2014).

The source, description of the remote sensing images and the derived indicators are detailed in the Appendix 2.1.

2.2.4 Random Forest Regression Model

We used a random forest regression tree to explore the performance of the different remote sensing data sources and derived indicators for AGB modelling and mapping. Regression trees are particularly efficient for remotely sensed indicators that show unknown multivariate patterns and nonlinear relationships (Breiman 2001).

2.2.4.1. Data Preparation

We resampled the indicators at 20-m resolution using GRASS libraries and stacked them all together to make sure they are georeferenced in the same system. This resolution matches with the size of the plot measurements. For each indicator, we generated an automatic process to extract the mean and standard deviation within the extent of each plot. We then compiled all the data in a file with the identification of each plot (row 1 to 121) and the estimated AGB followed by the mean and standard deviation of the 38 indicators (columns). Finally, this dataset is randomly mixed to avoid any biases related to its original structure and is split into 10 folds (Fig 2.2). This number of folds (k) is often suggested in order to balance bias limitation (lower value of k) and variability (higher value of k) (Kohavi 1995).

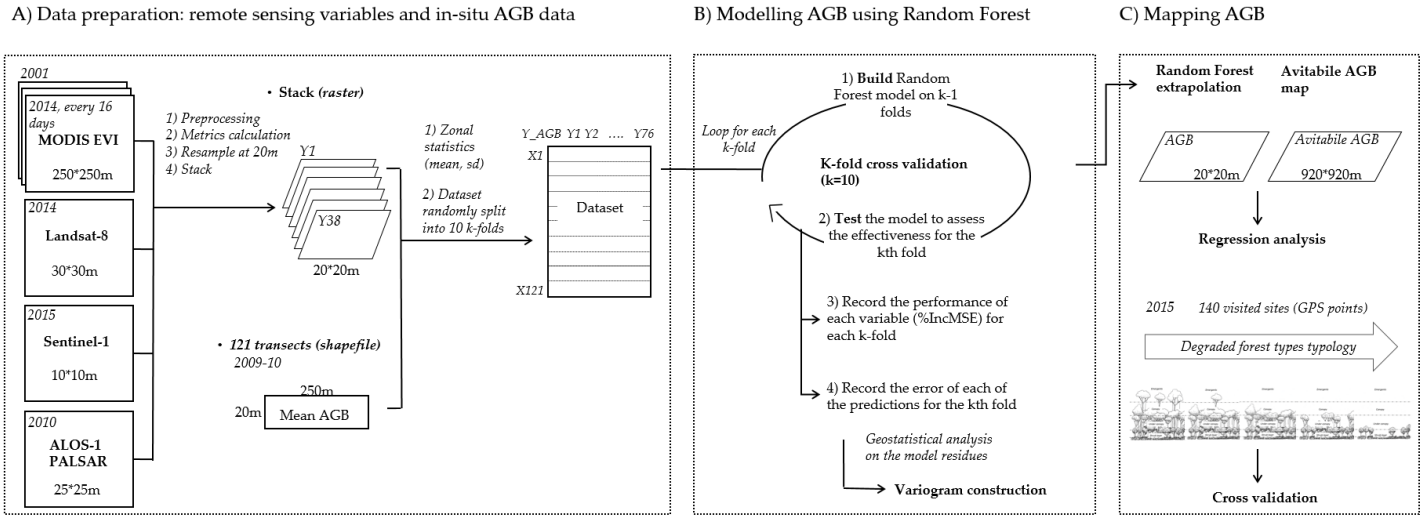

Figure 2.2 **Workflow of the evaluation of the indicators performance in AGB modelling and mapping.**

2.2.4.2. Modelling AGB with Random Forest

For each independent indicator, regression trees recurrently split the data into more homogeneous samples and identify the most significant indicator that gives best homogeneous sets of samples (Strobl et al. 2009). Random Forest grows multiple trees (500 trees in our study) by randomization of data subsampling in order to improve the predictive power of regression and to limit overfitting which is the most practical difficulty for decision tree models. Random forest provides for each independent indicator an increase in mean-squared error (Percentage of IncMSE), which quantifies how much MSE increases when that indicator is randomly permuted. This error measures the relative importance of each indicator, where a low IncMSE implies that the indicator does not have much weight on the model prediction and inversely (Mascaro et al. 2014). Random Forest is used as a regression and mapping tool, but also as an investigation tool to assess the importance of each indicator in the creation of the model and on its global error. Random Forest is used more and more to estimate carbon reservoirs and perform biomass regression (Asner et al. 2012; Goetz et al. 2009; Mutanga et al. 2012).

Due to the limited number of AGB plots, we used the k-fold cross validation technique to estimate regression performance (Kohavi 1995; Borra and Di Ciaccio 2010). This technique involves reserving a particular sample of the dataset on which the Random Forest model will be tested, while the rest of the dataset is used for training. For each of the 10 folds, the Random Forest model is trained on 9 folds (k - 1) and the 10th fold is used to test the model and check its effectiveness. This process goes through each of the 10 folds until each of the kfolds has served as a test set. After the end of each loop, we

record the percentage of IncMSE calculated for each of the 76 indicators and the predicted value of AGB. The average RMSE will serve as the performance metric for the model.

We finally invert the model using the values of the remote sensed indicators across Paragominas municipality to predict AGB.

2.2.5 Geostatistical Analysis of Random Forest Model Residuals

Geostatistical analysis is used to explore the spatial autocorrelation of the model residuals and evaluate whether model residuals data are independent (in the case of absence of autocorrelation) (Rossi et al. 1992). The presence of spatial autocorrelation or spatial structure of the model residuals would refer to any patterns of gradients or cluster within the data that the AGB Random Forest model would not have adequately been able to capture. To explore this spatial structure, we estimated an omnidirectional variogram at short distances (6 km) on Random Forest residuals, and we used the usual permutation test to compute a bi-lateral confidence band of pure spatial randomness (Gräler et al. 2016; Ribeiro and Diggle 2001).

2.2.6 Comparison with Avitabile et al. AGB Dataset

The available Avitabile et al. (2016) forest pantropical biomass map that displays aboveground biomass density in units of $Mg \cdot ha^{-1}$ at a 920-m spatial resolution was used to compare the spatial distribution of aboveground biomass of the degraded forest with the Random Forest predicted map. In the Amazon basin, the Avitabile AGB map provides lower RMSE and bias compared to the Baccini and Saatchi pantropical maps (Saatchi et al. 2011; Baccini et al. 2012; Avitabile et al. 2016). However, at the regional scale (e.g., Paragominas municipality), the Avitabile map can present error patterns because the quality reference data of the highly degraded forest were lacking and could not be used to calibrate the model (Avitabile et al. 2016).

2.2.7 Comparison with Degraded Forest Typology

To conduct a field validation of the predicted aboveground biomass values, we built a degraded forest typology based on the observation of 140 forest sites in May 2015. Each observation is associated with a GPS point (Garmin 60CSx, Garmin, Olathe, U.S), a description of the forest site and illustrative photos. We extracted the values of the predicted AGB at the location of each forest site. We finally used one-way ANOVA with post hoc Tukey tests to evaluate differences in predicted AGB between the different forest classes of the typology.

This typology is a result of the combination of in-situ qualitative indicators of forest degradation and semi-quantitative observations of the forest structure. First, we noted the presence or absence of fire and logging marks (burned trees, strains, trunks, logging trails), of pioneer species (mainly Cecropia species), which may indicate a recent opening of the canopy, and of trees with a diameter at breast height (DBH) greater than 80 cm. Then, we measured canopy height and the number of vegetative strata using a laser rangefinder and estimated the forest canopy texture (roughness) and the percentage of gaps between emergent trees. These four forest structure indicators provide relevant information on the vertical and horizontal process of forest degradation.

In order to make the typology representative of the diversity of degraded forest types (conserved, legally logged, illegally logged and/or burned), we made sure that the sampling covered the different forest landscapes and main zoning that can be found in Paragominas (see Fig 2.1).

2.2.8 Computational Aspects

Except for the statistics performed with the software ArcGIS (Esri, Redlands, U.S), all developments were programmed under the R environment. We used the Raster, Random Forest, shapefile, rgdal, geoR and gstat packages (Breiman 2001; Ribeiro and Diggle 2001; « CRAN - Package gstat ».; « CRAN - Package raster »; Stabler 2013; Bivand et al. 2019).

2.3 Results

2.3.1 Model and Indicator Performance

The mean variance explained by the random forest model is 28%, with a root mean squared residual error (RMSE) of 97.1 Mg·ha^{-1}. Depending on the AGB calibrated data and the associated remotely sensed indictors, the random forest model performs differently with an explained variance that ranges between 24% and 30% and an RMSE that ranges between 75.7 and 101.2 Mg·ha^{-1} (Table 2.2).

Table 2.2 Random Forest model performance (mean squared residuals and percentage of variance explained for each of the 10 k-fold random forest models).

Random Forest kfold [1]	1	2	3	4	5	6	7	8	9	10	Average
Mean of squared residuals (Mg·ha^{-1})	97.8	95.5	100.5	91.8	99.6	100.3	93.9	75.7	97.8	101.2	97.1
Percentage of variance explained	26	24	25	30	26	22	27	30	26	25	28

[1] Number of Trees: 500, No. of Indicators Tried at Each Split: 25

Six indicators (out of the 76) contribute the most to the 10 regression models, showing the highest and most stable IncMSE scores (Fig 2.3). Three are derived from MODIS: mean of annual standard deviation EVI, mean and standard deviation of annual mean EVI and three from Landsat: mean infra-red (MIR), mean and standard deviation of bare soils.

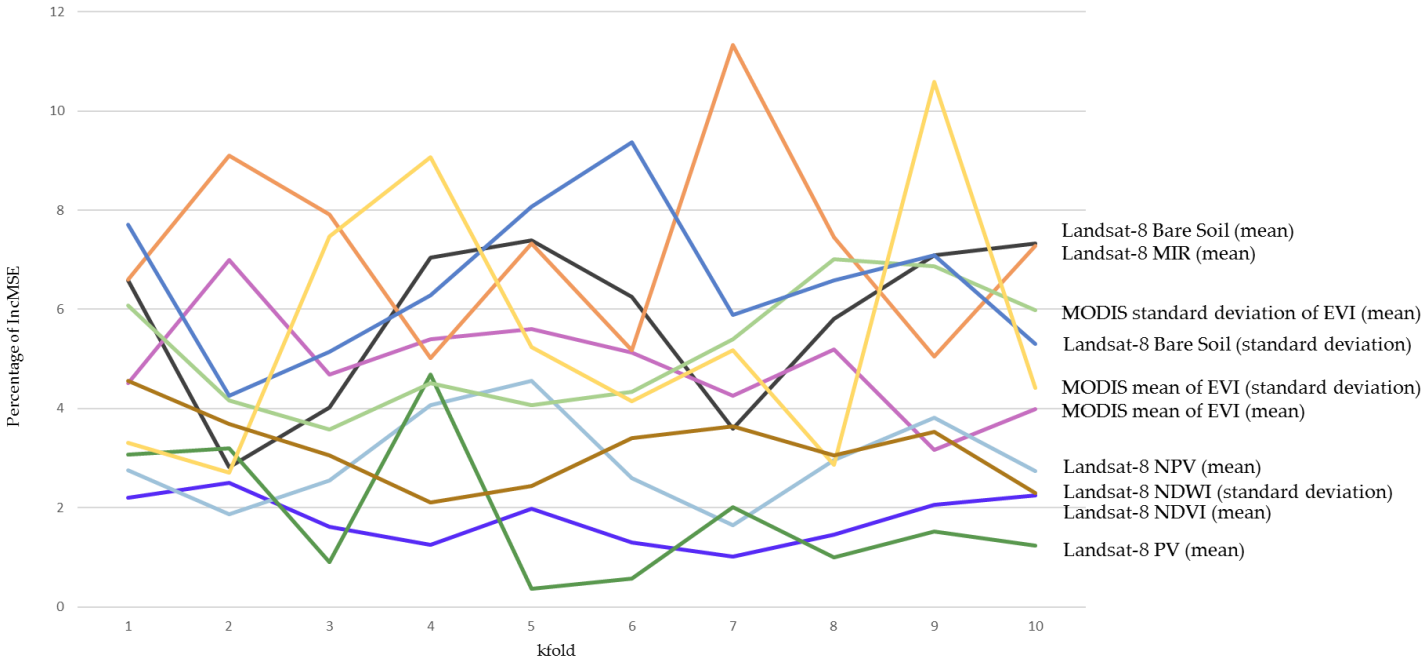

Figure 2.3 Explained indicator performance (Percentage of IncMSE) of the Random Forest model.

2.3.2 Geostatistical Analysis of Random Forest Model Residuals

The main spatial variability in the AGB data was captured by the Random Forest model, and no additive spatial variability can be explained through model residual interpolation. Figure 2.4 shows a flat empirical variogram contained within the confidence band which validates the absence of spatial structure within the Random Forest model residuals. We found similar results at smaller (0 to 1500 m) and larger (0–200,000 m) spatial scales. The distribution of the residuals shows an overall overestimation (high frequency of positive values, Fig 2.4B), which is important to consider when predicting AGB for the Paragominas municipality.

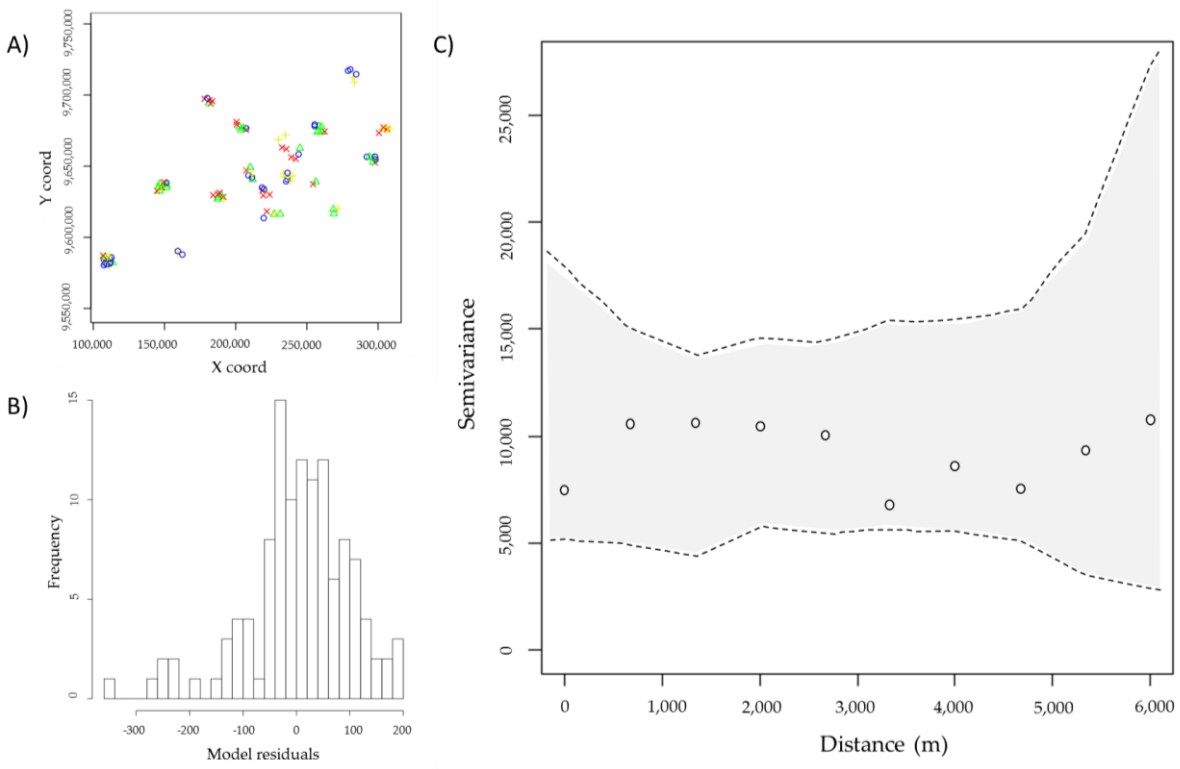

Figure 2.4 (A) Spatial distribution of the model residuals (blue, green, yellow and red colors for the respective four quartiles); (B) Histogram of the model residuals; (C) Variogram of biomass model residuals (The grey shape shows the confidence band interval expected for each distance class).

2.3.3 Above Ground Biomass Map

The range of AGB predicted values was large, spanning from 57 to 454 Mg·ha^{-1}. AGB was unequally spatially distributed over the municipality (Fig 2.5). The forests in the 80-km-wide central corridor have the lowest AGB values and are highly fragmented. The forests in the far-eastern and western part of the municipality contain the highest AGB. The percentage of degraded forest (below the threshold of 286 Mg·ha^{-1}, see Section 2.2.2) reached 87%.

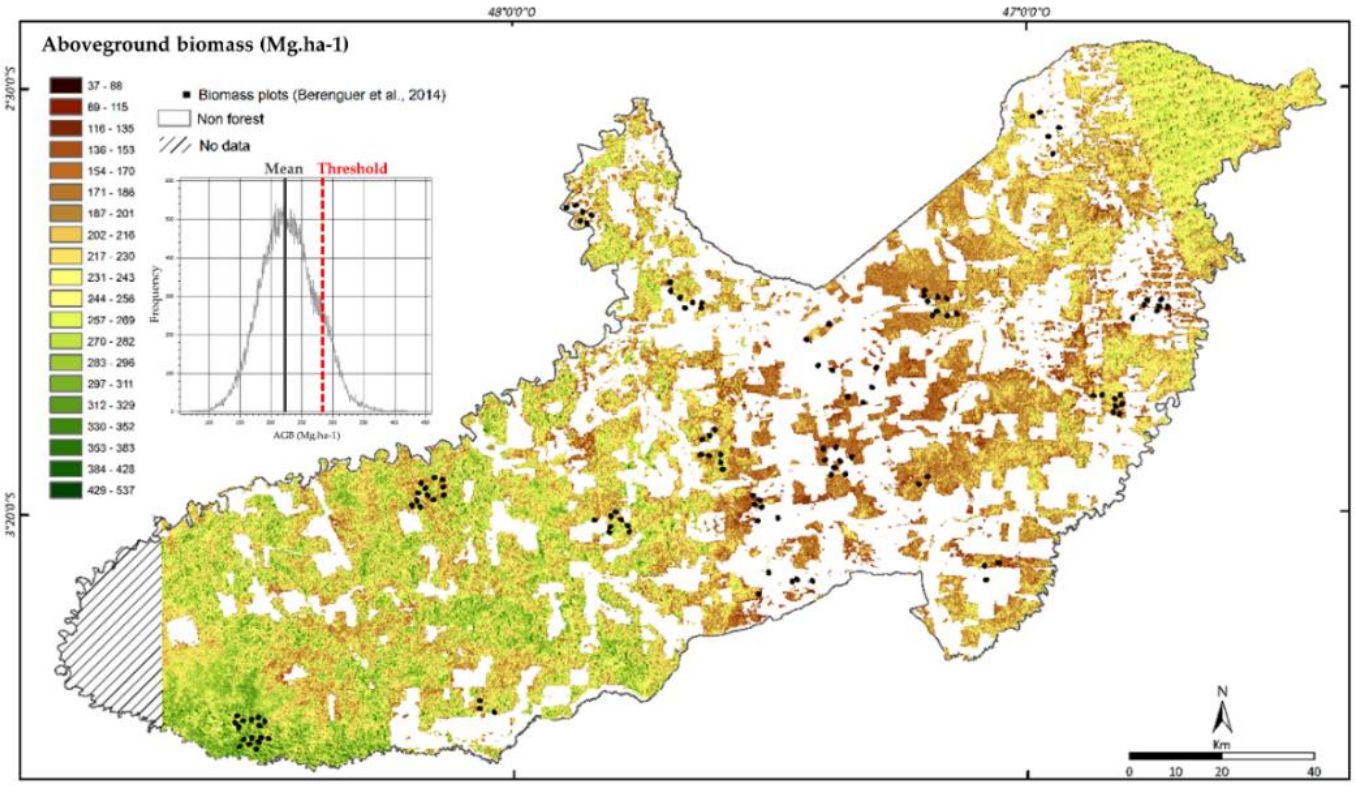

Figure 2.5 Random Forest predicted values of Aboveground Biomass across Paragominas municipality. In the western part of the municipality (stripped area), Sentinel-1 data was not available.

2.3.4 Comparison with Avitabile Pantropical Biomass Map

Figure 2.6 shows that our Random Forest model is more accurate than the Avitabile AGB map (R^2 higher and RMSE lower). The two models tend to overestimate for values of AGB lower than 200 $Mg \cdot ha^{-1}$ and underestimate for values higher than 300 $Mg \cdot ha^{-1}$. Despite the fact that the Random Forest has a higher explained variance and lower RMSE, the Avitabile dataset has a better potential to capture the large variability of AGB, particularly for extreme values where the dispersion follows the identity line. Random forest data are overall less scattered than Avitabile but display a much lower deviation between estimated and observed AGB for values from 100 to 300 $Mg \cdot ha^{-1}$ (Random Forest R^2 = 0.28, Avitabile R^2 = 0.14). This result is particularly interesting in the case of degraded forests where biomass values are contained within this window (Table 2.1).

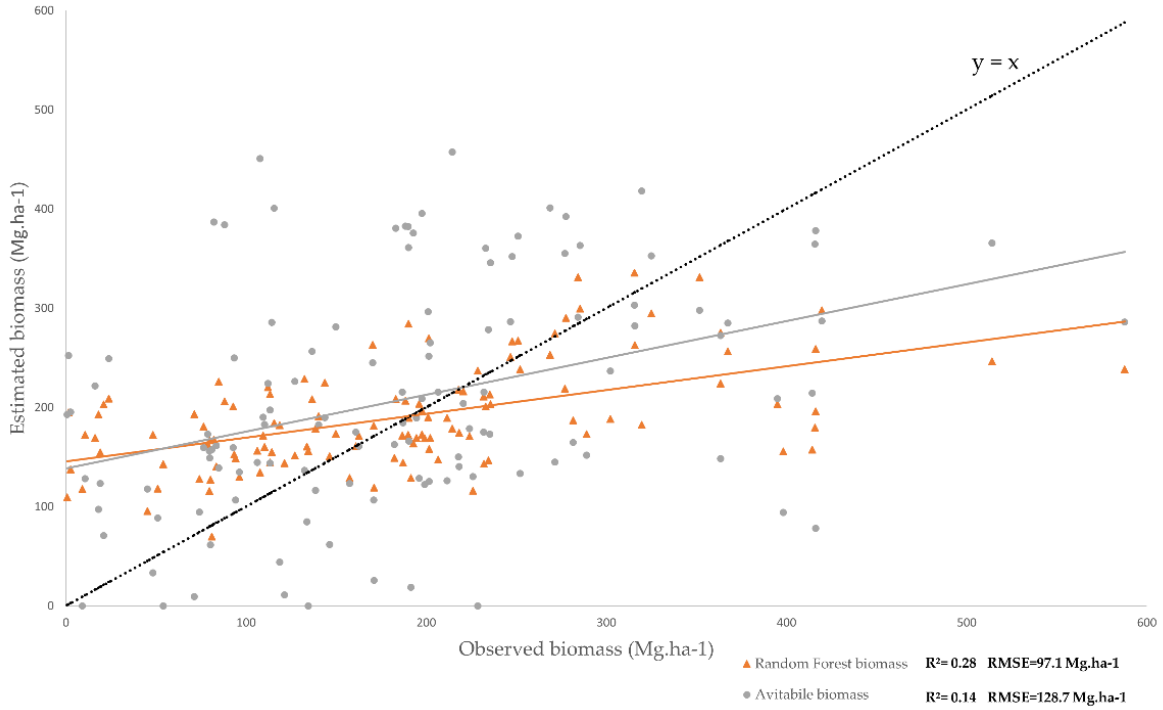

Figure 2.6 Observed (see Section 2.2.2.) and estimated biomass from Avitabile [23] and the Random Forest model.

The Avitabile map is less detailed than the Random Forest biomass map. It can be explained by the difference of spatial resolution between the two datasets and also the contribution of local remotely sensed indicators. After aggregating the Random Forest biomass map at the resolution of Avitabile's (Fig 2.7(3)), the difference between these two datasets shows similar AGB estimation in non-degraded areas and an overestimation of AGB values in degraded (logged) forests for Avitabile's dataset (differences lower than −100 Mg·ha^{-1}). The Random Forest map captures small-scale forest disturbances such as roads, i.e., skids trails and log-landing areas and canopy gaps (pictures 1 and 2). It also displays lower biomass values around the areas impacted by selective logging. These finely detailed forest disturbances are not translated into the 920-m resolution Avitabile map. In this figure, we can see that the forest-non forest transition is much better detailed with the Random Forest map than with Avitabile maps. The transect (Figure 2.7(4)) and the map show that the north forest edge is more degraded (probably burned with agriculture encroachment) than the south edge where the transition between the two land uses is much clearer and sharper (Transect A–B, see Figure 1 for its location). At this local scale, Avitabile data appear to stretch the values of AGB and thus smoothen the distribution of AGB in transition areas.

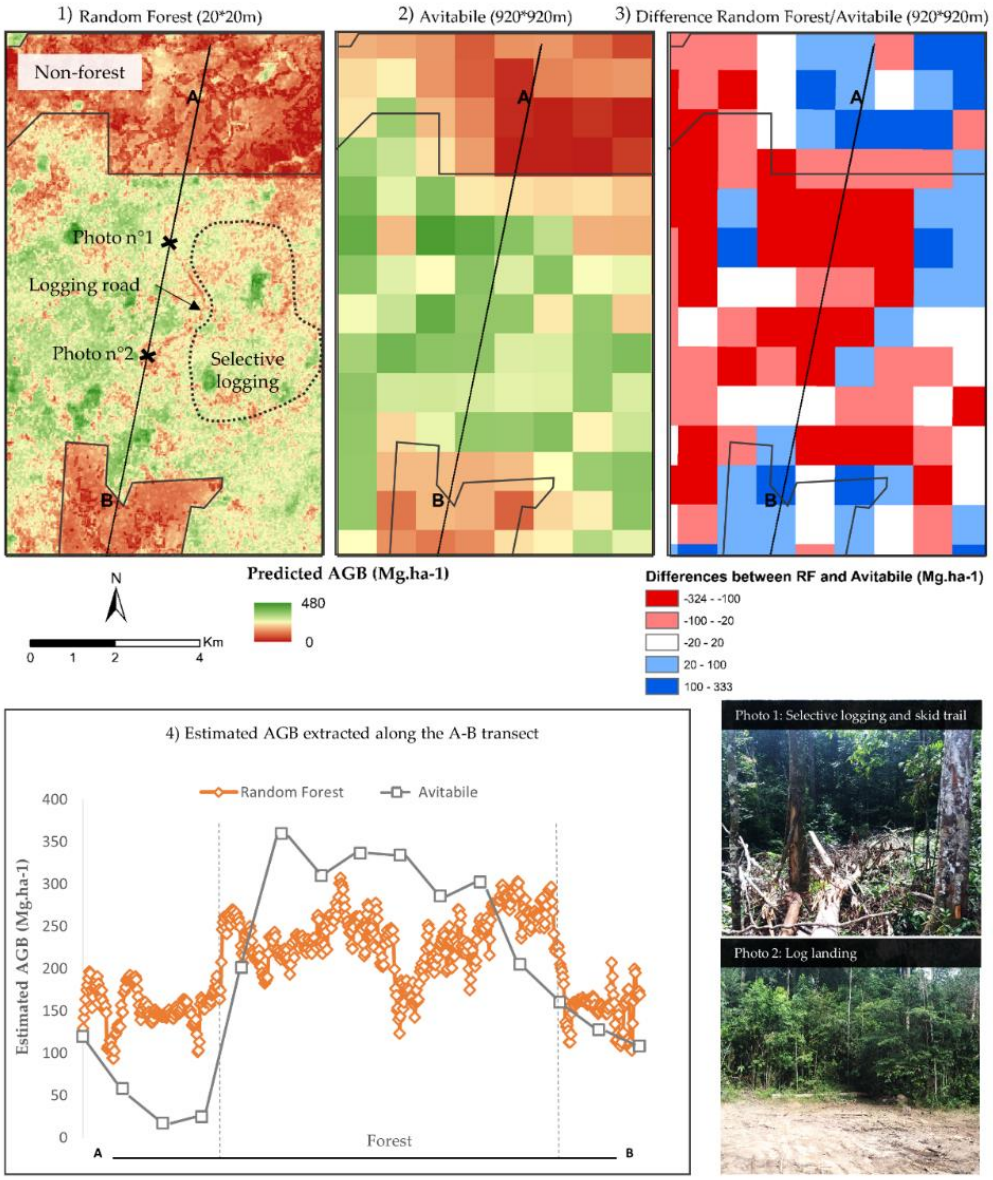

Figure 2.7 Comparison of AGB estimations, Random Forest, Avitabile (2016) and the difference map (1–3 respectively) in a selected zone representing the transition between non-forest to forest area (see Figure 1 for precise location in Paragominas). The selective logging area and the logging road were validated during the field trip.

2.3.5 Comparison with Degraded Forest Typology

The less degraded forest type (type F1) presents a closed canopy above 35 m, no signs of human impact and 4 vegetative strata defined as follows: the shrub layer below 5 m, the under canopy layer located around 15 m, the canopy layer at 25 m and the emergent layer that goes beyond 35 m. The most valuable tree species harvested first are the emergent trees with a large diameter (higher than 80 cm). This selective logging can cause small degradation vertically, with an impacted and lower canopy and

also horizontal damages generated by the extraction of the tree (type F2). When the selective logging becomes more intense (type F3), all the trees taller than 35 m and larger than 80 cm diameter are harvested, which causes a lowering of the canopy line at 25 m and big gaps inside the forest structure with the presence of skid tracks, broken and unrooted trees, log landing and other logging roads. Consequently, the degraded forest is much more sensitive to drought and fires, which can lead to severe disturbance, lowering the canopy at 15 m with only two remaining vegetative strata. This degraded forest type (F4) is often characterized by a high density of vegetative regrowth (pioneers species). Trees with DBH less than 80 cm are also harvested which causes an opened and destructed canopy. Finally, the intensification of fire leads to the most degraded type (F5) with only the shrub layer remaining and a few trees from the under canopy layer (Figure 2.8).

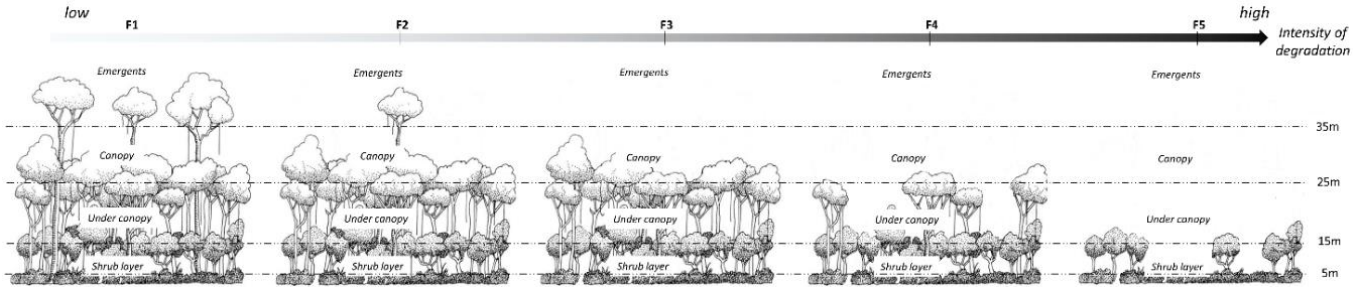

Figure 2.8 Five classes of degraded forest typology based on the observation of 140 forest sites in May 2015.

The typology of the degraded forest allows us to evaluate the relevance of the regional forest AGB mapping at the stand scale. The boxplots of Figure 2.9 show a relationship between the intensity of degradation identified in the field and the Random Forest prediction. We can assume the homogeneity of variances in the five degraded forest types (p-value = 0.09 > 0.05). Among the five types, only type F1 is significantly different from the other types F2, F3, F4, F5 (ANOVA test with p-value < 0.05). Degraded type F1 presented the highest values of AGB (average of 270 $Mg \cdot ha^{-1}$). Types F2, F3, F4, F5 had statistically similar values of AGB (200 $Mg \cdot ha^{-1}$), although we found a decreasing trend in the mean predicted AGB.

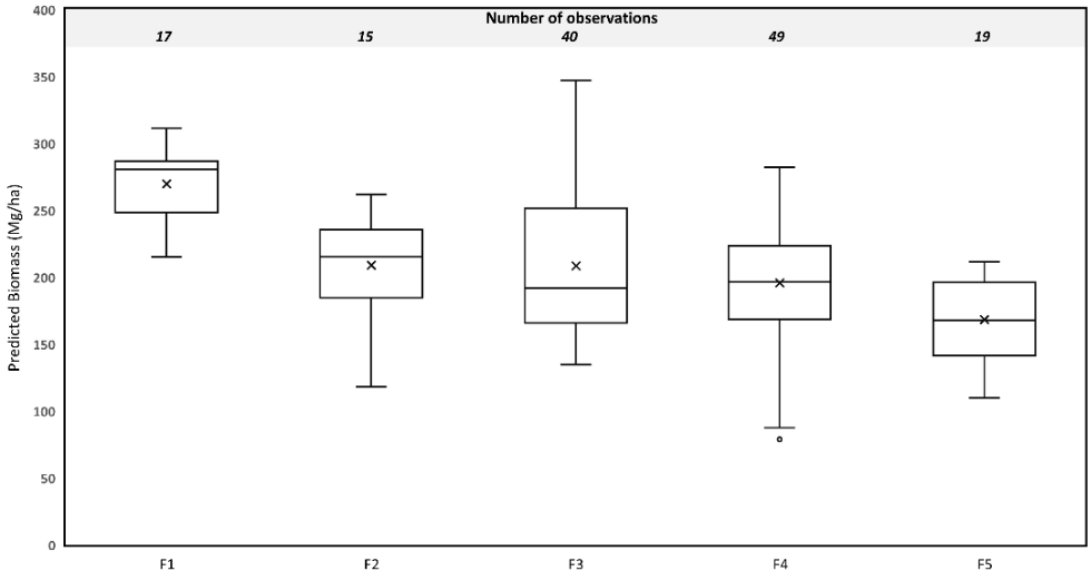

Figure 2.9 Boxplots of predicted values of AGB calculated for the five-class typology of degraded forest with the range (1st and 3rd quartile), the mean (line) and the median (cross).

2.4 Discussion

In this paper, we propose a novel approach to model and map AGB of degraded forests at the regional scale, which provides more detailed and accurate information than the pantropical dataset. We demonstrated that the model captures all spatial variability of the AGB data and identified the most robust remotely sensed indicators. Besides the model bias in underestimating AGB values greater than 300 $Mg \cdot ha^{-1}$, this AGB map constitutes key spatial information for the future management of degraded forest.

2.4.1 Model Performance Analysis

Extraction and selection of suitable indicators from remote sensing and future promising development in AGB mapping

There is a need to rank and prioritize the most suitable indicators to characterize degraded forests from multisource remote sensing (Hirschmugl et al. 2017; Herold et al. 2011; Mitchell et al. 2017; De Sy et al. 2012). Our results show that Landsat spectral unmixing bare soil, mid infrared and MODIS EVI standard deviation from the 2001 to 2014 time series were the most suitable indicators to model AGB and are the less data input driven. These indicators thus have the highest potential to map AGB. Unmixing approaches did perform well in our case, which confirms reports of other authors (Souza et

al. 2013; Tritsch et al. 2016) within the Amazon forest landscape. The bare soil Landsat indicator best translates the proportion of bare soil within a 30 × 30 m Landsat pixels while mid infrared is sensitive to humidity and therefore to forest structure and functioning (Hirschmugl et al. 2017). These results are coherent with the degradation process happening in the Paragominas forest. The emergent and most valuable trees are targeted first through legal and illegal selective logging which triggers a vertical and horizontal opening of the canopy (Ferreira et al. 2015). This type of degradation directly affects the internal forest structure, which leads to forest drying and a decrease in the local forest evapotranspiration and photosynthetic activity. Another degradation type is located along forest edges, which are always very degraded and impacted by local drying effect, fire or slow encroachment due to agriculture expansion (i.e., swidden agriculture)(Briant et al. 2010). The MODIS compiled standard deviation of EVI represents the stability over time of the annual mean EVI and thus annual photosynthetic activity. A drop in this activity in one particular year will lead to a high standard deviation value and information on potential degradation activity (Briant et al. 2010).

The other indicators have a much lower performance score, which indicates a lower sensitivity to the AGB range of values. The usual vegetation indices extracted from Landsat such as NDVI or SAVI are not sensitive enough for AGB of degraded forests. This may be related to the over saturation of the signal in the case of a tropical forest canopy and the measured photosynthesis activity, which do not allow differentiation between two types of degraded forests (Huete et al. 2002).

For radar data, one single data and related derived indicators (intensity coefficients and texture) are not sensitive enough to model AGB. To further develop this modelling approach, radar needs to be used as time series data, which would provide better information on the forest canopy status. Further investigation is also required on the preprocessing steps (e.g., filtering noise method) and on the derived texture indicators. To the extent of our knowledge, degraded forest structure and status remain understudied, with a lot of technical aspects (frequency of the time series, spatial resolution, polarizations, incident angles and frequency bands) that need to be tackled (Trisasongko 2010; Deutscher et al. 2013; Solberg et al. 2013).

The integration of Sentinel-1 and Sentinel-2 time series would be an interesting way to improve the model performance combined with daily Planet images that can map at 3-m resolution the forest canopy. Very high resolution remote sensing offers a unique opportunity to characterize degraded forest structure using canopy texture mapping (Ploton et al. 2017; Barbier et al. 2010). These analysis provide perspective for future space-borne LIDAR and RADAR data satellites (US GEDI mission and ESA Biomass) which will enable us to provide data sets on forest structure dynamics and forest biomass around the pantropical belt (Le Toan et al. 2011).

Identification of proper algorithms to develop biomass estimation models and their related uncertainty analysis

Although the model is robust because it has been trained and tested 10 times on independent and randomly selected datasets, we identified three potential error sources. First, the limitations can be linked to the large diversity of degraded forest types that are modelled and the limited number of ground truth data. More in-situ AGB data would help to train the model on large portion of the data set and better capture its underlying trend (Guitet et al. 2015). Then, a certain time gap between the collection of AGB and the remote sensing data needs to be noted and accounted. This gap is due to remote sensing data quality and availability and can be up to 5 years in the case of Sentinel-1 images. In the case of MODIS time series, there is also a temporal gap as we modelled single date forest status (i.e., AGB) with temporal indicators that are sensitive to photosynthetic activity dynamics. These temporal mismatches could introduce some uncertainty in the model. However, in light of the minimal increases in AGB within burned and illegally logged forests (representing 88 out of 121 field plots) over a five-year period, we do not consider this uncertainty to be meaningful (Blanc et al. 2009). Finally, the resampling of the remote sensing indicators to a higher resolution (20 m resolution) may introduce bias referring to the "ecological fallacy" problems (Robinson 2009). These problems are recurrent in the aggregation/disaggregation of remote sensing data and could be minimized by adapting the field collection protocol to the remote sensing data.

Despite these limitations and the low variance explained, we demonstrated that all spatial variability of the AGB data has been captured by the model through its input indicators. This gives interesting insights into how to improve local models to characterize degraded forests using biomass and how to quantify the influence of input indicators on the final modelling result.

Comparison with existing AGB maps

When comparing with pantropical datasets such as the Avitabile AGB map, we noted differences in the statistical accuracy with local AGB datasets and in the levels of details which are particularly important for degraded forest biomass mapping. Avitabile data do not capture all the details of local AGB distribution in small-scale degraded and complex mosaic forest due mainly to their coarse spatial resolution. Transition zones from forest/non-forest areas are better and more precisely described using local trained models, where logging roads, degraded forest edges and other distribution are mapped.

2.4.2 AGB Spatial Distribution in the Municipality

In the map produced, the spatial distribution of AGB varies depending on land-uses and landscape organization (Laurent et al. 2017). Degraded forests are dominant in the Paragominas forest landscape. The central corridor is a mosaic of agricultural lands (agribusiness) dominated by large-scale soybean cultivation and pasturelands and with fragmented patches of degraded forests. Forest biomass values range between 100 to 150 $Mg \cdot ha^{-1}$ with the lowest values within the first 200 m of forest edge which is consistent with previous studies (Briant et al. 2010). Forest fragmentation is even more important in smallholder areas (see Fig 2.1) where population density is high. These areas were major charcoal production hotspots (prohibited since 2008), which caused severe impacts on the forest resource. The transition between these areas and the indigenous protected reserve is sharp within the forest AGB values (with AGB higher than 250 $Mg \cdot ha^{-1}$ in the reserve).

2.4.3 Characterization of Degraded Forests

From a field point of view, degraded forests are a gradient of forest types marked by a certain canopy height and forest structure that vary depending on the intensity of past degradation trajectories. The five-class typology does not represent all the complexity of degraded forests but remains relevant in terms of modelled forest biomass. Besides the fact that only type F1 was significantly different from the four others, we found an interesting trend in the modelled biomass that requires further investigation. Type F3 presented the highest variability, which could be linked with an over-evaluation of the level of degradation in the field and the disproportionate size sample of this class. Type 5, the most degraded stage, presents the lowest predicted biomass (around 150 Mg·ha). These findings accord with those identified by the RAS team during the collection of in-situ AGB data (Table 2.1). This typology based on the observation of structural parameters (canopy height, number of vegetative strata, canopy rugosity, presence of emergent trees) constitutes a first step in the characterization of degraded forests which could help in the calibration and validation of other forest biomass and carbon stock assessment or the monitoring of forest degradation (Mitchell et al. 2017; DeVries et al. 2015). It also summarizes a one-shot time visualization of the status of degraded forests. From this, the next priority is to monitor the dynamics of degraded forest status over time using time series remote sensing (DeVries et al. 2015).

2.4.4 How Can These Data Be Useful for Forest Management at the Regional Scale?

Besides the limitations of the proposed modelling approach and the evaluated bias, we showed the importance of regional AGB mapping in Paragominas human-modified forest landscapes, in particular with the capacity to identify patterns of different forest status values linked with degradation and agricultural activities at the regional scale. This agricultural frontier is characterized by fragmented forest impacted by the accumulation of small-scale human disturbances that cannot be captured by pantropical databases, by forest field inventories or by high detailed/low extent coverage remote sensing sources (LIDAR).

In the context of zero deforestation commitment, this forest AGB modelling and mapping is particularly important in order to provide to decision makers with spatially detailed information on the status of the 50% remnant forest (« Climate-KIC | The EU's main climate innovation initiative »; « Observatory of the dynamics of interactions between societies and environnement in the Amazon, ODYSSEA »). The agricultural expansion over forest areas is now severely restricted (Piketty et al. 2015). Hence, the sustainable management of degraded forests is becoming a priority in order to enhance forest resources at different levels of disturbance (Goldstein 2014) as much as the urgent obligation to prevent further degradation. The quantification of the forest status and the understanding of the drivers of degradation are necessary in order to improve the management of forest landscape.

2.5 Conclusion

In this chapter, we proposed a rigorous evaluation of the potential of optical (Landsat-8, MODIS) and radar (Alos-1, Sentinel-1) remote sensing sources in modelling and mapping aboveground biomass of degraded forests. We combined a large dataset of plots providing abovegound biomass data with diverse remotely sensed indicators in a Random Forest model. The two major results we presented in this chapter are highly significant. First, our model captures all spatial variability of the biomass data. Second, the map produced for the municipality of Paragominas provides more detailed and accurate information than the only pantropical map proposed by Avitabile (2016).

However, the large range of forest structures spanning from conserved to highly degraded was not entirely captured by the models. There is a need to better understand how forest degradation changes forest structures. Current degraded forest structures are the result from long-term accumulation of disturbances of varying intensity and frequency. In this sense, Chapter 3 proposes a zoom from regional scale to forest stand scale to better understand the interactions between degradation and forest structures. This chapter relies on canopy texture analysis and data derived from unmanned aerial vehicule (UAV) and 33 years of Landsat archive.

Chapter 3 - UAV-based canopy textures assess changes in forest structure from long-term degradation

Understanding present situation to reconstruct the past: while both forest patches showed similar degraded structures, the fire following the 2015 El Niño event radically modified the structure of one patch but its propagation was stopped by the road (picture by Clément Bourgoin)

Reproduced from the article:

Bourgoin C., Betbeder J., Couteron P., Blanc L., Dessard H., Oszwald J., Le Roux R., Cornu G., Reymondin L., Mazzei L., Sist P., Läderach P., Gond V. (2019 submitted) UAV-based canopy textures assess changes in forest structure from long-term degradation. Ecological Indicators.

UAV-based canopy textures assess changes in forest structure from long-term degradation

Bourgoin C.[1,2,3], Betbeder J.[1,2,4], Couteron P.[5], Blanc L.[1,2], Dessard H.[1,2], Oszwald J.[6], Le Roux R.[1,2], Cornu G.[1,2], Reymondin L.[3], Mazzei L.[7], Sist P.[1,2], Läderach P.[3] and Gond V.[1,2]

1 CIRAD, Forêts et Sociétés, F-34398 Montpellier, France
2 Forêts et Sociétés, Univ Montpellier, CIRAD, Montpellier, France.
3 International Center for Tropical Agriculture (CIAT), Hanoi, Vietnam
4 Ecosystems Modelling Unity, Forests, Biodiversity and Climate Change Program, Tropical Agricultural Research and Higher Education Center (CATIE), Turrialba, Cartago, Costa Rica
5 UMR AMAP-IRD, Montpellier, France
6 UMR CNRS LETG 6554, Laboratory of Geography and Remote Sensing COSTEL, Université de Rennes 2
7 EMBRAPA Amazônia Oriental, Trav. Dr. Enéas Pinheiro, Bairro Marco, CEP, 66095-903 Belém, Pará, Brazil

Abstract

Degraded tropical forests dominate agricultural frontiers and their management is becoming an urgent priority. This calls for a better understanding of the different forest cover states and cost-efficient techniques to quantify the impact of degradation on forest structure. Canopy texture analyses based on Very High Spatial Resolution (VHSR) optical imagery provide proxies to assess forest structures but the mechanisms linking them with degradation have rarely been investigated. To address this gap, we used a lightweight Unmanned Aerial Vehicle (UAV) to map 739 ha of degraded forests and acquire both canopy VHSR images and height model. Thirty-three years of degradation history from Landsat archives allowed us to sample 40 plots in undisturbed, logged, over-logged and burned and regrowth forests in tropical forested landscapes (Paragominas, Pará, Brazil). Fourier (FOTO) and lacunarity textures were used to assess forest canopy structure and to build a typology linking degradation history and current states. Texture metrics capture canopy grain, heterogeneity and openness gradients and correlate with forest structure variability (r^2: 0.58). Similar structures share common degradation history and can be discriminated on the basis of canopy texture alone (accuracy: 55%). Over logging causes a lowering in forest height, which brings homogeneous textures and of finer grain. We identified the major changes in structures due to fire following logging which changes heterogeneous and intermediate grain into coarse textures. Our findings highlight the potential of canopy texture metrics to characterize degraded forests and thus be used as indicators for forest management and degradation mitigation. Cheap and agile UAV open promising perspectives at the interface between field inventory and satellite characterization of forest structure using texture metrics.

Keywords Canopy structure, Forest degradation, Remote Sensing, Texture, Tropical forest, Unmanned Aerial Vehicle.

3.1 Introduction

Forest degradation is a threat (Potapov et al. 2017) to the provision of ecosystem services by tropical forests. Degradation causes loss of biodiversity through habitat disturbance and fragmentation (Barlow et al. 2016; Broadbent et al. 2008), erosion of hydrological and soil properties, the reduction of non-timber forest resources (Lewis et al., 2015; Thompson et al., 2009), and currently accounts for 68.9% of overall carbon losses from tropical forests (Baccini et al. 2017).

The accumulation of forest disturbances such as selective logging and understory fires affects the states of the forest by destroying the canopy and the internal structure without triggering any changes in land use (Ghazoul and Chazdon 2017b; Putz and Redford 2010b). Degraded forests are therefore the consequence of complex degradation and recovery processes, which creates a gradient of varying structures within the forest landscape (Chazdon et al. 2016; Malhi et al. 2014).

Measuring the current forest structure and its degree of degradation are crucial for effective but sustainable management of degraded forests to guarantee the conservation, management and betterment of their ecological values (Goldstein 2014).

However, the identification, characterization and measurement of forest degradation remains a scientific challenge, in particular in the remote sensing community (Frolking et al. 2009; Herold et al. 2011; Hirschmugl et al. 2017; Mitchell et al. 2017a). Among the wide range of remote sensing approaches, optical time series of high resolution Landsat images have been used to derive forest states indicators and to reconstruct forest degradation history through the detection and quantification of disturbances within the canopy (Asner et al., 2009; Bullock et al., 2018; DeVries et al., 2015; Souza et al., 2013). These approaches are steps towards degradation monitoring and informing Reducing Emissions from Deforestation and Degradation (REDD+) systems (Goetz et al. 2014) but do not provide quantitative information on the forest structure which is directly related to carbon stocks. Airborne Light Detection and Ranging (A-LiDAR) is the most successful technique to retrieve three-dimensional forest structural parameters and estimate aboveground biomass (AGB) stocks (Asner et al. 2012; Longo et al. 2016; Rappaport et al. 2018) but the data are often costly to acquire and to replicate both in space and over time (Silva et al. 2017).

In addition to the spectral properties of optical remote sensing, Very High Spatial Resolution (VHSR) sensors also acquire information on the distribution of dominant tree crowns that define the forest canopy and also canopy gaps, thereby providing important indirect indicators of forest three-dimensional structure (Meyer et al. 2018). The spatial distribution of trees, the shapes and dimensions

of their crowns and the characteristics of the inter-crown gaps interact to define the forest canopy grain and can be assessed through canopy texture analysis (Couteron et al., 2005). Several authors have demonstrated the potential of texture methods to characterize VHSR canopy images (Couteron et al., 2005; Frazer et al., 2005). Among them, the FOurier-based Textural Ordination (FOTO) method has been used in a variety of tropical forests to characterize gradients of canopy grain, heterogeneity and crown size distribution (Barbier et al., 2010; Bastin et al., 2014; Couteron et al., 2005; Ploton et al., 2012; Singh et al., 2014). Case studies have shown that FOTO indices can correlate with forest structural parameters along gradients of natural variation (Couteron et al. 2005) of degradation (Ploton et al. 2012; Singh et al. 2014) or in landscapes mixing both (Bastin et al. 2014; Pargal et al. 2017). Other approaches to texture such as the lacunarity spectra also capture spatial heterogeneity of forest canopies and provide a quantitative measure of canopy 'gapiness' that correlates with canopy cover and gap fraction (Frazer et al. 2005; Malhi and Román-Cuesta 2008; Ploton et al. 2017). However, the possible links between canopy texture and forest structure parameters are context dependent (Ploton et al. 2017), and relationships have to be verified and calibrated using reference data from either field plots or airborne canopy altimetry, and such data are not available in many tropical landscapes or regions. Moreover, one cannot expect the variety of stand structures generated by degradation processes to display unequivocal relationships with canopy texture variables (Rappaport et al. 2018). For instance, severe degradation may result in coarse texture (e.g. because of big gaps) as well as fine-grained aspects owing to small crowns in regenerating patches. In this sense, there is a lack in understanding and quantifying the consequences of forest degradation on canopy texture. Using unmanned aerial vehicles (UAV), the aim of this paper is to demonstrate that texture information can efficiently characterize degraded forest types. UAVs are thus a new promising tool to acquire altimetry data and very high resolution images of the canopy (Koh and Wich 2012; Zhang et al. 2016).

Here, we used very high resolution UAV images to sample a broad range of degraded and intact forests conditions in an old deforestation pioneer front of the Brazilian Amazon. For each forest site, we combined degradation history from Landsat time series with UAV data including canopy elevation and grey-level images. Our large-area and diverse UAV coverage addressed two questions: (1) How do canopy textures correlate with forest structure parameters within a large range of degraded forest types? (2) How do disturbance type and frequency contribute to variability in texture metrics through heterogeneity, coarseness and openness canopy gradients?

In so doing, our study aims to pave the way for interpreting canopy texture in VHSR satellite images from agile UAV-based ground truthing and consequently help decision makers improve the management of degraded forests.

3.2 Materials and Methods

3.2.1 Study area

The study was carried out in the municipality of Paragominas, located in the northeastern part of the State of Pará, Brazil, and covered an area of 19,342 km² (Fig 3.1). The municipality experienced different colonization processes since its foundation in 1965, which led to significant deforestation with conversion of land to pasture for cattle ranching and forest degradation through overexploitation of timber. Deforestation was accentuated by the grain agro-industry in the 2000s, dominated by intensive soybean and maize cultivation mainly in the center of the municipality (Piketty et al., 2015). We demonstrated in previous studies that the history and processes of colonization spatially differ within Paragominas (Laurent et al. 2017). This led to a mosaic of forests in very different cover states within heterogeneous landscape mosaics dominated by different land uses (Bourgoin et al. 2018; Mercier et al. 2019). In this region, forest management plans with selective logging (SL) have rarely been adopted except in CIKEL Brasil Verde Madeiras Ltda forestry company (Mazzei et al. 2010b). Forest suffered from two major anthropogenic disturbances. Unplanned logging with over logging (OL) intensity is marked by repeated frequencies over time. Fire alters deeply the understory and generate high mortality rates for canopy trees (Fig 3.1)(Hasan et al. 2019a; Tritsch et al. 2016).

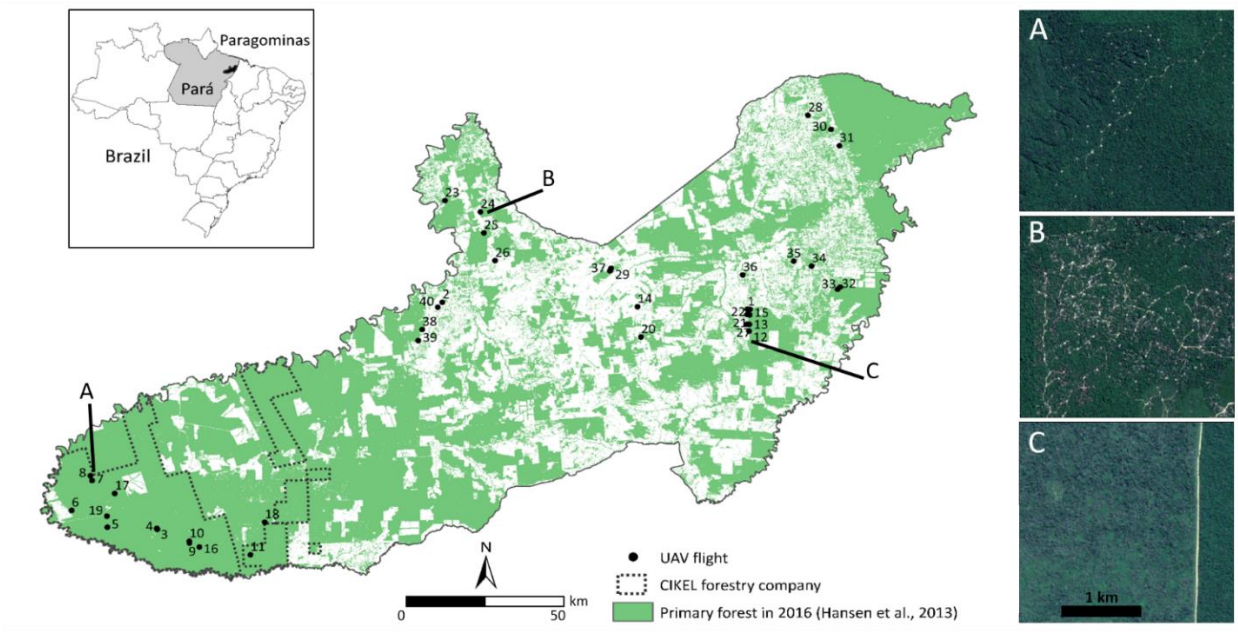

Figure 3.1 Location of the study site, Paragominas municipality, in Pará state in the Brazilian Amazon. Distribution of the 40 forest plots covered using UAV. Illustrations of selective logging (A), over logging (B) and fire (C) from Google Earth® 2017

3.2.2 Data collection

3.2.2.1 UAV surveys and processing

Forty forest sites were selected in various forested landscapes to cover a large variation of disturbance types (Fig 3.1). Using visual interpretation from Google Earth® VHRS images validated by in-situ UAV observations, we distinguished between sites that experienced disturbances such as logging and fire and intact sites with no human-induced disturbance. We also used the management plan of the Cikel forestry company (Fig 3.1) that provides spatial information on undisturbed and SL forests at different dates over the last 20 years.

We used a Dji mavic pro UAV carrying a RGB camera of 12.71 MP resolution (4000 x 3000 pixels). The acquisition plan was designed with Pix4D Capture software (Pix4D, Lausanne, Switzerland). We used a single grid with 80% of front and side overlap between images and a constant flight altitude of 300 meters above ground level. The objective was to maximize the overlap between each image and the total surface area mapped. As a result, the average surface mapped in each forest plot was 24 ha (~600 by 400 meters) at 10 centimeters spatial resolution (Appendix 3.3) for a total of 739 ha. In order to generate a high quality digital height model, each flight was constrained by several conditions:

- Flat terrain was selected with imaged areas that overlapped with roads or agricultural fields to allow us to retrieve the ground elevation during the preprocessing step;
- Acquisition in the morning (9 to 11 am) and afternoon (3 to 5 pm) was preferred to avoid zenithal effects (halo and low image contrast);
- Either cloud free or totally cloudy sky conditions were necessary to avoid cloud shadows;
- Absence of wind to low wind conditions were needed to generate crisp images of the forest canopy.

Raw image data were processed to the highest density point cloud using structure from motion (SfM) followed by densification using multi-view stereo algorithms in the Pix4D software (Alonzo et al. 2018; Westoby et al. 2012). Final point cloud densities were ~27 pts.m-3 depending on the availability of viable tie points, and some other acquisition parameters. Using the georectified point clouds, we corrected the raw images to generate RGB mosaics, which were then converted into single-band panchromatic grey level mosaics. Digital Surface Models (DSM) of the canopy at 0.10 m resolution were directly computed from the point cloud. We extracted the average ground elevation data in non-

forest areas (e.g. roads, agricultural fields or canopy gaps) from the DSMs and derived Digital Height Models (DHM) for each forest plot.

3.2.2.2 Landsat time series to detect forest disturbances and reconstruct degradation history

We acquired Landsat data from 1984 to 2017 (Appendix 3.1) to detect forest disturbances along time and reconstruct degradation history for each forest site. The images at Level 1 (Tier 1 product) were pre-processed to surface reflectance by the algorithm developed by the NASA Goddard Space Flight Center (http://earthexplorer.usgs.gov/). We computed the Normalized Difference Moisture Index (NDMI) from the Short-Wave InfraRed (SWIR) and Near InfraRed (NIR) bands as follows (Gao 1996):

$$NDMI = NIR - SWIR/NIR + SWIR$$

This index previously used to monitor forest degradation (DeVries et al. 2015) allowed us to identify disturbance type and frequency (Selective Logging, Over-Logging and fire) at forest plot scale, using photointerpretation (Appendix 3.2). The disturbance type was identified based on its spatial extent and shape and on NDMI values. SL is marked by regular and spaced logging roads (A, Fig 3.1), over logging (OL) is marked by irregular logging roads (B, Fig 3.1) and fire presents open canopy structure and low value of NDMI (Silva et al. 2018; Tritsch et al. 2016). We also recorded the date of the most recent disturbance (Appendix 3.3) which has a significant influence on the current forest structure (Rappaport et al. 2018). Figure 3.2 shows the diversity of forest degradation history of our sampling such as SL forests, OL forests and OL and burned forests.

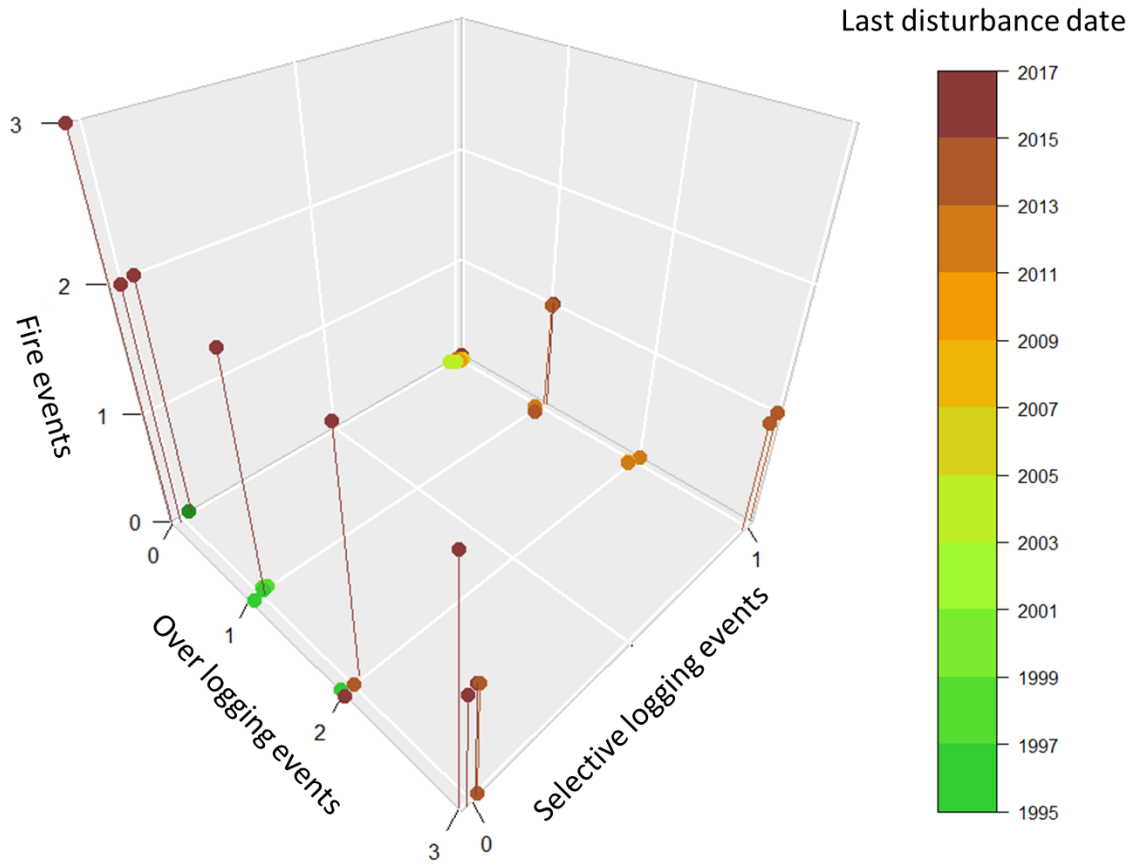

Figure 3.2 Forest degradation history of each forest plot (based on the frequency of selective logging, over logging, fire events and date of last disturbance).

3.2.3 Method

The data analysis was based on two steps: (1) use canopy texture metrics derived from grey-level UAV images to retrieve canopy structure metrics (based on canopy digital height models) derived from UAV structure from motion within a large range of degraded forest types at 1 ha scale and (2) potential of canopy texture metrics to discriminate degradation history and the resulting changes in forest structures at the forest plot scale (Fig 3.3).

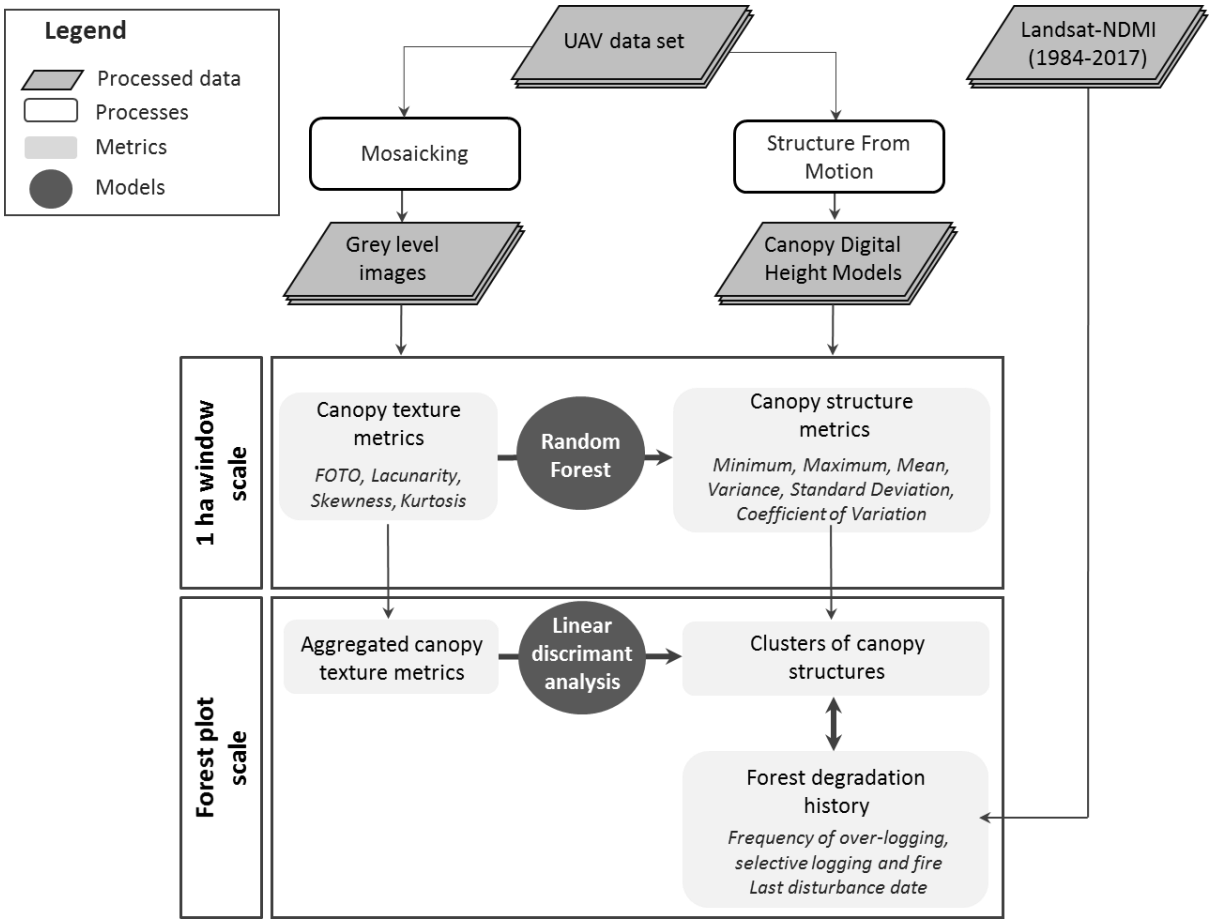

Figure 3.3 Workflow of the method used to evaluate the potential of canopy texture metrics to retrieve the canopy structure along the gradient of forest degradation and their relation with forest degradation history.

3.2.3.1 Computation of forest canopy texture metrics from grey level UAV images at 1 ha scale

We performed texture analysis of grey level canopy images using FOTO (Couteron 2002) and lacunarity (Frazer et al. 2005) algorithms. We also used basic descriptors of statistical grey level distributions such as skewness and kurtosis. Each of the UAV canopy images was divided into canopy 100*100 m windows (fixed grid) for texture analysis. This size was shown in previous studies to be appropriate to capture several repetitions of the largest tree crowns (in our case 45 meters of maximum tree crown diameter) in forest stands (Ploton et al. 2017).

The FOTO method is extensively described elsewhere (Couteron, 2002; Couteron et al., 2005; Ploton et al., 2017), hence we only give here a brief outline of the procedure. When applying FOTO, each of the windows originating from the UAV images is subjected to a two-dimensional Fourier transform to enable computation of the two-dimensional periodogram. 'Radial-' or 'r-spectra' are extracted from

the periodogram to provide simplified, azimuthally-averaged textural characterization. Spectra are systematically compared using the two first axes of a principal component analysis (FOTO_PCA1, FOTO_PCA2), providing an ordination along a limited number of coarseness vs. fineness gradients. In this process, windows are treated as statistical observations that are characterized and compared on the basis of their spectral profile, i.e., the way in which window grey scale variance is broken down in relation to Fourier harmonic spatial frequencies (ranging from 50 to 240 cycles/km for this study).

Lacunarity was defined following Frazer et al. (2005) and Malhi and Roman-Cuesta (2008). For each 100*100 m window, a moving square box of size 's' was glided by one pixel at a time and the sum of all pixel spectral radiance, called the mass, was computed at each gliding position. The probability of distribution was calculated using the frequency distribution of the mass divided by the number of boxes. Lacunarity at box size 's' is the squared ratio of the first and second moment of this distribution. This process was repeated for 100 box sizes ranging from 1 to 99 m and the resulting lacunarity spectrum was normalized by lacunarity at size 1. Finally, the spectra were compared using the two first axes of a PCA (Lacu_PCA1 and Lacu_PCA2 respectively), to provide an ordination of windows along inter-crown canopy openness gradients.

Routines for both FOTO (http://doi.org/10.5281/zenodo.1216005) and lacunarity methods were developed in the MatLab® environment (The MathWorks, Inc., Natick, Massachusetts, USA).

3.2.3.2 Computation of forest canopy structure metrics from digital height models at 1 ha scale

From the digital height model, six Canopy Structure Metrics (CSM) were computed in the same 100*100m window grid previously described: mean elevation (mean), minimum (min), maximum (max), variance (var), Standard Deviation (SD) and Coefficient of Variation (CV) defined as the ratio between standard deviation and mean elevation. We then compiled the six Canopy Texture Metrics, noted CTM, (FOTO_PCA1, FOTO_PCA2, Lacu_PCA1, Lacu_PCA2, Skewness, Kurtosis) and the 6 CSM.

3.2.3.3 Relationships between canopy textures metrics and canopy structure metrics within a large range of degraded forest types at 1 ha scale

The ability of CTM to predict forest canopy structures was tested using regression models for each CSM based on Random Forest machine learning (RF) (Breiman 2001).

The learning set is randomly partitioned into k equal size sub-samples with k=10. Each regression process is then applied where k-1 sub samples are used as training data and the remaining ones for validation. This process is repeated by changing the training/validation sub-samples in such a way that all learning samples are used for validation. Cross-validation is a common and sound procedure in machine learning processes (Arlot and Celisse 2010; Kohavi 1995). The R-squared, average Root Mean Square Error (RMSE) and relative RMSE will serve as the performance metrics for the model. The number of trees and the number of variables used for tree nodes splitting were randomly determined using the tune function implemented in the randomForest package (Liaw and Wiener 2002). The number of tree was set to 500 to reduce computation times without notable loss in accuracy.

3.2.3.4 Potential of canopy texture metrics to discriminate degradation history and the resulting changes in forest structures at the plot scale

The forest plot scale was used to combine canopy texture and canopy structure metrics with forest degradation history.

We first classified forest plots according to their canopy structures (mean CSM calculated at the plot scale) using PCA and hierarchical clustering (Ward's criterion). The number of clusters was optimized by calculating the inter-cluster variance (Ketchen and Shook 1996). Each cluster of forest canopy structure was then related to forest degradation history by calculating the average disturbance frequency of OL, SL and fire events.

We then used Linear Discriminant Analysis (LDA) to predict membership of forest structure clusters from averaged value of CTM at the plot scale. LDA algorithm tries to find a linear combination within the canopy textural metrics averaged at plot scale that maximizes separation between the barycenters of the clusters while minimizing the variation within each group of the dataset (Hamsici and Martinez 2008; Kuhn and Johnson 2013). We used MANOVA with Pillai's Trace tests to evaluate the significance of the multivariate inter-cluster difference computed from the 6 CTM. All processes were computed using the R packages FactoMineR (Husson et al. 2010; Lê et al. 2008) and the MASS package (Venables and Ripley 2002).

3.3 Results

3.3.1 Forest canopy texture metrics from grey level UAV images at 1 ha scale

The two first factorial axes of the PCA accounted for 51.6% of the total variability of the r-spectra observed (Fig 3.4b). FOTO_PCA1 expresses a gradient between coarse and fine texture corresponding to spatial frequencies of less than 90 cycles/km and more than 120 cycles/km, respectively (Fig 3.4c). FOTO_PCA2 expresses a gradient leading from heterogeneous textures with the coexistence of low and high frequencies (negative scores) toward homogeneous intermediate frequencies in the range 90-120 cycles/km (high scores). Fine textures correspond to homogeneous distribution of small tree crowns reflecting ongoing regeneration after probable over logging. Intermediate textures along axis 1 associate large and smaller tree crowns that characterize preserved forest with the natural distribution of high emergent trees and lower canopy trees. The left part of the scatter plot groups coarse textures corresponding to large gaps in the canopy related to logging activities. Finally, the two examples at the bottom of the plot show mixed coarse (remaining trees) and fine (low understory or shrub stratum) textures that characterize OL and recently burned forests.

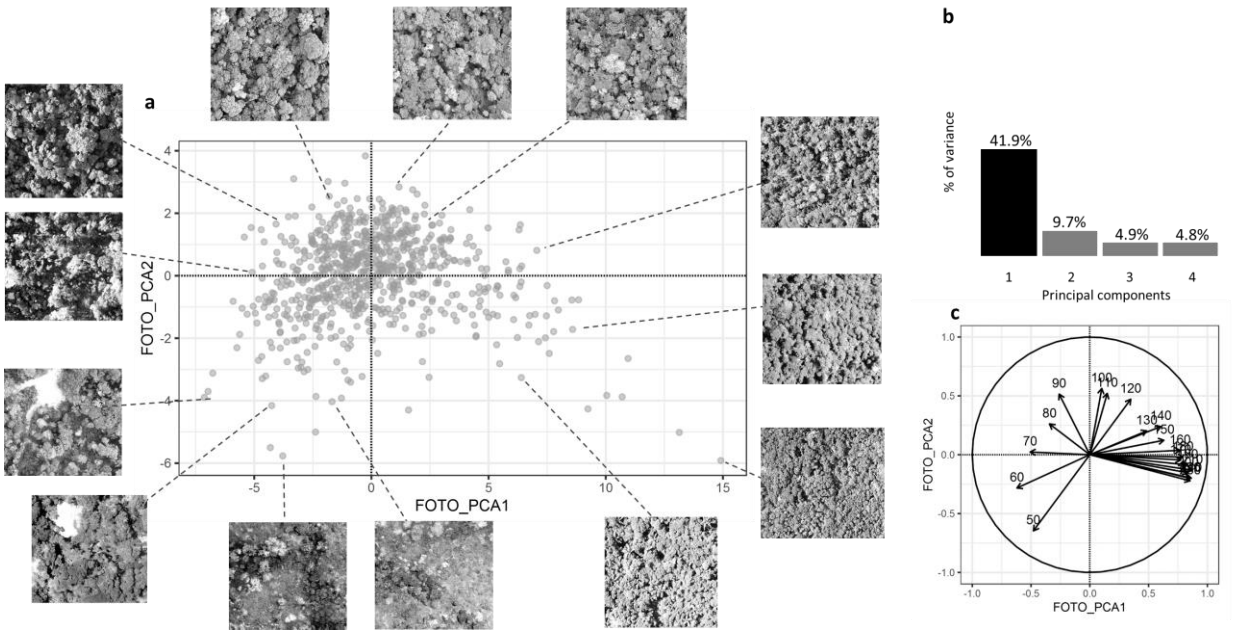

Figure 3.4 Canopy texture ordination based on the FOTO method applied to UAV-acquired grey level images. (a) Scatter plots of PCA scores along F1 and F2 and windows selected as illustrations. (b) Histogram of eigenvalues expressed as % of total variance. (c) Correlation circles with frequencies ranging from 50 to 240 (cycles/km).

The first factorial axe of the PCA on the lacunarity spectra account for more than 70% of total variability (Fig 3.5b). Lacu_PCA1 expresses a gradient of gapiness with large gaps appearing in the extreme left part of the scatter plot (Fig 3.5a) and closed canopy forest with no gaps in the extreme right part. Large gaps are tree shadows projected over large canopy gaps. Homogeneous canopies, i.e. smooth grain and a closed canopy characterizing low degradation forests were found on the positive side of the second axis (Lacu_PCA2)(11% of total variability) and vice versa for heterogeneous canopies. These are highly degraded forests (over logged at different ages and recently burned forests) with destroyed canopies and patches of small crowns linked to the understory or to regeneration. Other axis did not reveal other structure. Substantial analogy can be observed between the main texture gradients provided by FOTO and by the lacunarity analyses.

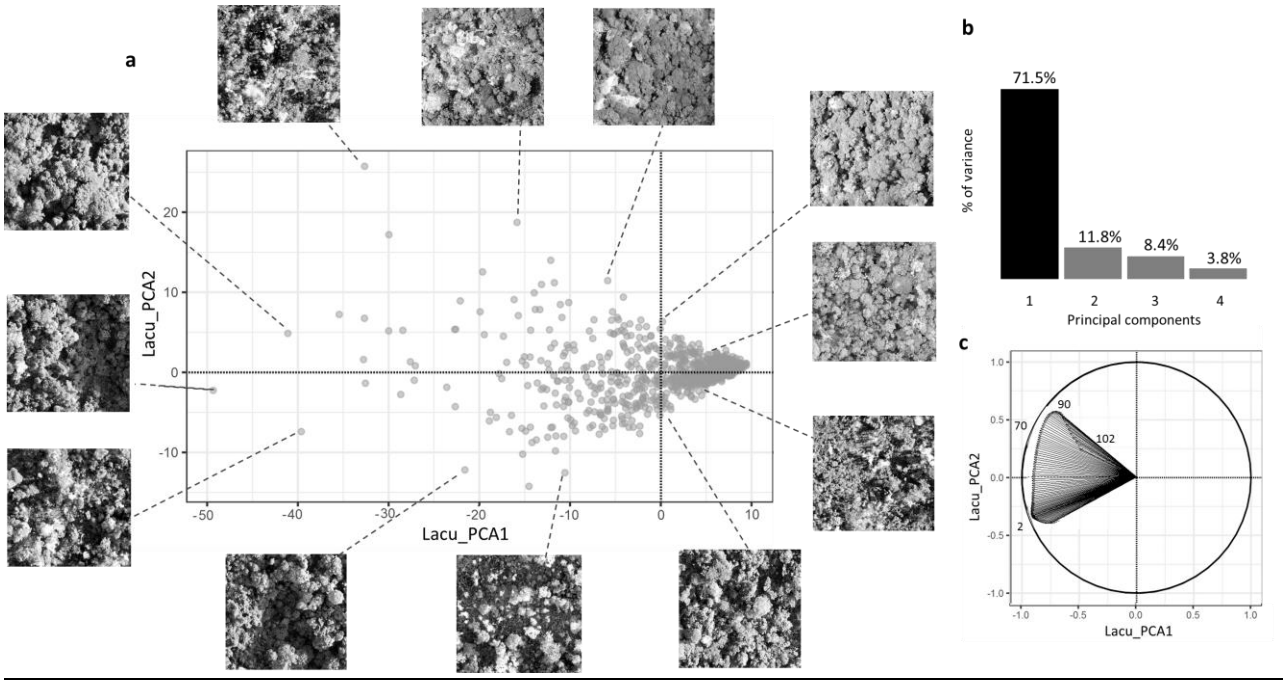

Figure 3.5 Canopy texture ordination based on the lacunarity method. (a) Scatter plots of PCA scores along F1 and F2 and windows selected as illustrations. (b) Histogram of eigenvalues expressed as % of total variance. (c) Correlation circles with sub-window sizes ranging from 2 to 102 pixels.

3.3.2 Relationships between canopy textures and forest structure parameters at 1 ha scale

The standard deviation and variance of canopy height were the CSM best explained by texture with a R^2 of 0.58 and 0.54 respectively (Table 3.1). These metrics pointing to the variability of canopy structure directly reflect the different processes of degradation and the associated gradients of canopy grain

texture. Maximum and mean canopy height and coefficient of variation show lower relationship (resp. R^2 of 0.43, 0.38 and 0.31). The minimum height showed a low R^2 of 0.13 with CTM.

Table 3.1 Random forest regression models for the prediction of canopy structure metrics (CSM) from canopy texture metrics (CTM) on grey level images.

CSM	R^2	RMSE	Relative RMSE
Minimum (m)	0.13	3.49	0.94
Maximum (m)	0.43	5.66	0.76
Mean (m)	0.38	4.88	0.79
Variance	0.54	13.03	0.68
Standard deviation	0.58	1.01	0.65
Coefficient of variation	0.31	0.17	0.83

3.3.3 Potential of canopy texture metrics to discriminate degradation history and the resulting changes in forest structures at the plot scale

3.3.3.1 Clusters of canopy structures and related degradation history

The clustering method allowed identifying 6 clusters of canopy structures (Fig 3.6). **Cluster 1** groups wide open and low canopy forests with a significantly lower average canopy height (9.9 m) than the other clusters and high Standard Deviation (SD) values (6.19 m). It groups forest plots that have mainly experienced OL (~1.4 events) and recent fire events identified between 2015 and 2017 (1.6 in average). **Cluster 2** groups 23-year-old secondary forests characterized by a homogeneous and low canopy (average height of 13.86m and SD of 2.28). **Cluster 3** groups forest plots with homogeneous (SD of 5.10), low average canopy height (14.13m) mainly marked by over logging (~1.5 events). **Cluster 4** has a heterogeneous canopy structure characterized by high standard deviation (SD of 7.03) which is explained by recent logging events detected in 2017 (~1.2 events) and other previous disturbances such as fire (~1 event). **Clusters 5 and 6** have similar canopy height (~22 m) but variable canopy roughness (SD ranging from 6.05 to 7.59). Their degradation histories differ as cluster 5 groups recently SL forest (~0.6 events) or OL forests (~1 event) while cluster 6 mostly groups undisturbed forest and old SL forests (more than 10 years ago). However both clusters are marked by very low (~0.1 events for cluster 5) to none fire disturbances detected. Further explanation on the different steps of the method and on the statistical results can be found in Appendix 3.4 and 3.5.

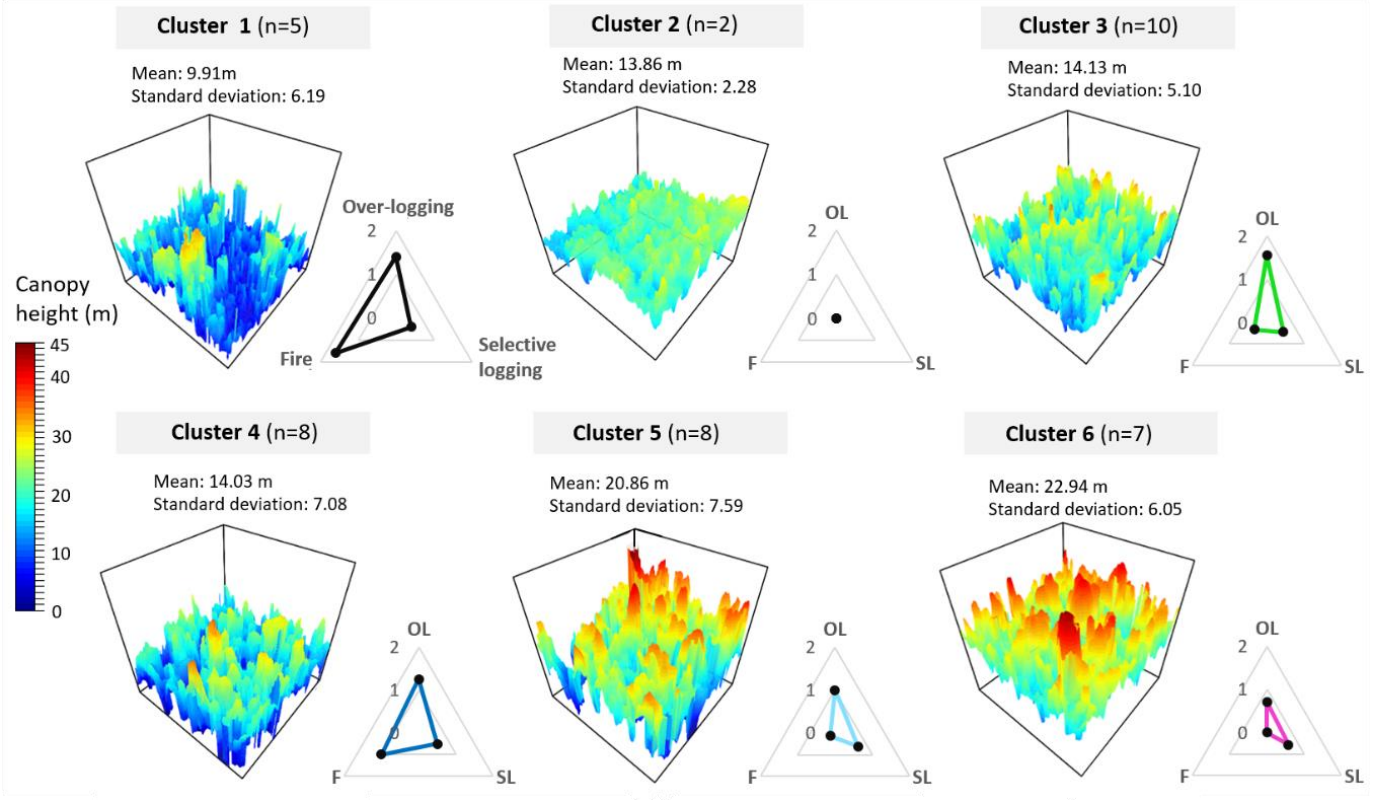

Figure 3.6 3D plots of digital height models of the (100x100 m) windows selected to illustrate the 6 forest structure clusters. Radar chart shows the average frequency of over-logging (OL), selective logging (SL) and fire (F) disturbances detected in all forest plots within a given cluster.

3.3.4.2 Linear discriminant analysis at the forest plot scale

The two first discriminant components (LD1 and LD2) account for 93.6% of the total proportion of the trace i.e. the proportion of inter-cluster discrimination of the LDA based on texture (MANOVA test with p-value < 0.05)(Fig 3.7a). The prominent first discriminant component is mainly correlated with FOTO_PCA1 (r=0.55 in LD1), FOTO_PCA2 (0.49 in LD1) and LACU_PCA2 (-0.79 in LD1) (Fig 3.7b). The second discriminant component is mainly correlated with LACU_PCA2. In the LD1-LD2 plane, clusters 2 and 3 are mainly separated from the rest of clusters thanks to axis LDA1. Cluster 1, 4 and 5 are discriminated along LD2. Cluster 6 has less discriminating capacity, especially compared with cluster 5. LDA results include misclassification errors corresponding to disagreement between texture-based and structural classifications of the plots (Fig 3.7a). The confusion matrix shows an overall accuracy of 55% and kappa index at 0.44 (Fig 3.7c). The LDA classification performed well for all clusters except cluster 6 which has the highest misclassification rate with a high rate of confusion with cluster 5. Based on

CTM, clusters 5 and 6 appeared to be similar because they mainly differ in their minimum height, which logically is difficult to predict from canopy texture metrics on 2D images.

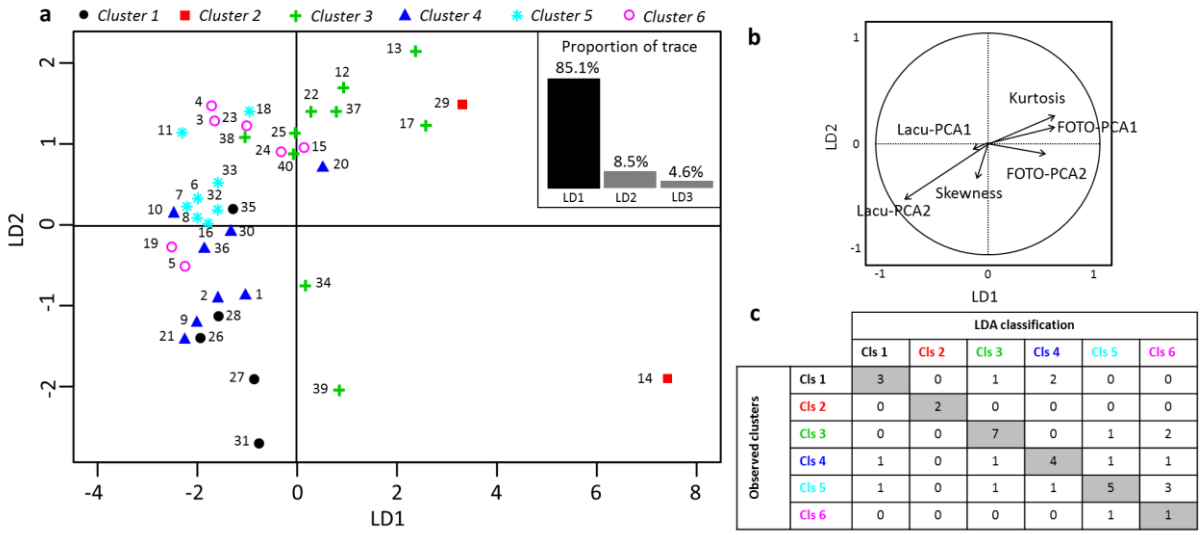

Figure 3.7 (a) Scatter plot showing the distribution of the 40 forest plots with color based on the color of canopy clusters on the linear discriminant plane (LD1-2). Inset: proportions of LDA trace (b) Correlation circle of CTM with respect to the two main components (axes) of the LDA (c) Confusion matrix between observed and predicted clusters for the 40 plots (LDA classifications)

Clusters 2, 3 and 5 are distinguished along a gradient of canopy textural grain that spans from fine to coarse (FOTO-PCA1) (Fig 3.8). Cluster 4 mainly presents the lowest FOTO-PCA1 and Lacunarity-PCA1 values, which correspond to the coarse texture and large gaps, respectively, typical of recent logging events. Cluster 1 has on average the coarse grain and homogeneous texture (FOTO-PCA1 and -PCA2) that characterize low vegetation strata. Finally cluster 6 (well preserved forest) has intermediate canopy grain (FOTO-PCA1 and 2) and canopy openness (Lacunarity-PCA2).

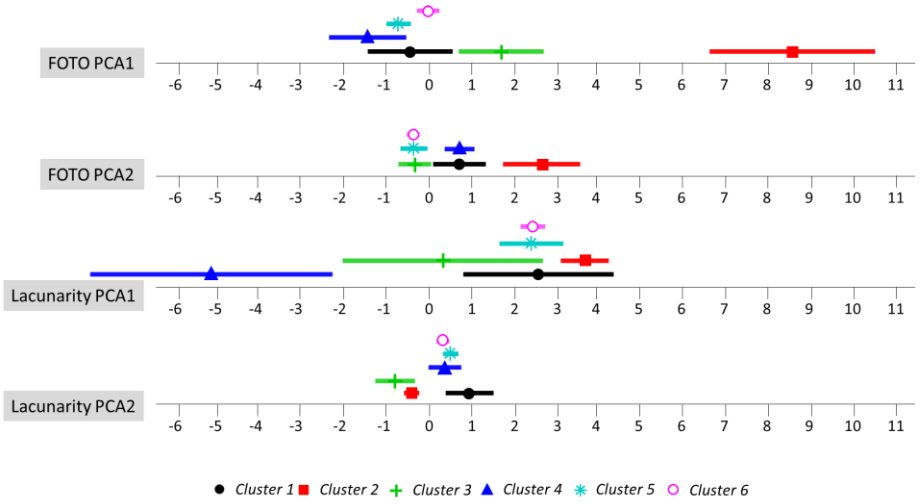

Figure 3.8 Mean and SD values of CTM calculated within the 6 predicted clusters using LDA.

3.4 Discussion

A better characterization of forest structure is crucial to tailoring forest management plans (Goldstein 2014). In this paper, we show that Canopy Textural Metrics (CTM) extracted from VHRS optical images acquired by UAV are clearly related to forest canopy digital height models and can reveal different and complex degradation history. The CTM provide complementary information on degraded forest states compared to other remotely sensed indicators based on vegetation photosynthesis activity (Asner et al., 2009; Bullock et al., 2018; Mitchell et al., 2017). The CTM can also be used in multidisciplinary approaches such as for the assessment of forest ecosystem services that require detailed information on forest structure (Barlow et al. 2016; Berenguer et al. 2014).

3.4.1 Potential of canopy texture metrics to assess degraded canopy structures

We showed that CTM can assess forest structure variability that reflects both horizontal and vertical heterogeneity induced by degradation. Through the expression of canopy grain and heterogeneity gradients, CTM provides reliable estimations of canopy roughness (standard deviation of canopy height) at 1 ha-scale. At the forest plot scale, we demonstrated the complementary of FOTO and lacunarity metrics in distinguishing between the different clusters. While FOTO and lacunarity express similar gradients of canopy texture (Fig 3.4 and 3.5), the measure of canopy openness in lacunarity provide useful additional information to distinguish large canopy gaps from large crowns, as underlined by Ploton et al. (2017). However, the first axis of lacunarity reveals a gradient of canopy textures that could be influenced by sun-angle conditions during the UAV data acquisition. Early morning and late afternoon data acquisitions generate higher projected shadow, which drives the distribution of the data towards the negative values of the first axis. Data acquisition parameters (sun and sensor angles, clouds etc.) are known to be able to disturb grey level values and textures (Barbier and Couteron 2015). One advantage of using UAV is that they allow better control of acquisition conditions than do satellites.

3.4.2 Long-term forest degradation consequences on structure explained using current canopy textures

In this study, we demonstrate the potential of single shot UAV-based canopy altimetry and texture to correlate with current structure that can reveal both past disturbances and recovery processes (Herold et al. 2011, Ghazoul and Chazdon 2017). At the forest plot scale (~24 ha), the average CSM and the variability of CSM enabled the identification of six forest clusters with specific degradation history. The link between long term degradation history and canopy structure has already been identified in previous studies that quantified carbon densities of Amazonian forests following successive logging and/or fire events (Berenguer et al. 2014; Longo et al. 2016; Rappaport et al. 2018). CTM proved to be able to differentiate between five types of degradation, although with some confusion between the less degraded forest types.

Undisturbed forests have a high closed canopy, and are homogeneous in texture with an intermediate grain associating large and medium-sized tree crowns (cluster 6). Any logging event will disrupt the canopy and create a coarse texture with greater variation in canopy height (cluster 4). Under a management plan, logging intensity is moderate (< 5 to 8 trees/ha) and the recovery time (35 years in Brazil) is respected. In that case, the coarse texture will recover and will turn back into intermediate grain (cluster 5 or 6). We showed that after 7 years, the canopy texture of a logged forest resembles that of undisturbed forest (Fig 3.6 and Appendix 3.3). For unmanaged forests, subject to higher uptake, the time for the forest to recover a canopy texture of intermediate grain will be longer (e.g. plots 23 and 24). In the case of additional impacts (progressive disappearance of large crowns), the coarse canopy texture will also be maintained longer. Repetitive and intense logging have therefore triggered the complete harvesting of emergent trees, thereby weakening the forest structure (Asner et al. 2002). During the recovery process, canopy is of low height and its texture is dominated by a fine and heterogeneous grain (cluster 3).

Additionally, we found that recent fire (single or multiple events) has a major impact on the damaged forest structure. The resulting highly degraded forests are characterized by coarse textures corresponding to large gaps and/or homogeneous regeneration stratum and highly damaged canopy (cluster 1). Moreover, most fires were detected in 2015, which correlates with the El Nino drought event (Berenguer et al. 2018). These findings underline the importance of the synergetic effects of logging and fire on forest structure (Dwomoh et al. 2019; Morton et al. 2013). We also found that fire was never detected (i.e. did not occur) in closed canopy and relatively low degradation forests. This confirms that heavily logged forests are more vulnerable to fire due to the presence of dead and dry

vegetation resulting from logging. At a larger scale, this vulnerability is linked with the fragmentation of forest patches, which facilitates access to forest resources, accentuates dry edge effects and increases potential pressure caused by agricultural expansion (Briant et al. 2010; Broadbent et al. 2008; Silva Junior et al. 2018). The mitigation of fire occurrence through improved landscape management is therefore a priority in order to prevent further degradation and forest carbon losses (Berenguer et al. 2014).

The results of the present study reveal possible ways to address questions concerning the future management of primary degraded forests by analyzing the structure and texture of their canopy in order to better differentiate forest states and the associated degradation history. This study also opens the way for further analysis of secondary forests in abandoned lands which will certainly play a crucial role in future scenarios of landscape restoration (Chazdon et al. 2016).

3.4.3 UAV technology: from data acquisition to limitations and perspectives

This paper reports the first large-scale application of low cost UAV to retrieve quantitative information on closed canopy forest structures. The UAV used is inexpensive (<2,000 US$) and a highly efficient cost/time ratio was found for data acquisition in the field. In a 20 minutes flight, around 25 hectares of forest was mapped at a resolution of 10 centimeters. Other studies using UAV produced results that are comparable with LiDAR in terms of point cloud densities (Dandois et al. 2015) and estimations of forest structural parameters (Alonzo et al., 2018). Finally, the computation of CTM using open-source Matlab® routines is automatic and only requires the window size used for texture analysis as user input. Window size can be adapted to forest canopy crown size and distribution, although limited variations do not alter the results much. Consequently, the workflow described here has great promise for future monitoring of tropical forest at low cost, which is interesting when airborne LiDAR is not affordable or available.

However, UAV remain limited by their inability to cover regions as large as those covered by satellite images, and climatic conditions (wind, cloud shadows) are likely to disturb the consistency of image texture and thus the automatic mapping process. Finally, regulations strongly limit the use of UAV in certain countries. Nonetheless, UAVs appears to be an efficient tool at the interface between field inventory and satellite characterization of forest structure (Koh and Wich, 2012). UAV-acquired reference data could be the basis of upscaling chains that would allow the use of spaceborne data of decreasing resolution yet increasing swath and affordability so as to reach broad scale, wall to wall mapping of forest state indicators of known accuracy.

3.5 Conclusion of Chapter 3

In this chapter, we described the first large-scale application of low cost UAV processes to acquire forest structural ground truth data across a wide range of degraded forest types. Canopy texture analysis and very high-resolution images are major cost-efficient alternatives to the use of LiDAR datasets and in the long run, could enable forest structure to be mapped at optimal spatial and temporal scales. We provided quantitative information to better interpret the different canopy textures that have resulted from the cumulative impacts of various types of degradation over the last 33 years. First, we built robust and significant correlations between Fourier, lacunarity texture metrics and forest structural parameters such as canopy variability and height. Second, we demonstrated that each type of degradation has a specific canopy grain, heterogeneity and openness signature. Deconstructing degradation complexities through canopy texture analysis also highlighted the destructive impacts of repetitive unsustainable logging and fire.

3.6 Perspectives

3.6.1 Multi-scale analysis of canopy structures of a tropical forest degradation gradient, from UAV to satellite VHSR

Based on UAV acquisitions that generate 2D and 3D images of the canopy using photogrammetry methods, the ability of texture metrics to characterize the variation in forest cover height, and thus degradation, has been demonstrated (Chapter 3). However, these data do not cover large areas. VHSR optical satellite data, such as SPOT 6 & 7, have already demonstrated their ability to characterize canopy structure variations at the regional scale through canopy texture analyses (Ploton et al. 2012; Singh et al. 2014; Pargal et al. 2017). However, the correct interpretation and calibration of texture indices requires a level of field data that is often not available. How can UAV data be combined with VHSR optical satellite data allow to characterize the forest structure and infer the state of degradation of tropical forests over large areas?

The objective of this study is therefore to evaluate the potential of VHSR optical images to analyze and map the structures of degraded tropical forests despite a lower resolution compared to UAV data. The study will therefore initially consist in carrying out a local scale analysis on reference sites using altimetry data derived from UAV imagery and VHSR optical satellite data (Fig 3.9). The aim will be to

demonstrate that the relationship between texture and structure is also significant with these data. Then, a large-scale analysis will be carried out in order to predict the structure of the forests and thus to estimate their state of degradation.

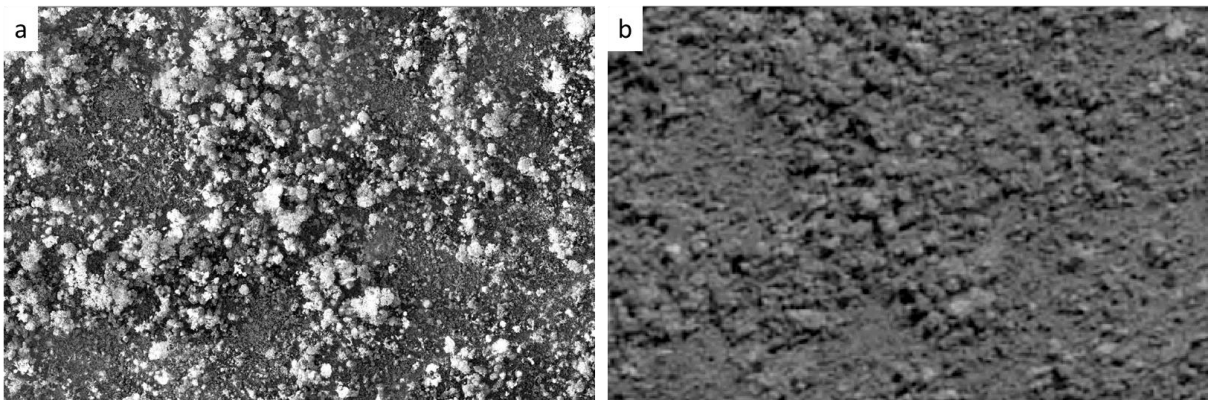

Figure 3.9 a) UAV greylevels (10cm) and b) SPOT-6 Panchromatic (1.5m)

The analysis is based on Canopy Digital Height Models extracted from 70 forest plots mapped using UAV in September 2017 and 2018. We also used six cloud-free SPOT-6 and 7 images to cover the municipality extent (1.5 spatial resolution in panchromatic mode) in 2017 dry season (from July to November). The scenes were mosaicked together, masked from clouds, shadows and other land cover/use different than primary and secondary forest (see Chapter 4).

Within the forest plots extent, the method used is similar that the one developed in Chapter 3. It involves using canopy texture metrics (from SPOT images in windows of 100*100 meters) as explanatory variables to model the canopy structure metrics derived from the UAV using Random Forest (k-fold validation). Due to the different configurations in angle sensor/sun conditions between the different SPOT images, we used an intercalibration method based on FOTO and linear regression in order to homogeneize the canopy structure metrics from one image to another (Barbier and Couteron 2015). This first step allows to characterize the relation texture (SPOT)/ structure (UAV). Then, we extracted intercalibrated canopy texture metrics from primary and secondary forest and used the texture/structure model to map canopystructure metrics over Paragominas (Fig 3.10).

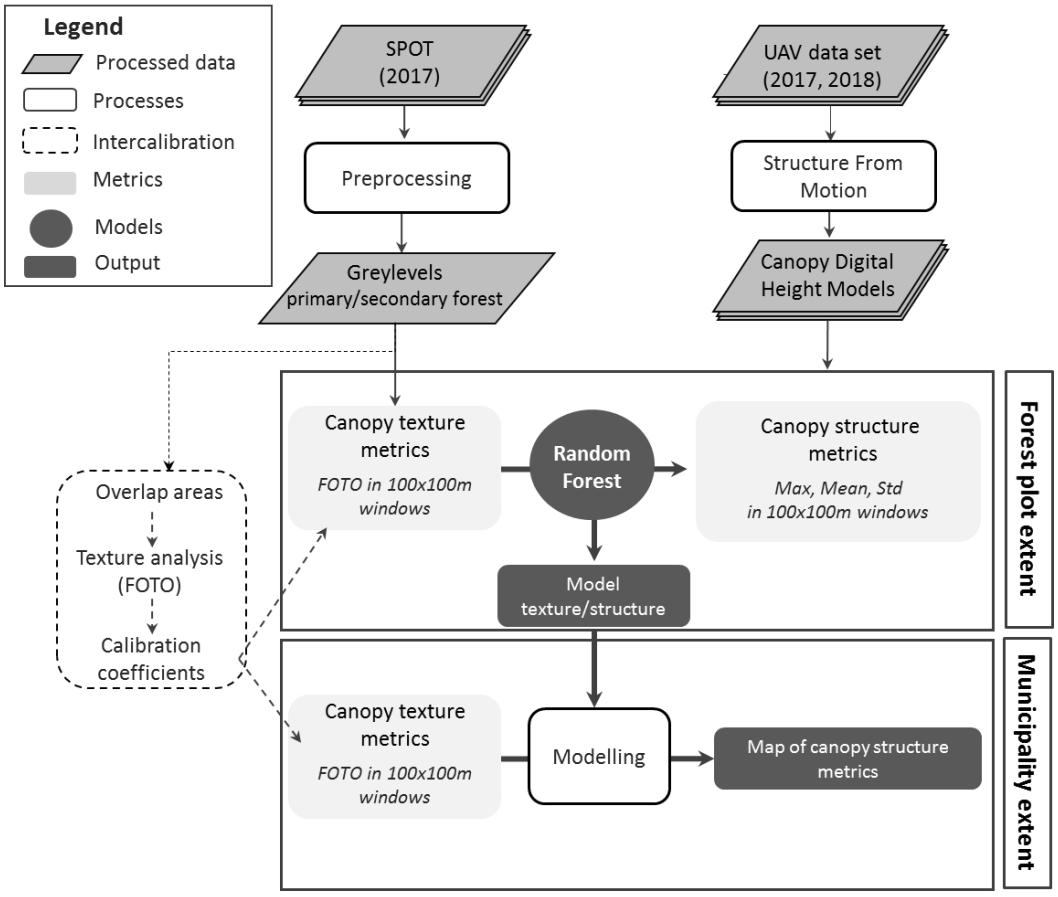

Figure 3.10 Method workflow from forest plot model texture/structure calibration to upscaling of canopy structure metrics using canopy texture analysis

At the forest plot scale, we found that the PCA shows that about 48% of the information is contained in the first two axes (axis inertia, Fig 3.11). The 20 spatial frequencies are ordered, as expected, in an increasing order in plane 1 - 2 along axis 1 following a gradient of canopy grain. Low values correspond to canopies with large crowns typical of conserved or low degraded primary forests. High values correspond to canopy with small crowns rather characteristic of secondary forests or highly degraded canopies. Axis 2 details more precisely all the intermediate textures with an average crown size which may correspond to regenerating forests or to different intensities of degradation.

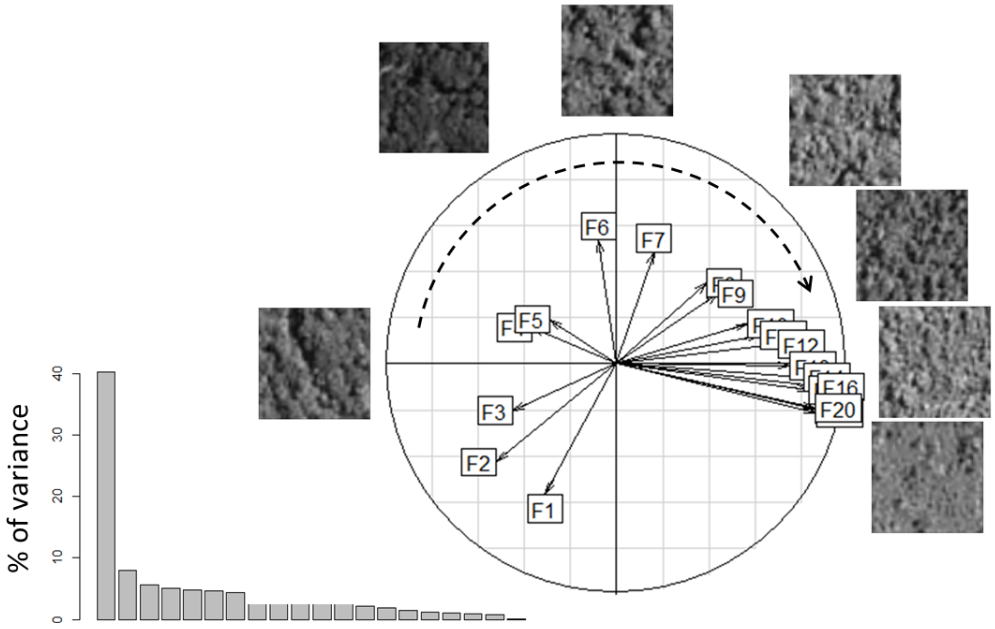

Figure 3.11 Canopy texture ordination based on the FOTO method applied to SPOT grey level images: Histogram of eigenvalues expressed as % of total variance and correlation circles with frequencies

The standard deviation and maximum canopy height are the structural metrics best correlated to texture with R^2 of about 0.5 and 0.4 respectively (Table 3.2). The mean and Q1 are less well correlated with R^2s of about 0.35 and 0.3 respectively. There therefore seems to be a significant relationship between the canopy structure and the texture determined from the SPOT scenes. Models will tend to overestimate low values (linear regression line in red higher than the first bisector in blue) and vice versa for high values.

Table 3.2 Random forest regression models for the prediction of canopy structure metrics from canopy texture metrics (FOTO and skewness) on SPOT grey level images.

Canopy structure metrics	R^2	RMSE	RRMSE
Standard deviation	0.501	1.222	0.706
Mean	0.347	5.559	0.808
Maximum	0.388	6.794	0.782
Q1	0.271	5.751	0.853

The prediction of the standard deviation of canopy height accurately reflects the forest degradation gradient in Paragominas (Figure 3.12). The areas of conserved forests at the West/East parts show a high standard deviation in contrast with the low values (i.e. high degradation) in the central part. The predictions are less good for the other structure metrics. The delimitations of the SPOT mosaic scenes

as well as the reduction of the contrast of the values are very visible and important. Average heights between 10 and 15 m are predicted for the indigenous reserve, while forest are low degraded. The values should be of the same order of magnitude as in the CIKEL where the predicted average height is much higher (between about 20 and 25 m).

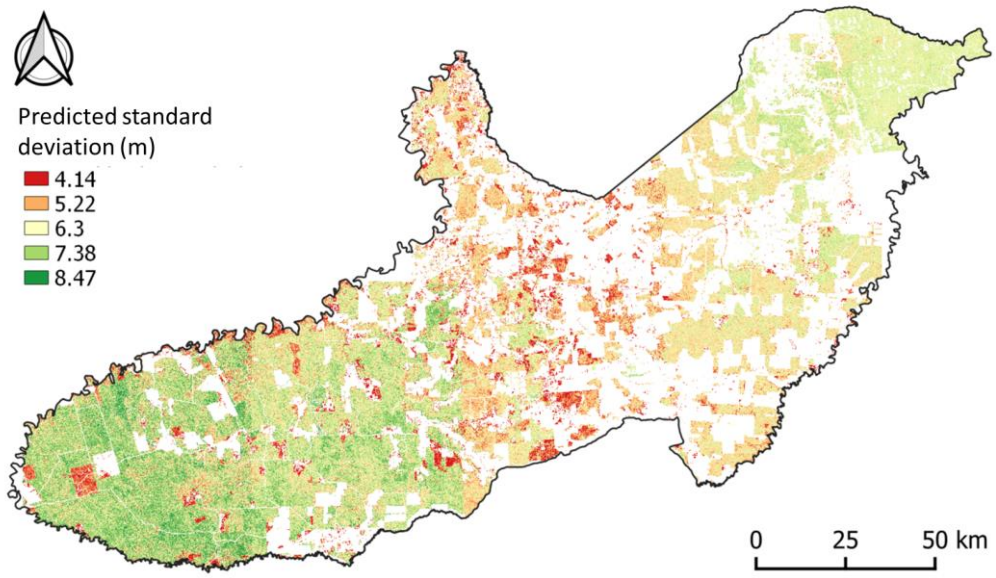

Figure 3.12 Prediction of standard deviation of canopy height (100m resolution)

This perspective demonstrated that VHSR optical satellite data can characterize tropical forest degradation. The use of the FOTO method makes it possible to produce canopy texture metrics significantly correlated to the three-dimensional structure of the forest cover. The upscaling achieved demonstrated the potential of the method to characterize degradation on a larger scale. By solving problems related to the calibration of VHSR scenes, it would be possible to produce mapping of an indicator of forest cover status. With the significant development of remote sensing in recent years, more and more satellite data with fine resolutions and high revisit frequencies are available (e.g. Planet Dove). It may therefore also be possible to monitor degradation over time using canopy texture analysis.

3.6.2 Reconstructing forest degradation history from Landsat time series

The replicability in time and space of canopy texture analysis to map degraded forest structures using the coupled UAV/VHSR methodology can be constrained by the availability of images (due to cloud cover or to acquisition parameters), their extent and related cost to cover large regions of the tropics. Furthermore, canopy texture analysis makes it possible to characterize the current state of forests by studying their structure but does not directly provide information on their history even if we showed that these two components were linked (Chapter 3). Reconstructing the degradation history using dense time series of remnant primary forests is thus an alternative and complementary method to characterize forest degradation. Most approaches rely on direct approaches and dense time series (inter-annual) to analyze the behavior of pixels (breakpoint detection). However, we showed in section 1.3.1 some limits to this approach. Spectral unmixing (direct punctual approach) informs at the sub-pixel scale on proportion of active and dead photosynthetic vegetation and bare soil but it is dependent on endmembers spectral libraries.

The objective of this perspective work is to characterize the frequency, intensity and type of the disturbances (logging and fire) altering the various primary forest patches of Paragominas municipality from annual Landsat time series (1980-2018). The method developed here is based on spectral unmixing to automatically identify and characterize the disturbances received by tropical forests. The objective is to move away from the spectral libraries and field data generally used in the selection of pure pixels, based in particular on unsupervised classification methods (Benhadj et al. 2012).

For this work, the study site is the extreme west of Paragominas, where the Cikel Brasil Verde Madeiras Ltda, founded in 2000, is located. This private forest estate governed by a forest management plan has been certified by the Forest Stewardship Council (FSC) since 2001. The work also includes forest plots outside of CIKEL where forest is subject to illegal selective logging.

The analysis is based on a time series of Landsat 5, 7 and 8 optical images of 30 meters spatial resolution (TIERS-1, Level-1), composed of one image per year between 2000 and 2017 with some data gaps, i.e. 15 images in total. The selection criteria for these images meets two conditions: i) cloud cover of less than 10% and ii) a date of acquisition between June and October (dry season), in order to respect the same climatic and phenological conditions.

The method is based on unsupervised classification (Baraldi et al. 2006), spectral unmixing and a series of image processing processes to extract each disturbance. Firstly, Baraldi unsupervised classification provides 46 classes identified through different combination of spectral bands and vegetation indices.

We extracted 10000 pixels for each of classes of vegetation, bare soil, water and shadow and identified using kmeans the most stable and robust spectral signature of each class. These signatures corresponds to endmembers attributes and were used for linear spectral unmixing following Benhadj et al. (2012). The resulting water, bare soil and vegetation components are combined and a set of GIS processes (threshold, morphological filters, kmeans) allowed to map most probable disturbances (e.g. selective logging, road network)(Fig 3.13).

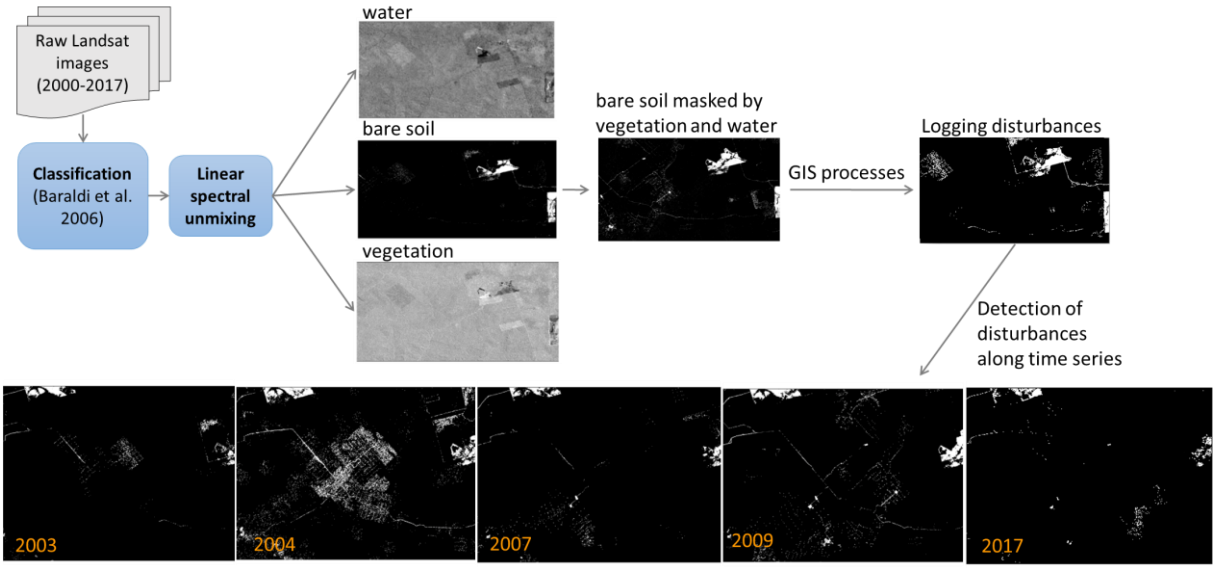

Figure 3.13 Workflow for detecting logging disturbances

Landscape metrics at the plot scale are then calculated to extract the evolution of the canopy opening area, and degradation indicators to identify types of forest exploitation. These indicators are: i) impact frequency (the number of times the forest is harvested), ii) maximum intensity (the maximum opening area of the canopy), iii) canopy opening frequency (the number of times the forest cover is opened more than 2%), iv) rotation (the average number of years between two farms).

We found that the generic method combining Baraldi's (2006) classification with spectral unmixing makes it possible to accurately extract degradation impacts such as main logging roads, skidding and skidding roads, log yards and logging gaps (Fig 3.14).

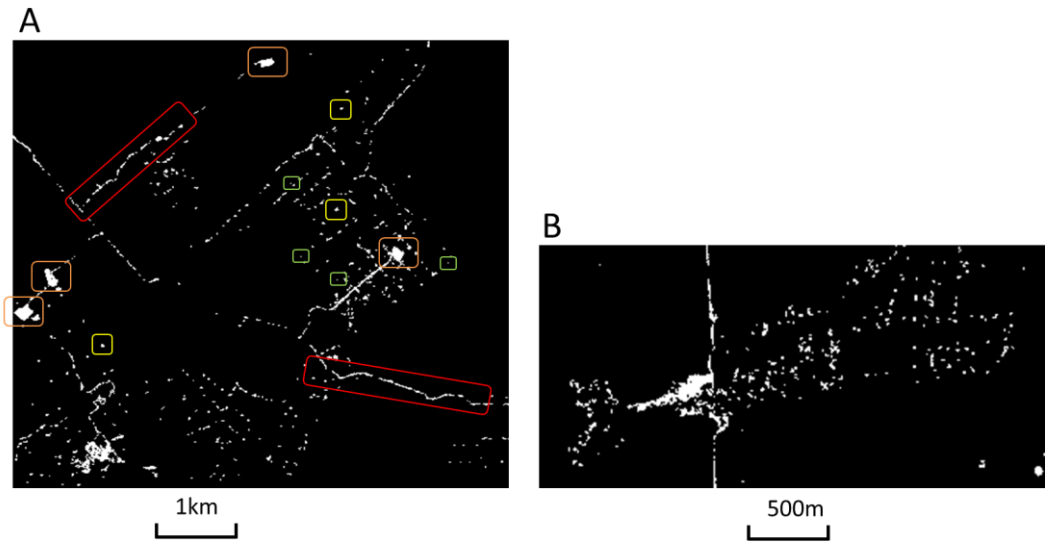

Figure 3.14 A) Detection of linear logging disturbances in 2009 in CIKEL (under forest management), detection of nonlinear disturbances outside of CIKEL in 2017

The evolution of the canopy's coverage area over time makes it possible to characterize forest degradation in terms of intensity and frequency. The combined analysis of the four degradation indicators makes it possible to differentiate between legal and conventional types of exploitation. In general, their values are higher in the case of non-legal exploitation (Fig 3.15).

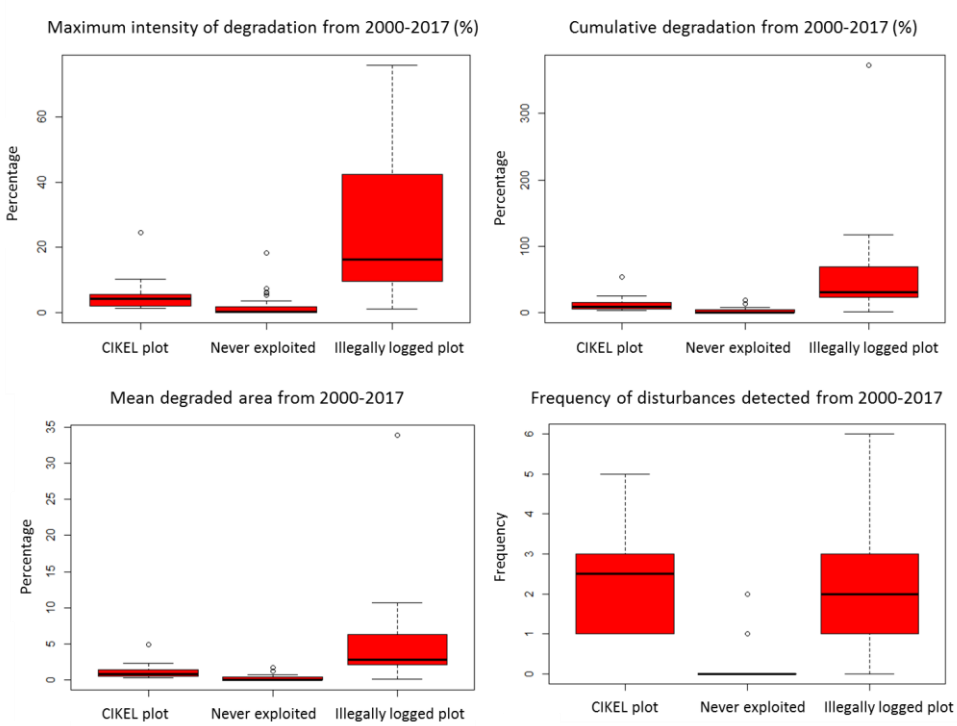

Fig 3.15 Indicators of forest degradation at the plot scale of a CIKEL plot (under forest management) and a plot never exploited (conserved primary forest) and a plot illegally logged outside of CIKEL

This study shows the potential of 30 m resolution Landsat satellite image time series to detect and identify the impacts of forest degradation in terms of canopy opening using an indirect approach. The method developed is semi-automatic, robust and reproducible because it is based on unsupervised classification and spectral unmixing to identify each impact of forest degradation such as logging roads, logyards and logging gaps. More study has to be made to add fire disturbances, which alters the canopy and thus the unmixing indicators differently. With the objective of operationality in mind, more study has to be made to adapt the method developed to the new Sentinel-2 data with a better spatial (10m) and temporal (6 days) resolution.

Chapter 4 - Primary forest degradation in the Amazon: a landscape approach to identify the main drivers

A gradient of vegetation structures from clean to wooded pasture up to a logged and burned primary forest in Paragominas municipality (picture by Jacques Baudry)

Reproduced from the article:

Bourgoin C., Blanc L., Betbeder J., Le Roux R., Le Clech S., Rumiano F., Baudry J., Boussard H., Oszwald J., Mercier A., Mazzei L., Dessard H., Laurent F., Hasan A., Poccard-Chapuis R., Burel F., Sist P., Läderach P., Reymondin L., Gond V. (2019 submitted) Primary forest degradation in the Amazon: a landscape approach to identify the main drivers. Environmental Research Letters.

Primary forest degradation in the Amazon: a landscape approach to identify the main drivers

Bourgoin C[1,2,3*], Blanc L[1,2], Betbeder J[1,2,4], Le Roux R[1,2], Le Clech S[5], Rumiano F[6,7], Baudry J[8], Boussard H[8], Oszwald J[9], Mercier A[9], Mazzei L[10], Dessard H[1,2], Laurent F[11], Hasan A[11], Poccard-Chapuis R[12,13], Burel F[14], Sist P[1,2], Läderach P[3], Reymondin L[3] and Gond V[1,2]

1 CIRAD, Forêts et Sociétés, F-34398 Montpellier, France
2 Forêts et Sociétés, Univ Montpellier, CIRAD, Montpellier, France
3 International Center for Tropical Agriculture (CIAT), Hanoi, Vietnam
4 Ecosystems Modelling Unity, Forests, Biodiversity and Climate Change Program, Tropical Agricultural Research and Higher Education Center (CATIE), Turrialba, Cartago, Costa Rica
5 Environmental Systems Analysis Group, Wageningen University and Research, Wageningen, The Netherlands
6 CIRAD, UMR TETIS, F-34398 Montpellier, France
7 TETIS, Univ Montpellier, AgroParisTech, CIRAD, CNRS, IRSTEA, F-34000 Montpellier, France
8 INRA, UMR BAGAP, 65 rue de St-Brieuc CS 84215, 35042 Rennes, France
9 LETG Rennes UMR 6554 LETG, Université Rennes 2, 35042 Rennes, France
10 EMBRAPA Amazônia Oriental, Trav. Dr. Enéas Pinheiro, Bairro Marco, CEP, 66095-903 Belém, Pará, Brazil
11 UMR ESO (Espaces et Sociétés), CNRS, Le Mans Université, 72000 Le Mans, France
12 CIRAD, UMR SELMET, Belém, Brazil
13 SELMET, Univ Montpellier, CIRAD, INRA, Montpellier SupAgro, Montpellier, France
14 UMR 6553 ECOBIO, CNRS, Rennes, France

Abstract

Deforestation shaped tropical landscapes into mosaics of land uses within which remnant primary forest are patches of varying land cover status. Degradation of primary forest with changes in structure but no change in land use is directly driven by selective logging and by fires set by humans. However, our understanding of the indirect drivers of forest degradation and the complex relations between degradation and land use processes at multiple scales is still limited. To fill this knowledge gap, we used a landscape approach to analyze the direct and indirect drivers of forest degradation at the old deforestation front in Paragominas municipality (Pará, Brazil). We used both regression and clustering methods to map the drivers of primary forest degradation from a large set of e.g. environmental and geographical factors, and landscape structure metrics derived from land use/cover classification. Models of forest degradation revealed that at the landscape scale, accessibility, geomorphology, fire occurrence and fragmentation were the key indirect and direct drivers of degradation (50-80% of explained variance). We clearly show that the indirect and direct drivers of degradation acted as a bundle and created homogenous patterns in the municipality thereby proving their spatial covariation and inter-dependency and revealing different land use dynamics and management practices. This paper provides a more holistic understanding of drivers of degradation and their sequential interactions. Our results underscore the need to tackle forest management at the landscape scale.

Keywords Forest degradation, remote sensing, land use/cover, Brazilian Amazon, landscape approach, fragmentation

4.1 Introduction

Forest degradation accounts for 68.9% of overall carbon losses from tropical forests (Baccini et al. 2017) and causes loss of biodiversity (Barlow et al. 2016; Broadbent et al. 2008), erosion of hydrological and soil properties and loss of non-timber forest resources (Lewis et al., 2015; Thompson et al., 2009). While the drivers of deforestation are well understood (Geist and Lambin 2002; Curtis et al. 2018; De Sy et al. 2019), knowledge of the drivers that cause gradual changes in the forest structure and composition with no change in land use is limited (Thompson et al. 2013; Putz and Redford 2010). Identifying the direct drivers (i.e. natural or human-induced factors that clearly influence forest ecosystems) and indirect drivers (i.e. natural or human-induced factors that are more diffuse as they alter direct drivers) of forest degradation is crucial for sustainable forest management and land-use planning (Nelson et al. 2006; Goldstein 2014).

Since the 1960s, around 20% of the Amazonian forest has been deforested and converted into agricultural land for cattle ranching and large-scale cultivation of cash crops (Fearnside 2005; Y. Malhi et al. 2008; Barona et al. 2010). The resulting landscapes along these old deforestation fronts are a complex mosaic of land uses. The state of primary forests in these human-dominated landscapes ranges from conserved to highly degraded due to the accumulation of severe disturbances over time and in space. The disturbances are mainly due to unsustainable logging practices (timber harvesting), biomass harvesting for energy (fuelwood and charcoal production) and fire (Asner et al. 2005; 2009; Souza, Jr et al. 2013). In the Brazilian Amazon, between 2000 and 2010, 50,815 km² of forest was degraded due to illegal selective logging and fire (Souza, Jr et al. 2013). While annual deforestation rates declined by 46%, degradation increased by 20%.

Although the direct drivers of forest degradation are well known (i.e. selective logging and understory fire) (Hosonuma et al. 2012; Asner et al. 2009b), so far, little is known about the indirect drivers of selective logging or forest burning in the Brazilian Amazon. There is thus a need to broaden our understanding of the drivers of forest degradation through a more integrative and holistic approach. The aim of the landscape approach is to deal with environmental, social and economic issues in unison in a defined geographical area characterized by a variety of competing land uses and multiple stakeholders (Reed et al. 2016; Opdam et al. 2018). Analyzing the forest and its degradation using a landscape approach consists in considering and characterizing the interconnections between the state of forest cover and the different land use processes at multiple scales (Melito et al. 2018). So far, most authors have analyzed degradation at the forest patch scale (Tyukavina et al. 2017) but this scale cannot explain how land use and agricultural practices influence the state of forest cover and whether forest degradation is at the origin of complex feedback loops (Morton et al. 2011). The landscape

approach has already been used to study the relation between deforestation and fragmentation (Laurance et al. 2002; 2011) where forests are spatially organized in patches of varying size, shape, with interconnections, and are influenced by the broader land use and cover change dynamics (Godron and Forman 1981). There is also a large body of literature focused on the negative impacts of fragmentation on forest structure triggered by deforestation (Briant et al. 2010; Shapiro et al. 2016; Melito et al. 2018; Almeida et al. 2019).

However, fragmentation is only one aspect of the influences land uses has on the state of forest cover. Land use conflicts between the protection of forest resources and growing pressure from the agricultural sector may trigger severe forest degradation, especially in areas where agricultural expansion is strictly limited (Nepstad et al. 2008). In addition, agricultural land management and agricultural practices may influence the state of proximate forest cover. To sum up, there is a lack of understanding of the different cascades of indirect and direct drivers leading to primary forest degradation in human-modified landscapes.

Here, we propose an innovative framework to disentangle how land use/land cover and landscape structure influence the state of the primary forest cover and degradation using an integrative landscape approach. The objective of this work was to identify the cascade of drivers of primary forest degradation at the landscape scale and to analyze their spatial complementary and variability. First, we assessed forest degradation using two proxies that capture forest degradation state in 2015 and degradation history between 2000 and 2015. Second, we collected data on the direct and indirect drivers of forest degradation from land cover/use classification, analysis of landscape structure and other environmental and geographical factors. Third, we used multiple linear regression analysis and clustering methods at the landscape scale to identify the most important drivers of forest degradation and to map their spatial distribution.

4.2 Materials and methods

4.2.1 Framing the degradation of primary forest in a landscape approach

Figure 4.1 depicts the interactions leading to primary forest degradation at different scales. Socio-economic and demographic factors, land policy (from management to land tenure) and environmental factors drive the expansion of farming and cattle ranching that trigger land use changes at the regional scale (Lambin et al. 2001; Geist and Lambin 2002). At the landscape scale, land use changes trigger

changes in landscape structure i.e. in the composition and configuration of landscape elements that make up the complex forest-agricultural mosaics (Burel and Baudry 1999). Different dynamics and practices are associated with agricultural land types and affect proximate forest patches through selective logging and understory fires (direct drivers of degradation). Land use change also modifies the configuration of landscape elements (e.g. heterogeneity and fragmentation). Higher fragmentation rates facilitate access to the forest patch and consequently to selective logging, leading to degradation (Broadbent et al. 2008). Edge effects increase forest flammability enhanced by climatic and topographic conditions (Phillips et al. 2009; Briant et al. 2010). Forest degradation also triggers feedback effects on landscape configuration (Morton et al. 2011).

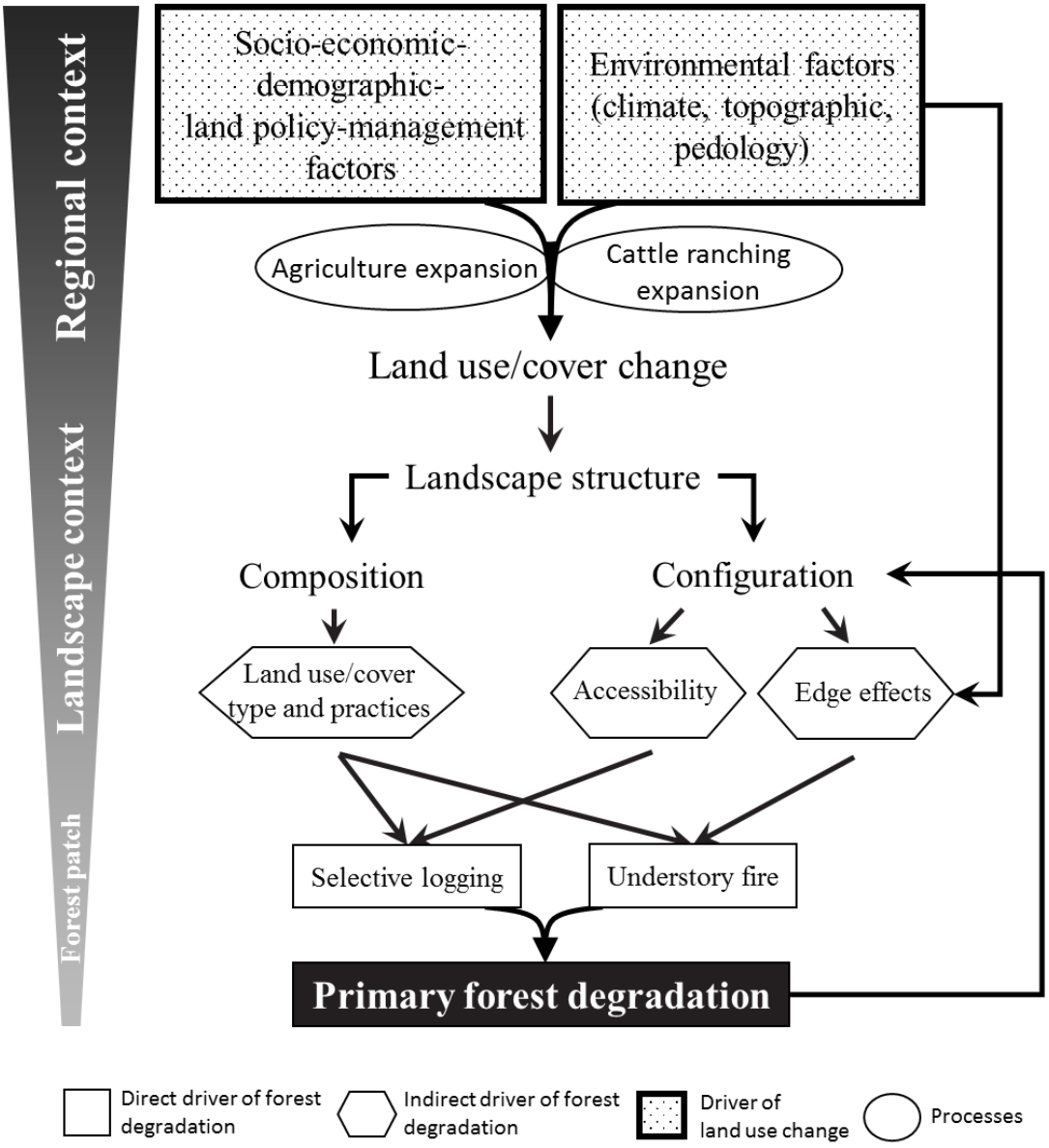

Figure 4.1 Conceptual framework of direct and indirect drivers of primary forest degradation at the forest patch, landscape and regional scales

4.2.2 Study site

The study area is the municipality of Paragominas located on the Brazilian deforestation front in the northeastern part of Pará State (Fig 4.2). The study area comprises 19,342 km² with a total population of 108,547 (IBGE, 2018). Colonization began in 1965 with the construction of the BR-010 road connecting Brasilia to Belém. The eastern part of the municipality is delimited by an indigenous reserve. Since 2000, the western part has been owned by a private forestry company *CIKEL Brazil Verde Madeiras Ltda*. Smallholder dominated areas can be found in the eastern and northern parts of the municipality. Smallholders practice small-scale cattle breeding, cultivate cash crops (pepper) extract acai, and practice subsistence agriculture (cassava)(Laurent et al. 2017).

The municipality went through successive development models (cattle ranching in the 1960s, the logging industry boom in the 1980s and of the grain agro-industry in 2000s) that resulted in a heterogeneous landscape mosaic of conserved to highly degraded forest associated with different land uses, mainly pasture and cereal crops, including soybean and maize (Viana et al. 2016; Piketty et al. 2015; Bourgoin et al. 2018; Mercier et al. 2019). Since 2008, the municipality is involved in a green development pact that aims to improve land and environmental regularization with a focus on reducing forest encroachment. However, forest degradation continues to exert increasing pressure on the remaining primary forest through unsustainable selective logging and fires (Hasan et al. 2019a).

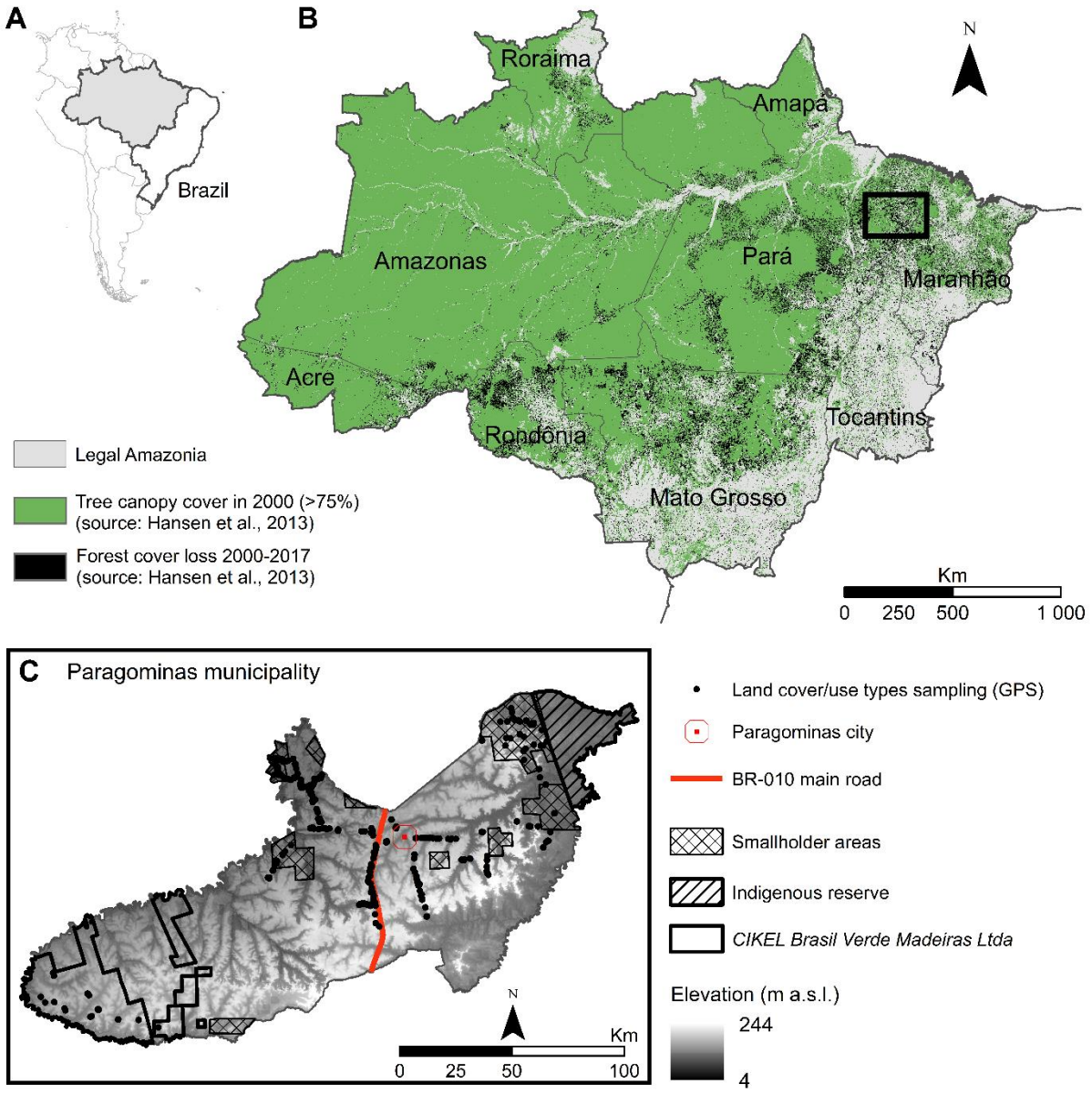

Figure 4.2 Paragominas municipality (C) and its location on the deforestation front (B) in the Legal Amazonia (A)

4.2.3 Data collection and methodology

We developed a framework to identify and map the direct and indirect drivers of forest degradation using a landscape approach (Fig 4.3): (1) collection of data for response and explanatory variables, (2) landscape analysis consisted in determining the appropriate scale to compute landscape structure metrics and zonal statistics of other explanatory variables and (3) analysis of drivers consisted in identifying the most significant drivers of degradation using linear regression models and mapping homogeneous clusters of degradation drivers.

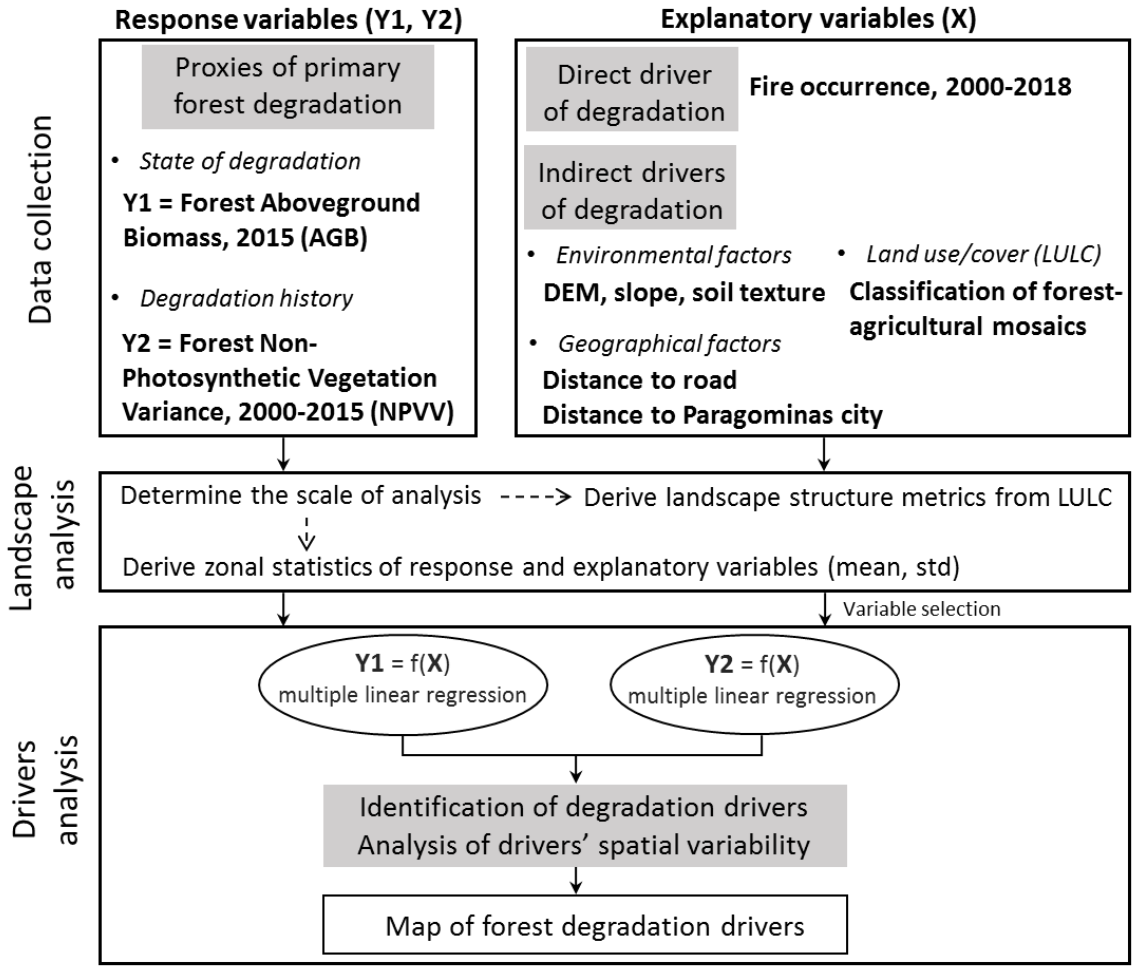

Figure 4.3 Workflow of the method used to identify and map forest degradation drivers at the landscape scale.

4.2.3.1 Proxies of primary forest degradation

Two proxies of forest degradation were used as response variables in this study. They provide spatial information on the state of forest degradation in 2015 and on the history of degradation between 2000 and 2015 (Fig 4.4).

The first proxy is the aboveground biomass (AGB) and forest structure assessed at a resolution of 20m in 2015 (Bourgoin et al. 2018). It was produced from multisource remote sensing calibrated using in-situ field inventory data and regression analysis (Berenguer et al. 2014). Values range from 57 to 454 $Mg{\cdot}ha^{-1}$ and the AGB of 87% of primary forest is below the degradation threshold of 286 $Mg{\cdot}ha^{-1}$ (specific for Paragominas)(see Bourgoin et al. 2018 section 4.2.2). Degraded forests are mainly located in the central part of the study area and along the edges of forest patches.

The second proxy is the non-photosynthetic vegetation variance (NPVV) (30m spatial resolution). It was produced using a time series of Landsat images (2000-2015) acquired during the dry season and Claslite spectral mixture analysis (Asner et al. 2009b). It is directly linked with forest degradation history and differentiates undisturbed forests, selectively logged forests (values between 2-5), overlogged forests with no management plan (values between 3-9) and burned forests (values higher than 8)(Hasan et al. 2019a).

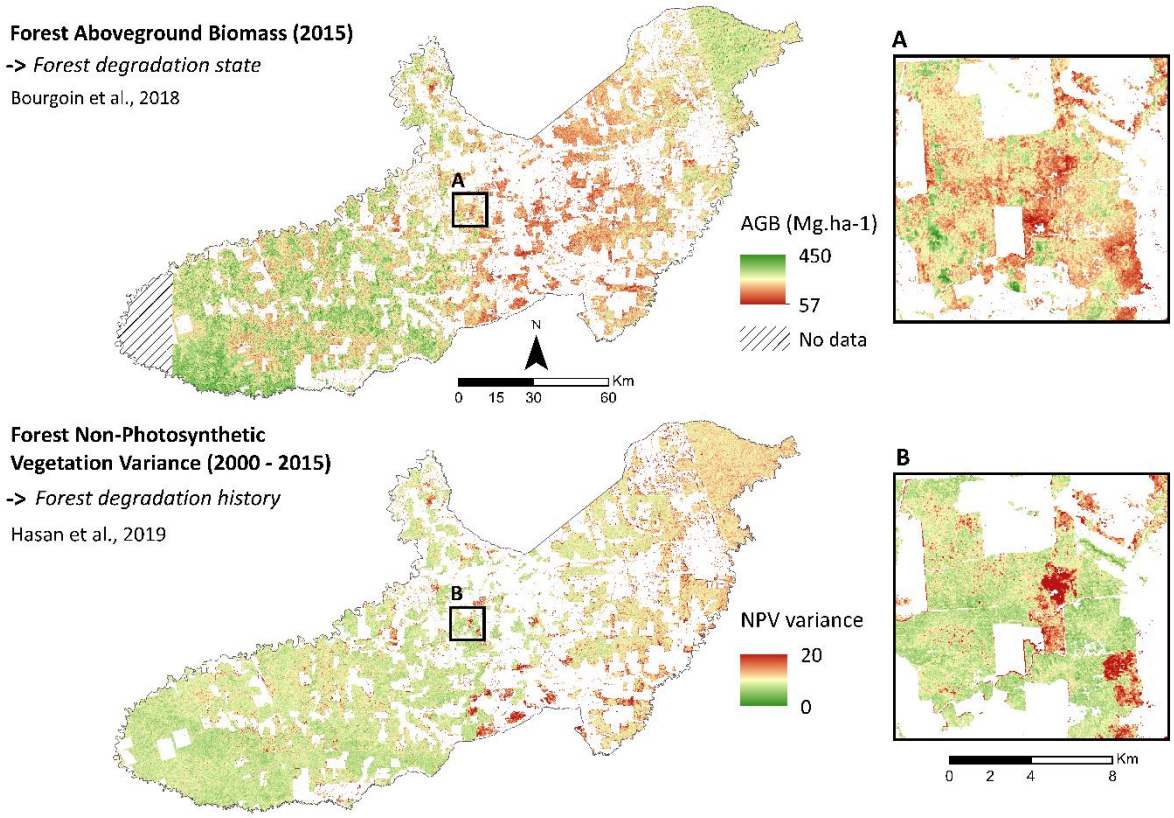

Figure 4.4 Aboveground biomass and non-photosynthetic vegetation variance as proxies of primary forest degradation (non-primary forest is shown in white).

4.2.3.2 Direct drivers of forest degradation

We collected inter-annual fire occurrence data from MODIS fire products (MOD14A2 and MYD14A2, high confidence values) between 2000 and 2018 (Giglio 2015). We resampled the data from 1km to 100m using the nearest neighbor algorithm (Fig 4.5).

4.2.3.3 Indirect drivers of forest degradation

Environmental factors

We used the SRTM 90m Digital Elevation Database v4.1 (Jarvis et al. 2008), derived slope and soil texture (Laurent et al. 2017) as environmental factors. The plateaus (100-220m elevation) are flat and the clay soils are fertile and consequently suitable for agriculture, the slopes are generally too steep for mechanization, while the valleys (45-80m elevation) are covered by loamy sand soil that is less suitable for agriculture (Fig 4.5).

Geographical factors

Distance to the road network (derived from OpenStreeMap) was created using the Euclidean distance and assessed forest patch accessibility (30m resolution). Distance to Paragominas city (Euclidean distance) was used to assess forest patch accessibility and market accessibility (Fig 4.5).

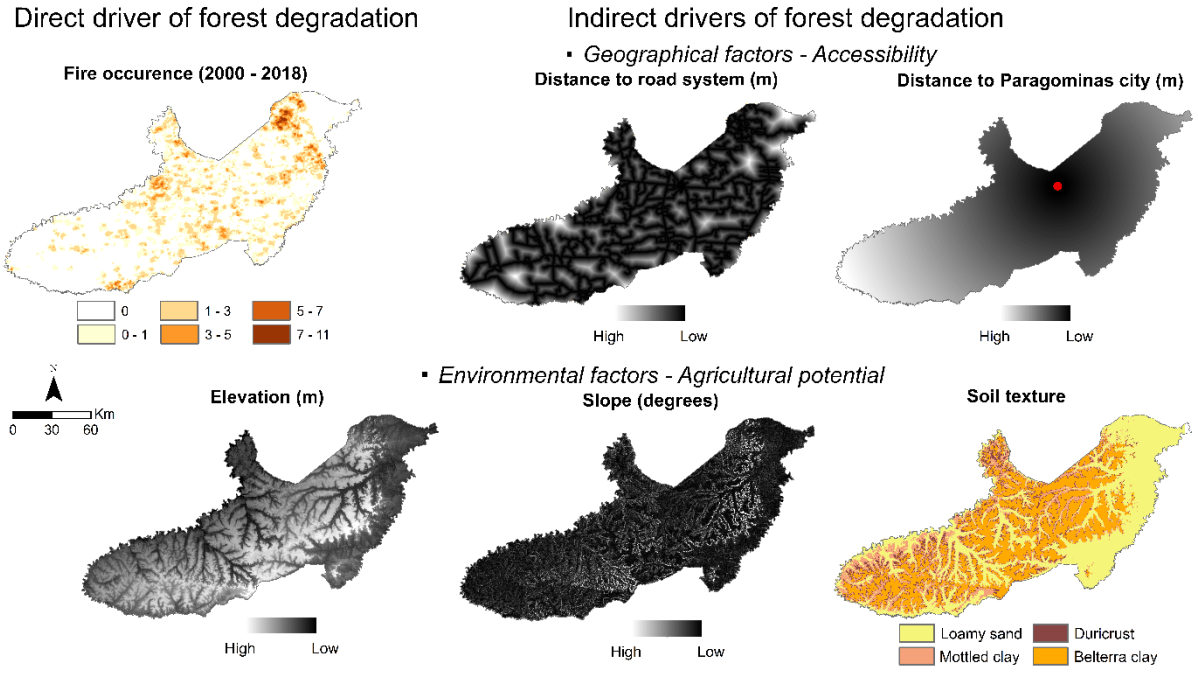

Figure 4.5 Direct and indirect drivers of forest degradation

Land use/land cover classification of forest-agriculture mosaics

Land use/land cover (LULC) was classified using Landsat images acquired at different dates (1988, 1995, 2001, 2009, 2017). These dates were chosen according to the main socio-economic phases in Paragominas (see Section 4.2.2). All the images presented less than 10% cloud cover, were acquired during the dry season (June to October), and were pre-processed to surface reflectance data using the algorithm developed by the NASA Goddard Space Flight Center (GSFC)(Appendix 4.1). Field data were collected in September 2017 to train and validate the classification algorithm. Based on 328 GPS points in different locations in the municipality (Fig 4.2) by visual interpretation of the 2017 image, we created a ground data set sub-divided into 10 classes (Appendix 4.2 and 4.3): cloud, shadow, artificial surface, water body, cropland, bare soil, pasture, plantation, forest and *juquiera* (initial stage of regrowth in pastures abandoned by low income owners). The ground data set for the other historical images was built using visual interpretation of forested and non-forested areas.

On the date of each analysis, the classification method used Landsat features (spectral bands and vegetation indices, see Appendix 4.1 and 4.4) and the ground data set (randomly separated into 50 pairs of training and validation samples) as inputs for the Random Forest (RF) classifier (Breiman 2001). This method is similar to the one developed by Mercier et al. (2019). We extracted overall accuracy, the kappa index, user and producer accuracy of each class from the confusion matrix. We used the RF package in R for the classification (Liaw and Wiener 2002). The 2017 forest cover class was divided into primary forest (classified as forest throughout the study period) and secondary forest (conversion from non-forest to forest cover) based on the historical classifications. Finally, we merged secondary forests detected between 1988-2017 with *juquiera* detected in 2017 using ArcGIS (Esri, Redlands, CA, USA).

4.2.3.4 Landscape analysis

First, we determined the landscape scale that best captures the spatial heterogeneity of landscape elements in order to define the size of a regular analytical grid (Bourgoin et al. 2020). Based on the land use/cover (section 4.2.3.2), we calculated the Shannon diversity index (SHDI) in 100 different regions (regular sampling at points located 15km apart) throughout the study area. This metric measures the proportion of landscape elements in a given area. We calculated the SHDI in buffer zones whose widths ranged from 90m to 20km around each region of interest. We estimated the plateauing of the average curve based on the resulting profiles of SHDI and recorded a corresponding distance of 6km. This value defines the size of the regular grid (total 504 units) applied to Paragominas municipality (Appendix 4.5).

Second, within each unit, we computed landscape structure metrics from the land use/cover to characterize landscape composition and configuration and hence specific spatial structures of forest-agricultural mosaics based on the concepts of heterogeneity, connectivity and fragmentation (Burel and Baudry 1999). These metrics reflect land use processes and their consequences for the spatial distribution of landscape elements and patches such as forest fragmentation and the heterogeneity of mosaics (Table 4.1). The selected landscape structure metrics were calculated using the free software Chloe 4.0 (Boussard and Baudry 2017).

Table 4.1 Landscape structure metrics (composition and configuration)

Metric	Code	Formula	Description
Extent of land under each land use/land cover (i)	pNV_i	$p(i)$	Percentage of pixels for class "i"
Interface between paired land uses i and j	pNC_i_j	$p(i,j)$	Percentage of edge pixels between paired land use types "i" and "j"
Shannon diversity index	SHDI	$-\sum p(i) * \ln(p(i))$	Diversity metric that takes both the number of classes and the abundance of each class into account (Shannon and Weaver 1949)
Complexity index	CSHDI	$NSHDI * (1 - NSHDI)$ with NSHDI is the normalization of SHDI	Parabolic transformation of SHDI
Heterogeneity composition index	HET_agg	$-\sum p(i,j) * \ln(p(i,j))$ with i=j	Heterogeneity for homogeneous couples (Burel and Baudry 1999)
Heterogeneity structure index	HET_frag	$-\sum p(i,j) * \ln(p(i,j))$ with i≠j	Heterogeneity for non-homogeneous couples (Burel and Baudry 1999)

Finally, we extracted the average ("mean") of other explanatory variables and the average and standard deviation ("std") of forest degradation proxies to capture the extent of spatial variability of primary forest degradation in each grid.

4.2.3.5 Drivers analysis

First, we analyzed the relationships between proxies of forest degradation (mean/std AGB, mean/std NPVV) and direct (fire occurrence) and indirect drivers (landscape structure metrics, geographical and environmental factors) to identify the most significant forest degradation drivers (Cornillon and Matzner-Løber 2007). We then applied multiple linear regression to each forest degradation proxy. Next, we applied stepwise selection using Cp criteria and the regsubset function of the leaps R package to select only the most significant explanatory variables (Mallows 1973; Le Clec'h et al. 2017; Lumley 2017). This procedure was necessary to obtain the model with the smallest number of variables that fitted the data and to avoid noise and collinearity. We then applied a cross-validation procedure in which the learning set was randomly partitioned into k equal size sub-samples with k=5 (Arlot and Celisse 2010; Kohavi 1995). Each regression process was then applied in which k-1 sub-samples were used as training data and the remaining samples were used for validation. This process was repeated by changing the training/validation sub-samples in such a way that all the learning samples were also used for validation. The R-squared and average root mean square error (RMSE) served as the performance metrics for each model. To facilitate their interpretation, the scores of each explanatory variable were standardized.

Second, we analyzed the spatial variability and complementarity of forest degradation drivers identified in the previous step. The most significant explanatory variables influencing forest degradation proxies were grouped into clusters using a three-step clustering method (Husson et al., 2010). The method combined principal component analysis, hierarchical clustering using Ward's criterion and k-means clustering to improve the initial partitioning. The number of clusters was identified using the elbow method, which calculates the total intra-cluster variation or total within-cluster sum of squares (WSS) for a range of cluster sizes varying from 1 to 15 (Charrad et al. 2014). Each cluster was then linked to the most significant drivers of forest degradation (ANOVA with $p < 0.05$ indicating if the mean driver value in the cluster is lower or higher than the overall mean for all clusters). The clustering was performed using the R package FactoMineR (Lê et al., 2008).

4.3 Results

4.3.1 Land use/land cover classification of forest-agriculture mosaics

Using Landsat-8 images, LULC classification in 2017 revealed high overall accuracy and kappa indexes (e.g. OA=0.87 and kappa=0.86). Most classes presented high user and producer accuracy (> 0.8). Bare soil, secondary forest and pasture classes presented omission and commission errors (Appendix 4.6). The classification errors and confusion were due to the difficulty in differentiating the complex gradient of vegetation structure among these three classes. Using historical Landsat images, forest/non-forest classifications were highly accurate (kappa= 0.9) (Appendix 4.7).

The 2017 land use/land cover map shows heterogeneous landscape mosaics dominated by different land uses (Fig 4.6a). The central region is dominated by large scale homogeneous cropland, tree plantations and pastureland with small isolated patches of primary forest (Fig 4.6d). Smallholder areas accounted for a diversity of land use mosaics ranging from secondary forests associated with large patches of primary forest and pastures (Fig 4.6b), to small fragmented patches of primary forest in pasture and croplands shaped by early deforestation in the 2000s (Fig 4.6e and Appendix 4.7) and secondary forests interspersed with very small patches of remnant forest (Fig 4.6g and Appendix 4.7). A large portion of the western part and, to a lesser extent, of the eastern and northern parts of the municipality, are marked by large homogeneous forest patches (Fig 4.6b and 4.6f) and highly heterogeneous fragmented landscape mosaics (Fig 4.6c). The eastern (indigenous reserve) and western (CIKEL) parts present a large homogeneous, contiguous patch of primary forest (Fig 4.6a).

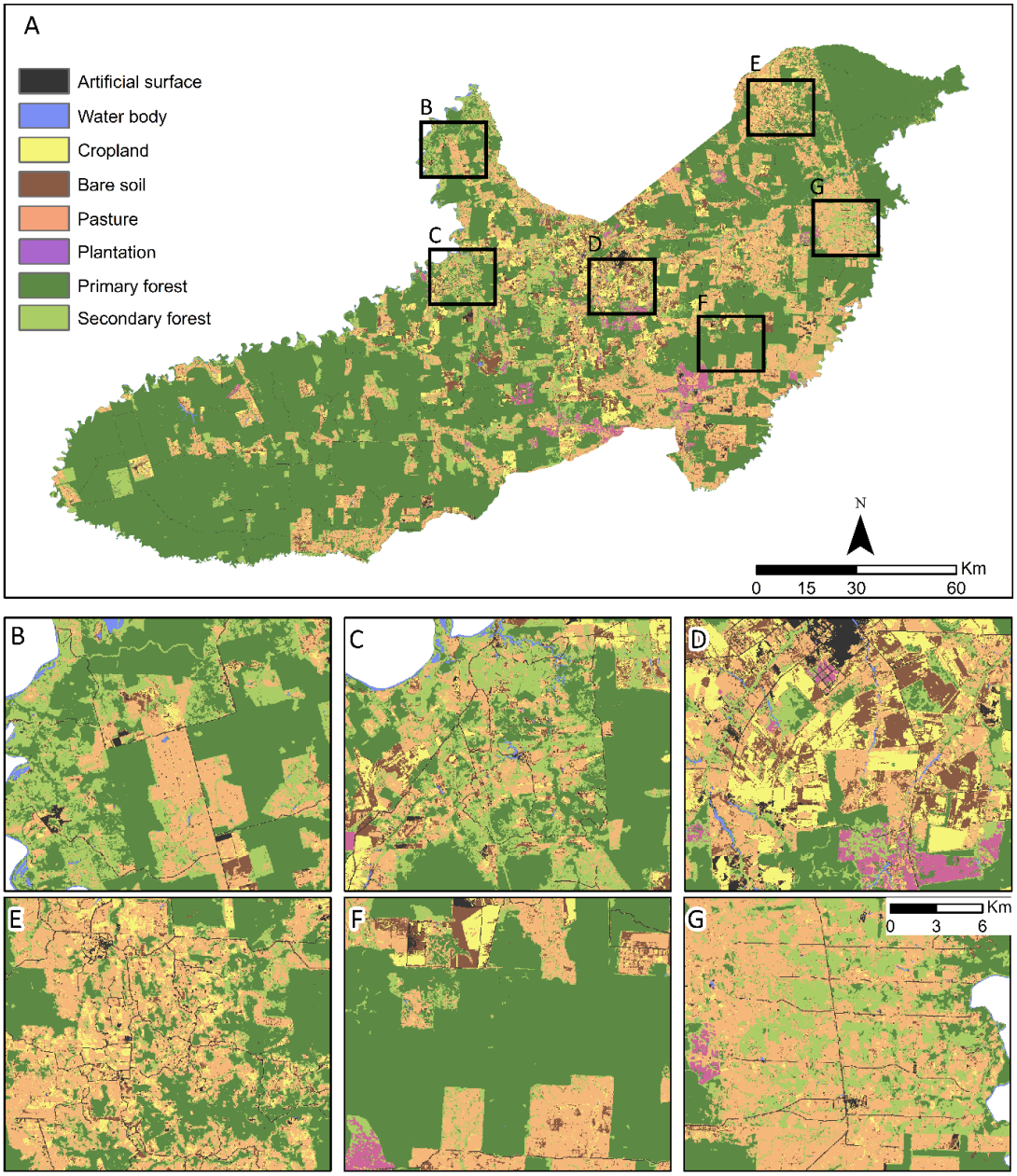

Figure 4.6 Land use/land cover classification combining current landscape mosaics and 29 years of secondary forest mapping using Landsat images (Fig 4.6b to Fig 4.6g are examples of the heterogeneity of land use/cover mosaics).

4.3.2 Identification of the drivers of primary forest degradation

Following cross validation, the models showed very high goodness-of-fit between the predicted and observed values (Table 4.2 and Appendix 4.8). The mean AGB model explained 80% of the variance and the most explanatory variables were distance to Paragominas city, topography (elevation and slope), the proportion of primary forest patches and the interfaces between forest/pasture and forest/bare soil. The results of the Std-AGB model were not taken into account due to its poor

performance (r^2: 0.31, RMSE: 5.49). The mean NPVV explained 58% of the variance and the most explanatory variables were distance to Paragominas city, the interfaces between forest/pasture, the proportion of primary forest patches, fire occurrence and the heterogeneity metric (HET_agg). The std-NPVV explained 67% of the variance and the most explanatory variables were the proportion of primary forest, elevation, the interfaces between forest/pasture, the proportion of forest patches, and the heterogeneity metric (HET_agg).

Table 4.2 Multiple linear regression models for the prediction of forest degradation proxies (mean of AGB, mean and standard deviation of NPVV) from direct and indirect drivers. The positive or negative sign refers to the type of correlation (positive or negative).

Models	R^2	RMSE	Most significant drivers (direct and indirect)
Mean AGB	0.80	14.26 $Mg.ha^{-1}$	Distance to Pgm (+), Elevation (-), Slope (+), pNV_Forest (+), pNC_Forest_Pasture (-), pNC_Forest_BareSoil (+)
Mean NPVV	0.58	0.85	Distance to Pgm (-), Sand_proportion (+), Fire occurrence (+), pNV_Forest (-), HET_agg (-), pNC_Forest_Pasture (+)
Std NPVV	0.67	0.55	pNV_Forest (-), HET_frag (+), SHDI (+), CSHDI (+), Elevation (+), Sand_proportion (+)

Proximity to Paragominas city (between 0 and 75km) had a significant negative impact on the average primary forest AGB (between 150 and 220 $Mg.ha^{-1}$ on average). Beyond 75km, the average AGB stabilized around 250 and 300 $Mg.ha^{-1}$ (Fig 4.7). Fire affected mean NPVV beyond the occurrence of two events in the period 2000-2018, with marked variability beyond this value. The length of the interface between forest and pastureland triggered an increase in Std-NPVV, which was interpreted as more variability in the extent of forest degradation. Heterogenous composition and structure of the landscape mosaics had a direct effect (sharp decrease) on mean AGB and (increase after 0.5) on Std NPVV. Finally, the proportion of forest patches representing primary forest fragmentation was positively correlated with mean AGB. Landscapes with less than 50% of forest area had less than 200 $Mg.ha^{-1}$ degraded forests, whereas landscapes with more than 50% of forest area had an AGB between 200 and 300 $Mg.ha^{-1}$ on average.

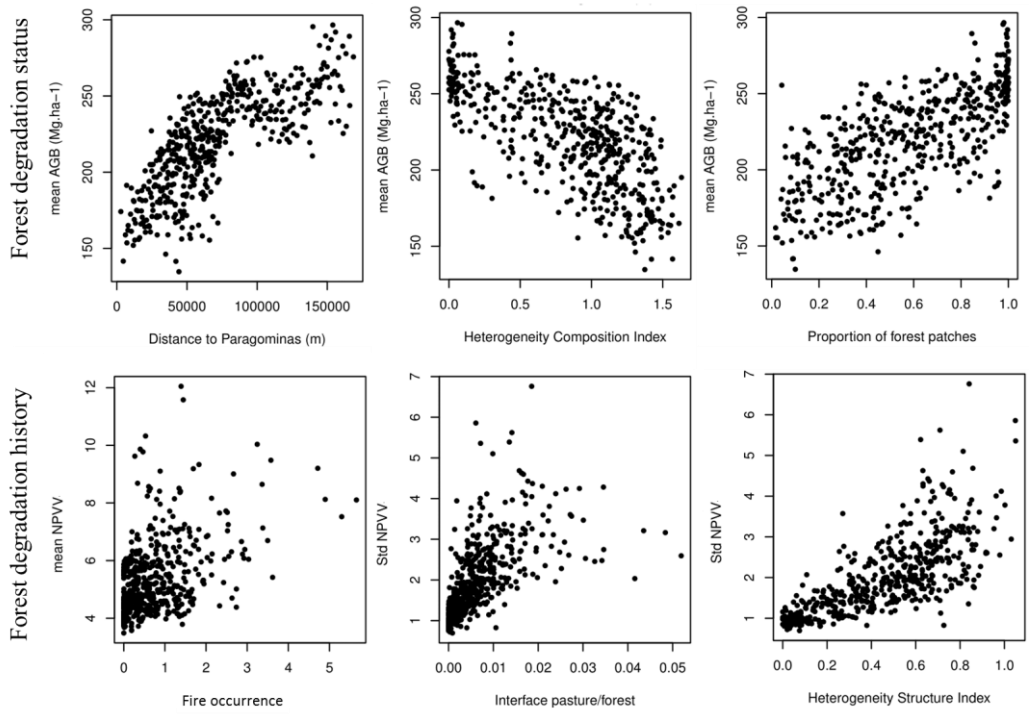

Figure 4.7 Forest degradation proxies and their relationship with some drivers of forest degradation

4.3.3 Mapping the drivers of primary forest degradation

The clustering method allowed us to identify six clusters of forest degradation drivers (corresponded to the location of a bend in the WSS curve). The resulting classification shows clusters grouped in distinct patches within Paragominas demonstrating that the drivers are unequally distributed in the municipality and that spatial covariation exists (Fig 4.8).

Cluster 1 groups landscapes located more than 100km from Paragominas city, in elevated terrain compared to the overall elevation of the terrain in the municipality, very low heterogeneity and absence of fire. These areas are largely dominated by patches of primary forest and limited interface between pasture and forest. **Cluster 2** has similar characteristics in terms of distance to Paragominas city and landscape structure to cluster 1 except that the elevation is below 80m (sandy soils). **Cluster 3** is located on elevated plateaus in the eastern and western central part of the municipality and is characterized by heterogeneous mosaics of large patches of primary forest interspersed with secondary forests and relativity longer interfaces between forest and pasture than cluster 2. **Cluster 4** groups landscapes located closer to Paragominas city (< 75km), in low areas (valleys) with considerable amount of interface between forest and pasture, high heterogeneity and fragmentation (proportion of forest < 0.5). **Cluster 5** is located in the central part of the municipality and groups landscapes located less than 50 km from Paragominas city, on elevated plateaus (around 120m a.s.l.),

characterized by high heterogeneity and primary forest fragmentation and an average of one fire detected. **Cluster 6** is specifically distributed between the northeastern and western central parts of the municipality where the landscapes are characterized by the longest forest/pastures interfaces and average fire occurrence (around three fire events detected annually between 2000 and 2018). These landscapes are also more fragmented and heterogeneous than average in the municipality (respectively HET_frag = 0.7 and pNV_Forest = 0.3 on average).

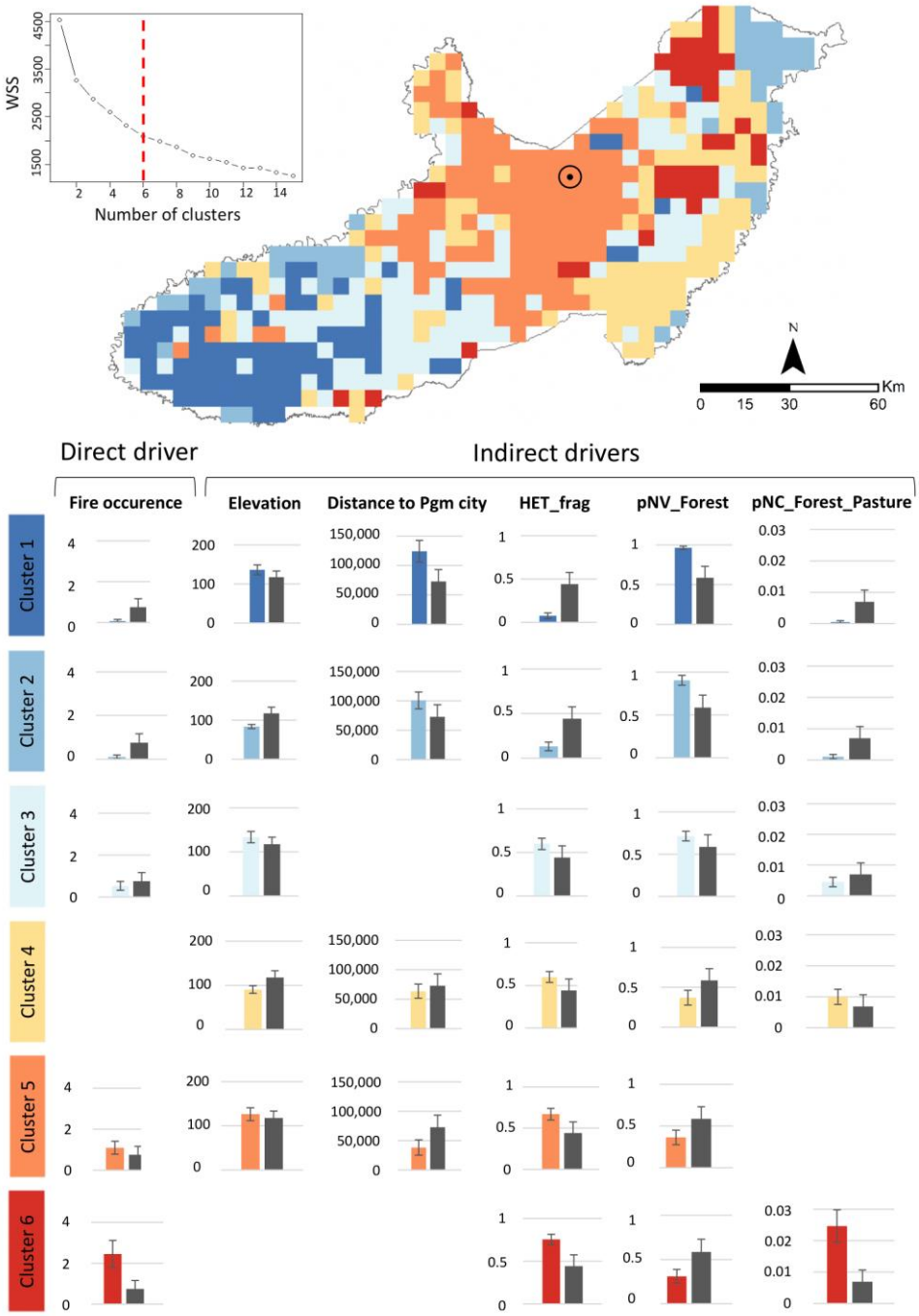

Figure 4.8 Map of clusters of proxies of direct and indirect forest degradation drivers. Grey bars represent the mean indicator value of all the clusters, empty slots mean the variable was not significant for that particular cluster.

4.4 Discussion

The aim of our study was to disentangle the drivers of primary forest degradation along an old Amazonian deforestation front using a landscape-level approach that was originally proposed by Melito et al. (2017). This approach responded to a clearly stated need for a more comprehensive understanding of forest degradation drivers at the landscape scale linking land use processes and the state of the forest cover that goes beyond the identification of direct logging and fire drivers (Nepstad et al. 2008; Morales-Barquero et al. 2015).

4.4.1 Cascades of indirect and direct drivers of forest degradation in human-modified landscapes

We demonstrate that the degradation of primary forest is the result of different land use processes at the regional scale and their multiple and combined consequences at the landscape scale. We provide clear evidence that the indirect and direct drivers of degradation act as a bundle and create homogenous patterns in this municipality. This attests to their spatial covariation and inter-dependency and reveals different land use dynamics and management practices.

Along the old deforestation front, a cascade of effects at multiple scales indirectly drove forest degradation (cluster 5). At regional level, the conversion of forest for the expansion of cattle ranching as part of the colonization process triggered large-scale land use change, which in turn, caused landscape fragmentation. Fragmentation amplified feedback loops through edge effects and fostered selective logging and the overexploitation of timber, causing increased fragmentation over time (Broadbent et al. 2008; Viana et al. 2016). More recently, agricultural expansion triggered new waves of deforestation but also conversion of pasture for the cultivation of cash crops (Osis et al. 2019). The consequences were changes in the configuration of the landscape (i.e. increased fragmentation and heterogeneity) that indirectly drove degradation (through edge effects and enhanced logging) but also changes in land use/land cover type and practices. In these heterogeneous landscape mosaics, the combined effects of forest fragmentation and high agricultural potential due to fertile soil suitable for agriculture were indirect drivers of forest degradation. Competition for land between agriculture (soybean and maize production) and primary forest patches located on the elevated plateaus resulted in increased human-set fires (three annual fire events detected between 2000 and 2018) as signs of agriculture expansion processes (Osis et al. 2019). These cascades were accentuated by the complex socio-economic, demographic and land management effects that are captured by proximity to

Paragominas (i.e. within a radius of 75km from the city). Indeed, this variable increased access to forest resources but also to areas suitable for the development of agriculture (Laurent et al. 2017).

We also showed that specific land tenure regimes such as smallholder dominated areas generate unique landscape structures (cluster 6). In these landscapes, the current state of forest cover (high degradation) is the joint result of historical processes (deforestation, degradation) prior to the installation of smallholder farmers and of recent interactions between degradation drivers. Our study provides insights into these recent processes. We found that frequent (up to seven fire events between 2000 and 2018) and recent fires (after 2015) were spatially coupled with high fragmentation and heterogeneity marked by forest and pasture interfaces. This can be explained by the use of fire in pasture management and in slash and burn agriculture used by smallholder farmers. Fires and their impact on forest structure increase due to the extreme fragmentation of forest patches (less than 30% of forest)(Silva Junior et al. 2018). Fragmentation triggers the desiccation of forest edges (Briant et al. 2010; Laurance et al. 2011) and the partial destruction of the canopy structure (Almeida et al. 2019; Shapiro et al. 2016). The damaged structure makes the forest more vulnerable to fire (Morton et al. 2011; Rappaport et al. 2018). The combined effects of forest edge and degraded forest structures may be amplified by severe and repetitive drought such as the El Niño 2015 event (Alencar et al. 2015; Le Page et al. 2017).

This study also showed that distance to roads was not a significant indirect driver of primary forest degradation whereas it was previously considered to be one of the main indirect drivers of deforestation (Laurance et al. 2002). This can be explained by the predominance of land use effects on forest degradation over road proximity in our modeling approach. However, more parameters regarding the type of road (quality, public/private) need to be taken into account as they may influence the results.

4.4.2 Limitations and future outlook

Although the identification and mapping of forest degradation drivers yielded good results, we identified several limitations that will be overcome in further study. Firstly, all the results presented here rely on the accuracy and validity of forest degradation proxies. These results are themselves the result of complex modeling and errors in the assessment of the state of forest cover are non-negligible (Bourgoin et al. 2018; Hasan et al. 2019a). Secondly, in the future, limitations due to data availability could be overcome by including supplementary data such as direct drivers (i.e. accumulation of logging events) and indirect drivers of degradation such as climate (environmental factor), land tenure (policy

and land management factor) as well as socio-economic data. Although the main accessibility effects are organized along the main road of the municipality, it is worth mentioning that we considered the study area as an isolated area and did not take other accessibility effects in neighboring municipalities into account. Thirdly, some of the variables used in this study capture mixed processes and could be further refined: (i) distance to Paragominas city assesses accessibility but also land tenure as two land tenure systems in the extreme eastern and western part of the study area host conserved forests, and (ii) fire occurrence groups both forest and land fires and is both a direct driver of degradation and a proxy of agricultural practices (slash and burn agriculture or wild fires).

Despite these limitations, our approach underlined the importance of using the landscape approach to characterize and map the drivers of degradation. More particularly, we reveal that the status of degradation of remnant forest patches is directly linked with their surrounding matrix and thus with land uses and land use changes occurring at that scale (Godron and Forman 1981). In this sense, we highlighted major benefits to be gained by characterizing degradation drivers at the landscape scale using land cover/land use mapping and remote sensing. Landscape structure metrics and the resulting indicators describing the heterogeneity of the mosaic depend on the validity and accuracy of LULC classifications. The remote sensing field of research is improving significantly thanks to the development of novel classification algorithms and the accessibility of near-real time and high resolution imagery (Bégué et al. 2018). The 2017 land cover/land use map was produced with a high degree of accuracy and required only a short processing time. Minor misclassifications were detected between the land cover classes that showed similar vegetation structure and were spatially difficult to identify in the field and to differentiate using Landsat images. Transition classes such as fallows, which often cause misclassification, proved difficult to map (Hett et al. 2012). High temporal resolution of optical and radar imagery could help describe and account for the phenology of vegetation when mapping forest-agriculture mosaics (Mercier et al. 2019). Furthermore, small agricultural systems can be mapped using combined pixel and object-based approaches and promising results have already been obtained with the characterization of fine cropland uses (Lebourgeois et al. 2017).

The robust relationships between forest degradation proxies and direct and indirect drivers of degradation we identified offer opportunities to assess the state of forest cover at a large scale based on regional LULC mapping. The identification, characterization and measurement of forest degradation remains a scientific challenge in the remote sensing community and there is as yet no consensus concerning the wide range of existing methodologies to map degraded forest at large scale (Frolking et al. 2009; Herold et al. 2011; Hirschmugl et al. 2017; Mitchell et al. 2017). Land cover/land use, landscape structure metrics, geographical and environmental factors would therefore be relevant indicators for estimating primary forest degradation. The Mapbiomas project (http://mapbiomas.org)

is a good example of cloud computing of Landsat archive images that would allow mapping land cover/land use of Brazil from 2000 to 2016 at a resolution of 30m.

4.4.3 Potential of characterizing and mapping forest degradation drivers for land use planning and targeted conservation actions

Our results emphasize the fact that the degradation of primary forest and the respective landscape-level drivers are found in specific areas, and consequently require spatially targeted forest management in a given territory. We have highlighted the complex interconnections between the forest patch and landscape scales that would enable the identification of levers of action to reduce the effects of land use and to mitigate degradation. For instance, policy reinforcement is crucial to prevent illegal logging and forest encroachment but also to support intensification of agriculture/ livestock activities in areas with high fragmentation and heterogeneity. Beyond fire bans which do not provide alternative ways of earning a living, the collective engagement of local people in improving fire management and control is essential to efficiently reduce fire risks, especially in highly degraded and fragmented landscapes (Cammelli et al. 2019).

We wish to emphasize that targeted management of forest landscapes in the clusters of forest degradation drivers we identified could be one of the main principles of Paragominas municipality's green development pact to ensure both production and conservation goals are reached (Griscom and Goodman 2015). This green development pact also involves the active engagement of stakeholders in sustainable land management. Despite the homogeneous clusters of forest degradation drivers, our study showed that in specific areas, degradation of forest patches was prevented regardless of easy access (proximity to Paragominas city), agricultural potential (fertile soils) and current level of heterogeneity of the surrounding mosaics (cluster 3). These particular areas may reflect the strategies of individual stakeholders who are willing to apply sustainable land management. The green development pact should therefore be guided by these strategies in order to reduce forest degradation risks.

Understanding the drivers of forest degradation is crucial for the development of policies and measures for effective but sustainable management of degraded forests at the landscape scale to guarantee the conservation and betterment of their ecological values (Goldstein 2014). Data concerning both the severity of degradation and the drivers of degradation provide key information to enable decision makers prioritize and tailor interventions at the landscape scale (Chazdon and Guariguata 2018). Forest landscape restoration appears to be an effective strategy to mitigate the

effect of forest degradation such as positive fragmentation feedback loops (Lamb et al. 2005). Beyond conserving biodiversity and improving ecological functioning, forest landscape restoration by increasing forest mosaic connectivity would enhance their resilience and functionality (Brancalion and Chazdon 2017).

4.5 Conclusion

In this Chapter, we identified and mapped the indirect and direct drivers of forest degradation. We also highlighted the interconnection between land use processes and landscape structures and how indirect factors affect forest cover. In the central part of the municipality, forests are degraded because of past overexploitation of timber, which has been indirectly enhanced by accessibility to forest patches and markets, and more recently due to conflicts associated with agricultural expansion processes and negative feedback loops generated by fragmentation, therefore affecting forest structure. In more complex landscape mosaics, forests are degraded due to the joint result of historical processes and recent interactions between degradation drivers such as fire used in the management of agricultural lands and forest landscape fragmentation.

4.6 Perspectives of forest potential impact assessment

In the framework of **forest ecological vulnerability assessment**, the identified drivers of degradation can be considered as **exposure** factors while forest aboveground biomass and forest non-photosynthetic vegetation variance are proxies of **sensitivity**. To complement the assessement of exposure component, another dimension that can be added is the temporal dynamic of agricultural expansion in terms of rates of changes in landscape composition and configuration. This would add additional weight to distinguish an area where the drivers of degradation are present but the dynamics of the deforestation front are slowed or stabilized from an area where the drivers are present and the dynamics of deforestation front are still active and can further accentuate the negative effects of degradation drivers (e.g. through increased fragmentation).

We used the same method developed in Chapter 5 (section 5.2.2.3) in order to identify landscape trajectories and thus characterize agricultural expansion dynamics. For each of the historical classification (1988, 1995, 2000, 2009 and 2017), we extracted forest/non-forest compositon in the same regular grid presented in section 4.2.3.4 (6*6km). We also calculated configuration metrics to

quantify size, proportion and aggregation, richness and shape of the landscape (see Chapter 5). The resulting 3D matrix (grid units/5 dates/structure metrics) was analyzed using PCA and ACT-STATIS and 10 classes of landscape trajectories were identified (Oszwald et al. 2011). The analysis of the average composition (forest and cropland) and configuration (Edge density) metrics over time showed that classes **T1 to T5** group forest-dominated units (mainly located in the eastern and western part of the municipality) (Fig 4.9). Classes **T9 and T10** group units where the balance between forested and non-forest areas remained unchanged throughout the study period (with constant average edge density). They are scattered in Paragominas and are stabilized forest/pasture landscapes. **T6** groups units dominated by cropland since 2000. It is mainly located in the central part and correspond to soybean cultivation after the boom in agro-industry. **T7** groups forest dominated units characterized by a slow decrease in forest cover since 1995 – 2000 associated with a gradual increase in cropland and edge density. T7 corresponded to areas of agricultural expansion that were slowed down in 2009 following the green development pact. **T8** groups forest dominated units experiencing a sharp decrease in forest cover with no stabilization at the end of the trajectory (compared with T7). T8 is mainly located in the northeast part of the municipality and scattered in other parts.

Compiling indictors of forest degradation, of drivers of degradation and dynamics of agricultural expansion would allow assessing **forest potential impact**. Assessing forest **adaptive capacity** remains a perspective that needs to be developed for mapping forest ecological vulnerability.

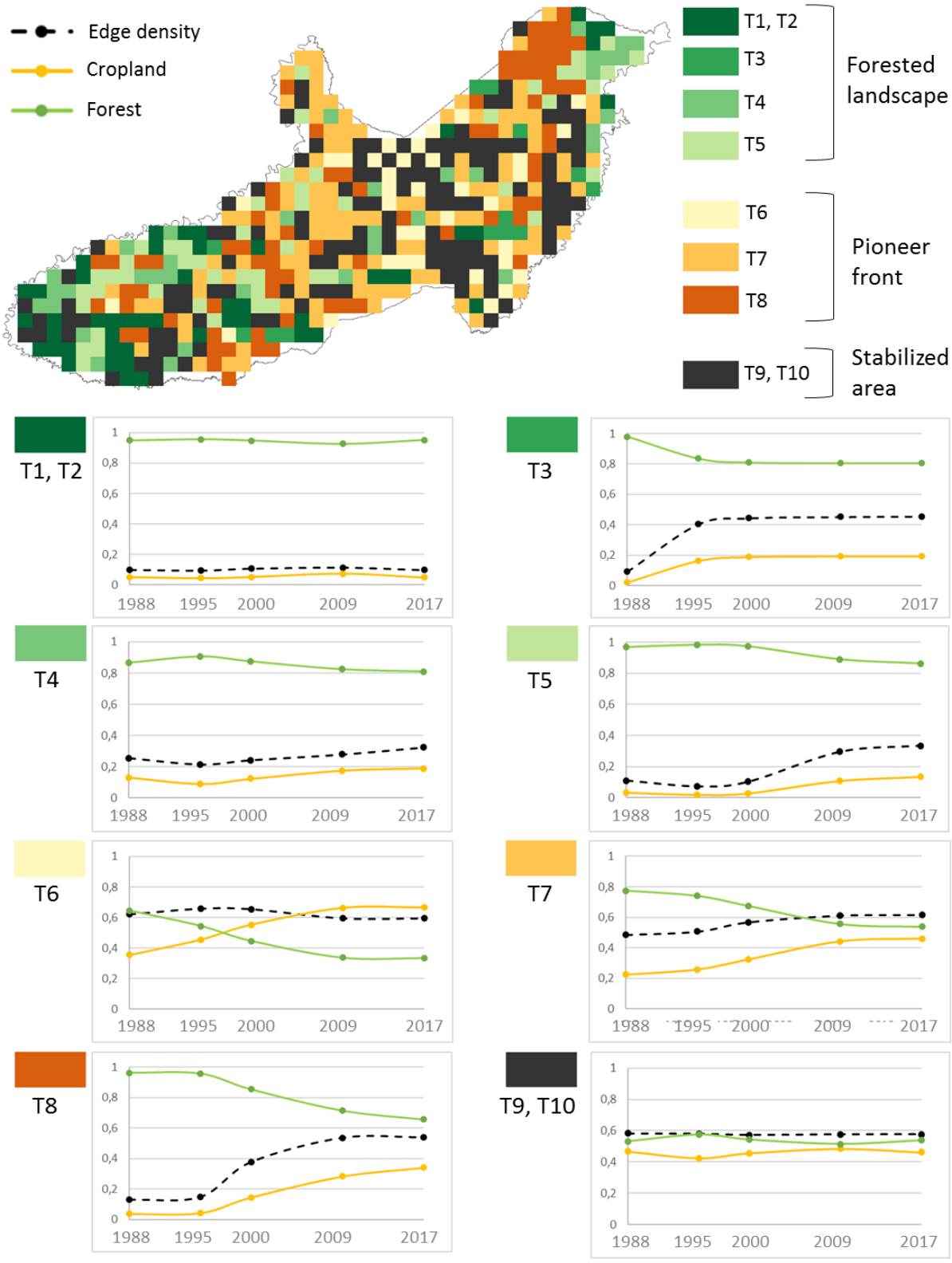

Figure 4.9 Classes of landscape trajectories (T1 to T10) based on land cover composition and configuration dynamics from 1988 to 2017 obtained using ACT-STATIS and clustering methods

Chapter 5 - Assessing the ecological vulnerability of forest landscape to agricultural frontier expansion in the Central Highlands of Vietnam

An agriculture frontier separating coffee plantation from primary evergreen forest (picture by Clément Bourgoin)

Reproduced from the article:

Bourgoin C., Oszwald J., Bourgoin J., Gond V., Blanc L., Dessard H., Phan VT., Plinio S., Läderach P. and Reymondin L. (2019) Assessing the ecological vulnerability of forest landscape to agricultural frontier expansion in the Central Highlands of Vietnam Environmental Research Letters. International Journal of Applied Earth Observation and Geoinformation, 84 : 13 p. https://doi.org/10.1016/j.jag.2019.101958

Assessing the ecological vulnerability of forest landscape to agricultural frontier expansion in the Central Highlands of Vietnam

Bourgoin C.[1,2,3]*, Oszwald J.[4], Bourgoin J.[5,6], Gond V.[1,2], Blanc L.[1,2], Dessard H.[1,2], Phan VT.[3], Plinio Sist[1,2], Läderach P.[3] and Reymondin L.[3]

[1] CIRAD, Forêts et Sociétés, F-34398 Montpellier, France
[2] Forêts et Sociétés, Université Montpellier, CIRAD, Montpellier, France.
[3] International Center for Tropical Agriculture (CIAT), Hanoi, Vietnam
[4] UMR CNRS LETG 6554, Laboratory of Geography and Remote Sensing COSTEL, Université de Rennes 2
[5] CIRAD, UMR TETIS, F-34398 Montpellier, France
[6] TETIS, Université Montpellier, AgroParisTech, CIRAD, CNRS, IRSTEA, Montpellier, France

Abstract

Forest conservation in human-dominated tropical landscapes ensures provision of major ecosystem services. However, conservation goals are threatened by growing demands for agricultural products. As the expansion of agricultural frontiers continues to exert increasing pressure on forest cover, it is crucial to provide indicators on forest vulnerability to improve our understanding of forest dynamics and prioritize management actions by local decision-makers. The purpose of this study is to develop a rigorous methodological framework to assess forest ecological vulnerability. We aim at evaluating the potential of remote sensing to characterize forest landscape dynamics in spatial and temporal dimensions. We present an innovative method that spatially integrates current landscape mosaic mapping with 45 years of landscape trajectories using Sentinel-2 and Landsat imagery. We derive indicators of exposure to cropland expansion, sensitivity linked with forest degradation and fragmentation, and forest capacity to respond based on forest landscape composition in Di Linh district in the Central Highlands of Vietnam. We map current forest-agricultural mosaics with high accuracy to assess landscape intensification (kappa index = 0.78). We also map the expansion of the agricultural frontier and highlighted heterogeneous agricultural encroachment on forested areas (kappa index = 0.72-0.93). Finally, we identify degradation and fragmentation trajectories that affect forest cover at different rates and intensity. Combined, these indicators pinpoint hotspots of forest vulnerability. This study provides tailored management responses and levers for action by local decision makers. The accessibility of multi-dimensional remote sensing data and the developed landscape approach open promising perspectives for continuously monitoring agricultural frontiers.

Keywords Deforestation, Forest degradation, Vietnam, Ecological vulnerability, Landscape approach

5.1 Introduction

The conservation of forest cover is a key to ensuring sustainable provision of multiple ecosystem services in ecological, climate, biogeochemical and biodiversity processes (I. Thompson et al. 2009). In human-modified landscapes, forest conservation must also be reconciled with agricultural productivity, food security actions and must support the livelihoods of human populations (Chazdon et al. 2009). Decentralized forest management and policies play a major role in balancing conservation and production, and in controlling the effective use and management of the forest, notably through the transfer of ownership and responsibilities to local forest decision makers (Persha et al. 2011; Phelps et al. 2010; Agrawal et al. 2008).

However, human-modified landscapes are often negatively impacted by the expansion and consolidation of agricultural frontiers, where forests are threatened by land use competition resulting in complex degradation and major habitat fragmentation (Foley 2005; Lambin et al. 2001). These effects are spatially interconnected and evolve rapidly over time. While deforestation refers to rapid conversion from forest to non-forest areas, degradation implies changes in forest structure following selective logging and fire disturbances, which also characterize progressive encroachment by agricultural activities (Putz and Redford 2010). Furthermore, deforestation and degradation lead to a feedback loop of fragmentation dynamics that facilitates access to forest habitats and hence to further disturbances (Broadbent et al. 2008). Historical land/ forest-use-associated drivers (i.e. degradation, fragmentation and agricultural expansion) determine the heterogeneous status and configuration of current forest landscapes. Future forest landscapes will thus be shaped by both ongoing pressures and management responses (Malhi et al. 2014). A first step to tailor effective management by local decision makers is to identify the forest areas that are most vulnerable to agricultural expansion and to characterize the underlying pressures (Klein et al. 2005).

Vulnerability assessments provide guidance on how to target interventions and to support decision making processes (Adger 2006). Originally formalized for climate change and the agricultural sector by the Intergovernmental Panel on Climate Change (IPCC), vulnerability frameworks make it possible to assess the key determinants of system responses to external stress and pressures (Marshall et al. 2010; Parker et al. 2019). Adapted from the IPCC definition, vulnerability is the degree to which a forest ecosystem is susceptible to, or unable to cope with, adverse effects of human-triggered impacts (McCarthy 2001). Vulnerability is commonly defined as the combination of three main components where exposure relates to the magnitude of stress undergone by a system; sensitivity refers to the degree to which the stress may affect the system, and the adaptive capacity is the system's ability to

respond to the stress (McCarthy 2001). This definition is widely used in the literature to describe human-environment interactions and the resulting pressure and response options in the framework of socio-ecological systems (Thiault et al. 2018; Metzger et al. 2006; A. Morel et al. 2019). However, the applicability and relevance of this approach for assessing forest ecological vulnerability in human-modified landscapes remains hypothetical. Hence, the implementation of vulnerability using available spatial datasets and the constitution of relevant indicators to model exposure, sensitivity and adaptive capacity remains challenging (Berrouet et al. 2018; Manuel-Navarrete et al. 2007).

Until now, agricultural frontier landscapes have never been analyzed through the vulnerability lens using spatio-temporal landscape indicators. In this paper, we propose an innovative method to assess the ecological vulnerability of forest cover at landscape scale. This methodology makes use of free and open source remote sensing images and combines temporal and spatial dimensions to capture the complexity of land use mosaics in human-modified landscapes. To characterize these complex landscape mosaics, we used a landscape approach, defined as an integrated framework to analyze competing land uses and involving local stakeholders to solve social and environmental issues (Oszwald et al. 2011; Reed et al. 2016). This framework is already well referenced and some authors have already highlighted the robustness of the framework for the analysis of spatial patterns of land use dynamics at the landscape scale and to provide further information on human-environment processes (Wu 2007; Messerli et al. 2009). Landscape structure metrics based on land use and cover information also enable the description of landscape patterns and variability. Some authors also demonstrated the relevance of indicators for the characterization of agricultural frontiers dominated by fragmentation dynamics (Oszwald et al. 2011; Wang et al. 2014; Hargis et al. 1998). Furthermore, the availability of time series of remote sensing images opens a wide range of perspectives to characterize agricultural frontiers through historical trajectories of landscape change (Lausch and Herzog 2002; Ernoult et al. 2006).

Given the above background, the objective of this work was to produce spatial indicators at the landscape scale using multidimensional remote sensing to assess forest ecological vulnerability. The specific steps were to:(1) characterize current landscape mosaics using land use inventory and mapping; (2) reconstruct historical land cover from Landsat time series; (3) identify trajectories of landscape structure dynamics; and (4) develop indicators of exposure, sensitivity and adaptive capacity that quantifies the expansion of agriculture, degradation and fragmentation dynamics and current landscape intensification.

5.2 Materials and Methods

5.2.1 Study area

The study was carried out in the district of Di Linh (Lam Dong province) in the Central Highlands region of Vietnam. The area was chosen for two reasons: 1) The district is located in a consolidated deforestation front where remnant forests are exposed to degradation risks linked to the expansion of coffee based-agriculture (Dien et al. 2013; J. Vogelmann et al. 2017); and 2) It is part of a REDD+ (Reducing Emissions from Deforestation and forest Degradation) pilot project that aim at facilitating forest monitoring with decisions makers such as land use planners and local forest rangers (Thuy 2013).

The town of Di Linh was founded in 1899 along the road connecting Ho Chi Minh City to Da Lat. The district went through a succession of colonization waves and economic transformations during the 20th century, which marked the continuous development of cash crops until the coffee boom in 1980s (Trædal and Vedeld 2017; Meyfroidt et al. 2013; Déry 2000; Ha and Shively 2008). This large-scale coffee production has been identified as one of the main drivers of deforestation and degradation and as responsible for triggering other environmental problems such as increased drought and soil erosion (Meyfroidt et al. 2013; Grosjean et al. 2016).

5.2.2 Conceptual framework for assessing forest vulnerability

We developed a framework to assess the ecological vulnerability of forest cover to deforestation and degradation at the landscape scale. Figure 5.1 presents the methodology, which is divided into four distinct steps: i. Data preparation involving acquisition and preprocessing of remote sensing images and collection of ground truth data; ii. Classification and assessment of the accuracy of 2018 Land-Use Land Cover (LULC) using Sentinel-2 or Landsat-8 and historical LC (simplified typology) using the Landsat archive; iii. Analysis of current landscape mosaics and historical trajectories of landscape dynamics in standard unit grids, and iv. Extraction of metrics to assess adaptive capacity, sensitivity and exposure components and forest ecological vulnerability (at the unit grid scale). Each step is described in detail in the following subsections.

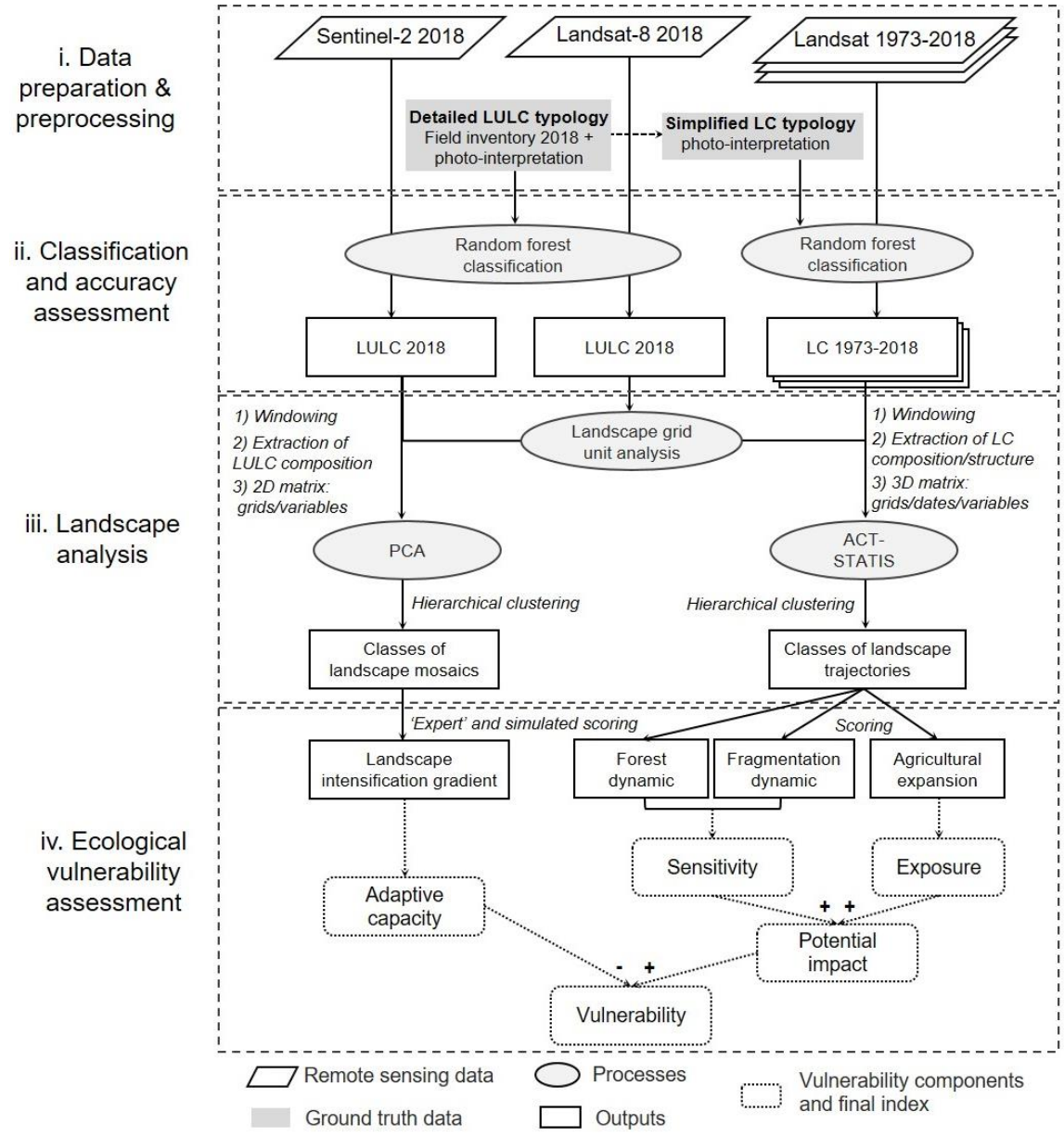

Figure 5.1 Methodological framework designed to assess forest ecological vulnerability with its four steps (i-iv)

5.2.2.1 Data preparation and preprocessing

In order to map current mosaics of LULC with high precision, data collection involved acquiring Sentinel-2 (S2) images and field data (Drusch et al. 2012) for 2018. For the analysis of LC change and landscape dynamics throughout the colonization period, we used two Landsat-8 (2014, 2016) and nine Landsat-5 images acquired in 1973, 1989, 1992, 1995, 1998, 2002, 2006, 2009 and 2011. We also used one Landsat-8 image acquired in 2018 to assess the difference between Sentinel-2 based classification

and to characterize landscape heterogeneity (section 5.2.2.3). All the images present less than 10% cloud cover and were taken during the dry season (December to March) (Appendix 5.1).

The Sen2Cor application developed by the European Space Agency (ESA) was used to transform S2 L1C tiles to surface reflectance L2A level (Main-Knorn et al. 2017). We acquired Landsat (L) surface reflectance data already pre-processed by the algorithm developed by the NASA Goddard Space Flight Center (GSFC). For each sensor, we derived vegetation indices that are related to vegetation photosynthetic activity, burned vegetation, soil brightness and vegetation moisture content (Appendix 5.2). The vegetation indices and the spectral bands were used as input features for the LULC classification.

Our field inventory allowed us to identify landscape elements. A set of 300 GPS points were recorded during a 2-week field survey conducted in Di Linh in March 2018 (Fig 5.2). Each GPS point (Garmin 60CSx, Garmin, Olathe, KS, USA) was associated with a qualitative description of the landscape element identified along with illustrative photos. Sampling (involving transects from agricultural land to natural habitats) was designed to cover agricultural, forested and mosaic landscapes along the main deforestation front (Oszwald et al. 2007). A detailed typology was constructed for the 2018 LULC classification that sums up the major landscape elements identified in the field (Appendix 5.3). For each class, a score was assigned with reference to a landscape intensification gradient ranging from natural (score close to 0) to anthropogenic (score close to 10). Degraded forest composed of logged or burned evergreen forest, natural or regenerated bamboo forest and bushes were judged to be more natural than pine forests, which are mostly planted for timber (Jong et al. 2016; Hiep et al. 2004). We also identified a simplified 4-class typology, which corresponds to general LC classes, to facilitate the historical classification.

Based on the field data and the detailed LULC typology, we manually discriminated polygons sampled around the GPS points and completed by photo interpretation of Sentinel-2 2018 images. We repeated this process using the simplified typology for each historical Landsat image. We created additional classes for cloud centers, edges and their projected shadows. We also differentiated shadowed and unshadowed evergreen forest due to the difference in reflectance that varied with the slope. For each date of the analysis, the resulting sample data sets were used as inputs for training and validating the classification detailed below.

5.2.2.2 Classification and accuracy assessment

For each date of the analysis, the classification method uses remotely sensed features (spectral band and vegetation indices) and samples of LULC typology (polygons) as inputs for the Random Forest (RF) classifier (Breiman 2001). The method is similar to the one developed by Mercier et al. (2019). We randomly generated 50 pairs of training and validation sample subsets from the sample dataset using a 70/30 ratio within which 300 pixels per class were randomly selected. An RF algorithm composed of 100 trees was applied to each selected subsample making it possible to rank the features using the mean decrease Gini (Calle and Urrea 2011) as well as to identify the optimal number of features using the kappa index (Rosenfield 1986). Then, we applied RF using the previously defined parameters and one training/validation sample file to generate the LULC classification. We extracted the overall accuracy, kappa index, user and producer accuracy of each class from the confusion matrix (Pontius and Millones 2011). These two steps were achieved using the RF package in R software. Finally, we applied an 8 x 8 pixel majority filter to reduce single pixel misclassifications using ArcGIS (Esri, Redlands, CA, USA).

5.2.2.3 Landscape analysis was conducted using the steps detailed below:

Identifying a landscape unit grid

Based on the classification of Landsat image (simplified typology) in 2018, we calculated the Shannon diversity index (SHDI) in different regions located along the agricultural frontier visited during the field survey (Sampling points in Fig 5.2). This metric measures both the richness i.e. number of land cover/use classes (compositional heterogeneity) and regularity i.e. distribution of the surface area of the LULC classes (configurational heterogeneity) in a given area. We calculated the SHDI in buffer zones spanning from 50 to 8000 m surrounding each region of interest. We estimated the plateauing of the average curve based on the resulting profiles of SHDI and recorded the corresponding distance. This distance reflects the optimal unit size to capture the diversity of landscape elements and heterogeneity and was used to define a regular grid of X units covering the study area.

Classifying landscape mosaics following an intensification gradient

Using the Sentinel-2 detailed classification, we extracted the composition as a percentage of LULC in each unit of the grid. We discarded units containing more than 80% of water bodies from the analysis. The resulting Y number of grid units were systematically compared using principal component analysis (PCA) and grouped in Z number of clusters using hierarchical clustering (Ward's criterion) applied on the first factorial axis of the PCA (Husson et al. 2010). The number Z of clusters is determined by the Huntsberger index that is a function of the number of units: $Z = 1 + 3.332*\log_{10}(Y)$ (Huntsberger 1961). The average composition of LULC describing each resulting cluster or landscape mosaic class is weighted by its respective 'expert based' land use score (Appendix 5.3). Each class of landscape mosaic is thus associated with a landscape intensification score.

Classifying landscape trajectories

For each of the historical classifications, we extracted the land cover composition in the same regular grid. We also calculated 11 configuration metrics to quantify size, proportion and aggregation, richness and shape of the landscape (Table 5.1), and in this way, characterized specific spatial structures of the agricultural frontier following the concepts of heterogeneity, connectivity and fragmentation (Burel and Baudry 2000). These metrics were computed with the R 'landscapemetrics' package (Nowosad and Stepinski 2018).

Table 5.1 Landscape configuration metrics (McGarigal 2012)

Aspect	Metric name	Description
Size, proportion, aggregation	Edge density (ED)	Equals the sum of the lengths (m) of all edge segments in the landscape in relation to the total landscape area (m²).
	Mean of patch area (MPA)	Mean of all patches in the landscape, describing the patch structure and the overall composition of the landscape.
	Standard deviation of patch area (SPD)	Standard deviation of all patches in the landscape, describing the differences among all patches in the landscape.
	Patch density (PD)	Describes fragmentation (patchiness) but does not necessarily contain information about the configuration or composition of the landscape.
	Aggregation Index (AI)	Equals the number of like adjacencies divided by the theoretical maximum possible number of like adjacencies for that class summed over each class for the entire landscape (He, DeZonia, & Mladenoff 1999).
Richness	Shannon diversity (SD)	Diversity metric that accounts for both the number of classes and the abundance of each class (Shannon & Weaver 1949).
	Patch richness density (PRD)	Measures the diversity of landscape composition.
Shape	Evergreen/Pine forest Mean perimeter area ratio (MPARF/MPARP)	Describes patch complexity but not standardized to a particular shape.
	Evergreen/Pine forest Mean Shape Index (MSIF/MSIP)	Describes the ratio between the actual perimeter of the patch and the hypothetical minimum perimeter of the patch if the patch were maximally compact (Patton 1975).

The resulting 3D matrix (grid units/12 dates/LC structure metrics) was analyzed using PCA and ACT-STATIS (Lavit et al. 1994; Oszwald et al. 2011). First, we defined the 'compromise' or common stationary spatial structures at the different dates using PCA, which provides a global description on the dynamics of overall spatial variability within the study area (Robert and Escoufier 1976). The second step allows the reproducibility of the compromise to be identified and the structure variability through each grid-variable table to be identified (Blanc et al. 1998). It informs on the variability of spatial dynamics i.e. the trajectory of each unit in the grid. Finally, we grouped these trajectories into Z number of classes using Hierarchical clustering (Ward's criterion) based on the Huntsberger index, which is similar. Consequently, units of a certain class of landscape trajectory share similar spatial landscape composition and structural dynamics from 1973 to 2018. The statistical analyses were carried out using the ade4 package in R (Thioulouse et al. 1996; Chessel et al. 2004).

5.2.2.4 Assessment of forest ecological vulnerability at the landscape scale

Ecological vulnerability (V) is constituted by components that include exposure to external stresses (E), sensitivity to perturbation (S) and capacity to cope or adapt (AC). V = S+E-AC (Fritzsche et al. 2014). Based on the adaptation of different conceptual frameworks, we defined indicators for each component to analyze the vulnerability of socio-ecological systems (Adger 2006; Gallopín 2006).

Sensitivity is defined by Gallopín (2006) as the degree to which the system is potentially modified or affected by a disturbance over time. We estimated sensitivity based on the combination of evergreen forest (EF) and fragmentation dynamics that provide information on the level of degradation that may affect a forest landscape over time (Shapiro et al. 2016; Vieilledent et al. 2018). These dynamics were calculated using the averaged values of the proportion of evergreen forest and edged density metrics composing each class of the landscape trajectory from 1998 to 2018 (Oszwald et al. 2011). This period makes it possible to capture recent trends that may impact the current landscape.

To capture EF dynamics, we extracted the rate of change (equation 1) and rescaled the values (equation 2) in order to compare EF trajectories with no change or increasing gradient (values close to 0) to decreasing gradient (values close to 10):

(1) Rate of change: $EF_{2018} – EF_{1998}$, where EF_{2018} is the proportion of EF in 2018.

(2) $X_{rescaled} = 10*(X - X_{min})/(X_{max} – X_{min})$ where X is the value of rate of change based on the change in EF for a given class of landscape trajectory, X_{min} and X_{max} are the minimum and maximum observed values of rate of change based on the changes in the EF in all landscape trajectory classes.

Finally, we multiplied the rescaled rate of change values by the average value of EF from 1998 to 2018 to yield a general score of EF dynamics that combines information on the rate and intensity of EF changes.

To calculate fragmentation dynamics based on the edge density metric, we followed the same procedure as that described above. The rate of change was rescaled to compare increasing gradient (values close to 10) to no change or decreasing gradient (values close to 0).

Sensitivity was obtained by combining (summing and rescaling) EF and fragmentation dynamic scores.

Exposure refers to the length of time the forest has been subjected to external stress or perturbation (Turner et al. 2003; Adger 2006). In our case, the stress is caused by encroaching cropland linked to the agricultural expansion of coffee. We applied the same procedure as that described above to assess

agricultural dynamics through the changes in the proportion of agricultural land for each class of landscape trajectory. The exposure score is thus influenced by the average proportion and rate of increase in the crop cover.

Adaptive or coping capacity refers to the ability of the system to respond to a perturbation (Smit and Wandel 2006). This potential is linked with the current level of intensification of a forest landscape (Messerli et al. 2009). We assessed adaptive capacity as the additive inverse of landscape intensification scores defined in section 5.2.2.3. Here we assume that high landscape intensification scores (i.e. fragmented coffee and degraded forest dominated landscape) correspond to low adaptive capacity. As the landscape intensification score is based on 'expert' scoring, we simulated different land use scores (LUS) for degraded and pine forest classes such that:

"LUS EF = 0 < LUS degraded forest <LUS pine forest < LUS agricultural elements = 9."

The 28 possible combinations of LUS for both landscape elements generated 28 possible landscape intensification scores and thus adaptive capacity scores related to the forest landscape mosaics we identified. Finally we analyzed the influence of scoring on vulnerability assessment by calculating and mapping the agreement, overestimation and underestimation of simulation and 'expert' ecological vulnerability classifications.

5.3 Results

5.3.1 Mapping LULC in 2018

Using Sentinel-2 images, LULC classification in 2018 revealed high overall accuracy and kappa indexes (e.g. OA=0.81 and kappa=0.78). Similar results were found for Landsat-8 classifications (Appendix 5.4). Clouds, water, projected shadow, infrastructure, irrigated rice and pine forest were the classes with the highest user and producer accuracy in both classifications (>0.8). Degraded forest class included omission errors (producer accuracy of 0.49) due to confusion between coffee and evergreen forest classes. Rainfed rice represents sparse vegetation cover in the dry season and can therefore be confused with the bare soil and infrastructure classes. Evergreen forest was correctly classified with little confusion between shadowed and unshadowed forest cover and degraded forest. Cropland was the least well classified class with 0.27 producer accuracy notably due to confusion with coffee and bare soil and the limited number of training samples (Appendix 5.5). Lowlands are dominated by irrigated rice, coffee and infrastructure. In the southern part of the district, LULC is driven by

topography where rainfed rice is cultivated in the valley bottoms, coffee on the slopes, degraded forest at the edges and evergreen forest grows on higher terrain. Pine forest is often located at the interface between coffee and evergreen forest (Fig 5.2).

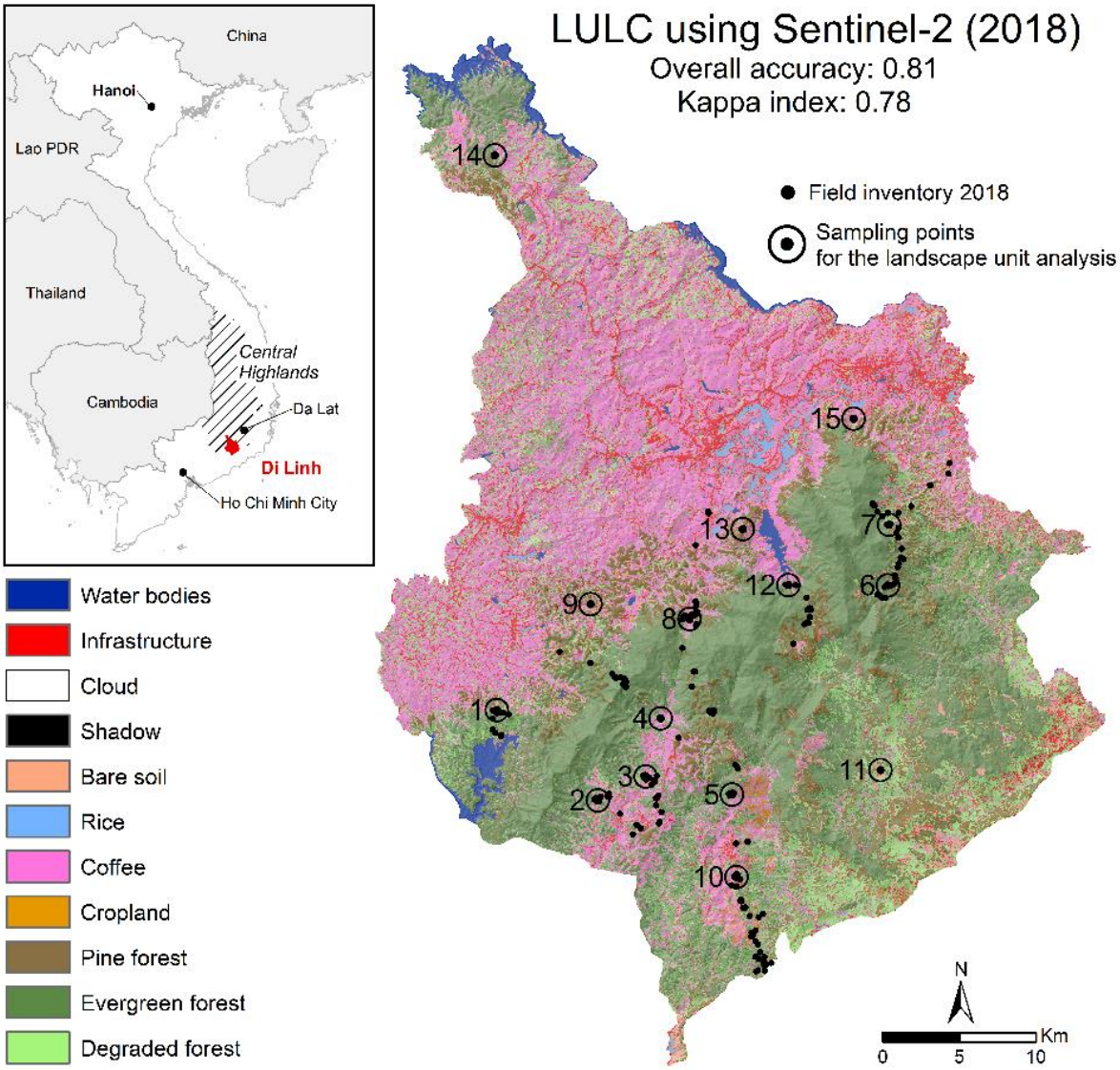

Figure 5.2 Location and classification of Di Linh district (Lam Dong province) in the Central Highlands of Vietnam.

5.3.2 Defining landscape mosaics from LULC classification

The inflexion point of the average curve summarizing 15 Shannon diversity profiles is reached at 0.85, which corresponds to a distance of 360 m (Appendix 5.6). This value defines the size of the landscape matrix grid applied to Di Linh district i.e. 12,259 units of 360 m. Similar inflexion points were found using Sentinel-2 based LULC classification (detailed and simplified typology).

The two first factorial axes of the PCA accounted for 40.2% of the total variability of the landscape elements composing each unit (Fig 5.3a). The first PCA axis shows an anthropogenic gradient between forest (evergreen and pine) and agricultural land (cropland, bare soil, coffee and infrastructure) (Fig 5.3b). The second axis of the PCA opposes degraded forest and the other landscape elements. Degraded forests are mostly found at the interface between natural and mainly agricultural landscapes.

Using the first seven axes of the PCA (83.4% of the total PCA variance) as inputs for hierarchical clustering and Huntsberger index, we obtained 15 classes of landscape mosaics (Fig 5.3c). We defined forest mosaics as those with between 10 and 96% evergreen forest cover and varying proportions of the other landscape elements. L4 landscape mosaics were mainly composed of degraded forest (71% on average) which corresponds to natural shrubland areas and was therefore excluded from the forest mosaic. Agricultural mosaics were characterized by a landscape intensification score higher than 6 in which the proportion of forest cover was very low (<0.07% on average). L9 landscape mosaics were dominated by water and consequently excluded from the analysis. Mapping the landscape intensification score highlights the spatial distribution of forest mosaic gradients from core evergreen forest landscapes (dark green) to complex landscape mosaics of fragmented elements made up of forest, coffee, degraded forest and pine (light green) (Fig 5.3d).

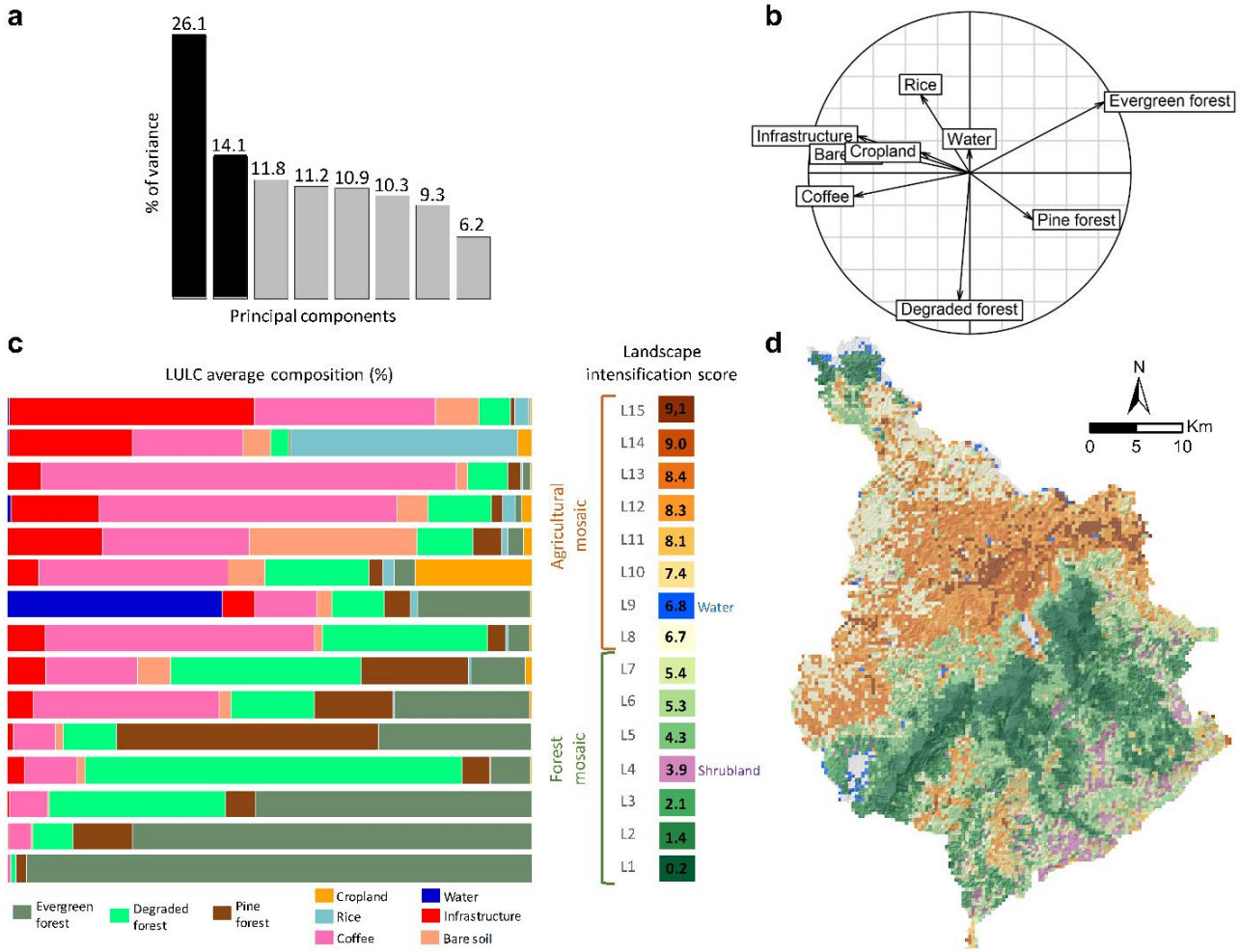

Figure 5.3 Transformation of land use/cover patches into landscape mosaics using a regular 360 m x 360 m grid and Sentinel-2 based classification at 10 m resolution (2018). a) Histogram of eigenvalues expressed as % of total variance. b) Correlation circle of the first two PCA components. c) Classes of landscape mosaics (L1 to L15) according to hierarchical clustering based on the first seven PCA components: Average composition of land cover/land use and landscape intensification score attributed to each landscape mosaic class. d) Landscape mosaics distinguished according to the landscape intensification gradient (see the legend to Fig 5.3c)

5.3.2 Mapping historical land cover using the Landsat 1973-2018 archive

LC historical classification from 1973 to 2018 highlights the expansion of cropland, i.e. of infrastructure, coffee, rice and other crops at the expense of evergreen forest. Kappa and overall accuracy indexes ranged from 0.95 for 2018 classification to 0.72 in 1973 (Appendix 5.7). Over the last 45 years, the evergreen forest cover was reduced from 100 M ha to 60 M ha to the direct benefit of cropland. Pine forests remained stable over the period with a slight decrease starting in 2008 (Fig 5.4). In 1973, 62% of the district was covered by evergreen forest and croplands were located along the main roads

crossing the district from east to west. Some agricultural regions were found in the south west but remained limited to the valley bottoms, typically rice fields. In 1989, some large patches of forest were deforested, mainly around Di Linh city. This trend continued until 2002 with deforestation reaching a peak in 1992. Starting in 2006, the cropland expansion started decreasing and became consolidated in the northern part of the district but continued in two main poles in the south that were previously inactive. In 2014, the agricultural frontier appears to have stopped advancing. Pine forest was largely reduced in the northern parts of the district. Along the current agricultural frontier, pine forest was conserved and was even still being planted at the interface between cropland and evergreen forest starting in 2009. The pine forest that was originally located in the central region of the district (low elevation, low slope) was rapidly converted into cropland.

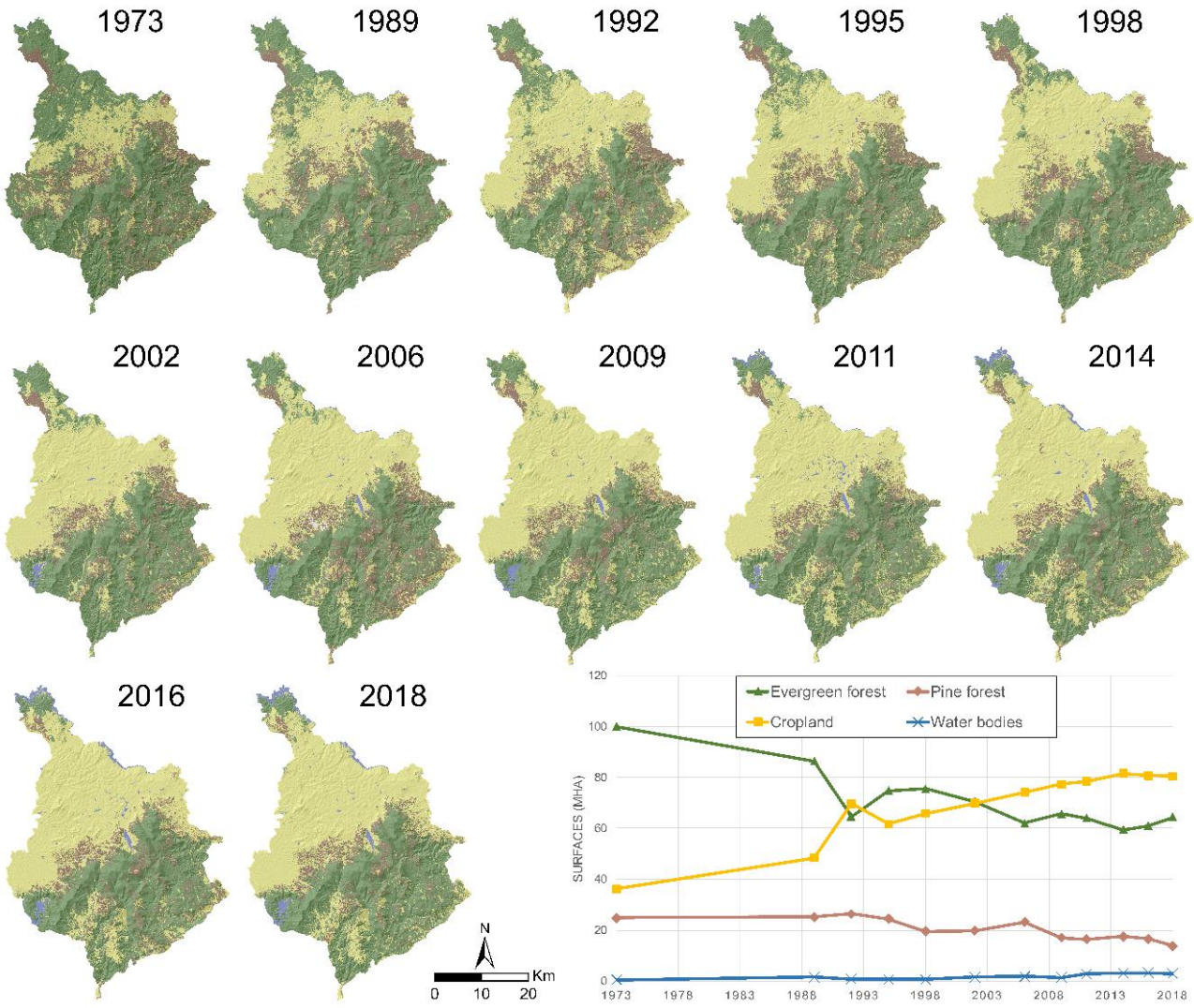

Figure 5.4 Maps showing 45 years of evergreen forest, pine forest, cropland and water cover using Landsat archives and random forest classification

5.3.4 Deriving classes of landscape trajectories

ACT-STATIS and clustering methods generated 15 classes of landscape trajectories within which we analyzed the average composition (evergreen forest, pine forest and cropland) and configuration (the Shannon diversity index and edge density) metrics over time. **Class T1** groups forest-dominated units were characterized by a slow decrease in EF cover from 1998 on associated with a gradual increase in cropland and a steep increase in edge density (Fig 5.5). **Class T2** groups units in which evergreen and pine forest decreased starting in 1973, with a shift in 2006 when cropland started to become the dominating class. Since then, deforestation and fragmentation processes have decreased and stabilized. With a similar configuration to Class T1 in 1973, **class T3** differed by a sharp decrease in EF cover (reduced by half) with an increase in edge density and cropland. This class underwent the biggest increase in edge density of all the classes. Classes T1, T2 and T3 are located along the current agricultural frontier. **Classes T4 to T8** group units dominated by forest that have remained constant over the last 45 years with the exception of T4 in which EF is gradually increasing and T7, which is marked by a fluctuating EF cover and edge density. **Classes T9 and T10** group units that were always dominated by croplands and remained unchanged throughout the study period. Typically, Di Linh city and its surrounding region belong to these groups. **Classes T11 to T15** group units showing chronological stages of deforestation:T11 (light grey), which is located close to Di Linh city, shows a deforestation process that started before 1973, while T15 (dark grey), which is mainly located in the northern part of the district groups units that were completely deforestated in 2006.

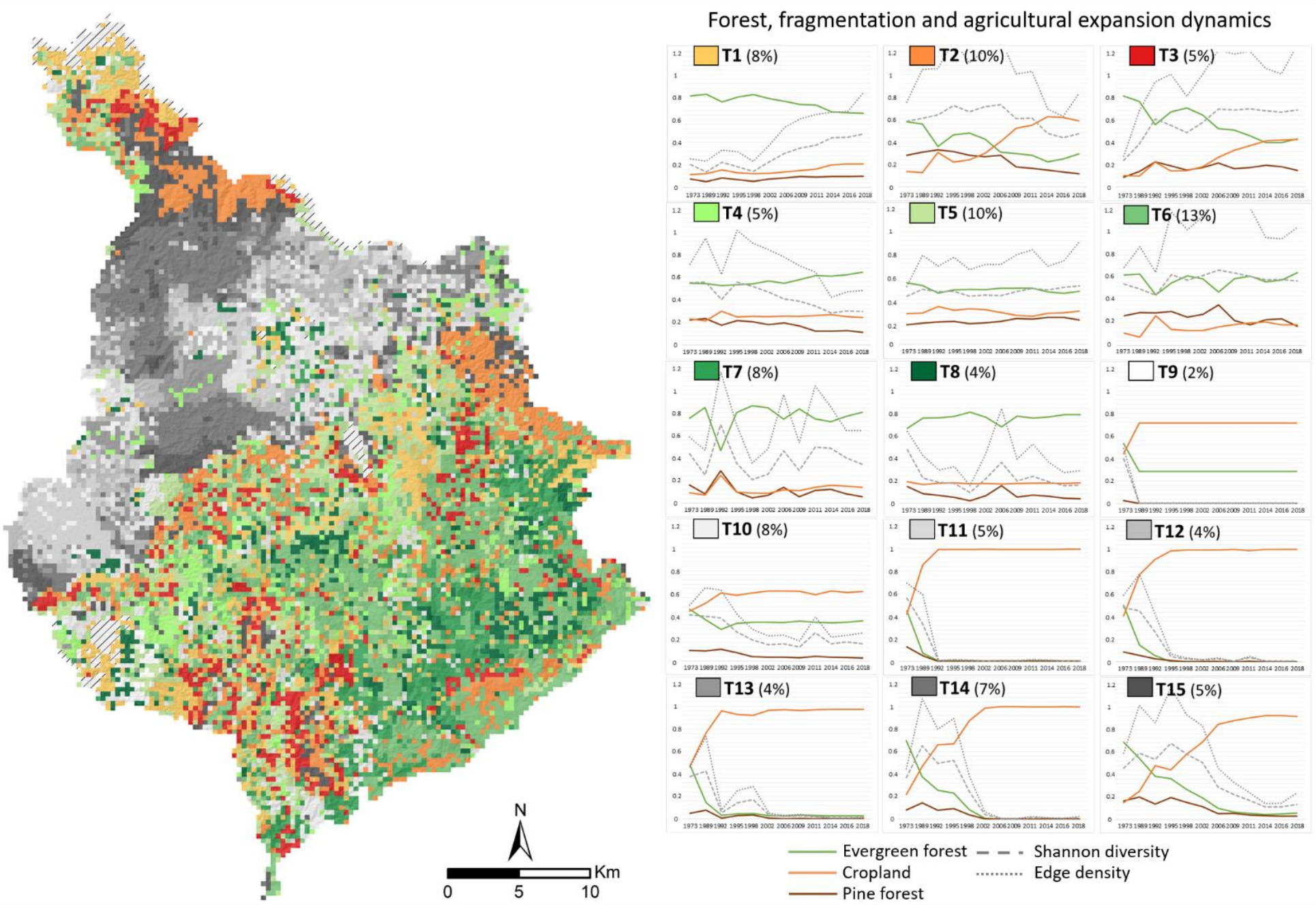

Figure 5.5 Classes of landscape trajectories (T1 to T15) based on land cover composition and configuration dynamics from 1973 to 2018 obtained using ACT-STATIS and clustering methods. Hatched areas represent water bodies in 2018 (2%).

5.3.5 Assessment of forest ecological vulnerability

Forest adaptive capacity is the lowest along the agricultural frontier, which corresponds to fragmented landscapes with mixtures of different land uses including evergreen forest, degraded forest and coffee plantations (Fig 5.6). These regions are mainly located along the main deforestation front and in the south of the district where complex forest mosaics were mapped. Forest adaptive capacity had the highest score in core forest regions isolated from agricultural frontiers, infrastructure networks or other forms of human activities; or in mixed evergreen and pine forest landscapes. Concerning sensitivity, a number of regions experienced a rapid decrease in forest cover over the last 20 years and an increase in fragmentation (high values). Exposure was highest in the eastern part of the agricultural frontier due to the recent rapid expansion of cropland (Appendix 5.8 and 5.9 for more details about the calculations).

All negative vulnerability scores (highest AC, lowest sensitivity and exposure) were reclassified as lowest vulnerability. All positive values were grouped in three classes (labelled low, medium and high) using Jenks Natural Break classification in ArcGIS. Overall vulnerability revealed heterogeneous distribution of values along agricultural frontiers. Frontiers A and B (Fig 5.6) are among the most vulnerable due to different combinations of sensitivity, exposure and adaptive capacity. Region A is vulnerable mostly because of low adaptive capacity and high sensitivity. Region B includes scattered highly vulnerable areas and overall low adaptive capacity. However, we also identified high sensitivity hotspots in the western part and a high exposure hotspot in the eastern part of the region.

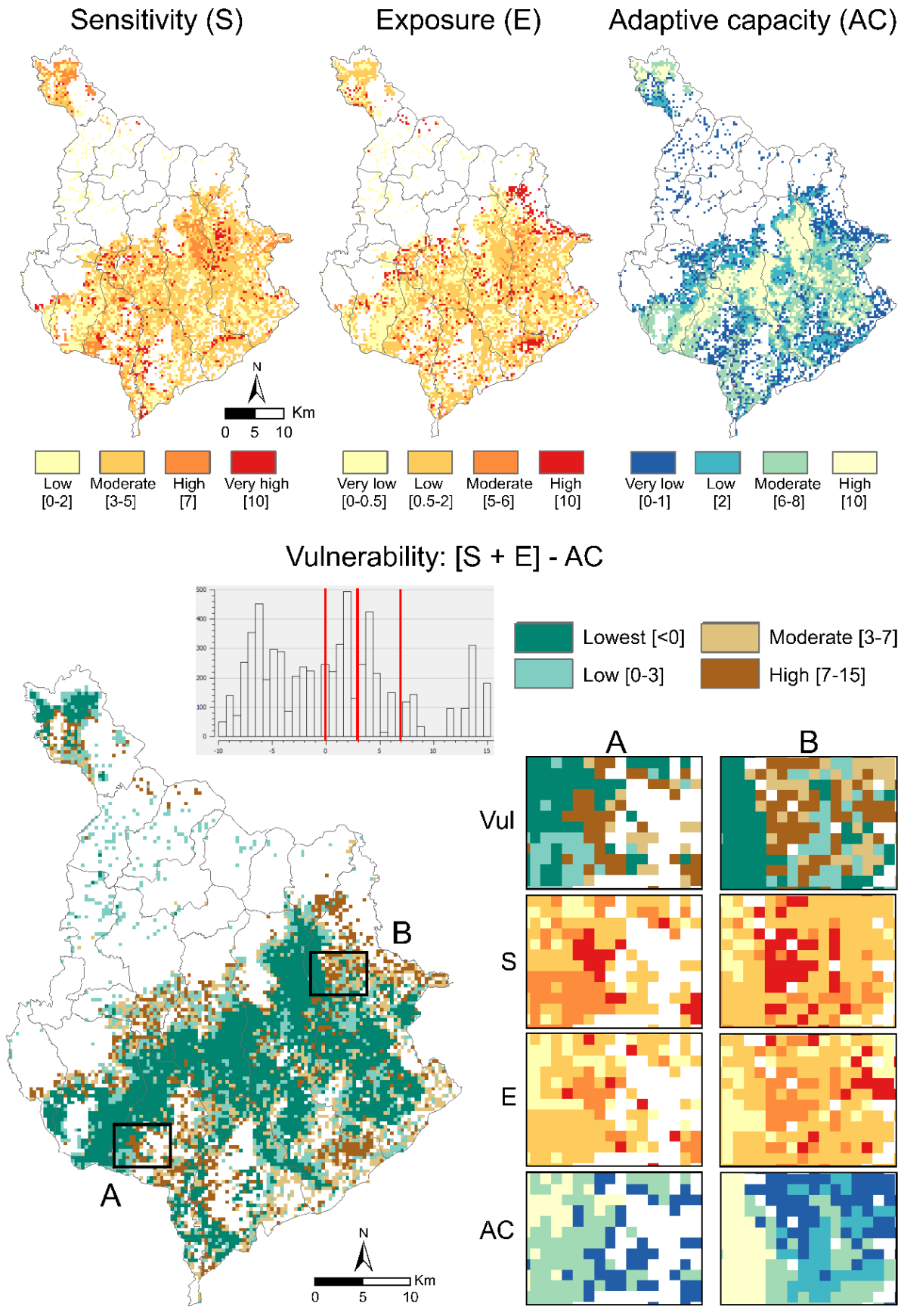

Figure 5.6 Forest ecological vulnerability to deforestation and degradation (agricultural landscapes are in white, communes are delimited in grey)

5.4 Discussion

5.4.1 Potential of vulnerability assessment for land use planning and targeted conservation actions

There is a growing consensus that integrating production and conservation is an efficient strategy to achieve conservation goals in human dominated landscapes (Griscom and Goodman 2015). However, agricultural expansion in forested areas achieved through degradation, deforestation and indirectly through fragmentation can jeopardize conservation goals and land use planning (Tilman 1999).

In this study, we proposed an innovative adaptation of the vulnerability framework defined by the Intergovernmental Panel on Climate Change (IPCC) to forest ecosystems on the only basis of remote sensing and statistical analysis. We provided indicators of forest vulnerability at landscape level to improve our understanding of forest and agricultural dynamics. Combined, these indicators allowed targeting regions that are most vulnerable to agricultural frontier expansion. We also provided tailored management responses and levers for action by decision makers depending on the importance of forest adaptive capacity, sensitivity and exposure. Consequently, our approach pinpointed where decision makers should prioritize management actions and conservation to prevent future forest degradation and deforestation. Global forest cover monitoring systems usually rely on moderate resolution remote sensing imageries. However, improved resolution and frequency of image acquisition are needed in key areas such as active deforestation fronts. Our work allowed targeting these areas and thus orientating where higher resolution is needed for improving the efficiency of near-real time monitoring systems (Reymondin et al. 2012). Finally, the forest ecological vulnerability approach can be coupled with forest ecosystem modelling such as soil erosion, water availability, biodiversity or forest carbon mapping to provide even more comprehensive and informed data, making it all the more constructive when applied in decision making (Le Clec'h et al. 2017; Grimaldi et al. 2014).

The results of this study pinpoint hotspots of vulnerability along the agricultural frontier. Most areas along the agricultural frontier displayed low adaptive capacity corresponding to fragmented forest mosaics dominated by coffee plantations, degraded forests and infrastructure. Improving the connectivity of forest habitat could increase the adaptive capacity of these landscapes (Ribeiro et al. 2009). One example in Di Linh district is the association of evergreen forest with pine forest (central and western part of the district) to stabilize and protect the agricultural frontier and increase forest surface area (Dien et al. 2013). Sensitivity and exposure indicators revealed localized patterns of forest

degradation and agricultural expansion, respectively. The southern part of the district was identified as an active agricultural front recently marked by encroachment of forest cover amplified by fragmentation of the forest edge (trajectory T3) due to an increasing importance of cash crop agriculture (e.g. coffee, maize and banana plantations). The eastern region is experiencing different dynamics with notable opening of the forest cover in the forest habitat. Although driven by different factors, these two regions should both be high on the list of priorities for intervention. We demonstrate the need to adapt conservation and management actions, for example, slower rates of reduction in forest cover were detected (trajectory T1) but they were still characterized by a closed forest habitat, leading to a lower vulnerability index and consequently lower priority for intervention.

It is important to stress that the ecological vulnerability index is not a measurable phenomenon but rather an aggregation of complex and interacting indicators (Fritzsche et al. 2014). Current landscape intensification scores and historical degradation trajectories are indicators that are assumed to affect the ecological vulnerability of forest cover to agricultural expansion, because vulnerability cannot be measured directly (Adger 2006). These indicators reflect human decisions through changes in land use and in land cover and hence indirectly provide information on social systems. Further research into social vulnerability and their related indicators at the household level is necessary to provide a complete picture of overall socio-ecosystem vulnerability as defined by Thiault et al. (2018). Our ecological vulnerability approach is therefore a first attempt to capture complex realities of forest cover vulnerability using only indicators based on free and open source data.

5.4.2 Methodological robustness and future outlook

The adaptive capacity indicator reflects a gradient of landscape intensification, which is based on the land use composition of each class of forest landscape and expert scoring. We evaluated the impact of this method of scoring on the vulnerability classification by simulating all possible intensification scores, adaptive capacity indexes and vulnerability scores. Figure 5.7 shows that most of the forest landscapes were classified as belonging to the same class of vulnerability when we compared expert based and simulation results. The areas of low agreement are mostly related to overestimation (i.e. the simulations yielded a higher class of vulnerability than the expert result). Vulnerability was rarely underestimated and did not concern any of the previously identified and characterized hotspots of vulnerability. This means that ‘expert’ qualitative inputs had no negative impacts on the ecological vulnerability assessment of forest cover and that the method can be used at other sites. The consequences of scoring are generally not assessed in studies (Lavelle et al. 2016).

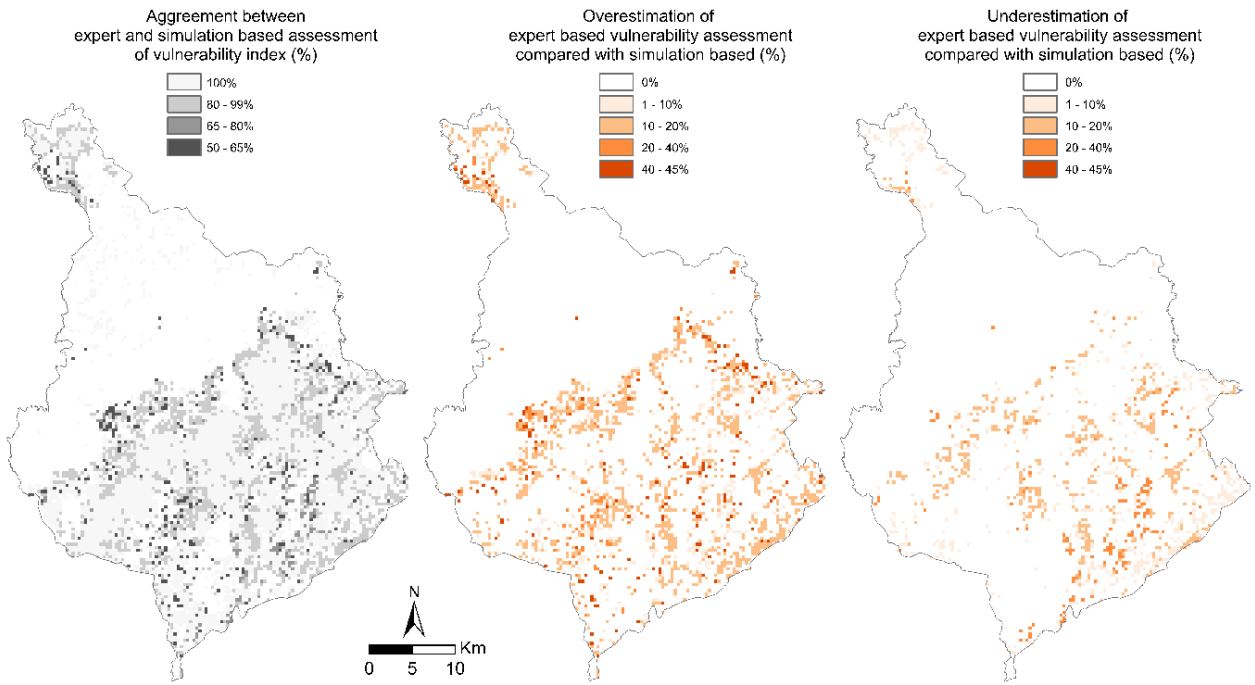

Figure 5.7 Agreement, overestimation and underestimation in expert and simulation based ecological vulnerability assessments

Landscape metrics, the trajectory classes obtained using the ACT-STATIS method and the resulting indicators of vulnerability depend on the validity and accuracy of LULC classifications. This remote sensing field of research is improving significantly thanks to the development of novel classification algortihms and the accessibility of near-real time and high resolution imagery (Bégué et al. 2018). The 2018 land cover and land use maps were produced with a high degree of accuracy and required only a short processing time. Minor misclassification were detected between the land cover and land use classes along the agricultural frontier as these elements are highly contrasted and clearly seperated in the landscape. Transition classes, which often cause misclassification, proved difficult to map (Mercier et al. 2019; Hett et al. 2012). In our case, they were grouped in the degraded forest class, which refers to different land uses with the same vegetation structure. Further work is necessary to be able to distinguish degraded forest due to logging and fire from shrubland and fallow. Spectral unmixing indicators assess the proportion of active photosynthetic vegetation, dead vegetation and bare soil within a pixel and could significantly improve the identification and classification of forest edges subject to degradation risks (Asner et al. 2009b). Time series optical images could also provide useful information to help improve the classification of degraded forest. In continental Asia, annual dfferences in the normalized burn ratio revealed highly accurate patterns of canopy disturbances linked with encroachment and logging (Langner et al. 2018). Cropland and rice classes showed misclassification errors due to confusion with bare soil because mapping was based on images

acquired in the dry season. High temporal resolution of optical and radar imagery could help describe and account for the phenology of vegetation to map forest-agriculture mosaics (Mercier et al. 2019). Furthermore, small agricultural systems can be mapped using combined pixel and object-based approaches and promising results have already been obtained with the characterization of fine cropland uses (Lebourgeois et al. 2017).

5.4.3 Landscape approaches that incorporate both spatial and temporal information are keys to characterizing complex agricultural frontiers

Major pressures and conflicts opposing human and natural elements are concentrated along agricultural pioneer fronts (Lambin et al. 2001). Today, remote sensing offers unique opportunities to map and characterize these regions using land cover classification and its contextual transformation into land use information, which is often used to describe landscape mosaics (Mercier et al. 2019). The landscape approach has been shown to be appropriate for studying agricultural frontiers as its scale encompasses spatial patterns that reveal the underlying social, environmental and ecological processes and hence human-environmental interactions (Wu 2007). The landscape approach is particularly useful when degradation and deforestation are the main drivers that shape the landscape through complex fragmentation patterns integrating agriculture and forest systems (Shapiro et al. 2016). Pixel-based approaches would provide limited information on the consequences of degradation and on their underlying drivers linked with agricultural frontier expansion (Oszwald et al. 2012). The landscape approach has proved to be particularly effective in complex mosaic landscapes marked by high heterogeneity, fragmentation and disconnection between the different landscape elements. The transformation of land use into landscape mosaic has been applied to different human-dominated landscapes such as Northern Laos where complex swidden systems have been successfully mapped and characterized using human-environment data (Hett et al. 2012; Messerli et al. 2009). In the case of Amazonian agricultural frontiers, Oszwald et al. (2011) demonstrated that the combination of structure metrics at both spatial and temporal dimensions are key indicators for characterizing landscape and for reflecting human-induced drivers of landscape change. Indeed, two landscape mosaics sharing similar characteristics at a given moment in time may have experienced different historical landscape dynamics. Our analysis demonstrates that the relationship between the spatial and temporal dimensions of landscape analysis is effectively verified, especially in regions that are highly vulnerable to agricultural expansion (Fig 5.8). Current mosaics and historical trajectories are complementary, providing dependent and non-redundant information to help understand landscape complexities. Highly vulnerable areas (brown areas in Fig 5.6) are five types of current forest landscape

mosaics with specific past trajectories and any given landscape can be the result of multiple types of dynamics.

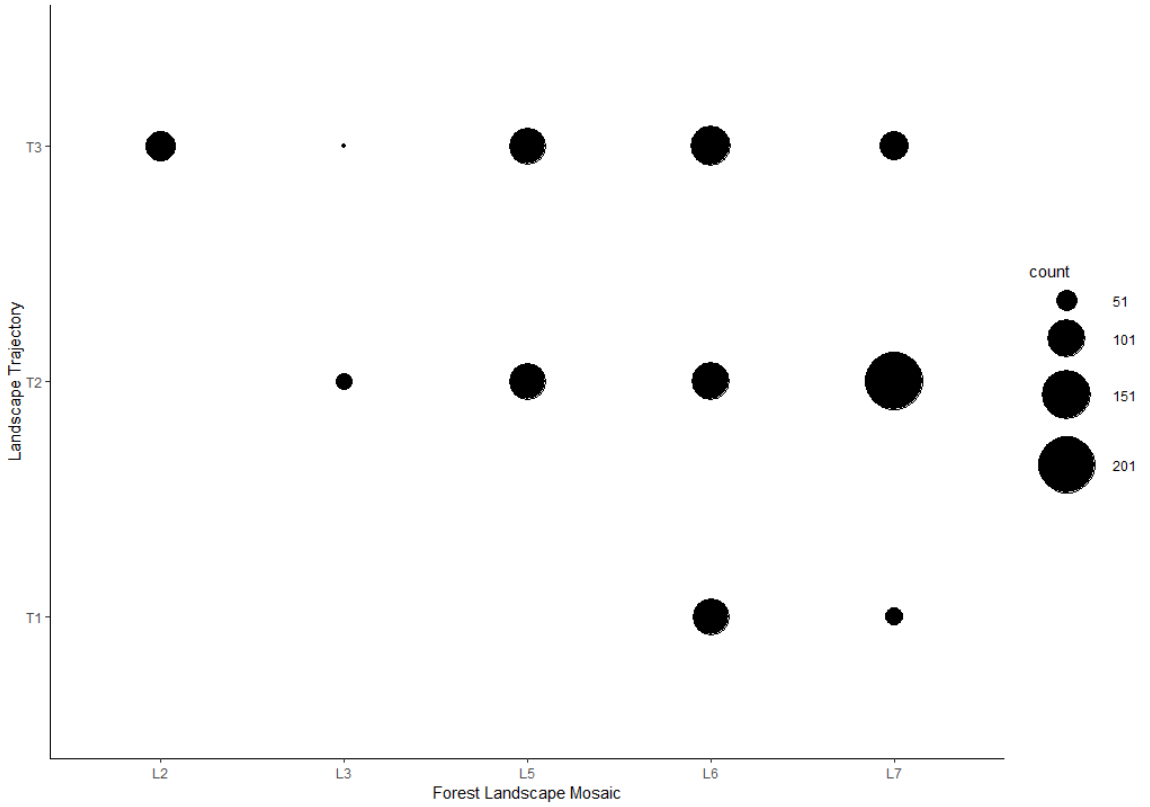

Figure 5.8 Number of forest landscape mosaic and landscape trajectory pairs identified in the most vulnerable forest cover areas

So far, the multiplication of scales in landscape analysis has been applied to the spatial dimension and has made it possible to capture trends at different organizational levels (Ostrom 2009). In this paper, we emphasize the importance and added value of including the temporal scale in the landscape approach conceptual framework in order to reconstruct landscape dynamics and analyze underlying drivers and pressures that drive agricultural frontiers and other areas where competition between land uses is high (Sayer et al. 2013; Reed et al. 2016). With accessibility, global coverage, temporally rich archives and frequency of acquisition of optical remote sensing images (Landsat and Sentinel), this study paves the way for replicating and scaling out the proposed framework to other agricultural frontiers for more effective management and conservation actions of forest landscapes.

5.5 Conclusion

A need exists to identify which forest areas are most vulnerable to agricultural expansion and thus require prioritized conservation. In light of this, this paper demonstrates the potential and robustness of the proposed innovative methodology based on multidimensional remote sensing and landscape analysis to assess forest ecological vulnerability. We successfully mapped current land uses using Sentinel-2 and retrospectively reconstructed land cover over a 45-year period using Landsat archive. Landscape structure dynamics revealed heterogeneous trajectories of cropland expansion, degradation and fragmentation while the composition of forest-agricultural mosaics highlighted different landscape intensification levels along the agricultural frontier. Most vulnerable forest areas were experiencing rapid and recent forest cover loss associated with landscape fragmentation, land use competition due to coffee production and forest degradation. Long-term landscape structure analysis coupled with detailed description of land uses opens up prospects for continuously monitoring forests within agricultural frontiers over time and space.

Chapter 6 – Synthesis, discussion, and conclusions

Human-modified landscapes of Paragominas and Di Linh study sites (pictures by Clément Bourgoin)

6.1 Summary of the findings

This thesis investigated four research questions related to the development of a multidimensional approach using remote sensing to assess forest degradation and the relationship between the broader dynamics of land use, land cover and landscape changes towards the evaluation of the ecological vulnerability of forest cover. The four research questions are recalled below, and the main findings are summarized with recommendations for improving the management of forests at the landscape scale.

Sub-research question 1: How to assess the state of forest cover across gradients of human-induced degradation using multisource remote sensing?

In Chapter 2, we evaluated the potential of optical (Landsat, MODIS) and radar (ALOS-1 PALSAR, Sentinel-1) remote sensing sources in modelling and mapping forest AGB in Paragominas municipality (Brazil). We extracted a wide range of vegetation and textural indices and combined them with AGB data collected in situ into a random forest regression model to predict AGB at a resolution of 20m. The model explained 28% of the variance with a root mean square error of 97.1 $Mg \cdot ha^{-1}$ and captured all spatial variability. We identified Landsat spectral unmixing and mid-infrared indicators as the most robust indicators with the highest explanatory power. AGB mapping reveals that 87% of forest is degraded, with illegal logging activities, impacted forest edges and other spatial distribution of AGB that are not captured with pantropical datasets. We validated this map with a field-based forest degradation typology built on canopy height and structure observations. This modelling framework combined with high-resolution vegetation status indicators can help improve the understanding of the complex gradients of forest structures as well as improving the management of degraded forests at the regional scale.

Sub-research question 2: How to quantify long-term changes in forest structures from degradation?

In Chapter 3, we assessed how canopy textural analysis could capture forest structure complexities resulting from different forest degradation histories. We used a lightweight Unmanned Aerial Vehicle (UAV) to map 739ha of degraded forests in Paragominas and 33 years of Landsat archives to reconstruct degradation history through the detection of logging and fire disturbances. Fourier (FOTO) and lacunarity textures were used to assess forest canopy structure and to build a typology linking degradation history and current status. Texture metrics capture canopy grain, heterogeneity and openness gradients and correlate with forest structure variability (r^2: 0.58). Similar forest structures shared common degradation history and could be discriminated on the basis of canopy texture alone (accuracy: 55%). Over logging causes a lowering in forest height, which is represented by homogeneous

textures of finer grain. We identified the major changes in structures due to fire following logging which changes heterogeneous and intermediate grain into coarse textures. Our findings highlighted the potential of canopy texture metrics to characterize the structures of degraded forests which could therefore be used as indicators for forest cover status using UAV up to VHSR satellite sources.

Sub-research question 3: How to identify and disentangle cascading effects of forest degradation drivers at the landscape scale?

In Chapter 4, we identified the direct and indirect drivers of forest degradation using a landscape approach, which goes beyond the direct detection of forest disturbances. We used both regression and clustering methods to map the drivers of primary forest degradation from a large set of environmental and geographical factors, and landscape structure metrics derived from land use/cover classification. Models of forest degradation revealed that at the landscape scale, accessibility, geomorphology, fire occurrence and fragmentation were the key indirect and direct drivers of degradation (80% of explained variance). We clearly showed that the indirect and direct drivers of degradation acted together and in sequence to create homogenous patterns in the municipality, thereby proving their spatial covariation and inter-dependency and revealing different land use dynamics and management practices. In the central part of the municipality, forests are degraded because of past overexploitation of timber, which has been indirectly enhanced by accessibility to forest patches and markets, and more recently due to conflicts associated with agricultural expansion processes and negative feedback loops generated by fragmentation, therefore affecting forest structure. In more complex landscape mosaics, forests are degraded due to the joint result of historical processes and recent interactions between degradation drivers such as fire used in the management of agricultural lands and forest landscape fragmentation. This holistic understanding of the drivers of degradation and their sequential interactions underscores the need to tackle forest management at the landscape scale.

Sub-research question 4: How to characterize the ecological vulnerability of forest cover?

In Chapter 5, we developed a rigorous methodological framework to assess forest ecological vulnerability and aimed at evaluating the potential of remote sensing to characterize forest landscape dynamics in spatial and temporal dimensions. We presented an innovative method that spatially integrates current landscape mosaic mapping with 45 years of landscape structure trajectories using Sentinel-2 and Landsat imagery. We extracted indicators of exposure to cropland expansion, sensitivity linked with forest degradation and fragmentation, and forest capacity to respond based on forest landscape composition in Di Linh district (Vietnam). We mapped current forest-agricultural mosaics with high accuracy to assess landscape intensification (kappa index = 0.78). We also mapped the

expansion of the agricultural frontier and highlighted heterogeneous agricultural encroachment on forested areas (kappa index = 0.72-0.93). Finally, we identified degradation and fragmentation trajectories that affected forest cover at different rates and intensity. Combined, these indicators pinpointed hotspots of forest vulnerability. Most vulnerable forest areas were experiencing rapid and recent forest cover loss associated with landscape fragmentation, land use competition due to coffee production and forest degradation. This study provided tailored management responses and levers for action for local decision makers in order to prioritize actions to prevent future forest degradation.

6.2 General discussion

Forest degradation is a multi-aspect phenomenon requiring multiple nested scale analyses and multidisciplinary approaches. In this section we will discuss the different methods used in this thesis, their respective limitations and how the results can be used for forest management.

6.2.1 Promising methods to characterize forest structures from degradation

Due to the natural diversity of forest types and variety (type, intensity and frequency) of anthropogenic disturbances, multiple forest structures can be observed within tropical forest landscape mosaics. This necessitates the need for indicators that characterizes the state of the forest as well as techniques to reliably assess those indicators from cost-efficient monitoring schemes. Multidimensional remote sensing alternatives must be found when LiDAR data, used to directly assess forest structures or at the basis of regional AGB mapping, is not available or affordable.

Mapping degraded forest structures through the modelling of aboveground biomass using remote sensing indicators showed promising results. Predicted values of AGB matched with a field established typology of degraded forests and provided improved accuracy and details compared with pantropical approaches. However, the large range of forest structures spanning from conserved to highly degraded was not entirely captured by the models. Beyond the contribution of each remote sensing derived indicator to model performance, the number of samples from field inventory was an important limiting factor given the large area of forest to cover and the complex gradients of degraded forest structures in place. Globally, forest inventories of degraded forest structures are rare as the majority of studies are carried out in undisturbed tropical forests or logged forests (under strict management)(Sist et al. 2015). The forest inventory used in this research has been sampled along gradients of overexploitation and fire disturbances which provided another level of understanding on the effects of human-induced

disturbances on above and below ground carbon dynamics (Gardner et al. 2013; Berenguer et al. 2014). However, such inventories are time consuming and expensive which makes the approach difficult to generalize and replicate.

Structural analysis of forests by UAV and 'Structure from motion' photogrammetry are low cost, time effective tools for forest inventory (Wallace et al. 2016; Westoby et al. 2012; Frey et al. 2018). However, UAVs are presently limited to small area mapping and specific flight conditions. Texture canopy analysis are promising 2D proxies of 3D forest structure to characterize degraded forest structures through gradients of canopy grain and heterogeneity as soon as the contrast between sunlit and shadowed tree crowns becomes perceptible by images. This property increases with the fineness of image spatial resolution. We showed the potential of UAV and VHSR satellite optical images to assess canopy height variation through FOTO derived indices. Further studies should continue in this vein as the influence of acquisition parameters (i.e. multiple sun/sensor angles and cloud shadow effects) are still limitations to operational broad scale applications of canopy textural analysis to characterize degraded forest structures (Barbier and Couteron 2015).

6.2.2 Landscape approach to analyze dynamics of land use and cover changes

Remote sensing is a globally adopted tool to detect, characterize and monitor land cover/use changes. However, remote sensing alone is not sufficient for understanding the different dynamics of landscape trajectories or for the analysis of underlying drivers, particularly in the context of deforestation fronts. Changes in pixel labels are often interpreted as land use changes but do not depict broader dynamics and underlying agricultural and forestry practices (Haro-Carrión and Southworth 2018).

In this thesis, we initially adopted a landscape quantitative approach to compute landscape pattern metrics based on heterogeneity and fragmentation concepts. These metrics were chosen specifically for studying the expansion of agricultural frontiers in both case studies. Despite a large range of existing landscape metrics, often closely correlating with one another, more information on isolation and contagion effects could have been added to improve the analysis (Wang et al. 2014). Indeed, connectivity between the different landscape elements is an essential factor in understanding the processes of landscape dynamics after disturbance or abandonment of agricultural areas (Lavelle et al. 2016). The computation of metrics within a given area can generate different biasses linked with edge effects due to the windowing process (which be attenuated by using sliding windows) and with the selection of the appropriate window size. Defining the appropriate window size or the appropriate

landscape scale are unresolved issues and depend on the scale of landscape phenomena that are analyzed (Burel and Baudry 1999). It is important to remember that there is no single scale sufficient for comprehensive landscape analysis. This considered, the adopted methodology identified the scale that best captures the diversity of landscape elements using nested-scale approach (heterogeneity metrics yielded similar results). A sensitivity analysis of the impact of the landscape scale on landscape structure metrics capturing fragmentation and heterogeneity and on forest degradation/landscape relationships would help to confirm the adopted methodology and to move forward in the applicability of landscape approaches to land use studies.

Secondly, remote sensing data and the derived landscape structure metrics were analyzed using multivariate statistics in order to generate landscape trajectories. This approach provides a quantitative synthesis of relative changes in both composition and configuration of elements within different units dividing the area of interest (Oszwald et al. 2011). Multivariate statistics (PCA and STATIS) were chosen in order to assign the same statistical weight to each unit (i.e. window) dividing the deforestation front. The rationale being that we can assume that there is a local geographical effect that differentiates each unit in relation to its neighbor. Common factors of evolution should be identified within units located in the same regions but also some units that experienced similar dynamics may be located in different parts of the deforestation front due to similar migration waves, agricultural practices or public policies. Variability in temporal dynamics of the deforestation front expansion and in socio-economic characteristics that are specific to each unit justified the need to use multivariate analysis for differentiating each unit in the analysis.

Landscape structure trajectories were built based on a simplified typology of land cover maps whereas current classification aimed to be as close as possible to landscape elements identified in the field. This was explained by the difficulty in the photointerpretation of historical images and the obtained commission and omission errors using supervised classification algorithms. Consistent detailed mapping of historical Landsat images would provide further information on landscape trajectories. Hybrid supervised and unsupervised classification methods (Baraldi et al. 2006), hybrid pixel and object based approaches taking into account shapes and texture of objects (Phiri et al. 2019) or fully unsupervised classification of dense time series to extract vegetation profiles (Tan et al. 2011; Picoli et al. 2018) could help classify historical land cover/uses and be less dependent on field data.

6.2.3 Vulnerability assessment to guide forest management and empower decision makers

Forest management in human-modified landscapes requires indicators to spatially prioritize areas of importance and therefore financially and efficiently optimize interventions in the field. Assessing the ecological vulnerability of forest cover can help to identify which forests are the most vulnerable to anthropogenic impacts, where they are located and what is driving this vulnerability. Due to the specific interpretation and construction of exposure, sensitivity and adaptive capacity components, vulnerability assessment can hardly be compared between Paragominas and Di Linh study sites. However, vulnerability mapping demonstrates to decision makers that each hotspot of vulnerability calls for a distinct form of management as the **forest status**, **landscape dynamics** and the **drivers of degradation** differ. Maps of forest ecological vulnerability and its components should be core elements in drafting scenarios of degraded forest future (Goldstein 2014). However, the development of these scenarios should be done using a landscape sharing approach in order to find trade-offs between forest conservation and the production of agriculture products (Griscom and Goodman 2015).

In Paragominas municipality, we showed that in areas where forests are highly degraded (overexploitation by timber and recent fire events) there lies different drivers of degradation and landscape dynamics. The adopted landscape approach informed us that the mitigation of exposure factors should be prioritized in areas where conflicts between agriculture and forest are high, while other regions should be targeted for drafting different forest restoration scenarios. However, imagining future landscape management must be conditioned and tailored to local socio-economic conditions (Brancalion et al. 2019; Sayer et al. 2013). Based on our results and field experience, several scenarios or options of restoration are proposed here depending on geomorphological parameters, diversity of local stakeholders (from farming agriculture to industrial agro-business farmers) and whether or not conflicts with agricultural expansion are present:

- In plateaus subject to agricultural expansion, interventions should rely on improved forest cover monitoring (higher spatial and temporal resolution) to prevent further encroachment and develop landscape strategies to prevent fire propagation in landscapes that are particularly prone to fire i.e. strong degradation of forest structures and high fragmentation of forest patches.
- In regions subject to negative feedback loops of degradation and fragmentation, fire controls should rely on the landscape management such as implementation of firebreaks and on participatory approaches to improve awareness of local smallholders to the negative impacts

of fire, with objective to sustain swidden agriculture and prevent further wildfires (Carmenta et al. 2013; Cammelli et al. 2019).

- In fragmented landscape mosaics where forests and soils are highly degraded and forest successional recoveries are often blocked therefore altering seed fluxes among forest patches, passive (i.e. natural) regeneration is less likely to succeed. Active regeneration through enrichment planting or agroforestry are possible alternatives, however only on the condition that preventative measures have been put in place to mitigate fire occurrences. However, some studies highlighted low rates of survival seedlings due to severe drought which may be exacerbated by the current level of fragmentation (Mangueira et al. 2018).
- The slopes generally too steep for mechanization (i.e. no agricultural potential) should be prioritized areas for passive restoration with one of several objectives to restore ecological continuity between the different of forest patches (Tambosi et al. 2014).
- In areas with no particular agricultural expansion dynamic (central Paragominas), enrichment planting to restore degraded primary and secondary forest fragments and reforestation in certain key areas could respectively improve the resilience of these forests to future edge effects and drought events and improve the connectivity of forest landscapes with minimal impact on current agricultural production (Rappaport et al. 2015).

In Di Linh district, we showed that degraded forests are spatially associated with coffee plantation at the forest edges but hotspots of agricultural expansion are not located homogenously along the agricultural frontier. Improving the connectivity of forest habitat could increase the adaptive capacity of these landscapes by reducing fragmentation levels. One example is the mix of evergreen forest with pine forest (central and western part of the district) to stabilize and protect the agricultural frontier, prevent soil erosion and increase forest surface area as well as ecological continuity (Dien et al. 2013). In areas with direct encroachment dynamics of coffee over forest areas, high resolution and frequent data acquisition are needed for improving the efficiency of near-real time monitoring systems and reporting loops to local decision makers (Reymondin et al. 2012).

6.3 Future perspectives

6.3.1 Scaling-up forest ecological vulnerability assessment from localized sites to regions

Large-scale analysis provides a global picture of spatial and temporal dynamics of a given phenomenon which is particularly conducive for grabbing the attention of decision-makers as well as multilateral supports. Recent good examples of large-scale analyses includes the global tree restoration potential calculated by excluding existing trees, agricultural and urban areas (Bastin et al. 2019) and the global restoration opportunities in tropical rainforest landscapes (Brancalion et al. 2019). Data limitation (e.g. availability, coverage, accessibility, cost), methods and computation time are non-exhaustive issues that both studies had to face. Analyzing forest ecological vulnerability at the large scale would provide key information to help orientate restoration initiatives, particularly at deforestation fronts where management responses are eagerly expected. This would therefore involve identifying trade-offs in the large range of possible data (i.e. spatial resolution, price, scale and frequency of acquisition), methods and approaches. We propose to raise some points of discussion following this reflection:

Which data and methods to evaluate forest degradation at large scale?

In the case of large scale studies, assessing the aboveground biomass or analyzing the structures of degraded forests using canopy textures from UAV or VHSR remote sensing are methods limited by inventory data availability, coverage, image extent and costs. Considering the perspective of chapter 3, we developed a method to semi-automatically detect forest disturbances (mainly logging gaps and roads associated with logging activity) using cloud-free Landsat images along a given time series. Instead of mapping forest structures or changes in structures (or carbon stocks) to evaluate the forest status, this proposed indirect approach shows promising alternatives to assess forest degradation defined here as the accumulation of disturbances. Moreover, the long historical depth of Landsat archive coupled with the frequent acquisition of Sentinel-2 images are real assets for the continuous monitoring of forest disturbances over large areas.

The technological and operational barriers that prevent forest structure mapping (and other direct approach methods) from being applicable at a large scale could be unlocked in the very near future. The number of satellite observations of global forests is increasing tremendously thanks to the upcoming launches of the NASA GEDI (2019), ESA BIOMASS (2021), NASA-ISRO NISAR (2022), along with the network of existing systems, such as NASA ICESat-2 (2018), DLR TanDEM-X, JAXA ALOS missions, ESA Copernicus missions, NASA Landsat and Planet microsatellites. The challenge that awaits

is how fast, efficient and accurate methods for forest structure mapping can make the most of these potential large datasets in order to provide the best picture of forest cover status how this can be employed actionable knowledge.

How to face data limitation?

This thesis is a good example of methodological adjustment facing data limitation. Inventories of aboveground biomass did not exist for the Vietnam study site nor did the possibility (due to legislation constraints) to use UAV to acquire forest structural parameters. In addition, the high terrain and strong slopes would have generated many biases when applying canopy texture analysis of VHSR images. Forest degradation was therefore assessed through current mapping of forest types and by analyzing trajectories of forest landscape dynamics, particularly the rate of forest cover changes and fragmentation (edge density). A good understanding of the drivers of forest degradation are also key for mapping degraded forests. In this case, most forest degradation is driven by coffee encroachment on the slopes and in to lesser extent, slow conversion over time to maize/banana production or pine forest plantation. To conclude, there is no a single definition or approach to characterize forest degradation. Forest degradation is site specific because it is linked with underlying direct and indirect drivers that are partially localized. This specificity is a limit for global scale approaches. However, the joint analysis of forest degradation and drivers that are spatially and temporally acting at the landscape scale provides a framework in order to adapt or transpose methodologies from one place of the tropics to another.

Limitations for applying a landscape quantitative approach at large scale

Beyond characterizing forest degradation, scaling-up forest ecological vulnerability also requires applying a landscape quantitative approach at large scale. This approach needs accurate and frequent maps of land cover and land uses in order to analyze the succession of land use processes and events linked with complex human-environmental interactions over a given period of time. The main limitation of applying a similar landscape quantitative approach at larger scale is linked with the large number of landscape units to handle within the method. First, the analysis would encompass a larger amount of landscape diversity and heterogeneity, which could make the identification of the unit size more difficult and variable among different landscapes (e.g. active or passive deforestation front, areas already dominated to agriculture etc). In the long-run, this variability would generate bias in the calculation of landscape metrics. One alternative to this issue would be to select administrative (e.g. villages) or farm boundaries to play the role of unit of analysis, as previously demonstrated by Oszwald et al. (2011) and Grimaldi et al. (2014) but this data is often missing at that scale of analysis. Second, the important number of units to analyze could cause some issues in the construction of unit-specific

landscape structure trajectories and in their classification into homogeneous and low intra-variance clusters. Other clustering methods better suited to large datasets has to be found in order to face these limitations.

6.3.2 Potential addition of indicators and approaches to enhance forest ecological vulnerability assessment

Adding forest functioning indicators to better characterize the ecological vulnerability assessment

It is important to understand that forest ecological vulnerability is not a measurable phenomenon, it is instead a dynamic state which is the result of multiple interacting indicators (Fritzsche et al. 2014). As forest ecological vulnerability cannot be measured directly (Adger 2006), a number of indicators which are presumed to affect vulnerability are aggregated to provide an indication, or an index of vulnerability. Indicators of forest degradation (e.g. degraded forest structures and disturbance accumulation) and landscape dynamics feed the different components of forest ecological vulnerability. Besides changes in structures, forest degradation also implies changes in the functioning of the forest, which was not directly captured in this thesis (Ghazoul and Chazdon 2017b). The functioning of forests following degradation processes could be added to vulnerability assessment as an indicator of forest sensitivity. Adding this indicator would improve how we analyze the reactions of forest ecosystems to degradation such as tree mortality and forest succession. It would also inform on how photosynthesis activity of degraded forests are linked with climate and thus provide significant information on how degraded forest are coping with climate variability and extreme drought events. Hasan (2019) demonstrated that degraded forests experience a progressive decline in photosynthesis activity during the dry season where precipitation are sparse. This decline may due to the fact that degraded forests have a more superficial root system, unable to access water stored in the deep layers of the soil. Additionally, opening of the canopy increases the radiation and heating in the understory and on the surface of the ground, which accelerates the drying process (Alencar et al. 2004).

Combining forest ecological vulnerability assessment with forest ecosystem services mapping

To further emphasize on the prioritization of intervention areas, forest ecological vulnerability assessment could be combined with the evaluation of ecosystem services provided by degraded forests such as soil protection, water availability or biodiversity (Oszwald et al. 2012; Le Clec'h et al. 2017). For instance, Sahraoui et al. (2017) proposed a method for assessing landscape connectivity

through a multi-species approach and identifying areas where conservation actions are needed to enhance or maintain connectivity for species at a landscape scale. These areas would gain extra emphasis if we were to combine this modelling with the assessment of forest ecological vulnerability to agricultural expansion. At the Vietnam study sites, we found that some forest areas located along the agricultural frontier (central part and east of the district) were vulnerable to coffee expansion and coincide with areas of steep slopes and therefore significant risks of soil erosion. The modelling and mapping of spatial patterns of soil erosion are essential for land use planning and could be strategically combined with the vulnerability of forest cover in order to give even more weight in the prioritization of decision making (Tamene et al. 2017).

Building forest ecological vulnerability assessment with local actors

The engagement of local actors in the preparation, evaluation and follow-up of the implementation of landscape approaches are key to their success (Reed et al. 2019). Similarly, their engagement and participation should be put at the forefront of forest ecological vulnerability assessment for a number of reasons:

- To ensure that their perceptions of forest vulnerability are taken into account and properly modelled in the approach. For instance, their conceptions of forest degradation is likely linked to their daily use of forest resources, which could greatly add some nuance to the choice of forest degradation indicators and its modelling and mapping.
- To collect feedback during the construction of the vulnerability framework and improve the understanding of drivers of vulnerability (especially when wider literature is missing) through consultation or participatory workshops.
- To collect validation on the identified areas of forest sensitivity, exposure and adaptive capacity and vulnerability
- To facilitate the discussion among actors in order to prioritize actions such as forest restoration and other types of management on the basis of forest ecological vulnerability assessment and other spatially explicit information

Mentions and notes to the reader

We would like to mention that the two study sites were part of CIRAD and CIAT respective projects:

- Paragominas municipality was part of Ecotera project (« ECOefficiences et développement TERritorial en Amazonie Brésilienne »). The project aimed at producing multidisciplinary knowledge and tools (e.g. eco-efficiency indicators at different scales) to enable local actors in a territory in reconciling their objective of sustainable development with the establishment of productive systems and eco-efficient land use.
- Paragominas municipality was part of ForLand project. The ForLand-Restoration project is developing a forest landscape restoration decision support platform co-designed with all the stakeholders in a given territory. This will involve mapping geographically referenced socioeconomic and environmental data. The indicators generated by the tool will give local stakeholders greater insight into their territory and the impact of their practices and thus help draft future restoration scenarios.
- Di Linh district was part of Terra-i/REDD+ project. Terra-i is a pan-tropical forest monitoring system that pinpoints most probable deforestation areas in near-real time. It was combined with a REDD+ (Reducing Emissions from Deforestation and forest Degradation) pilot project that aim at facilitating forest monitoring with decisions makers such as land use planners and local forest rangers.

Several field trips were organized in Paragominas and Di Linh in the framework of this projects. Two field trips were undergone in Paragominas. The first one was in September 2017 (3 weeks) in order to collect land use/cover type data and UAV data of different forest structures and the second one was in September 2018 (3 weeks) in order to validate land use/cover classifications and acquire additional UAV data. Two field trips were undergone in Di Linh district. The first one was to participate in non-structured interviews with local stakeholders to know more the drivers of land use change and forest degradation in the area and to visit some landscapes of the study site (1 week). The second one was dedicated to field collection of the different land use/cover types (2 weeks).

The first article (chapter 2) presented in this thesis was published in the journal Forest in 2018, the second (chapter 3) was submitted to Ecological Indicator in June 2019, the third (chapter 4) was submitted in Environmental Research Letters in October 2019 and the fourth (chapter 5) was published in International Journal of Applied Earth Observation and Geoinformation in September 2019.

It is also worth noting the oral participation in two international conferences in 2017 and 2018 where the general framework of this thesis and chapter 3 were presented respectively:

- VII World Conference on Ecological Restoration (SER 2017) in Foz Do Iguassu, Brazil. C Bourgoin, L Blanc, J Oszwald, L Reymondin P Laderach, V Gond. *Remote sensing of degraded tropical forest trajectories in the Brazilian Amazon: New insights for landscape restoration.* Oral presentation.
- Association for Forest Spatial Analysis Technologies (ForestSAT 2018) in College Park, Maryland, USA. C Bourgoin, J Betbeder, P Couteron, L Blanc, N Baghdadi, L Reymondin P Laderach, V Gond. *Assessing canopy structures of degraded Amazonian forests using UAV.* Oral presentation.

It is also worth noting the participation in the supervision of two first-year master students from Grenoble university who worked respectively on the environmental and socio-economic conditions of the two study sites (related to Chapter 1) and of three second-year master students who contributed to the different chapter:

- *Landsat analysis of land use and land cover changes in Paragominas, Pará, Brazil* by Florent Rumiano (2018) who contributed to the chapter 4.
- *Analysis of forest degradation trajectories from dense time series in Paragominas, Pará, Brazil* by Sarah Vanacker (2018) who contributed to chapter 3.
- *Multi-scale analysis of canopy structures of a tropical forest degradation gradient* by Etienne Duperron (2019) who contributed to the perspectives of chapter 3.

Other studies written as co-authors and related to the thesis topic have been published (Tritsch et al. 2016; Mercier et al. 2019; Hasan et al. 2019b).

- The article Tritsch et al. (2016) complements chapter 3 and proposes an efficient remote sensing methodology based on Landsat imagery to detect and track logging activity based on the monitoring of canopy openings: Tritsch, Isabelle, Plinio Sist, Igor Narvaes, Lucas Mazzei, Lilian Blanc, Clément Bourgoin, Guillaume Cornu, et Valery Gond. 2016. « Multiple Patterns of Forest Disturbance and Logging Shape Forest Landscapes in Paragominas, Brazil ». Forests 7 (12): 315. https://doi.org/10.3390/f7120315.

- The article Mercier et al. (2019) presents a robust classification method to map forest-agricultural mosaics and assess the complementary of Sentinel-1 and 2 time series. The methodology and script was used in chapter 4 and chapter 5: Mercier, Audrey, Julie Betbeder,

Florent Rumiano, Valéry Gond, Lilian Blanc, Clément Bourgoin, Guillaume Cornu, René Poccard-Chapuis, Jacques Baudry, et Laurence Hubert-Moy. 2019. « Evaluation of Sentinel-1 and 2 Time Series for Land Cover Classification of Forest–Agriculture Mosaics in Temperate and Tropical Landscapes », 20. https://doi.org/10.3390/rs11080979.

- The article Hasan et al. (2019) is based on one of the result of chapter 2, which identified spectral unmixing indicators relevant for identifying degraded forest types. The study presents an indicator of forest degradation used in chapter 4 and built from Landsat annual imagery (2000 to 2015) and non-photosynthetic vegetation variance: Hasan, Ali Fadhil, François Laurent, François Messner, Clément Bourgoin, et Lilian Blanc. 2019a. « Cumulative Disturbances to Assess Forest Degradation Using Spectral Unmixing in the North-eastern Amazon ». Applied Vegetation Science, mai, avsc.12441. https://doi.org/10.1111/avsc.12441.

References

Achard, F., L. Boschetti, S. Brown, M. Brady, R. DeFries, G. Grassi, M. Herold, et al. 2014. « A sourcebook of methods and procedures for monitoring and reporting anthropogenic greenhouse gas emissions and removals associated with deforestation, gains and losses of carbon stocks in forests remaining forests, and forestation ». GOFC-GOLD. http://library.wur.nl/WebQuery/wurpubs/481317.

Achard, F, R DeFries, H Eva, M Hansen, P Mayaux, et H-J Stibig. 2007. « Pan-Tropical Monitoring of Deforestation ». *Environmental Research Letters* 2 (4): 045022. https://doi.org/10.1088/1748-9326/2/4/045022.

Adger, W. Neil. 2006. « Vulnerability ». *Global Environmental Change* 16 (3): 268-81. https://doi.org/10.1016/j.gloenvcha.2006.02.006.

Agrawal, A., A. Chhatre, et R. Hardin. 2008. « Changing Governance of the World's Forests ». *Science* 320 (5882): 1460-62. https://doi.org/10.1126/science.1155369.

Alencar, Ane A., Paulo M. Brando, Gregory P. Asner, et Francis E. Putz. 2015. « Landscape Fragmentation, Severe Drought, and the New Amazon Forest Fire Regime ». *Ecological Applications* 25 (6): 1493-1505. https://doi.org/10.1890/14-1528.1.

Alencar, Ane A. C., Luis A. Solórzano, et Daniel C. Nepstad. 2004. « Modeling Forest Understory Fires in an Eastern Amazonian Landscape ». *Ecological Applications* 14 (sp4): 139-49. https://doi.org/10.1890/01-6029.

Almeida, D. R. A, S. C. Stark, J. Schietti, J. L. C. Camargo, N. T. Amazonas, E. B. Gorgens, D. M Rosa, et al. 2019. « Persistent Effects of Fragmentation on Tropical Rainforest Canopy Structure after 20 Years of Isolation ». *Ecological Applications*, juin, e01952. https://doi.org/10.1002/eap.1952.

Almeida, Danilo R. A., Scott C. Stark, Juliana Schietti, Jose L. C. Camargo, Nino T. Amazonas, Eric B. Gorgens, Diogo M. Rosa, et al. 2019. « Persistent Effects of Fragmentation on Tropical Rainforest Canopy Structure after 20 Yr of Isolation ». *Ecological Applications*, juillet. https://doi.org/10.1002/eap.1952.

Alonzo, Michael, Hans-Erik Andersen, Douglas Morton, et Bruce Cook. 2018. « Quantifying Boreal Forest Structure and Composition Using UAV Structure from Motion ». *Forests* 9 (3): 119. https://doi.org/10.3390/f9030119.

Andrade, Fabiano Soares. 2011. « Variabilidade da precipitação pluviométrica de um município do estado do Pará » 8 (4): 8.

Arlot, Sylvain, et Alain Celisse. 2010. « A Survey of Cross-Validation Procedures for Model Selection ». *Statistics Surveys* 4 (0): 40-79. https://doi.org/10.1214/09-SS054.

Asner, Gregory P. 2009. « Tropical forest carbon assessment: integrating satellite and airborne mapping approaches ». *Environmental Research Letters* 4 (3): 034009. https://doi.org/10.1088/1748-9326/4/3/034009.

Asner, Gregory P., Philip G. Brodrick, Christopher Philipson, Nicolas R. Vaughn, Roberta E. Martin, David E. Knapp, Joseph Heckler, et al. 2018. « Mapped Aboveground Carbon Stocks to Advance Forest Conservation and Recovery in Malaysian Borneo ». *Biological Conservation* 217 (janvier): 289-310. https://doi.org/10.1016/j.biocon.2017.10.020.

Asner, Gregory P., Michael Keller, Rodrigo Pereira, et Johan C. Zweede. 2002. « Remote sensing of selective logging in Amazonia: Assessing limitations based on detailed field observations, Landsat ETM+, and textural analysis ». *Remote Sensing of Environment* 80 (3): 483–496.

Asner, Gregory P., David E. Knapp, Aravindh Balaji, et Guayana Páez-Acosta. 2009a. « Automated mapping of tropical deforestation and forest degradation: CLASlite ». *Journal of Applied Remote Sensing* 3 (1): 033543–033543.

———. 2009b. « Automated mapping of tropical deforestation and forest degradation: CLASlite ». *Journal of Applied Remote Sensing* 3 (1): 033543–033543.

Asner, Gregory P., David E. Knapp, Eben N. Broadbent, Paulo JC Oliveira, Michael Keller, et Jose N. Silva. 2005. « Selective logging in the Brazilian Amazon ». *Science* 310 (5747): 480–482.

Asner, Gregory P., et Joseph Mascaro. 2014. « Mapping Tropical Forest Carbon: Calibrating Plot Estimates to a Simple LiDAR Metric ». *Remote Sensing of Environment* 140 (janvier): 614-24. https://doi.org/10.1016/j.rse.2013.09.023.

Asner, Gregory P., Joseph Mascaro, Helene C. Muller-Landau, Ghislain Vieilledent, Romuald Vaudry, Maminiaina Rasamoelina, Jefferson S. Hall, et Michiel van Breugel. 2012. « A Universal Airborne LiDAR Approach for Tropical Forest Carbon Mapping ». *Oecologia* 168 (4): 1147-60. https://doi.org/10.1007/s00442-011-2165-z.

Avitabile, Valerio, Martin Herold, Gerard B. M. Heuvelink, Simon L. Lewis, Oliver L. Phillips, Gregory P. Asner, John Armston, et al. 2016. « An Integrated Pan-Tropical Biomass Map Using Multiple Reference Datasets ». *Global Change Biology* 22 (4): 1406-20. https://doi.org/10.1111/gcb.13139.

Baccini, A., S. J. Goetz, W. S. Walker, N. T. Laporte, M. Sun, D. Sulla-Menashe, J. Hackler, et al. 2012. « Estimated carbon dioxide emissions from tropical deforestation improved by carbon-density maps ». *Nature Climate Change* 2 (3): 182-85. https://doi.org/10.1038/nclimate1354.

Baccini, A, N Laporte, S J Goetz, M Sun, et H Dong. 2008. « A first map of tropical Africa's above-ground biomass derived from satellite imagery ». *Environmental Research Letters* 3 (4): 045011. https://doi.org/10.1088/1748-9326/3/4/045011.

Baccini, A., W. Walker, L. Carvalho, M. Farina, D. Sulla-Menashe, et R. A. Houghton. 2017. « Tropical Forests Are a Net Carbon Source Based on Aboveground Measurements of Gain and Loss ». *Science* 358 (6360): 230-34. https://doi.org/10.1126/science.aam5962.

Baraldi, A., V. Puzzolo, P. Blonda, L. Bruzzone, et C. Tarantino. 2006. « Automatic Spectral Rule-Based Preliminary Mapping of Calibrated Landsat TM and ETM+ Images ». *IEEE Transactions on Geoscience and Remote Sensing* 44 (9): 2563-86. https://doi.org/10.1109/TGRS.2006.874140.

Barbier, Nicolas, et Pierre Couteron. 2015. « Attenuating the Bidirectional Texture Variation of Satellite Images of Tropical Forest Canopies ». *Remote Sensing of Environment* 171 (décembre): 245-60. https://doi.org/10.1016/j.rse.2015.10.007.

Barbier, Nicolas, Pierre Couteron, Christophe Proisy, Yadvinder Malhi, et Jean-Philippe Gastellu-Etchegorry. 2010. « The Variation of Apparent Crown Size and Canopy Heterogeneity across Lowland Amazonian Forests: Amazon Forest Canopy Properties ». *Global Ecology and Biogeography* 19 (1): 72-84. https://doi.org/10.1111/j.1466-8238.2009.00493.x.

Barlow, Jos, Gareth D. Lennox, Joice Ferreira, Erika Berenguer, Alexander C. Lees, Ralph Mac Nally, James R. Thomson, et al. 2016. « Anthropogenic disturbance in tropical forests can double biodiversity loss from deforestation ». *Nature* 535 (7610): 144-47. https://doi.org/10.1038/nature18326.

Barona, Elizabeth, Navin Ramankutty, Glenn Hyman, et Oliver T Coomes. 2010. « The Role of Pasture and Soybean in Deforestation of the Brazilian Amazon ». *Environmental Research Letters* 5 (2): 024002. https://doi.org/10.1088/1748-9326/5/2/024002.

Bastin, Jean-François, Nicolas Barbier, Pierre Couteron, Benoît Adams, Aurélie Shapiro, Jan Bogaert, et Charles De Cannière. 2014. « Aboveground biomass mapping of African forest mosaics using canopy texture analysis: toward a regional approach ». *Ecological applications* 24 (8): 1984–2001.

Bastin, Jean-Francois, Yelena Finegold, Claude Garcia, Danilo Mollicone, Marcelo Rezende, Devin Routh, Constantin M. Zohner, et Thomas W. Crowther. 2019. « The Global Tree Restoration Potential ». *Science* 365 (6448): 76-79. https://doi.org/10.1126/science.aax0848.

Bastin, J.-F., N. Barbier, M. Réjou-Méchain, A. Fayolle, S. Gourlet-Fleury, D. Maniatis, T. de Haulleville, et al. 2015. « Seeing Central African forests through their largest trees ». *Scientific Reports* 5 (août): 13156. https://doi.org/10.1038/srep13156.

Bégué, Agnès, Damien Arvor, Beatriz Bellon, Julie Betbeder, Diego de Abelleyra, Rodrigo P. D. Ferraz, Valentine Lebourgeois, Camille Lelong, Margareth Simões, et Santiago R. Verón. 2018. « Remote Sensing and Cropping Practices: A Review ». *Remote Sensing* 10 (2): 99. https://doi.org/10.3390/rs10010099.

Benhadj, Iskander, Benoit Duchemin, Philippe Maisongrande, Vincent Simonneaux, Saïd Khabba, et Abdelghani Chehbouni. 2012. « Automatic Unmixing of MODIS Multi-Temporal Data for Inter-Annual Monitoring of Land Use at a Regional Scale (Tensift, Morocco) ». *International Journal of Remote Sensing* 33 (5): 1325-48. https://doi.org/10.1080/01431161.2011.564220.

Berenguer, Erika, Joice Ferreira, Toby Alan Gardner, Luiz Eduardo Oliveira Cruz Aragão, Plínio Barbosa De Camargo, Carlos Eduardo Cerri, Mariana Durigan, Raimundo Cosme De Oliveira, Ima Célia Guimarães Vieira, et Jos Barlow. 2014. « A Large-Scale Field Assessment of Carbon Stocks in Human-Modified Tropical Forests ». *Global Change Biology* 20 (12): 3713-26. https://doi.org/10.1111/gcb.12627.

Berenguer, Erika, Yadvinder Malhi, Paulo Brando, Amanda Cardoso, Nunes Cordeiro, Joice Ferreira, Filipe Franca, et Liana Chesini Rossi. 2018. « Tree Growth and Stem Carbon Accumulation in Human-Modified Amazonian Forests Following Drought and Fire », 8.

Bernier, P Y, D Paré, G Stinson, S R J Bridge, B E Kishchuk, T C Lemprière, E Thiffault, B D Titus, et W Vasbinder. 2016. « Moving beyond the Concept of "Primary Forest" as a Metric of Forest Environment Quality ». *Ecological Applications*, décembre. https://doi.org/10.1002/eap.1477.

Berrouet, Lina María, Jenny Machado, et Clara Villegas-Palacio. 2018. « Vulnerability of Socio—Ecological Systems: A Conceptual Framework ». *Ecological Indicators* 84 (janvier): 632-47. https://doi.org/10.1016/j.ecolind.2017.07.051.

Bivand, Roger, Tim Keitt, Barry Rowlingson, Edzer Pebesma, Michael Sumner, Robert Hijmans, Even Rouault, et Jeroen Ooms. 2019. « CRAN - Package rgdal ». 2019. https://cran.r-project.org/web/packages/rgdal/.

Blanc, L., D. Chessel, et S. Doledec. 1998. « Etude de la stabilité temporelle des structures spatiales par analyses d'une série de tableaux de relevés faunistiques totalement appariés ». *Bulletin Français de la Pêche et de la Pisciculture*, n° 348: 1-21. https://doi.org/10.1051/kmae:1998049.

Blanc, Lilian, Marion Echard, Bruno Herault, Damien Bonal, Eric Marcon, Jerome Chave, et Christopher Baraloto. 2009. « Dynamics of aboveground carbon stocks in a selectively logged tropical forest ». *Ecological Applications* 19 (6): 1397–1404.

Borra, Simone, et Agostino Di Ciaccio. 2010. « Measuring the Prediction Error. A Comparison of Cross-Validation, Bootstrap and Covariance Penalty Methods ». *Computational Statistics & Data Analysis* 54 (12): 2976-89. https://doi.org/10.1016/j.csda.2010.03.004.

Bourbier, Lucas, Guillaume Cornu, Alexandre Pennec, Christine Brognoli, et Valéry Gond. 2013. « Large-scale estimation of forest canopy opening using remote sensing in Central Africa ». *Bois et forêts des tropiques*, n° 315: 1.

Bourgoin, Clément, Lilian Blanc, Jean-Stéphane Bailly, Guillaume Cornu, Erika Berenguer, Johan Oszwald, Isabelle Tritsch, et al. 2018. « The Potential of Multisource Remote Sensing for Mapping the Biomass of a Degraded Amazonian Forest ». *Forests*, 21. https://doi.org/10.3390/f9060303.

Bourgoin, Clément, Johan Oszwald, Jeremy Bourgoin, Valéry Gond, Lilian Blanc, Hélène Dessard, Trong Van Phan, Plinio Sist, Peter Läderach, et Louis Reymondin. 2020. « Assessing the Ecological Vulnerability of Forest Landscape to Agricultural Frontier Expansion in the Central Highlands of Vietnam ». *International Journal of Applied Earth Observation and Geoinformation* 84 (février): 101958. https://doi.org/10.1016/j.jag.2019.101958.

Boussard, H, et J Baudry. 2017. « Chloe4.0: a software for landscape pattern analysis ». 2017. https://www6.rennes.inra.fr/bagap/PRODUCTIONS/Logiciels.

Bouvet, Alexandre, Stéphane Mermoz, Marie Ballère, Thierry Koleck, et Thuy Le Toan. 2018. « Use of the SAR Shadowing Effect for Deforestation Detection with Sentinel-1 Time Series ». *Remote Sensing* 10 (8): 1250. https://doi.org/10.3390/rs10081250.

Brancalion, Pedro H. S., et Robin L. Chazdon. 2017. « Beyond Hectares: Four Principles to Guide Reforestation in the Context of Tropical Forest and Landscape Restoration: Forest and Landscape Restoration Principles ». *Restoration Ecology* 25 (4): 491-96. https://doi.org/10.1111/rec.12519.

Brancalion, Pedro H. S., Aidin Niamir, Eben Broadbent, Renato Crouzeilles, Felipe S. M. Barros, Angelica M. Almeyda Zambrano, Alessandro Baccini, et al. 2019. « Global Restoration Opportunities in Tropical Rainforest Landscapes ». *Science Advances* 5 (7): eaav3223. https://doi.org/10.1126/sciadv.aav3223.

Brandon, Katrina. 2014. « Ecosystem Services from Tropical Forests: Review of Current Science ». *SSRN Electronic Journal*. https://doi.org/10.2139/ssrn.2622749.

Breiman, Leo. 2001. « Random forests ». *Machine learning* 45 (1): 5–32.

Briant, Gaël, Valéry Gond, et Susan G.W. Laurance. 2010. « Habitat Fragmentation and the Desiccation of Forest Canopies: A Case Study from Eastern Amazonia ». *Biological Conservation* 143 (11): 2763-69. https://doi.org/10.1016/j.biocon.2010.07.024.

Broadbent, E, G Asner, M Keller, D Knapp, P Oliveira, et J Silva. 2008. « Forest Fragmentation and Edge Effects from Deforestation and Selective Logging in the Brazilian Amazon ». *Biological Conservation* 141 (7): 1745-57. https://doi.org/10.1016/j.biocon.2008.04.024.

Bullock, Eric L., Curtis E. Woodcock, et Pontus Olofsson. 2018. « Monitoring Tropical Forest Degradation Using Spectral Unmixing and Landsat Time Series Analysis ». *Remote Sensing of Environment*, novembre. https://doi.org/10.1016/j.rse.2018.11.011.

Burel, Françoise, et Jacques Baudry. 1999. « Ecologie du paysage. Concepts, Méthodes et Applications, Technique & Documentation ».

Bustamante, Mercedes M. C., Iris Roitman, T. Mitchell Aide, Ane Alencar, Liana O. Anderson, Luiz Aragão, Gregory P. Asner, et al. 2016a. « Toward an Integrated Monitoring Framework to Assess the Effects of Tropical Forest Degradation and Recovery on Carbon Stocks and Biodiversity ». *Global Change Biology* 22 (1): 92-109. https://doi.org/10.1111/gcb.13087.

———. 2016b. « Toward an Integrated Monitoring Framework to Assess the Effects of Tropical Forest Degradation and Recovery on Carbon Stocks and Biodiversity ». *Global Change Biology* 22 (1): 92-109. https://doi.org/10.1111/gcb.13087.

Calle, M. L., et V. Urrea. 2011. « Letter to the Editor: Stability of Random Forest Importance Measures ». *Briefings in Bioinformatics* 12 (1): 86-89. https://doi.org/10.1093/bib/bbq011.

Cammelli, Federico, Emilie Coudel, et Livia de Freitas Navegantes Alves. 2019. « Smallholders' Perceptions of Fire in the Brazilian Amazon: Exploring Implications for Governance Arrangements ». *Human Ecology*, août. https://doi.org/10.1007/s10745-019-00096-6.

Carmenta, Rachel, Saskia Vermeylen, Luke Parry, et Jos Barlow. 2013. « Shifting Cultivation and Fire Policy: Insights from the Brazilian Amazon ». *Human Ecology* 41 (4): 603-14. https://doi.org/10.1007/s10745-013-9600-1.

Champion, Isabelle, Christian Germain, Jean Pierre Da Costa, Arnaud Alborini, et Pascale Dubois-Fernandez. 2014. « Retrieval of forest stand age from SAR image texture for varying distance and orientation values of the gray level co-occurrence matrix ». *IEEE Geoscience and Remote Sensing Letters* 11 (1): 5–9.

Charrad, Malika, Nadia Ghazzali, Véronique Boiteau, et Azam Niknafs. 2014. « NbClust: An R Package for Determining the Relevant Number of Clusters in a Data Set ». *Journal of Statistical Software* 61 (6). https://doi.org/10.18637/jss.v061.i06.

Chave, J., C. Andalo, S. Brown, M. A. Cairns, J. Q. Chambers, D. Eamus, H. Fölster, et al. 2005. « Tree Allometry and Improved Estimation of Carbon Stocks and Balance in Tropical Forests ». *Oecologia* 145 (1): 87-99. https://doi.org/10.1007/s00442-005-0100-x.

Chazdon, RL, et MR Guariguata. 2018. *Decision Support Tools for Forest Landscape Restoration: Current Status and Future Outlook*. Center for International Forestry Research (CIFOR).

Chazdon, Robin L., Pedro H. S. Brancalion, Lars Laestadius, Aoife Bennett-Curry, Kathleen Buckingham, Chetan Kumar, Julian Moll-Rocek, Ima Célia Guimarães Vieira, et Sarah Jane Wilson. 2016. « When Is a Forest a Forest? Forest Concepts and Definitions in the Era of Forest and Landscape Restoration ». *Ambio* 45 (5): 538-50. https://doi.org/10.1007/s13280-016-0772-y.

Chazdon, Robin L., Celia A. Harvey, Oliver Komar, Daniel M. Griffith, Bruce G. Ferguson, Miguel Martinez-Ramos, Helda Morales, et al. 2009. « Beyond Reserves: A Research Agenda for Conserving Biodiversity in Human-Modified Tropical Landscapes ». *Biotropica* 41 (2): 142-53. https://doi.org/10.1111/j.1744-7429.2008.00471.x.

Chessel, Daniel, Anne B Dufour, et Jean Thioulouse. 2004. « The Ade4 Package - I : One-Table Methods » 4: 6.

« Climate-KIC | The EU's main climate innovation initiative ». s. d. Consulté le 18 mai 2018. http://www.climate-kic.org/.

Cohen, Warren B., Zhiqiang Yang, Sean P. Healey, Robert E. Kennedy, et Noel Gorelick. 2018. « A LandTrendr Multispectral Ensemble for Forest Disturbance Detection ». *Remote Sensing of Environment* 205 (février): 131-40. https://doi.org/10.1016/j.rse.2017.11.015.

Cornillon, Pierre-André, et Eric Matzner-Løber. 2007. *Régression : Théorie et Applications*. https://hal.archives-ouvertes.fr/hal-00955892.

Couteron, P., R. Pelissier, E. A. Nicolini, et D. Paget. 2005. « Predicting tropical forest stand structure parameters from Fourier transform of very high-resolution remotely sensed canopy images ». *Journal of applied ecology* 42 (6): 1121-28.

Couteron, Pierre. 2002. « Quantifying Change in Patterned Semi-Arid Vegetation by Fourier Analysis of Digitized Aerial Photographs ». *International Journal of Remote Sensing* 23 (17): 3407-25. https://doi.org/10.1080/01431160110107699.

Couteron, Pierre, Raphael Pelissier, Eric A. Nicolini, et Dominique Paget. 2005. « Predicting Tropical Forest Stand Structure Parameters from Fourier Transform of Very High-Resolution Remotely Sensed Canopy Images: *Predicting Tropical Forest Stand Structure* ». *Journal of Applied Ecology* 42 (6): 1121-28. https://doi.org/10.1111/j.1365-2664.2005.01097.x.

« CRAN - Package gstat ». s. d. Consulté le 13 avril 2018. https://cran.r-project.org/web/packages/gstat/index.html.

« CRAN - Package raster ». s. d. Consulté le 13 avril 2018. https://cran.r-project.org/web/packages/raster/index.html.

Curtis, Philip G., Christy M. Slay, Nancy L. Harris, Alexandra Tyukavina, et Matthew C. Hansen. 2018. « Classifying Drivers of Global Forest Loss ». *Science* 361 (6407): 1108-11. https://doi.org/10.1126/science.aau3445.

Dandois, Jonathan, Marc Olano, et Erle Ellis. 2015. « Optimal Altitude, Overlap, and Weather Conditions for Computer Vision UAV Estimates of Forest Structure ». *Remote Sensing* 7 (10): 13895-920. https://doi.org/10.3390/rs71013895.

De Sy, Veronique, Martin Herold, Frédéric Achard, Gregory P Asner, Alex Held, Josef Kellndorfer, et Jan Verbesselt. 2012. « Synergies of Multiple Remote Sensing Data Sources for REDD+ Monitoring ». *Current Opinion in Environmental Sustainability* 4 (6): 696-706. https://doi.org/10.1016/j.cosust.2012.09.013.

De Sy, Veronique, Martin Herold, Frederic Achard, Valerio Avitabile, Alessandro Baccini, Sarah Carter, Jan G P W Clevers, Erik Lindquist, Maria Pereira, et Louis Verchot. 2019. « Tropical Deforestation Drivers and Associated Carbon Emission Factors Derived from Remote Sensing Data ». *Environmental Research Letters*, août. https://doi.org/10.1088/1748-9326/ab3dc6.

« DEGRAD — Coordenação-Geral de Observação da Terra ». s. d. Consulté le 10 avril 2018. http://www.obt.inpe.br/OBT/assuntos/programas/amazonia/degrad.

Deng, Yingbin, Changshan Wu, Miao Li, et Renrong Chen. 2015. « RNDSI: A Ratio Normalized Difference Soil Index for Remote Sensing of Urban/Suburban Environments ». *International Journal of Applied Earth Observation and Geoinformation* 39 (juillet): 40-48. https://doi.org/10.1016/j.jag.2015.02.010.

Déry, Steve. 2000. « Agricultural Colonisation in Lam Dong Province, Vietnam ». *Asia Pacific Viewpoint* 41 (1): 35-49. https://doi.org/10.1111/1467-8373.00105.

Deutscher, Janik, Roland Perko, Karlheinz Gutjahr, Manuela Hirschmugl, et Mathias Schardt. 2013. « Mapping Tropical Rainforest Canopy Disturbances in 3D by COSMO-SkyMed Spotlight InSAR-Stereo Data to Detect Areas of Forest Degradation ». *Remote Sensing* 5 (2): 648-63. https://doi.org/10.3390/rs5020648.

DeVries, Ben, Mathieu Decuyper, Jan Verbesselt, Achim Zeileis, Martin Herold, et Shijo Joseph. 2015. « Tracking Disturbance-Regrowth Dynamics in Tropical Forests Using Structural Change Detection and Landsat Time Series ». *Remote Sensing of Environment* 169 (novembre): 320-34. https://doi.org/10.1016/j.rse.2015.08.020.

DeVries, Ben, Jan Verbesselt, Lammert Kooistra, et Martin Herold. 2015. « Robust Monitoring of Small-Scale Forest Disturbances in a Tropical Montane Forest Using Landsat Time Series ». *Remote Sensing of Environment* 161 (mai): 107-21. https://doi.org/10.1016/j.rse.2015.02.012.

Dien, Vu Tien, Pham Ngoc Bay, Peter Stephen, Tran Van Chau, Alexandre Grais, et Silvia Petrova. 2013. « Land use, forest cover change and historical GHG emission, From 1990 to 2010, Lam Dong province, Vietnam ». 2013. https://theredddesk.org/resources/land-use-forest-cover-change-and-historical-ghg-emission.

Drusch, M., U. Del Bello, S. Carlier, O. Colin, V. Fernandez, F. Gascon, B. Hoersch, et al. 2012. « Sentinel-2: ESA's Optical High-Resolution Mission for GMES Operational Services ». *Remote Sensing of Environment* 120 (mai): 25-36. https://doi.org/10.1016/j.rse.2011.11.026.

Dwomoh, Francis K., Michael C. Wimberly, Mark A. Cochrane, et Izaya Numata. 2019. « Forest Degradation Promotes Fire during Drought in Moist Tropical Forests of Ghana ». *Forest Ecology and Management* 440 (mai): 158-68. https://doi.org/10.1016/j.foreco.2019.03.014.

Englhart, S., V. Keuck, et F. Siegert. 2011. « Aboveground Biomass Retrieval in Tropical Forests — The Potential of Combined X- and L-Band SAR Data Use ». *Remote Sensing of Environment* 115 (5): 1260-71. https://doi.org/10.1016/j.rse.2011.01.008.

Ernoult, Aude, Sylviano Freiré-Diaz, Estelle Langlois, et Didier Alard. 2006. « Are Similar Landscapes the Result of Similar Histories? » *Landscape Ecology* 21 (5): 631-39. https://doi.org/10.1007/s10980-005-5321-1.

Fahrig, Lenore, Jacques Baudry, Lluís Brotons, Françoise G. Burel, Thomas O. Crist, Robert J. Fuller, Clelia Sirami, Gavin M. Siriwardena, et Jean-Louis Martin. 2011. « Functional Landscape Heterogeneity and Animal Biodiversity in Agricultural Landscapes ». *Ecology Letters* 14 (2): 101-12. https://doi.org/10.1111/j.1461-0248.2010.01559.x.

Fayad, Ibrahim, Nicolas Baghdadi, Jean-Stéphane Bailly, Nicolas Barbier, Valéry Gond, Mahmoud Hajj, Frédéric Fabre, et Bernard Bourgine. 2014. « Canopy Height Estimation in French Guiana with LiDAR ICESat/GLAS Data Using Principal Component Analysis and Random Forest Regressions ». *Remote Sensing* 6 (12): 11883-914. https://doi.org/10.3390/rs61211883.

Fayad, Mohammad, Nicolas Baghdadi, Ibrahim Fayad, Ghislain Vieilledent, Jean-Stéphane Bailly, et Dinh Minh. 2017. « Interest of Integrating Spaceborne LiDAR Data to Improve the Estimation of Biomass in High Biomass Forested Areas ». *Remote Sensing* 9 (3): 213. https://doi.org/10.3390/rs9030213.

Fearnside, Philip M. 2005. « Deforestation in Brazilian Amazonia: history, rates, and consequences ». *Conservation biology* 19 (3): 680–688.

Ferreira, Joice, Lilian Blanc, Milton Kanashiro, Alexander Charles Lees, Jeremy Bourgoin, Joberto Veloso de Freitas, Michelliny Bentes Gama, François Laurent, Marlucia Bonifacio Martins, et Nargila Moura. 2015. « Degradação florestal na Amazônia: como ultrapassar os limites conceituais, científicos e técnicos para mudar esse cenário ».

Finer, Matt, Sidney Novoa, Mikaela J. Weisse, Rachael Petersen, Joseph Mascaro, Tamia Souto, Forest Stearns, et Raúl García Martinez. 2018. « Combating Deforestation: From Satellite to Intervention ». *Science* 360 (6395): 1303-5. https://doi.org/10.1126/science.aat1203.

« Florestas do Brasil em Resumo 2013 ». s. d. Consulté le 10 avril 2018. http://www.florestal.gov.br/publicacoes/572-florestas-do-brasil-em-resumo-2013.
Foley, J. A. 2005. « Global Consequences of Land Use ». *Science* 309 (5734): 570-74. https://doi.org/10.1126/science.1111772.
Folke, Carl, Steve Carpenter, Brian Walker, Marten Scheffer, Thomas Elmqvist, Lance Gunderson, et C.S. Holling. 2004. « Regime Shifts, Resilience, and Biodiversity in Ecosystem Management ». *Annual Review of Ecology, Evolution, and Systematics* 35 (1): 557-81. https://doi.org/10.1146/annurev.ecolsys.35.021103.105711.
Folke, Carl, Thomas Hahn, Per Olsson, et Jon Norberg. 2005. « Adaptive Governance of Social-Ecological Systems ». *Annual Review of Environment and Resources* 30 (1): 441-73. https://doi.org/10.1146/annurev.energy.30.050504.144511.
Forman, RT, et Michel Godron. 1981. « Patches and Structural Components for a Landscape Ecology ». *BioScience* 31 (10): 733-40. https://doi.org/10.2307/1308780.
Frazer, Gordon W., Michael A. Wulder, et K. Olaf Niemann. 2005. « Simulation and Quantification of the Fine-Scale Spatial Pattern and Heterogeneity of Forest Canopy Structure: A Lacunarity-Based Method Designed for Analysis of Continuous Canopy Heights ». *Forest Ecology and Management* 214 (1-3): 65-90. https://doi.org/10.1016/j.foreco.2005.03.056.
Frey, Julian, Kyle Kovach, Simon Stemmler, et Barbara Koch. 2018. « UAV Photogrammetry of Forests as a Vulnerable Process. A Sensitivity Analysis for a Structure from Motion RGB-Image Pipeline ». *Remote Sensing* 10 (6): 912. https://doi.org/10.3390/rs10060912.
Fritzsche, Kerstin, Stefan Schneiderbauer, Philip Bubeck, Stefan Kienberger, Mareike Buth, Marc Zebisch, et Walter Kahlenborn. 2014. « The Vulnerability Sourcebook: Concept and Guidelines for Standardised Vulnerability Assessments ». Adelphi. 2014. http://www.adaptationcommunity.net/?wpfb_dl=203.
Frolking, S., M. W. Palace, D. B. Clark, J. Q. Chambers, H. H. Shugart, et G. C. Hurtt. 2009. « Forest Disturbance and Recovery: A General Review in the Context of Spaceborne Remote Sensing of Impacts on Aboveground Biomass and Canopy Structure ». *Journal of Geophysical Research* 114 (juillet). https://doi.org/10.1029/2008JG000911.
Gallopín, Gilberto C. 2006. « Linkages between Vulnerability, Resilience, and Adaptive Capacity ». *Global Environmental Change* 16 (3): 293-303. https://doi.org/10.1016/j.gloenvcha.2006.02.004.
Gao, Bo-cai. 1996. « NDWI—A Normalized Difference Water Index for Remote Sensing of Vegetation Liquid Water from Space ». *Remote Sensing of Environment* 58 (3): 257-66. https://doi.org/10.1016/S0034-4257(96)00067-3.
Gardner, T. A., J. Ferreira, J. Barlow, A. C. Lees, L. Parry, I. C. G. Vieira, E. Berenguer, et al. 2013. « A Social and Ecological Assessment of Tropical Land Uses at Multiple Scales: The Sustainable Amazon Network ». *Philosophical Transactions of the Royal Society B: Biological Sciences* 368 (1619): 20120166-20120166. https://doi.org/10.1098/rstb.2012.0166.
Gardner, Toby A., Jos Barlow, Robin Chazdon, Robert M. Ewers, Celia A. Harvey, Carlos A. Peres, et Navjot S. Sodhi. 2009. « Prospects for Tropical Forest Biodiversity in a Human-Modified World ». *Ecology Letters* 12 (6): 561-82. https://doi.org/10.1111/j.1461-0248.2009.01294.x.
Gardner, Toby A., Neil D. Burgess, Naikoa Aguilar-Amuchastegui, Jos Barlow, Erika Berenguer, Tom Clements, Finn Danielsen, et al. 2012. « A Framework for Integrating Biodiversity Concerns into National REDD+ Programmes ». *Biological Conservation* 154 (octobre): 61-71. https://doi.org/10.1016/j.biocon.2011.11.018.
Geist, Helmut J., et Eric F. Lambin. 2002. « Proximate Causes and Underlying Driving Forces of Tropical Deforestation ». *BioScience* 52 (2): 143. https://doi.org/10.1641/0006-3568(2002)052[0143:PCAUDF]2.0.CO;2.
Ghazoul, Jaboury, Zuzana Burivalova, John Garcia-Ulloa, et Lisa A. King. 2015. « Conceptualizing Forest Degradation ». *Trends in Ecology & Evolution* 30 (10): 622-32. https://doi.org/10.1016/j.tree.2015.08.001.

Ghazoul, Jaboury, et Robin Chazdon. 2017a. « Degradation and Recovery in Changing Forest Landscapes: A Multiscale Conceptual Framework ». *Annual Review of Environment and Resources* 42: 161–188.
———. 2017b. « Degradation and Recovery in Changing Forest Landscapes: A Multiscale Conceptual Framework ». *Annual Review of Environment and Resources* 42: 161–188.
Goetz, Scott, Matthew Hansen, Richard A Houghton, Wayne Walker, Nadine T Laporte, et Jonah Busch. 2014. « Measurement and Monitoring for REDD+: The Needs, Current Technological Capabilities, and Future Potential ». *SSRN Electronic Journal*. https://doi.org/10.2139/ssrn.2623076.
Goetz, Scott J, Alessandro Baccini, Nadine T Laporte, Tracy Johns, Wayne Walker, Josef Kellndorfer, Richard A Houghton, et Mindy Sun. 2009. « Mapping and Monitoring Carbon Stocks with Satellite Observations: A Comparison of Methods ». *Carbon Balance and Management* 4 (1): 2. https://doi.org/10.1186/1750-0680-4-2.
Goldstein, Jenny E. 2014. « The Afterlives of Degraded Tropical Forests: New Value for Conservation and Development ». *Environment and Society: Advances in Research* 5 (1): 124-40. https://doi.org/10.3167/ares.2014.050108.
Gond, V., E. Bartholomé, F. Ouattara, A. Nonguierma, et L. Bado. 2004. « Surveillance et cartographie des plans d'eau et des zones humides et inondables en régions arides avec l'instrument VEGETATION embarqué sur SPOT-4 ». *International Journal of Remote Sensing* 25 (5): 987-1004. https://doi.org/10.1080/0143116031000139908.
Gond, V., A. Fayolle, A. Pennec, G. Cornu, P. Mayaux, P. Camberlin, C. Doumenge, N. Fauvet, et S. Gourlet-Fleury. 2013. « Vegetation Structure and Greenness in Central Africa from Modis Multi-Temporal Data ». *Philosophical Transactions of the Royal Society B: Biological Sciences* 368 (1625): 20120309-20120309. https://doi.org/10.1098/rstb.2012.0309.
Gräler, Benedikt, Edzer Pebesma, et Gerard Heuvelink. 2016. « Spatio-temporal interpolation using gstat ». *R Journal* 8 (1): 204–218.
Grimaldi, Michel, Johan Oszwald, Sylvain Dolédec, Maria del Pilar Hurtado, Izildinha de Souza Miranda, Xavier Arnauld de Sartre, William Santos de Assis, et al. 2014. « Ecosystem Services of Regulation and Support in Amazonian Pioneer Fronts: Searching for Landscape Drivers ». *Landscape Ecology* 29 (2): 311-28. https://doi.org/10.1007/s10980-013-9981-y.
Griscom, B. W., et R. C. Goodman. 2015. « Reframing the Sharing VS Sparing Debate for Tropical Forestry Landscapes ». *Journal of Tropical Forest Science* 27 (2): 145–147.
Grosjean, Godefroy, F. Monteils, S. D. Hamilton, D. Blaustein-Rejto, M. Gatto, T. Talsma, C. Bourgoin, L. S. Sebastian, D. Catacutan, et R. Mulia. 2016. « Increasing resilience to droughts in Viet Nam: The role of forests, agroforestry, and climate smart agriculture ».
Guitet, Stéphane, Bruno Hérault, Quentin Molto, Olivier Brunaux, et Pierre Couteron. 2015. « Spatial Structure of Above-Ground Biomass Limits Accuracy of Carbon Mapping in Rainforest but Large Scale Forest Inventories Can Help to Overcome ». Édité par Krishna Prasad Vadrevu. *PLOS ONE* 10 (9): e0138456. https://doi.org/10.1371/journal.pone.0138456.
Gunderson, Lance H. 2000. « Ecological resilience–in theory and application ». *Annual review of ecology and systematics*, 425–439.
Ha, Dang Thanh, et Gerald Shively. 2008. « Coffee Boom, Coffee Bust and Smallholder Response in Vietnam's Central Highlands ». *Review of Development Economics* 12 (2): 312-26. https://doi.org/10.1111/j.1467-9361.2007.00391.x.
Hamsici, O.C., et A.M. Martinez. 2008. « Bayes Optimality in Linear Discriminant Analysis ». *IEEE Transactions on Pattern Analysis and Machine Intelligence* 30 (4): 647-57. https://doi.org/10.1109/TPAMI.2007.70717.
Hansen, M. C., P. V. Potapov, R. Moore, M. Hancher, S. A. Turubanova, A. Tyukavina, D. Thau, et al. 2013. « High-Resolution Global Maps of 21st-Century Forest Cover Change ». *Science* 342 (6160): 850-53. https://doi.org/10.1126/science.1244693.

Hansen, M. C., S. V. Stehman, et P. V. Potapov. 2010. « Quantification of Global Gross Forest Cover Loss ». *Proceedings of the National Academy of Sciences* 107 (19): 8650-55. https://doi.org/10.1073/pnas.0912668107.

Haralick, Robert M., K. Shanmugam, et Its'Hak Dinstein. 1973. « Textural Features for Image Classification ». *IEEE Transactions on Systems, Man, and Cybernetics* SMC-3 (6): 610-21. https://doi.org/10.1109/TSMC.1973.4309314.

Hargis, Christina D., John A. Bissonette, et John L. David. 1998. « The behavior of landscape metrics commonly used in the study of habitat fragmentation ». *Landscape ecology* 13 (3): 167–186.

Haro-Carrión, Xavier, et Jane Southworth. 2018. « Understanding Land Cover Change in a Fragmented Forest Landscape in a Biodiversity Hotspot of Coastal Ecuador ». *Remote Sensing* 10 (12): 1980. https://doi.org/10.3390/rs10121980.

Hasan, Ali Fadhil. 2019. « Évaluation de la dégradation des forêts primaires par télédétection dans un espace de front pionnier consolidé d'Amazonie orientale (Paragominas) », mars. https://tel.archives-ouvertes.fr/tel-02275810/document.

Hasan, Ali Fadhil, François Laurent, François Messner, Clément Bourgoin, et Lilian Blanc. 2019a. « Cumulative Disturbances to Assess Forest Degradation Using Spectral Unmixing in the North-eastern Amazon ». *Applied Vegetation Science*, mai, avsc.12441. https://doi.org/10.1111/avsc.12441.

———. 2019b. « Cumulative Disturbances to Assess Forest Degradation Using Spectral Unmixing in the Northeastern Amazon ». Édité par Duccio Rocchini. *Applied Vegetation Science*, juin, avsc.12441. https://doi.org/10.1111/avsc.12441.

He, Hong S, Barry E DeZonia, et David J Mladenoff. 1999. « An Aggregation Index (AI) to Quantify Spatial Patterns of Landscapes », 11.

Herold, Martin, Rosa María Román-Cuesta, Danilo Mollicone, Yasumasa Hirata, Patrick Van Laake, Gregory P. Asner, Carlos Souza, Margaret Skutsch, Valerio Avitabile, et Ken MacDicken. 2011. « Options for monitoring and estimating historical carbon emissions from forest degradation in the context of REDD+ ». *Carbon balance and management* 6 (1): 13.

Hethcoat, M.G., D.P. Edwards, J.M.B. Carreiras, R.G. Bryant, F.M. França, et S. Quegan. 2019. « A Machine Learning Approach to Map Tropical Selective Logging ». *Remote Sensing of Environment* 221 (février): 569-82. https://doi.org/10.1016/j.rse.2018.11.044.

Hett, Cornelia, Jean-Christophe Castella, Andreas Heinimann, Peter Messerli, et Jean-Laurent Pfund. 2012. « A Landscape Mosaics Approach for Characterizing Swidden Systems from a REDD+ Perspective ». *Applied Geography* 32 (2): 608-18. https://doi.org/10.1016/j.apgeog.2011.07.011.

Hiep, Nguyen Tien, Phan Ke Loc, Nguyen Duc To Luu, P.I. Thomas, A. Farjon, L. Averyanov, et J. Regalado. 2004. « Vietnam Conifers: Conservation Status Review ». Global Trees. 2004. http://globaltrees.org/resources/vietnam-conifers-conservation-status-review-nguyen-et-al-2004/.

Hirschmugl, Manuela, Heinz Gallaun, Matthias Dees, Pawan Datta, Janik Deutscher, Nikos Koutsias, et Mathias Schardt. 2017. « Methods for mapping forest disturbance and degradation from optical earth observation data: A review ». *Current Forestry Reports* 3 (1): 32–45.

Holling, C S. 1973. « Resilience and Stability of Ecological Systems ». *Annual Review of Ecology and Systematics* 4 (1): 1-23. https://doi.org/10.1146/annurev.es.04.110173.000245.

Hosonuma, Noriko, Martin Herold, Veronique De Sy, Ruth S De Fries, Maria Brockhaus, Louis Verchot, Arild Angelsen, et Erika Romijn. 2012. « An Assessment of Deforestation and Forest Degradation Drivers in Developing Countries ». *Environmental Research Letters* 7 (4): 044009. https://doi.org/10.1088/1748-9326/7/4/044009.

Houghton, Richard A. 2013. « The Emissions of Carbon from Deforestation and Degradation in the Tropics: Past Trends and Future Potential ». *Carbon Management* 4 (5): 539-46. https://doi.org/10.4155/cmt.13.41.

Huete, A., Kamel Didan, Tomoaki Miura, E. Patricia Rodriguez, Xiang Gao, et Laerte G. Ferreira. 2002. « Overview of the radiometric and biophysical performance of the MODIS vegetation indices ». *Remote sensing of environment* 83 (1): 195–213.

Huete, A.R. 1988. « A Soil-Adjusted Vegetation Index (SAVI) ». *Remote Sensing of Environment* 25 (3): 295-309. https://doi.org/10.1016/0034-4257(88)90106-X.

Huntsberger, David V. 1961. *Elements of statistical inference*. Elements of statistical inference. Needham Heights, MA, US: Allyn & Bacon. https://doi.org/10.1037/11778-000.

Husson, Francois, Julie Josse, et Jerome Pages. 2010. « Principal Component Methods - Hierarchical Clustering - Partitional Clustering: Why Would We Need to Choose for Visualizing Data? », 17.

« IBGE, Paragominas ». s. d. Consulté le 17 mai 2018. https://cidades.ibge.gov.br/brasil/pa/paragominas/panorama.

« Imazon – Instituto do Homem e Meio Ambiente da Amazônia ». s. d. Consulté le 18 mai 2018. http://imazon.org.br/en/.

Inglada, Jordi, Arthur Vincent, Marcela Arias, et Claire Marais-Sicre. 2016. « Improved Early Crop Type Identification By Joint Use of High Temporal Resolution SAR And Optical Image Time Series ». *Remote Sensing* 8 (5): 362. https://doi.org/10.3390/rs8050362.

International Tropical Timber Organization. 2002. *ITTO Guidelines for the Restoration, Management and Rehabilitation of Degraded and Secondary Tropical Forests.* Yokohama, Japan: Internaitonal Tropical Timber Organization.

Jarvis, A., E. Guevara, H. I. Reuter, et A. D. Nelson. 2008. « Hole-Filled SRTM for the Globe : Version 4 : Data Grid ». Web publication/site, CGIAR Consortium for Spatial Information. Retrieved from http://srtm.csi.cgiar.org/.

Jong, Wil de, Jinlong Liu, et Yeo-Chang Youn. 2016. « Land and Forests in the Anthropocene: Trends and Outlooks in Asia ». *Forest Policy and Economics*, octobre. https://doi.org/10.1016/j.forpol.2016.09.019.

Joshi, Neha, Edward TA Mitchard, Natalia Woo, Jorge Torres, Julian Moll-Rocek, Andrea Ehammer, Murray Collins, Martin R Jepsen, et Rasmus Fensholt. 2015. « Mapping dynamics of deforestation and forest degradation in tropical forests using radar satellite data ». *Environmental Research Letters* 10 (3): 034014. https://doi.org/10.1088/1748-9326/10/3/034014.

Justice, C. O., Louis Giglio, S. Korontzi, J. Owens, J. T. Morisette, D. Roy, J. Descloitres, S. Alleaume, F. Petitcolin, et Y. Kaufman. 2002. « The MODIS fire products ». *Remote Sensing of Environment* 83 (1-2): 244–262.

Kalnay, Eugenia, et Ming Cai. 2003. « Impact of Urbanization and Land-Use Change on Climate ». *Nature* 423 (6939): 528-31. https://doi.org/10.1038/nature01675.

Katayama, Naoki, Tatsuya Amano, Shoji Naoe, Takehisa Yamakita, Isamu Komatsu, Shin-ichi Takagawa, Naoto Sato, Mutsuyuki Ueta, et Tadashi Miyashita. 2014. « Landscape Heterogeneity–Biodiversity Relationship: Effect of Range Size ». Édité par Ben Bond-Lamberty. *PLoS ONE* 9 (3): e93359. https://doi.org/10.1371/journal.pone.0093359.

Kennedy, Robert E., Zhiqiang Yang, et Warren B. Cohen. 2010. « Detecting Trends in Forest Disturbance and Recovery Using Yearly Landsat Time Series: 1. LandTrendr — Temporal Segmentation Algorithms ». *Remote Sensing of Environment* 114 (12): 2897-2910. https://doi.org/10.1016/j.rse.2010.07.008.

Ketchen Jr., David J., et Christopher L. Shook. 1996. « The Application Of Cluster Analysis In Strategic Management Research: An Analysis And Critique ». *Strategic Management Journal* 17 (6): 441-58. https://doi.org/10.1002/(SICI)1097-0266(199606)17:6<441::AID-SMJ819>3.0.CO;2-G.

Klein, Richard J.T., E. Lisa F. Schipper, et Suraje Dessai. 2005. « Integrating Mitigation and Adaptation into Climate and Development Policy: Three Research Questions ». *Environmental Science & Policy* 8 (6): 579-88. https://doi.org/10.1016/j.envsci.2005.06.010.

Koh, Lian Pin, et Serge A. Wich. 2012. « Dawn of Drone Ecology: Low-Cost Autonomous Aerial Vehicles for Conservation ». *Tropical Conservation Science* 5 (2): 121-32. https://doi.org/10.1177/194008291200500202.

Kohavi, Ron. 1995. « A Study of Cross-Validation and Bootstrap for Accuracy Estimation and Model Selection », 7.

Kuhn, Max, et Kjell Johnson. 2013. *Applied Predictive Modeling*. New York: Springer.

Kuplich, T. M., P. J. Curran, et P. M. Atkinson. 2005. « Relating SAR Image Texture to the Biomass of Regenerating Tropical Forests ». *International Journal of Remote Sensing* 26 (21): 4829-54. https://doi.org/10.1080/01431160500239107.

L. Giglio, C. Justice. 2015. « MOD14A2 MODIS/Terra Thermal Anomalies/Fire 8-Day L3 Global 1km SIN Grid V006 ». https://doi.org/10.5067/modis/mod14a2.006.

Lamb, David, Peter D. Erskine, et John A. Parrotta. 2005. « Restoration of degraded tropical forest landscapes ». *Science* 310 (5754): 1628–1632.

Lambin, Eric F. 1999. « Monitoring forest degradation in tropical regions by remote sensing: some methodological issues ». *Global ecology and biogeography* 8 (3-4): 191–198.

Lambin, Eric F., Helmut J. Geist, et Erika Lepers. 2003. « Dynamics of Land-Use and Land-Cover-Change in Tropical Regions ». *Annual Review of Environment and Resources* 28 (1): 205-41. https://doi.org/10.1146/annurev.energy.28.050302.105459.

Lambin, Eric F., et Patrick Meyfroidt. 2010. « Land Use Transitions: Socio-Ecological Feedback versus Socio-Economic Change ». *Land Use Policy* 27 (2): 108-18. https://doi.org/10.1016/j.landusepol.2009.09.003.

Lambin, Eric F., Bi L. Turner, Helmut J. Geist, Samuel B. Agbola, Arild Angelsen, John W. Bruce, Oliver T. Coomes, et al. 2001. « The causes of land-use and land-cover change: moving beyond the myths ». *Global environmental change* 11 (4): 261–269.

Langner, Andreas, Jukka Miettinen, Markus Kukkonen, Christelle Vancutsem, Dario Simonetti, Ghislain Vieilledent, Astrid Verhegghen, Javier Gallego, et Hans-Jürgen Stibig. 2018. « Towards Operational Monitoring of Forest Canopy Disturbance in Evergreen Rain Forests: A Test Case in Continental Southeast Asia ». *Remote Sensing* 10 (4): 544. https://doi.org/10.3390/rs10040544.

Laurance, William F., Ana K. M. Albernaz, Gotz Schroth, Philip M. Fearnside, Scott Bergen, Eduardo M. Venticinque, et Carlos Da Costa. 2002. « Predictors of Deforestation in the Brazilian Amazon ». *Journal of Biogeography* 29 (5-6): 737-48. https://doi.org/10.1046/j.1365-2699.2002.00721.x.

Laurance, William F., José L.C. Camargo, Regina C.C. Luizão, Susan G. Laurance, Stuart L. Pimm, Emilio M. Bruna, Philip C. Stouffer, G. Bruce Williamson, Julieta Benítez-Malvido, et Heraldo L. Vasconcelos. 2011. « The Fate of Amazonian Forest Fragments: A 32-Year Investigation ». *Biological Conservation* 144 (1): 56-67. https://doi.org/10.1016/j.biocon.2010.09.021.

Laurance, William F., Miriam Goosem, et Susan G.W. Laurance. 2009. « Impacts of Roads and Linear Clearings on Tropical Forests ». *Trends in Ecology & Evolution* 24 (12): 659-69. https://doi.org/10.1016/j.tree.2009.06.009.

Laurance, William F., Thomas E. Lovejoy, Heraldo L. Vasconcelos, Emilio M. Bruna, Raphael K. Didham, Philip C. Stouffer, Claude Gascon, Richard O. Bierregaard, Susan G. Laurance, et Erica Sampaio. 2002. « Ecosystem Decay of Amazonian Forest Fragments: A 22-Year Investigation ». *Conservation Biology* 16 (3): 605-18. https://doi.org/10.1046/j.1523-1739.2002.01025.x.

Laurent, François, Damien Arvor, Marion Daugeard, Reinis Osis, Isabelle Tritsch, Emilie Coudel, Marie-Gabrielle Piketty, et al. 2017. « Le tournant environnemental en Amazonie : ampleur et limites du découplage entre production et déforestation ». *EchoGéo*, nº 41 (septembre). https://doi.org/10.4000/echogeo.15035.

Laurent, François, René Poccard-Chapuis, Sophie Plassin, et Gustavo Pimentel Martinez. 2017. « Soil Texture Derived from Topography in North-Eastern Amazonia ». *Journal of Maps* 13 (2): 109-15. https://doi.org/10.1080/17445647.2016.1266524.

Lausch, A., et F. Herzog. 2002. « Applicability of landscape metrics for the monitoring of landscape change: issues of scale, resolution and interpretability ». *Ecological indicators* 2 (1): 3–15.
Lavelle, Patrick, Sylvain Dolédec, Xavier Arnauld de Sartre, Thibaud Decaëns, Valery Gond, Michel Grimaldi, Johan Oszwald, et al. 2016. « Unsustainable Landscapes of Deforested Amazonia: An Analysis of the Relationships among Landscapes and the Social, Economic and Environmental Profiles of Farms at Different Ages Following Deforestation ». *Global Environmental Change* 40 (septembre): 137-55. https://doi.org/10.1016/j.gloenvcha.2016.04.009.
Lavit, Christine, Yves Escoufier, Robert Sabatier, et Pierre Traissac. 1994. « The ACT (STATIS Method) ». *Computational Statistics & Data Analysis* 18 (1): 97-119. https://doi.org/10.1016/0167-9473(94)90134-1.
Le Clec'h, Solen, Nicolas Jégou, Thibaud Decaens, Simon Dufour, Michel Grimaldi, et Johan Oszwald. 2017. « From Field Data to Ecosystem Services Maps: Using Regressions for the Case of Deforested Areas Within the Amazon ». *Ecosystems*, avril. https://doi.org/10.1007/s10021-017-0145-9.
Le Page, Yannick, Douglas Morton, Corinne Hartin, Ben Bond-Lamberty, José Miguel Cardoso Pereira, George Hurtt, et Ghassem Asrar. 2017. « Synergy between Land Use and Climate Change Increases Future Fire Risk in Amazon Forests ». *Earth System Dynamics* 8 (4): 1237-46. https://doi.org/10.5194/esd-8-1237-2017.
Lê, Sébastien, Julie Josse, et François Husson. 2008. « FactoMineR : An R Package for Multivariate Analysis ». *Journal of Statistical Software* 25 (1). https://doi.org/10.18637/jss.v025.i01.
Le Toan, T., S. Quegan, M.W.J. Davidson, H. Balzter, P. Paillou, K. Papathanassiou, S. Plummer, et al. 2011. « The BIOMASS Mission: Mapping Global Forest Biomass to Better Understand the Terrestrial Carbon Cycle ». *Remote Sensing of Environment* 115 (11): 2850-60. https://doi.org/10.1016/j.rse.2011.03.020.
Lebourgeois, Valentine, Stéphane Dupuy, Élodie Vintrou, Maël Ameline, Suzanne Butler, et Agnès Bégué. 2017. « A Combined Random Forest and OBIA Classification Scheme for Mapping Smallholder Agriculture at Different Nomenclature Levels Using Multisource Data (Simulated Sentinel-2 Time Series, VHRS and DEM) ». *Remote Sensing* 9 (3): 259. https://doi.org/10.3390/rs9030259.
Lei, Yang, Robert Treuhaft, Michael Keller, Maiza dos-Santos, Fabio Gonçalves, et Maxim Neumann. 2018. « Quantification of Selective Logging in Tropical Forest with Spaceborne SAR Interferometry ». *Remote Sensing of Environment* 211 (juin): 167-83. https://doi.org/10.1016/j.rse.2018.04.009.
Leisher, Craig, Jerome Touval, Sebastiaan Hess, Timothy Boucher, et Louis Reymondin. 2013. « Land and Forest Degradation inside Protected Areas in Latin America ». *Diversity* 5 (4): 779-95. https://doi.org/10.3390/d5040779.
Lewis, S. L., D. P. Edwards, et D. Galbraith. 2015. « Increasing Human Dominance of Tropical Forests ». *Science* 349 (6250): 827-32. https://doi.org/10.1126/science.aaa9932.
Li, S., et X. Chen. 2014. « A New Bare-Soil Index for Rapid Mapping Developing Areas Using LANDSAT 8 Data ». *ISPRS - International Archives of the Photogrammetry, Remote Sensing and Spatial Information Sciences* XL-4 (avril): 139-44. https://doi.org/10.5194/isprsarchives-XL-4-139-2014.
Liaw, Andy, et Matthew Wiener. 2002. « Classification and regression by randomForest ». *R news* 2 (3): 18–22.
Longo, Marcos, Michael Keller, Maiza N. dos-Santos, Veronika Leitold, Ekena R. Pinagé, Alessandro Baccini, Sassan Saatchi, Euler M. Nogueira, Mateus Batistella, et Douglas C. Morton. 2016. « Aboveground Biomass Variability across Intact and Degraded Forests in the Brazilian Amazon: AMAZON INTACT AND DEGRADED FOREST BIOMASS ». *Global Biogeochemical Cycles* 30 (11): 1639-60. https://doi.org/10.1002/2016GB005465.

Luckman, A. J., A. C. Frery, C. C. F. Yanasse, et G. B. Groom. 1997. « Texture in Airborne SAR Imagery of Tropical Forest and Its Relationship to Forest Regeneration Stage ». *International Journal of Remote Sensing* 18 (6): 1333-49. https://doi.org/10.1080/014311697218458.

Lumley, Thomas. 2017. *leaps: Regression Subset Selection* (version 3.0). https://CRAN.R-project.org/package=leaps.

Lund, HG. 2009. « What Is a Degraded Forest? Forest Information Services: Gainesville, VA, USA ». ResearchGate. 2009. https://www.researchgate.net/publication/280921178_What_is_a_degraded_forest.

Main-Knorn, Magdalena, Bringfried Pflug, Jerome Louis, Vincent Debaecker, Uwe Müller-Wilm, et Ferran Gascon. 2017. « Sen2Cor for Sentinel-2 ». In *Image and Signal Processing for Remote Sensing XXIII*, édité par Lorenzo Bruzzone, Francesca Bovolo, et Jon Atli Benediktsson, 3. Warsaw, Poland: SPIE. https://doi.org/10.1117/12.2278218.

Malhi, Y., J. T. Roberts, R. A. Betts, T. J. Killeen, W. Li, et C. A. Nobre. 2008. « Climate Change, Deforestation, and the Fate of the Amazon ». *Science* 319 (5860): 169-72. https://doi.org/10.1126/science.1146961.

Malhi, Yadvinder, Toby A. Gardner, Gregory R. Goldsmith, Miles R. Silman, et Przemyslaw Zelazowski. 2014. « Tropical Forests in the Anthropocene ». *Annual Review of Environment and Resources* 39 (1): 125-59. https://doi.org/10.1146/annurev-environ-030713-155141.

Malhi, Yadvinder, et Rosa María Román-Cuesta. 2008. « Analysis of Lacunarity and Scales of Spatial Homogeneity in IKONOS Images of Amazonian Tropical Forest Canopies ». *Remote Sensing of Environment* 112 (5): 2074-87. https://doi.org/10.1016/j.rse.2008.01.009.

Malhi, Yadvinder, Daniel Wood, Timothy R. Baker, James Wright, Oliver L. Phillips, Thomas Cochrane, Patrick Meir, et al. 2006. « The Regional Variation of Aboveground Live Biomass in Old-Growth Amazonian Forests ». *Global Change Biology* 12 (7): 1107-38. https://doi.org/10.1111/j.1365-2486.2006.01120.x.

Mallows, C. L. 1973. « Some Comments on C p ». *Technometrics* 15 (4): 661-75. https://doi.org/10.1080/00401706.1973.10489103.

Mangueira, Julia Raquel S. A., Karen D. Holl, et Ricardo R. Rodrigues. 2018. « Enrichment Planting to Restore Degraded Tropical Forest Fragments in Brazil ». *Ecosystems and People*, novembre. https://www.tandfonline.com/action/showCopyRight?scroll=top&doi=10.1080%2F21513732.2018.1529707.

Manuel-Navarrete, David, José Javier Gómez, et Gilberto Gallopín. 2007. « Syndromes of Sustainability of Development for Assessing the Vulnerability of Coupled Human–Environmental Systems. The Case of Hydrometeorological Disasters in Central America and the Caribbean ». *Global Environmental Change* 17 (2): 207-17. https://doi.org/10.1016/j.gloenvcha.2006.07.002.

Marshall, NA, PA Marshall, J Tamelander, D Obura, D Malleret-King, et JE Cinner. 2010. « A Framework for Social Adaptation to Climate Change Sustaining Tropical Coastal Communitites and Industries. » 188 (4752): 716-17. https://doi.org/10.1038/188716b0.

Mascaro, Joseph, Gregory P. Asner, David E. Knapp, Ty Kennedy-Bowdoin, Roberta E. Martin, Christopher Anderson, Mark Higgins, et K. Dana Chadwick. 2014. « A Tale of Two "Forests": Random Forest Machine Learning Aids Tropical Forest Carbon Mapping ». Édité par Ben Bond-Lamberty. *PLoS ONE* 9 (1): e85993. https://doi.org/10.1371/journal.pone.0085993.

Mascaro, Joseph, Matteo Detto, Gregory P. Asner, et Helene C. Muller-Landau. 2011. « Evaluating Uncertainty in Mapping Forest Carbon with Airborne LiDAR ». *Remote Sensing of Environment* 115 (12): 3770-74. https://doi.org/10.1016/j.rse.2011.07.019.

Mather, A S, et C L Needle. 1998. « The forest transition: a theoretical basis ». *Area* 30 (2): 117-24. https://doi.org/10.1111/j.1475-4762.1998.tb00055.x.

Matricardi, Eraldo A.T., David L. Skole, Marcos A. Pedlowski, Walter Chomentowski, et Luis Claudio Fernandes. 2010. « Assessment of Tropical Forest Degradation by Selective Logging and Fire Using Landsat Imagery ». *Remote Sensing of Environment* 114 (5): 1117-29. https://doi.org/10.1016/j.rse.2010.01.001.

Mazzei, Lucas, Plinio Sist, Ademir Ruschel, Francis E. Putz, Phidias Marco, Wagner Pena, et Josué Evandro Ribeiro Ferreira. 2010a. « Above-Ground Biomass Dynamics after Reduced-Impact Logging in the Eastern Amazon ». *Forest Ecology and Management* 259 (3): 367-73. https://doi.org/10.1016/j.foreco.2009.10.031.

———. 2010b. « Above-Ground Biomass Dynamics after Reduced-Impact Logging in the Eastern Amazon ». *Forest Ecology and Management* 259 (3): 367-73. https://doi.org/10.1016/j.foreco.2009.10.031.

McCarthy, James J., et Intergovernmental Panel on Climate Change, éd. 2001. *Climate Change 2001: Impacts, Adaptation, and Vulnerability: Contribution of Working Group II to the Third Assessment Report of the Intergovernmental Panel on Climate Change*. Cambridge, UK ; New York: Cambridge University Press.

McFeeterts, S. K. 1996. « The use of the Normalized Difference Water Index (NDWI) in the delineation of open water features ». *International Journal of Remote Sensing* 17 (7): 1425-32. https://doi.org/10.1080/01431169608948714.

McGarigal, K, S.A. Cushman, et E. Ene. 2012. « FRAGSTATS v4: Spatial Pattern Analysis Program for Categorical and Continuous Maps. Computer software program produced by the authors at the University of Massachusetts, Amherst. Available at the following web site: http://www.umass.edu/landeco/research/fragstats/fragstats.html ». 2012. http://www.umass.edu/landeco/research/fragstats/fragstats.html.

Melito, Melina, Jean Paul Metzger, et Alexandre A. de Oliveira. 2017. « Landscape-Level Effects on Aboveground Biomass of Tropical Forests: A Conceptual Framework ». *Global Change Biology*, novembre. https://doi.org/10.1111/gcb.13970.

———. 2018. « Landscape-level Effects on Aboveground Biomass of Tropical Forests: A Conceptual Framework ». *Global Change Biology* 24 (2): 597-607. https://doi.org/10.1111/gcb.13970.

Mercier, Audrey, Julie Betbeder, Florent Rumiano, Valéry Gond, Lilian Blanc, Clément Bourgoin, Guillaume Cornu, René Poccard-Chapuis, Jacques Baudry, et Laurence Hubert-Moy. 2019. « Evaluation of Sentinel-1 and 2 Time Series for Land Cover Classification of Forest–Agriculture Mosaics in Temperate and Tropical Landscapes », 20. https://doi.org/10.3390/rs11080979.

Mermoz, Stéphane, Thuy Le Toan, Ludovic Villard, Maxime Réjou-Méchain, et Joerg Seifert-Granzin. 2014. « Biomass assessment in the Cameroon savanna using ALOS PALSAR data ». *Remote Sensing of Environment* 155: 109–119.

Messerli, Peter, Andreas Heinimann, et Michael Epprecht. 2009. « Finding Homogeneity in Heterogeneity—A New Approach to Quantifying Landscape Mosaics Developed for the Lao PDR ». *Human Ecology* 37 (3): 291-304. https://doi.org/10.1007/s10745-009-9238-1.

Metzger, M.J., M.D.A. Rounsevell, L. Acosta-Michlik, R. Leemans, et D. Schröter. 2006. « The Vulnerability of Ecosystem Services to Land Use Change ». *Agriculture, Ecosystems & Environment* 114 (1): 69-85. https://doi.org/10.1016/j.agee.2005.11.025.

Meyer, V., S. S. Saatchi, J. Chave, J. W. Dalling, S. Bohlman, G. A. Fricker, C. Robinson, M. Neumann, et S. Hubbell. 2013. « Detecting Tropical Forest Biomass Dynamics from Repeated Airborne Lidar Measurements ». *Biogeosciences* 10 (8): 5421-38. https://doi.org/10.5194/bg-10-5421-2013.

Meyer, Victoria, Sassan Saatchi, David B. Clark, Michael Keller, Grégoire Vincent, António Ferraz, Fernando Espírito-Santo, Marcus V. N. d'Oliveira, Dahlia Kaki, et Jérôme Chave. 2018. « Canopy Area of Large Trees Explains Aboveground Biomass Variations across Neotropical Forest Landscapes ». *Biogeosciences* 15 (11): 3377-90. https://doi.org/10.5194/bg-15-3377-2018.

Meyer, Victoria, Sassan Saatchi, António Ferraz, Liang Xu, Alvaro Duque, Mariano García, et Jérôme Chave. 2019. « Forest Degradation and Biomass Loss along the Chocó Region of Colombia ». *Carbon Balance and Management* 14 (1). https://doi.org/10.1186/s13021-019-0117-9.

Meyfroidt, Patrick, et Eric F. Lambin. 2008. « Forest Transition in Vietnam and Its Environmental Impacts ». *Global Change Biology* 14 (6): 1319-36. https://doi.org/10.1111/j.1365-2486.2008.01575.x.

Meyfroidt, Patrick, Tan Phuong Vu, et Viet Anh Hoang. 2013. « Trajectories of Deforestation, Coffee Expansion and Displacement of Shifting Cultivation in the Central Highlands of Vietnam ». *Global Environmental Change* 23 (5): 1187-98. https://doi.org/10.1016/j.gloenvcha.2013.04.005.

Millennium Ecosystem Assessment (Program), éd. 2005. *Ecosystems and human well-being: synthesis*. Washington, DC: Island Press.

Miller, Jay D., et Andrea E. Thode. 2007. « Quantifying Burn Severity in a Heterogeneous Landscape with a Relative Version of the Delta Normalized Burn Ratio (DNBR) ». *Remote Sensing of Environment* 109 (1): 66-80. https://doi.org/10.1016/j.rse.2006.12.006.

Mitchard, E.T.A., S.S. Saatchi, S.L. Lewis, T.R. Feldpausch, I.H. Woodhouse, B. Sonké, C. Rowland, et P. Meir. 2011. « Measuring Biomass Changes Due to Woody Encroachment and Deforestation/Degradation in a Forest–Savanna Boundary Region of Central Africa Using Multi-Temporal L-Band Radar Backscatter ». *Remote Sensing of Environment* 115 (11): 2861-73. https://doi.org/10.1016/j.rse.2010.02.022.

Mitchell, Anthea L., Ake Rosenqvist, et Brice Mora. 2017a. « Current Remote Sensing Approaches to Monitoring Forest Degradation in Support of Countries Measurement, Reporting and Verification (MRV) Systems for REDD+ ». *Carbon Balance and Management* 12 (1). https://doi.org/10.1186/s13021-017-0078-9.

———. 2017b. « Current Remote Sensing Approaches to Monitoring Forest Degradation in Support of Countries Measurement, Reporting and Verification (MRV) Systems for REDD+ ». *Carbon Balance and Management* 12 (1). https://doi.org/10.1186/s13021-017-0078-9.

Morales-Barquero, Lucia, Armonia Borrego, Margaret Skutsch, Christoph Kleinn, et John R. Healey. 2015. « Identification and Quantification of Drivers of Forest Degradation in Tropical Dry Forests: A Case Study in Western Mexico ». *Land Use Policy* 49 (décembre): 296-309. https://doi.org/10.1016/j.landusepol.2015.07.006.

Morales-Barquero, Lucia, Margaret Skutsch, Enrique Jardel-Peláez, Adrian Ghilardi, Christoph Kleinn, et John Healey. 2014. « Operationalizing the Definition of Forest Degradation for REDD+, with Application to Mexico ». *Forests* 5 (7): 1653-81. https://doi.org/10.3390/f5071653.

Morel, Alexandra C., Sassan S. Saatchi, Yadvinder Malhi, Nicholas J. Berry, Lindsay Banin, David Burslem, Reuben Nilus, et Robert C. Ong. 2011. « Estimating Aboveground Biomass in Forest and Oil Palm Plantation in Sabah, Malaysian Borneo Using ALOS PALSAR Data ». *Forest Ecology and Management* 262 (9): 1786-98. https://doi.org/10.1016/j.foreco.2011.07.008.

Morel, Alexandra, Mark Hirons, Sheleme Demissie, Techane Gonfa, Zia Mehrabi, Peter R Long, Sami Rifai, et al. 2019. « The Structures Underpinning Vulnerability: Examining Landscape-Society Interactions in a Smallholder Coffee Agroforestry System ». *Environmental Research Letters*, mai. https://doi.org/10.1088/1748-9326/ab2280.

Morton, D. C., Y. Le Page, R. DeFries, G. J. Collatz, et G. C. Hurtt. 2013. « Understorey Fire Frequency and the Fate of Burned Forests in Southern Amazonia ». *Philosophical Transactions of the Royal Society B: Biological Sciences* 368 (1619): 20120163-20120163. https://doi.org/10.1098/rstb.2012.0163.

Morton, Douglas C., Ruth S. DeFries, Jyoteshwar Nagol, Carlos M. Souza, Eric S. Kasischke, George C. Hurtt, et Ralph Dubayah. 2011. « Mapping Canopy Damage from Understory Fires in Amazon Forests Using Annual Time Series of Landsat and MODIS Data ». *Remote Sensing of Environment* 115 (7): 1706-20. https://doi.org/10.1016/j.rse.2011.03.002.

Mutanga, Onisimo, Elhadi Adam, et Moses Azong Cho. 2012. « High Density Biomass Estimation for Wetland Vegetation Using WorldView-2 Imagery and Random Forest Regression Algorithm ». *International Journal of Applied Earth Observation and Geoinformation* 18 (août): 399-406. https://doi.org/10.1016/j.jag.2012.03.012.

Nelson, Gerald C., A. Dobermann, N. Nakicenovic, et B. C. O'Neill. 2006. « Anthropogenic drivers of ecosystem change: an overview ». *Ecology and Society* 11 (2). http://pure.iiasa.ac.at/7882.

Nepstad, D. C, C. M Stickler, B. S. Filho, et F. Merry. 2008. « Interactions among Amazon Land Use, Forests and Climate: Prospects for a near-Term Forest Tipping Point ». *Philosophical Transactions of the Royal Society B: Biological Sciences* 363 (1498): 1737-46. https://doi.org/10.1098/rstb.2007.0036.

Nepstad, Daniel, Britaldo S. Soares-Filho, Frank Merry, André Lima, Paulo Moutinho, John Carter, Maria Bowman, et al. 2009. « The end of deforestation in the Brazilian Amazon ». *Science* 326 (5958): 1350–1351.

Nowosad, Jakub, et Tomasz Stepinski. 2018. « Information-Theoretical Approach to Measuring Landscape Complexity ». Preprint. Ecology. https://doi.org/10.1101/383281.

« Observatory of the dynamics of interactions between societies and environnement in the Amazon, ODYSSEA ». s. d. Consulté le 18 mai 2018. https://odyssea-amazonia.org/.

O'Neill, Robert V., Carolyn T. Hunsaker, K. Bruce Jones, Kurt H. Riitters, James D. Wickham, Paul M. Schwartz, Iris A. Goodman, Barbara L. Jackson, et William S. Baillargeon. 1997. « Monitoring environmental quality at the landscape scale ». *BioScience*, 513–519.

O'Neill, Robert V., K.H. Riitters, J.D. Wickham, et K. Bruce Jones. 1999. « Landscape Pattern Metrics and Regional Assessment ». *Ecosystem Health* 5 (4): 225-33. https://doi.org/10.1046/j.1526-0992.1999.09942.x.

Opdam, Paul, Sandra Luque, Joan Nassauer, Peter H. Verburg, et Jianguo Wu. 2018. « How Can Landscape Ecology Contribute to Sustainability Science? » *Landscape Ecology* 33 (1): 1-7. https://doi.org/10.1007/s10980-018-0610-7.

« Orfeo ToolBox – Orfeo ToolBox is not a black box ». s. d. Consulté le 13 avril 2018. https://www.orfeo-toolbox.org/.

Osis, Reinis, François Laurent, et René Poccard-Chapuis. 2019. « Spatial Determinants and Future Land Use Scenarios of Paragominas Municipality, an Old Agricultural Frontier in Amazonia ». *Journal of Land Use Science*, juillet, 1-22. https://doi.org/10.1080/1747423X.2019.1643422.

Ostrom, E. 2009. « A General Framework for Analyzing Sustainability of Social-Ecological Systems ». *Science* 325 (5939): 419-22. https://doi.org/10.1126/science.1172133.

Oszwald, Johan, Xavier Arnauld de Sartre, Thibaud Decaëns, Valéry Gond, Michel Grimaldi, Antoine Lefebvre, RL De Araujo Fretas, et al. 2012. « Utilisation de la télédétection et de données socio-économiques et écologiques pour comprendre l'impact des dynamiques de l'occupation des sols à Pacajá (Brésil). » *Revue Française de Photogrammétrie et de Télédétection* 198 (199): 199.

Oszwald, Johan, Jean-Marie Kouacou Atta, Claude Kergomard, et Marc Robin. 2007. « Représenter l'espace pour structurer le temps: approche des dynamiques de changements forestiers dans le sud-est de la Côte d'Ivoire par télédétection ». *Télédétection* 7 (1-2-3-4): 271–282.

Oszwald, Johan, Valéry Gond, Sylvain Doledec, et Patrick Lavelle. 2011. « Identification d'indicateurs de changement d'occupation du sol pour le suivi des mosaïques paysagères ». *Bois et forêts des tropiques* 307 (1): 7–21.

Pal, M., et P. M. Mather. 2005. « Support Vector Machines for Classification in Remote Sensing ». *International Journal of Remote Sensing* 26 (5): 1007-11. https://doi.org/10.1080/01431160512331314083.

Panagiotidis, Dimitrios, Azadeh Abdollahnejad, Peter Surový, et Vasco Chiteculo. 2017. « Determining Tree Height and Crown Diameter from High-Resolution UAV Imagery ». *International Journal of Remote Sensing* 38 (8-10): 2392-2410. https://doi.org/10.1080/01431161.2016.1264028.

Pargal, Sourabh, Rakesh Fararoda, Gopalakrishnan Rajashekar, Natesan Balachandran, Maxime Réjou-Méchain, Nicolas Barbier, Chandra Jha, Raphaël Pélissier, Vinay Dadhwal, et Pierre Couteron. 2017. « Inverting Aboveground Biomass–Canopy Texture Relationships in a Landscape of Forest Mosaic in the Western Ghats of India Using Very High Resolution Cartosat Imagery ». *Remote Sensing* 9 (3): 228. https://doi.org/10.3390/rs9030228.

Parker, Louis, Clement Bourgoin, Armando Martinez-Valle, et Peter Läderach. 2019. « Vulnerability of the Agricultural Sector to Climate Change: The Development of a Pan-Tropical Climate Risk Vulnerability Assessment to Inform Sub-National Decision Making ». Édité par Shahbaz Mushtaq. *PLOS ONE* 14 (3): e0213641. https://doi.org/10.1371/journal.pone.0213641.

Patton, David R. 1975. « A Diversity Index for Quantifying Habitat "Edge" ». *Wildlife Society Bulletin (1973-2006)* 3 (4): 171-73.

Pearson, Timothy R. H., Sandra Brown, Lara Murray, et Gabriel Sidman. 2017. « Greenhouse Gas Emissions from Tropical Forest Degradation: An Underestimated Source ». *Carbon Balance and Management* 12 (1). https://doi.org/10.1186/s13021-017-0072-2.

Persha, L., A. Agrawal, et A. Chhatre. 2011. « Social and Ecological Synergy: Local Rulemaking, Forest Livelihoods, and Biodiversity Conservation ». *Science* 331 (6024): 1606-8. https://doi.org/10.1126/science.1199343.

Phelps, J., E. L. Webb, et A. Agrawal. 2010. « Does REDD+ Threaten to Recentralize Forest Governance? » *Science* 328 (5976): 312-13. https://doi.org/10.1126/science.1187774.

Phillips, Oliver L., Luiz EOC Aragão, Simon L. Lewis, Joshua B. Fisher, Jon Lloyd, Gabriela López-González, Yadvinder Malhi, et al. 2009. « Drought sensitivity of the Amazon rainforest ». *Science* 323 (5919): 1344–1347.

Phiri, Darius, Justin Morgenroth, et Cong Xu. 2019. « Four Decades of Land Cover and Forest Connectivity Study in Zambia—An Object-Based Image Analysis Approach ». *International Journal of Applied Earth Observation and Geoinformation* 79 (juillet): 97-109. https://doi.org/10.1016/j.jag.2019.03.001.

Piazza, Gustavo Antonio, Alexander Christian Vibrans, Veraldo Liesenberg, et Júlio Cesar Refosco. 2016. « Object-Oriented and Pixel-Based Classification Approaches to Classify Tropical Successional Stages Using Airborne High–Spatial Resolution Images ». *GIScience & Remote Sensing* 53 (2): 206-26. https://doi.org/10.1080/15481603.2015.1130589.

Picoli, Michelle Cristina Araujo, Gilberto Camara, Ieda Sanches, Rolf Simões, Alexandre Carvalho, Adeline Maciel, Alexandre Coutinho, et al. 2018. « Big Earth Observation Time Series Analysis for Monitoring Brazilian Agriculture ». *ISPRS Journal of Photogrammetry and Remote Sensing*, août. https://doi.org/10.1016/j.isprsjprs.2018.08.007.

Pielke, RA. 2005. « Land Use and Climate Change ». *Science*, 3.

Piketty, Marie-Gabrielle, René Poccard-Chapuis, Isabel Drigo, Emilie Coudel, Sophie Plassin, François Laurent, et Marcelo Thâles. 2015. « Multi-Level Governance of Land Use Changes in the Brazilian Amazon: Lessons from Paragominas, State of Pará ». *Forests* 6 (5): 1516-36. https://doi.org/10.3390/f6051516.

Piponiot, Camille, Plinio Sist, Lucas Mazzei, Marielos Peña-Claros, Francis E Putz, Ervan Rutishauser, Alexander Shenkin, et al. 2016. « Carbon Recovery Dynamics Following Disturbance by Selective Logging in Amazonian Forests ». *ELife* 5 (décembre). https://doi.org/10.7554/eLife.21394.

Ploton, P., N. Barbier, P. Couteron, C.M. Antin, N. Ayyappan, N. Balachandran, N. Barathan, et al. 2017. « Toward a General Tropical Forest Biomass Prediction Model from Very High Resolution Optical Satellite Images ». *Remote Sensing of Environment* 200 (octobre): 140-53. https://doi.org/10.1016/j.rse.2017.08.001.

Ploton, Pierre, Raphaël Pélissier, Christophe Proisy, Théo Flavenot, Nicolas Barbier, S. N. Rai, et Pierre Couteron. 2012. « Assessing aboveground tropical forest biomass using Google Earth canopy images ». *Ecological Applications* 22 (3): 993–1003.

Pontius, Robert Gilmore, et Marco Millones. 2011. « Death to Kappa: Birth of Quantity Disagreement and Allocation Disagreement for Accuracy Assessment ». *International Journal of Remote Sensing* 32 (15): 4407-29. https://doi.org/10.1080/01431161.2011.552923.

Potapov, P., A. Tyukavina, S. Turubanova, Y. Talero, A. Hernandez-Serna, M.C. Hansen, D. Saah, et al. 2019. « Annual Continuous Fields of Woody Vegetation Structure in the Lower Mekong Region from 2000-2017 Landsat Time-Series ». *Remote Sensing of Environment* 232 (octobre): 111278. https://doi.org/10.1016/j.rse.2019.111278.

Potapov, Peter, Matthew C. Hansen, Lars Laestadius, Svetlana Turubanova, Alexey Yaroshenko, Christoph Thies, Wynet Smith, et al. 2017. « The last frontiers of wilderness: Tracking loss of intact forest landscapes from 2000 to 2013 ». *Science Advances* 3 (1): e1600821.

« PRODES — Coordenação-Geral de Observação da Terra ». s. d. Consulté le 13 avril 2018. http://www.obt.inpe.br/OBT/assuntos/programas/amazonia/prodes.

Proisy, Christophe, Pierre Couteron, et François Fromard. 2007. « Predicting and Mapping Mangrove Biomass from Canopy Grain Analysis Using Fourier-Based Textural Ordination of IKONOS Images ». *Remote Sensing of Environment* 109 (3): 379-92. https://doi.org/10.1016/j.rse.2007.01.009.

Proisy, Christophe, Pierre Couteron, Raphaël Pélissier, Nicolas Barbier, et Julien Engel. 2007. « Monitoring canopy grain of tropical forest using Fourier-based textural ordination (FOTO) of very high resolution images ». In *Geoscience and Remote Sensing Symposium, 2007. IGARSS 2007. IEEE International*, 4324–4326. IEEE. http://ieeexplore.ieee.org/xpls/abs_all.jsp?arnumber=4423808.

Putz, Francis E., et Kent H. Redford. 2010a. « The Importance of Defining 'Forest': Tropical Forest Degradation, Deforestation, Long-Term Phase Shifts, and Further Transitions: Importance of Defining 'Forest' ». *Biotropica* 42 (1): 10-20. https://doi.org/10.1111/j.1744-7429.2009.00567.x.

———. 2010b. « The Importance of Defining 'Forest': Tropical Forest Degradation, Deforestation, Long-Term Phase Shifts, and Further Transitions: Importance of Defining 'Forest' ». *Biotropica* 42 (1): 10-20. https://doi.org/10.1111/j.1744-7429.2009.00567.x.

Qi, J., A. Chehbouni, A.R. Huete, Y.H. Kerr, et S. Sorooshian. 1994. « A Modified Soil Adjusted Vegetation Index ». *Remote Sensing of Environment* 48 (2): 119-26. https://doi.org/10.1016/0034-4257(94)90134-1.

Rappaport, Danielle I, Douglas C Morton, Marcos Longo, Michael Keller, Ralph Dubayah, et Maiza Nara dos-Santos. 2018. « Quantifying Long-Term Changes in Carbon Stocks and Forest Structure from Amazon Forest Degradation ». *Environmental Research Letters*, mai. https://doi.org/10.1088/1748-9326/aac331.

Rappaport, Danielle I., Leandro R. Tambosi, et Jean P. Metzger. 2015. « A Landscape Triage Approach: Combining Spatial and Temporal Dynamics to Prioritize Restoration and Conservation ». Édité par Marc Cadotte. *Journal of Applied Ecology* 52 (3): 590-601. https://doi.org/10.1111/1365-2664.12405.

Reed, James, Jos Barlow, Rachel Carmenta, Josh van Vianen, et Terry Sunderland. 2019. « Engaging Multiple Stakeholders to Reconcile Climate, Conservation and Development Objectives in Tropical Landscapes ». *Biological Conservation* 238 (octobre): 108229. https://doi.org/10.1016/j.biocon.2019.108229.

Reed, James, Josh Van Vianen, Elizabeth L. Deakin, Jos Barlow, et Terry Sunderland. 2016. « Integrated Landscape Approaches to Managing Social and Environmental Issues in the Tropics: Learning from the Past to Guide the Future ». *Global Change Biology* 22 (7): 2540-54. https://doi.org/10.1111/gcb.13284.

Reed, James, Josh van Vianen, Jos Barlow, et Terry Sunderland. 2017. « Have Integrated Landscape Approaches Reconciled Societal and Environmental Issues in the Tropics? » *Land Use Policy* 63 (avril): 481-92. https://doi.org/10.1016/j.landusepol.2017.02.021.

Reiche, Johannes, Jan Verbesselt, Dirk Hoekman, et Martin Herold. 2015. « Fusing Landsat and SAR Time Series to Detect Deforestation in the Tropics ». *Remote Sensing of Environment* 156 (janvier): 276-93. https://doi.org/10.1016/j.rse.2014.10.001.

Reiche, Johannes, Rob Verhoeven, Jan Verbesselt, Eliakim Hamunyela, Niels Wielaard, et Martin Herold. 2018. « Characterizing Tropical Forest Cover Loss Using Dense Sentinel-1 Data and Active Fire Alerts ». *Remote Sensing* 10 (5): 777. https://doi.org/10.3390/rs10050777.

Reymondin, Louis, Andrew Jarvis, Andres Perez-Uribe, Jerry Touval, Karolina Argote, Alejandro Coca, Julien Rebetez, Edward Guevara, et Mark Mulligan. 2012. « A methodology for near real-time monitoring of habitat change at continental scales using MODIS-NDVI and TRMM ».

RIBEIRO, JR., et P.J. DIGGLE. 2001. « geoR: A package for geostatistical analysis. R-NEWS Vol 1, No 2. ISSN. » 2001. http://www.leg.ufpr.br/geoR/.

Ribeiro, Milton Cezar, Jean Paul Metzger, Alexandre Camargo Martensen, Flávio Jorge Ponzoni, et Márcia Makiko Hirota. 2009. « The Brazilian Atlantic Forest: How Much Is Left, and How Is the Remaining Forest Distributed? Implications for Conservation ». *Biological Conservation* 142 (6): 1141-53. https://doi.org/10.1016/j.biocon.2009.02.021.

Robert, P, et Y Escoufier. 1976. « A Unifying Tool for Linear Multivariate Statistical Methods: The RV-Coefficient ». *Journal of the Royal Statistical Society. Series C (Applied Statistics)* 25 (3). http://www.jstor.org/stable/2347233.

Robinson, Ws. 2009. « Ecological Correlations and the Behavior of Individuals* ». *International Journal of Epidemiology* 38 (2): 337-41. https://doi.org/10.1093/ije/dyn357.

Rosenfield, George H. 1986. « A Coefficient of Agreement as a Measure of Thematic Classification Accuracy ». *PHOTOGRAMMETRIC ENGINEERING*, 5.

Rossi, Richard E., David J. Mulla, Andre G. Journel, et Eldon H. Franz. 1992. « Geostatistical Tools for Modeling and Interpreting Ecological Spatial Dependence ». *Ecological Monographs* 62 (2): 277-314. https://doi.org/10.2307/2937096.

Rouse, W, et R H Haas. 1974. « Monitoring Vegetation Systems In The Great Plains With Erts » Vol. 1: 309–317.

Roy, David P., Haiyan Huang, Luigi Boschetti, Louis Giglio, Lin Yan, Hankui H. Zhang, et Zhongbin Li. 2019. « Landsat-8 and Sentinel-2 Burned Area Mapping - A Combined Sensor Multi-Temporal Change Detection Approach ». *Remote Sensing of Environment* 231 (septembre): 111254. https://doi.org/10.1016/j.rse.2019.111254.

Saatchi, Sassan S., Nancy L. Harris, Sandra Brown, Michael Lefsky, Edward TA Mitchard, William Salas, Brian R. Zutta, et al. 2011. « Benchmark map of forest carbon stocks in tropical regions across three continents ». *Proceedings of the National Academy of Sciences* 108 (24): 9899–9904.

Sahraoui, Yohan, Jean-Christophe Foltête, et Céline Clauzel. 2017. « A Multi-Species Approach for Assessing the Impact of Land-Cover Changes on Landscape Connectivity ». *Landscape Ecology* 32 (9): 1819-35. https://doi.org/10.1007/s10980-017-0551-6.

Sasaki, Nophea, et Francis E. Putz. 2009a. « Critical Need for New Definitions of “Forest” and “Forest Degradation” in Global Climate Change Agreements ». *Conservation Letters* 2 (5): 226-32. https://doi.org/10.1111/j.1755-263X.2009.00067.x.

———. 2009b. « Critical Need for New Definitions of “Forest” and “Forest Degradation” in Global Climate Change Agreements ». *Conservation Letters* 2 (5): 226-32. https://doi.org/10.1111/j.1755-263X.2009.00067.x.

Sayer, J., T. Sunderland, J. Ghazoul, J.-L. Pfund, D. Sheil, E. Meijaard, M. Venter, et al. 2013. « Ten Principles for a Landscape Approach to Reconciling Agriculture, Conservation, and Other Competing Land Uses ». *Proceedings of the National Academy of Sciences* 110 (21): 8349-56. https://doi.org/10.1073/pnas.1210595110.

Sayer, Jeffrey, Terry Sunderland, Jaboury Ghazoul, Jean-Laurent Pfund, Douglas Sheil, Erik Meijaard, Michelle Venter, et al. 2013. « Ten principles for a landscape approach to reconciling agriculture, conservation, and other competing land uses ». *Proceedings of the national academy of sciences* 110 (21): 8349–8356.

Seymour, Frances, et Jonah Busch. 2016. *Why Forests? Why Now? The Science, Economics, and Politics of Tropical Forests and Climate Change*. Washington DC: Center for Global Development.

Shannon, Claude, et Warren Weaver. 1949. « The Mathematical Theory of Communication », 132.

Shapiro, Aurélie C., Naikoa Aguilar-Amuchastegui, Patrick Hostert, et Jean-François Bastin. 2016. « Using Fragmentation to Assess Degradation of Forest Edges in Democratic Republic of Congo ». *Carbon Balance and Management* 11 (1). https://doi.org/10.1186/s13021-016-0054-9.

Shimada, Masanobu, Takuya Itoh, Takeshi Motooka, Manabu Watanabe, Tomohiro Shiraishi, Rajesh Thapa, et Richard Lucas. 2014. « New Global Forest/Non-Forest Maps from ALOS PALSAR

Data (2007–2010) ». *Remote Sensing of Environment* 155 (décembre): 13-31. https://doi.org/10.1016/j.rse.2014.04.014.
Silva, Carlos, Andrew Hudak, Lee Vierling, Carine Klauberg, Mariano Garcia, António Ferraz, Michael Keller, Jan Eitel, et Sassan Saatchi. 2017. « Impacts of Airborne Lidar Pulse Density on Estimating Biomass Stocks and Changes in a Selectively Logged Tropical Forest ». *Remote Sensing* 9 (10): 1068. https://doi.org/10.3390/rs9101068.
Silva Junior, Celso, Luiz Aragão, Marisa Fonseca, Catherine Almeida, Laura Vedovato, et Liana Anderson. 2018. « Deforestation-Induced Fragmentation Increases Forest Fire Occurrence in Central Brazilian Amazonia ». *Forests* 9 (6): 305. https://doi.org/10.3390/f9060305.
Silva, Sonaira Souza da, Philip Martin Fearnside, Paulo Mauricio Lima de Alencastro Graça, Irving Foster Brown, Ane Alencar, et Antonio Willian Flores de Melo. 2018. « Dynamics of Forest Fires in the Southwestern Amazon ». *Forest Ecology and Management* 424 (septembre): 312-22. https://doi.org/10.1016/j.foreco.2018.04.041.
Simula, M., et E. Mansur. 2011. « A global challenge needing local response ». *Unasylva* 62 (2): 238.
Simula, Markku. 2009. « Towards defining forest degradation: comparative analysis of existing definitions ». *Forest Resources Assessment Working Paper* 154. http://www.ardot.fi/Documents_2/Degradationdefintions.pdf.
Singh, Minerva, Yadvinder Malhi, et Shonil Bhagwat. 2014. « Biomass Estimation of Mixed Forest Landscape Using a Fourier Transform Texture-Based Approach on Very-High-Resolution Optical Satellite Imagery ». *International Journal of Remote Sensing* 35 (9): 3331-49. https://doi.org/10.1080/01431161.2014.903441.
Sist, Plinio, Ervan Rutishauser, Marielos Peña-Claros, Alexander Shenkin, Bruno Hérault, Lilian Blanc, Christopher Baraloto, et al. 2015. « The Tropical Managed Forests Observatory: A Research Network Addressing the Future of Tropical Logged Forests ». *Applied Vegetation Science* 18 (1): 171-74. https://doi.org/10.1111/avsc.12125.
Smit, Barry, et Johanna Wandel. 2006. « Adaptation, Adaptive Capacity and Vulnerability ». *Global Environmental Change* 16 (3): 282-92. https://doi.org/10.1016/j.gloenvcha.2006.03.008.
Solberg, Svein, Rasmus Astrup, Johannes Breidenbach, Barbi Nilsen, et Dan Weydahl. 2013. « Monitoring Spruce Volume and Biomass with InSAR Data from TanDEM-X ». *Remote Sensing of Environment* 139 (décembre): 60-67. https://doi.org/10.1016/j.rse.2013.07.036.
Song, Xiao-Peng, Matthew C. Hansen, Stephen V. Stehman, Peter V. Potapov, Alexandra Tyukavina, Eric F. Vermote, et John R. Townshend. 2018. « Global Land Change from 1982 to 2016 ». *Nature* 560 (7720): 639-43. https://doi.org/10.1038/s41586-018-0411-9.
Sothe, Camile, Cláudia Almeida, Veraldo Liesenberg, et Marcos Schimalski. 2017. « Evaluating Sentinel-2 and Landsat-8 Data to Map Sucessional Forest Stages in a Subtropical Forest in Southern Brazil ». *Remote Sensing* 9 (8): 838. https://doi.org/10.3390/rs9080838.
Souza, Carlos M., Dar A. Roberts, et Mark A. Cochrane. 2005a. « Combining Spectral and Spatial Information to Map Canopy Damage from Selective Logging and Forest Fires ». *Remote Sensing of Environment* 98 (2-3): 329-43. https://doi.org/10.1016/j.rse.2005.07.013.
———. 2005b. « Combining Spectral and Spatial Information to Map Canopy Damage from Selective Logging and Forest Fires ». *Remote Sensing of Environment* 98 (2-3): 329-43. https://doi.org/10.1016/j.rse.2005.07.013.
Souza, Jr, Carlos, João Siqueira, Marcio Sales, Antônio Fonseca, Júlia Ribeiro, Izaya Numata, Mark Cochrane, Christopher Barber, Dar Roberts, et Jos Barlow. 2013. « Ten-Year Landsat Classification of Deforestation and Forest Degradation in the Brazilian Amazon ». *Remote Sensing* 5 (11): 5493-5513. https://doi.org/10.3390/rs5115493.
Stabler, Ben. 2013. « CRAN - Package shapefiles ». 2013. https://cran.r-project.org/web/packages/shapefiles/.
Storey, Emanuel A., Douglas A. Stow, et John F. O'Leary. 2016. « Assessing Postfire Recovery of Chamise Chaparral Using Multi-Temporal Spectral Vegetation Index Trajectories Derived from Landsat Imagery ». *Remote Sensing of Environment* 183 (septembre): 53-64. https://doi.org/10.1016/j.rse.2016.05.018.

Strobl, Carolin, James Malley, et Gerhard Tutz. 2009. « An Introduction to Recursive Partitioning: Rationale, Application, and Characteristics of Classification and Regression Trees, Bagging, and Random Forests. » *Psychological Methods* 14 (4): 323-48. https://doi.org/10.1037/a0016973.

Tambosi, Leandro R., Alexandre C. Martensen, Milton C. Ribeiro, et Jean P. Metzger. 2014. « A Framework to Optimize Biodiversity Restoration Efforts Based on Habitat Amount and Landscape Connectivity: Optimizing Restoration Based on Landscape Resilience ». *Restoration Ecology* 22 (2): 169-77. https://doi.org/10.1111/rec.12049.

Tamene, Lulseged, Zenebe Adimassu, James Ellison, Tesfaye Yaekob, Kifle Woldearegay, Kindu Mekonnen, Peter Thorne, et Quang Bao Le. 2017. « Mapping soil erosion hotspots and assessing the potential impacts of land management practices in the highlands of Ethiopia ». *Geomorphology* 292: 153-63. https://doi.org/10.1016/j.geomorph.2017.04.038.

Tan, Bin, Jeffrey T. Morisette, Robert E. Wolfe, Feng Gao, Gregory A. Ederer, Joanne Nightingale, et Jeffrey A. Pedelty. 2011. « An enhanced TIMESAT algorithm for estimating vegetation phenology metrics from MODIS data ». *Selected Topics in Applied Earth Observations and Remote Sensing, IEEE Journal of* 4 (2): 361–371.

Thiault, Lauric, Paul Marshall, Stefan Gelcich, Antoine Collin, Frédérique Chlous, et Joachim Claudet. 2018. « Mapping Social-Ecological Vulnerability to Inform Local Decision Making: Mapping Social-Ecological Vulnerability ». *Conservation Biology* 32 (2): 447-56. https://doi.org/10.1111/cobi.12989.

Thioulouse, Jean, Daniel Chessel, Sylvain Dolédec Dec, et Jean-Michel Olivier. 1996. « ADE-4: A Multivariate Analysis and Graphical Display Software », 9.

Thompson, Ian D., Manuel R. Guariguata, Kimiko Okabe, Carlos Bahamondez, Robert Nasi, Victoria Heymell, Cesar Sabogal, et others. 2013a. « An operational framework for defining and monitoring forest degradation ». *Ecology and Society* 18 (2): 20.

———. 2013b. « An operational framework for defining and monitoring forest degradation ». *Ecology and Society* 18 (2): 20.

Thompson, Ian, Brendan Mackey, Steven McNulty, Alex Mosseler, et Secretariat of the convention on the biological diversity. 2009. *Forest Resilience, Biodiversity, and Climate Change: A Synthesis of the Biodiversity, Resilience, Stabiblity Relationship in Forest Ecosystems*. http://alltitles.ebrary.com/Doc?id=10886304.

Thuy, Pham Thu. 2012. *The Context of REDD+ in Vietnam Drivers, Agents and Institutions*. Bogor: CIFOR. http://webdoc.sub.gwdg.de/ebook/serien/yo/CIFOR_OP/75.pdf.

———. 2013. *Payments for Forest Environmental Services in Vietnam from Policy to Practice*. Bogor: CIFOR. http://webdoc.sub.gwdg.de/ebook/serien/yo/CIFOR_OP/93.pdf.

Tilman, D. 1999. « Global Environmental Impacts of Agricultural Expansion: The Need for Sustainable and Efficient Practices ». *Proceedings of the National Academy of Sciences* 96 (11): 5995-6000. https://doi.org/10.1073/pnas.96.11.5995.

Trædal, Leif, et Pål Vedeld. 2017. « Livelihoods and Land Uses in Environmental Policy Approaches: The Case of PES and REDD+ in the Lam Dong Province of Vietnam ». *Forests* 8 (12): 39. https://doi.org/10.3390/f8020039.

Trisasongko, Bambang H. 2010. « The Use of Polarimetric SAR Data for Forest Disturbance Monitoring ». *Sensing and Imaging: An International Journal* 11 (1): 1-13. https://doi.org/10.1007/s11220-010-0048-8.

Tritsch, Isabelle, Plinio Sist, Igor Narvaes, Lucas Mazzei, Lilian Blanc, Clément Bourgoin, Guillaume Cornu, et Valery Gond. 2016. « Multiple Patterns of Forest Disturbance and Logging Shape Forest Landscapes in Paragominas, Brazil ». *Forests* 7 (12): 315. https://doi.org/10.3390/f7120315.

Tucker, Catherine M., J. C. Randolph, Tom Evans, Krister P. Andersson, Lauren Persha, et Glen M. Green. 2008. « An Approach to Assess Relative Degradation in Dissimilar Forests: Toward a Comparative Assessment of Institutional Outcomes ». *Ecology and Society* 13 (1): art4. https://doi.org/10.5751/ES-02262-130104.

Turner, B. L., Roger E. Kasperson, Pamela A. Matson, James J. McCarthy, Robert W. Corell, Lindsey Christensen, Noelle Eckley, et al. 2003. « A Framework for Vulnerability Analysis in Sustainability Science ». *Proceedings of the National Academy of Sciences* 100 (14): 8074-79. https://doi.org/10.1073/pnas.1231335100.

Turner, B. L., E. F. Lambin, et A. Reenberg. 2007. « The Emergence of Land Change Science for Global Environmental Change and Sustainability ». *Proceedings of the National Academy of Sciences* 104 (52): 20666-71. https://doi.org/10.1073/pnas.0704119104.

Turner, Billie, D. Skole, S. Sanderson, G. Fischer, L. Fresco, et R. Leemans. 1995. « Land-Use and Land-Cover Change: Science/Research Plan ». *[No Source Information Available]*, janvier. https://asu.pure.elsevier.com/en/publications/land-use-and-land-cover-change-scienceresearch-plan-2.

Tyukavina, A., M. C. Hansen, P. V. Potapov, A. M. Krylov, et S. J. Goetz. 2016. « Pan-Tropical Hinterland Forests: Mapping Minimally Disturbed Forests: Pan-Tropical Hinterland Forests ». *Global Ecology and Biogeography* 25 (2): 151-63. https://doi.org/10.1111/geb.12394.

Tyukavina, Alexandra, Matthew C. Hansen, Peter V. Potapov, Stephen V. Stehman, Kevin Smith-Rodriguez, Chima Okpa, et Ricardo Aguilar. 2017. « Types and rates of forest disturbance in Brazilian Legal Amazon, 2000–2013 ». *Science Advances* 3 (4): e1601047.

Van Der Werf, G. R., D. C. Morton, R. S. DeFries, J. G. J. Olivier, P. S. Kasibhatla, R. B. Jackson, G. J. Collatz, et J. T. Randerson. 2009. « CO2 Emissions from Forest Loss ». *Nature Geoscience* 2 (11): 737-38. https://doi.org/10.1038/ngeo671.

Vásquez-Grandón, Angélica, Pablo Donoso, et Víctor Gerding. 2018. « Forest Degradation: When Is a Forest Degraded? » *Forests* 9 (11): 726. https://doi.org/10.3390/f9110726.

Venables, W N, et B D Ripley. 2002. « Modern Applied Statistics with S », 504.

Verbesselt, Jan, Rob Hyndman, Glenn Newnham, et Darius Culvenor. 2010. « Detecting Trend and Seasonal Changes in Satellite Image Time Series ». *Remote Sensing of Environment* 114 (1): 106-15. https://doi.org/10.1016/j.rse.2009.08.014.

Verburg, Peter H., Neville Crossman, Erle C. Ellis, Andreas Heinimann, Patrick Hostert, Ole Mertz, Harini Nagendra, et al. 2015. « Land System Science and Sustainable Development of the Earth System: A Global Land Project Perspective ». *Anthropocene* 12 (décembre): 29-41. https://doi.org/10.1016/j.ancene.2015.09.004.

Verhegghen, Astrid, Hugh Eva, Guido Ceccherini, Frederic Achard, Valery Gond, Sylvie Gourlet-Fleury, et Paolo Cerutti. 2016. « The Potential of Sentinel Satellites for Burnt Area Mapping and Monitoring in the Congo Basin Forests ». *Remote Sensing* 8 (12): 986. https://doi.org/10.3390/rs8120986.

Viana, Cecilia, Emilie Coudel, Jos Barlow, Joice Ferreira, Toby Gardner, et Luke Parry. 2016. « How Does Hybrid Governance Emerge? Role of the Elite in Building a Green Municipality in the Eastern Brazilian Amazon: Role of the Elite in Building a Green Municipality ». *Environmental Policy and Governance* 26 (5): 337-50. https://doi.org/10.1002/eet.1720.

Vieilledent, Ghislain, Clovis Grinand, Fety A. Rakotomalala, Rija Ranaivosoa, Jean-Roger Rakotoarijaona, Thomas F. Allnutt, et Frédéric Achard. 2018. « Combining Global Tree Cover Loss Data with Historical National Forest Cover Maps to Look at Six Decades of Deforestation and Forest Fragmentation in Madagascar ». *Biological Conservation* 222 (juin): 189-97. https://doi.org/10.1016/j.biocon.2018.04.008.

Vogelmann, James E, et Barrett N Rock. 1988. « Assessing Forest Damage in High-Elevation Coniferous Forests in Vermont and New Hampshire Using Thematic Mapper Data ». *Remote Sensing of Environment* 24 (2): 227-46. https://doi.org/10.1016/0034-4257(88)90027-2.

Vogelmann, James, Phung Khoa, Do Lan, Jacob Shermeyer, Hua Shi, Michael Wimberly, Hoang Duong, et Le Huong. 2017. « Assessment of Forest Degradation in Vietnam Using Landsat Time Series Data ». *Forests* 8 (12): 238. https://doi.org/10.3390/f8070238.

Wallace, Luke, Arko Lucieer, Zbyněk Malenovský, Darren Turner, et Petr Vopěnka. 2016. « Assessment of Forest Structure Using Two UAV Techniques: A Comparison of Airborne

Laser Scanning and Structure from Motion (SfM) Point Clouds ». *Forests* 7 (12): 62. https://doi.org/10.3390/f7030062.

Wang, Xianli, F. Guillaume Blanchet, et Nicola Koper. 2014. « Measuring Habitat Fragmentation: An Evaluation of Landscape Pattern Metrics ». Édité par Andrew Tatem. *Methods in Ecology and Evolution* 5 (7): 634-46. https://doi.org/10.1111/2041-210X.12198.

Westoby, M.J., J. Brasington, N.F. Glasser, M.J. Hambrey, et J.M. Reynolds. 2012. « 'Structure-from-Motion' Photogrammetry: A Low-Cost, Effective Tool for Geoscience Applications ». *Geomorphology* 179 (décembre): 300-314. https://doi.org/10.1016/j.geomorph.2012.08.021.

Wu, Jianguo. 2007. « Scale and Scaling: A Cross-Disciplinary Perspective ». In *Key Topics in Landscape Ecology*, édité par Jianguo Wu et Richard J. Hobbs, 115-42. Cambridge: Cambridge University Press. https://doi.org/10.1017/CBO9780511618581.008.

———. 2013. « Landscape Sustainability Science: Ecosystem Services and Human Well-Being in Changing Landscapes ». *Landscape Ecology* 28 (6): 999-1023. https://doi.org/10.1007/s10980-013-9894-9.

Wulder, Michael A., Ronald J. Hall, Nicholas C. Coops, et Steven E. Franklin. 2004. « High Spatial Resolution Remotely Sensed Data for Ecosystem Characterization ». *BioScience* 54 (6): 511. https://doi.org/10.1641/0006-3568(2004)054[0511:HSRRSD]2.0.CO;2.

Yanai, Aurora Miho, Euler Melo Nogueira, Paulo Maurício Lima de Alencastro Graça, et Philip Martin Fearnside. 2017. « Deforestation and Carbon Stock Loss in Brazil's Amazonian Settlements ». *Environmental Management* 59 (3): 393-409. https://doi.org/10.1007/s00267-016-0783-2.

Zhang, Jian, Jianbo Hu, Juyu Lian, Zongji Fan, Xuejun Ouyang, et Wanhui Ye. 2016. « Seeing the Forest from Drones: Testing the Potential of Lightweight Drones as a Tool for Long-Term Forest Monitoring ». *Biological Conservation* 198 (juin): 60-69. https://doi.org/10.1016/j.biocon.2016.03.027.

Zhu, Zhe. 2017. « Change Detection Using Landsat Time Series: A Review of Frequencies, Preprocessing, Algorithms, and Applications ». *ISPRS Journal of Photogrammetry and Remote Sensing* 130 (août): 370-84. https://doi.org/10.1016/j.isprsjprs.2017.06.013.

Zhu, Zhe, et Curtis E. Woodcock. 2014. « Continuous Change Detection and Classification of Land Cover Using All Available Landsat Data ». *Remote Sensing of Environment* 144 (mars): 152-71. https://doi.org/10.1016/j.rse.2014.01.011.

Zhu, Zhe, Michael A. Wulder, David P. Roy, Curtis E. Woodcock, Matthew C. Hansen, Volker C. Radeloff, Sean P. Healey, et al. 2019. « Benefits of the Free and Open Landsat Data Policy ». *Remote Sensing of Environment* 224 (avril): 382-85. https://doi.org/10.1016/j.rse.2019.02.016.

Annexes

Appendix 2.1 Remote sensing metadata and derived indicators (R=Red, G= Green, B=Blue, NIR= Near infrared, SWIR= Shortwave infrared)

Satellite Sources	Links	Date	Resolution	ID	Preprocessing	Spectral Bands	Indicators
MODIS	http://modis.gsfc.nasa.gov/	2001–2014 every 16 days	250 m	MOD13Q1: h13v09	Georeferenced, removed cloud covered pixels, atmospheric corrections	R (620–670 nm), NIR (841–876 nm)	EVI mean, EVI standard deviation, EVI variance
Landsat 8	http://earthexplorer.usgs.gov/	27/10/2014 16/09/2014 12/06/2014	30 m	LC82206220 14300LGN0 0 LC82206220 14259LGN0 0 LC82206220 14163LGN0 0	Georeferenced and reflectance product	B (450–515 nm), G (525–600 nm), R (630–680 nm), NIR (845–885 nm), SWIR (1560–1660 nm)	PV, NPV, Bare Soil (Claslite unmixing indicators) B, G, R, NIR, SWIR NDVI, RVI, RI, SAVI, NDWI, MSAVI, GEMI, WDVI, NDTI, TSAVI, NDPI, IPVI, TNDVI (Orfeo Toolbox derived indicators)
ALOS-1 PALSAR	http://global.jaxa.jp/	26/05/2010 18/07/2010 23/07/2010 28/07/2010 07/08/2010 09/09/2010	25 m	N00W050	Georeferenced and calibrated: 1) gamma [dB] 2) sigma [dB]	L-band (1,27 Ghz), dual-polarisation (HH,HV)	Gamma [dB], Sigma [dB]
Sentinel-1	https://scihub.esa.int/	04/05/2015	10 m	L1 (Ground Range Detected)	Calibration and georeferenced (Sentinel-Toolbox Software)	C-band dual-polarisation (VV,VH)	Sigma [dB] Grey Level Co-occurence matrix (9 × 9 pixels): Contrast, Dissimilarity, Energy, Entropy, Correlation, Mean, Variance, Homogeneity, Maximum (Sentinel Toolbox derived indicators)

Appendix 3.1 Landsat archive Metadata (Product identifier) from 1984 to 2017 (3 path/row)

Path/row 222062	Path/row 223062	Path/row 223062
LC08_L1TP_222062_20170731_20170811_01_T1	LC08_L1TP_223062_20170706_20170716_01_T1	LC08_L1TP_223063_20170706_20170716_01_T1
LC08_L1TP_222062_20151201_20170401_01_T1	LC08_L1TP_223062_20160921_20170321_01_T1	LC08_L1TP_223063_20160719_20170323_01_T1
LC08_L1TP_222062_20131109_20170428_01_T1	LC08_L1TP_223062_20150717_20170407_01_T1	LC08_L1TP_223063_20151005_20170403_01_T1
LT05_L1TP_222062_20100626_20161014_01_T1	LC08_L1TP_223062_20150802_20170406_01_T1	LC08_L1TP_223063_20140612_20170422_01_T1
LT05_L1TP_222062_20090810_20161022_01_T1	LC08_L1TP_223062_20130727_20170503_01_T1	LC08_L1TP_223063_20131015_20170429_01_T1
LT05_L1TP_222062_20081010_20161029_01_T1	LT05_L1TP_223062_20090817_20161022_01_T1	LT05_L1TP_223063_20110604_20161009_01_T1
LT05_L1TP_222062_20060615_20161121_01_T1	LT05_L1TP_223062_20080713_20161030_01_T1	LT05_L1TP_223063_20100905_20161013_01_T1
LT05_L1TP_222062_20050714_20161125_01_T1	LT05_L1TP_223062_20070625_20161112_01_T1	LT05_L1TP_223063_20090817_20161022_01_T1
LT05_L1TP_222062_20010804_20161210_01_T1	LT05_L1TP_223062_20060724_20161120_01_T1	LT05_L1TP_223063_20080713_20161030_01_T1
LT05_L1TP_222062_19990714_20161217_01_T1	LT05_L1TP_223062_20040904_20161130_01_T1	LT05_L1TP_223063_20070625_20161112_01_T1
LT05_L1TP_222062_19960705_20170104_01_T1	LT05_L1TP_223062_20030716_20161205_01_T1	LT05_L1TP_223063_20060724_20161120_01_T1
LT05_L1TP_222062_19950719_20170107_01_T1	LE07_L1TP_223062_20020907_20170128_01_T1	LT05_L1TP_223063_20040904_20161129_01_T1
LT05_L1TP_222062_19940918_20170112_01_T1	LE07_L1TP_223062_20010803_20170204_01_T1	LT05_L1TP_223063_20030716_20161205_01_T1
LT05_L1TP_222062_19880816_20170206_01_T1	LE07_L1TP_223062_20000731_20170210_01_T1	LE07_L1TP_223063_20020705_20170130_01_T1
LT05_L1TP_222062_19840618_20170220_01_T1	LE07_L1TP_223062_19990713_20170218_01_T1	LE07_L1TP_223063_20010803_20170204_01_T1
	LT05_L1TP_223062_19990705_20161217_01_T1	LE07_L1TP_223063_20000731_20170210_01_T1
	LT05_L1TP_223062_19970528_20161231_01_T1	
	LT05_L1TP_223062_19950710_20170107_01_T1	
	LT05_L1TP_223062_19910816_20170126_01_T1	
	LT05_L1TP_223062_19890927_20170201_01_T1	
	LT05_L1TP_223062_19880924_20170206_01_T1	
	LT05_L1TP_223062_19860615_20170217_01_T1	

Appendix 3.2 Example of reconstruction of degradation history (1984-2017) of a logged and burned forest plot mapped in September 2017: photointerpretation of forest disturbances (over logging, selective logging and fire) using Landsat annual imageries and derived Normalized Difference Moisture Index (NDMI).

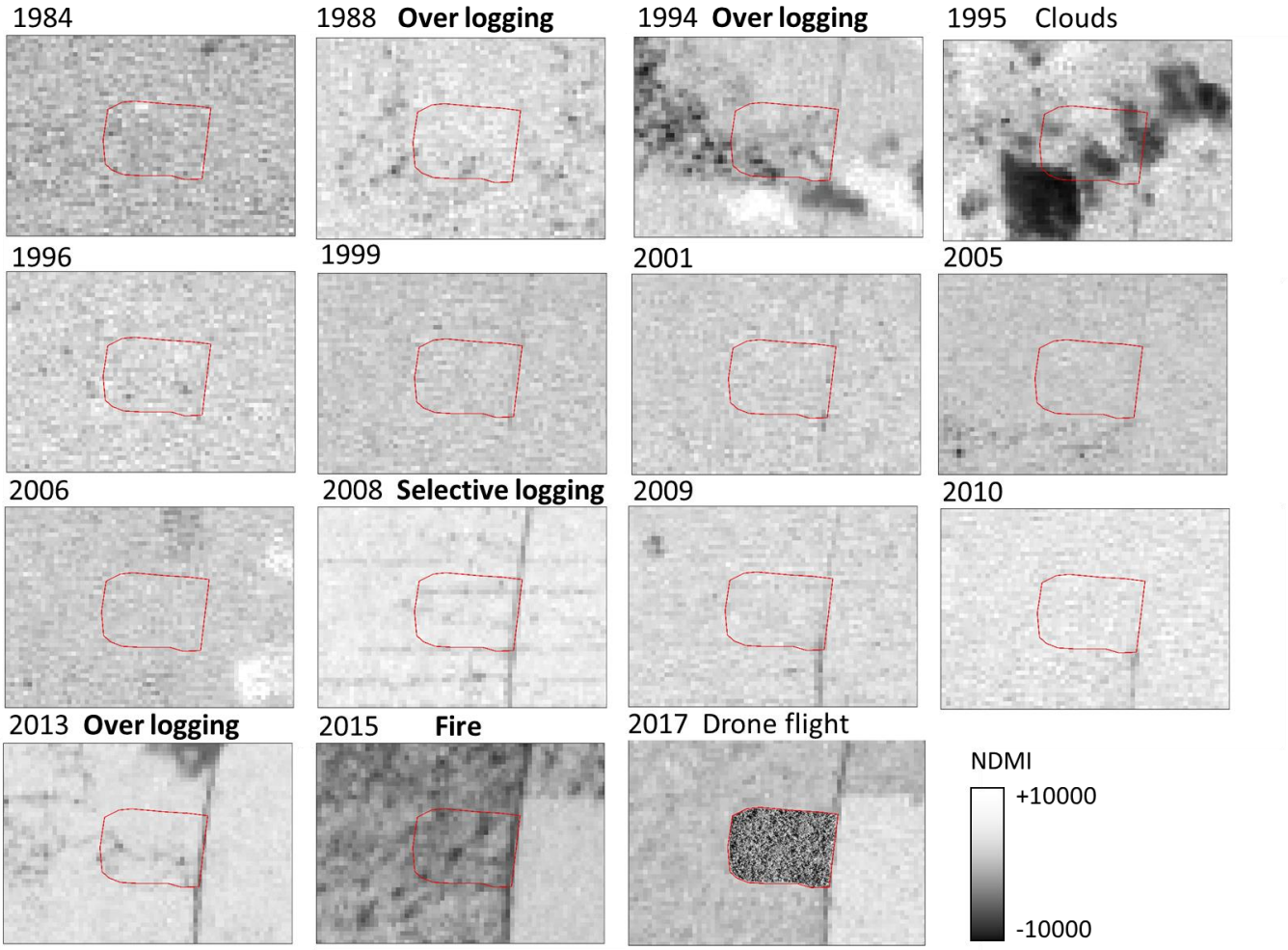

Appendix 3.3 Information on 1) UAV data collection (plot ID, surface mapped, date, hour and point cloud average density), 2) Landsat reconstruction of degradation history simplified in four indicators (number of over logging, selective logging and fire detected events, and date of the last disturbance) and 3) Cluster id of canopy structure

ID	UAV data collection				Landsat reconstruction of degradation history				Canopy structure cluster id
	Surface (ha)	Date	Hour	Average density (per m^3)	Over logging events	Selective logging events	Fires events	Last impact date	
1	33.5	18/09/2017	15:35	17.28	3	1	1	2015	4
2	14.7	19/09/2017	16:58	19.27	0	0	2	2016	4
3	53.5	21/09/2017	08:31	27.29	0	1	0	2004	6
4	50.2	21/09/2017	09:50	29.73	0	1	0	2004	6
5	41.1	21/09/2017	17:07	20.81	0	1	0	2010	6
6	19.6	22/09/2017	07:35	29.85	0	1	0	2013	5
7	41.7	22/09/2017	08:14	18.53	0	1	0	2014	5
8	16.6	22/09/2017	08:44	13.01	0	1	0	2014	5
9	35.0	22/09/2017	12:56	19.4	0	1	0	2017	4
10	32.4	22/09/2017	13:21	17.65	0	1	0	2017	4
11	36.2	22/09/2017	15:54	14.28	0	1	0	2017	5
12	29.2	23/09/2017	09:41	17.04	1	1	0	2013	3
13	25.1	23/09/2017	10:09	18.47	2	1	0	2013	3
14	14.7	13/09/2017	15:04	30.18	Secondary forest since 1994 (pasture before)				2
15	31.1	18/09/2017	15:56	18.93	2	1	0	2008	6
16	41.4	14/09/2018	14 :43	7.42	0	1	0	2006	5
17	37.3	14/09/2018	14 :43	7.42	Secondary forest since 1990 (pasture before)				3
18	39.8	24/09/2018	16 :57	7.51	2	0	0	2016	5
19	34.7	12/09/2018	11 :24	8.37	0	0	0	/	6

20	24.0	13/09/2017	09:07	18.68	1	0	0	1995	4
21	33.3	18/09/2017	16:28	17.37	3	1	1	2015	4
22	33.2	18/09/2017	16:49	18.64	2	1	0	2013	3
23	35.8	14/09/2017	14:46	15.80	1	0	0	1999	6
24	36.1	14/09/2017	15:52	17.65	2	0	0	1995	6
25	33.1	14/09/2017	16:31	19.93	2	0	0	2015	3
26	29.3	14/09/2017	17:18	23.52	3	0	2	2016	1
27	32.1	18/09/2017	17:18	18.83	1	1	1	2015	1
28	24.0	16/09/2017	08:44	17.33	0	0	2	2017	1
29	25.1	12/09/2017	14:52	16.6	Secondary forest since 1995 (pasture before)				2
30	32.3	16/09/2017	10:22	17.61	0	0	3	2017	4
31	26.1	16/09/2017	11:20	16.02	2	0	2	2017	1
32	23.9	17/09/2017	09:16	27.49	3	0	0	2015	5
33	27.8	17/09/2017	10:29	13.40	3	0	1	2017	5
34	15.8	17/09/2017	12:52	21.25	1	0	0	1999	3
35	24.1	17/09/2017	13:52	23.80	1	1	1	2017	1
36	25.8	17/09/2017	14:58	20.36	3	0	1	2017	4
37	40.4	12/09/2017	15:53	15.99	1	1	0	2015	3
38	32.1	19/09/2017	15:00	20.12	1	0	0	1997	3
39	22.6	19/09/2017	15:34	16.58	1	0	2	2016	3
40	26.5	19/09/2017	16:33	21.25	3	0	1	2015	3

Appendix 3.4 Unsupervised clustering of canopy structure

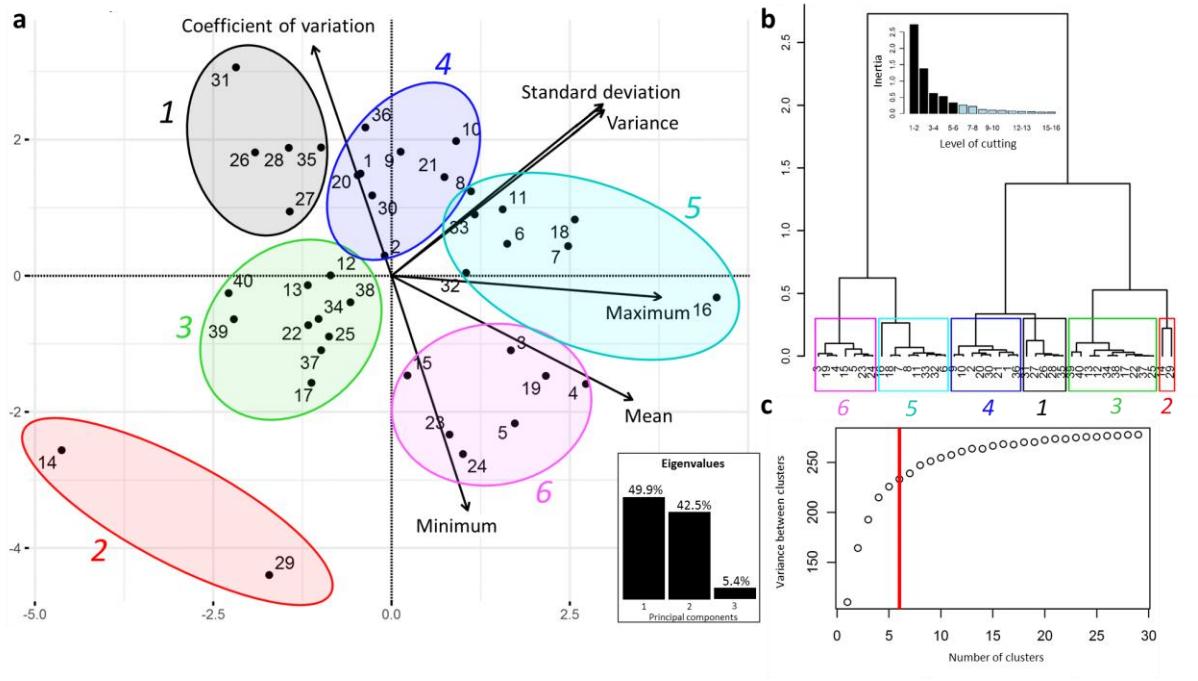

a) Principal component analysis (PCA) of the DHM (arrows) for each of the 40 forest plots and representation of the 6 clusters obtained on the 1-2 factorial plane of the PCA. b) Dendrogram and absolute loss of inertia related to the clustering of the 6 clusters. c) Plot of the inter-cluster variance calculated with the kmeans clustering method as a function of the number of clusters tested (from 2 to 30). Beyond 6 clusters, the variance between clusters tended to saturate to a constant value of 250.

Appendix 3.5 Average of Canopy Height Model metrics defining each forest structure cluster.

Forest structural metrics	Cluster 1	Cluster 2	Cluster 3	Cluster 4	Cluster 5	Cluster 6	Overall mean (all clusters)
Minimum (m)	0.64	6.48	2.66	0.96	2.26	6.26	2.81
Maximum (m)	27.88	20.71	30.03	32.01	39.47	39.49	33.23
Mean (m)	9.91	13.86	14.13	14.03	20.86	22.94	16.46
Variance	39.81	5.53	26.72	51.03	58.96	37.81	40.55
Standard deviation	6.19	2.28	5.10	7.08	7.59	6.05	6.16
Coefficient of variation CV	0.72	0.18	0.38	0.53	0.38	0.23	0.42

Appendix 4.1 Landsat images metadata (source USGS[1])

		Landsat-5				Landsat-8
	Spectral resolution	Blue (450-520), Green (520-600), Red (630-690), NIR (760-900), SWIR1 (1550-1750), SWIR2 (2080-2350)				Ultra Blue (435-451), Blue (452-512), Green (533-590), Red (636-673), NIR (851-879), SWIR1(1566-1651), SWIR2 (2107-2294)
Path/row		1988	1995-1996	2000-2001	2009	2017
222/062	Date	1988-08-16	1996-07-05	2001-08-04	2009-08-10	2017-07-31
	Cloud cover	0%	2%	5%	2%	5.1%
223/062	Date	1988-09-24	1995-07-10	2000-06-05	2009-08-17	2017-07-06
	Cloud cover	0%	0%	4%	0%	1.39%
223/063	Date	1988-09-24	1995-07-10	2000-06-05	2009-08-17	2017-07-06
	Cloud cover	0%	1%	0%	0%	0.01%

[1] https://earthexplorer.usgs.gov/ (accessed on 7 March 2019)

Appendix 4.2 Landscape elements identified and the land use/ land cover typology

Land use / Land cover typology	Landscape elements identified in the field	Photo (Bourgoin 2017)
Artificial surface	Concrete road and buildings	
Water body	Natural and anthropized lakes and rivers	
Cropland	Maize, Soybean, Millet and sorghum	
Bare soil	Dirt road or mining or bare soil (no crops)	
Pasture	Managed pasture (Herbaceous layer <1m) and unmanaged pasture (Herbaceous layer >1m and woody vegetation)	
Plantation	Eucalyptus or Parika plantation of various ages	
Forest	Forest in various states (from conserved to degraded) that has never been deforested	
Juquiera	An initial stade of forest regrowth, mainly associated with abandoned or small-income-owner's pastures	

Appendix 4.3 Field inventory and visual interpretation of the different land uses (Landsat-8 2017 image with RGB composite color).

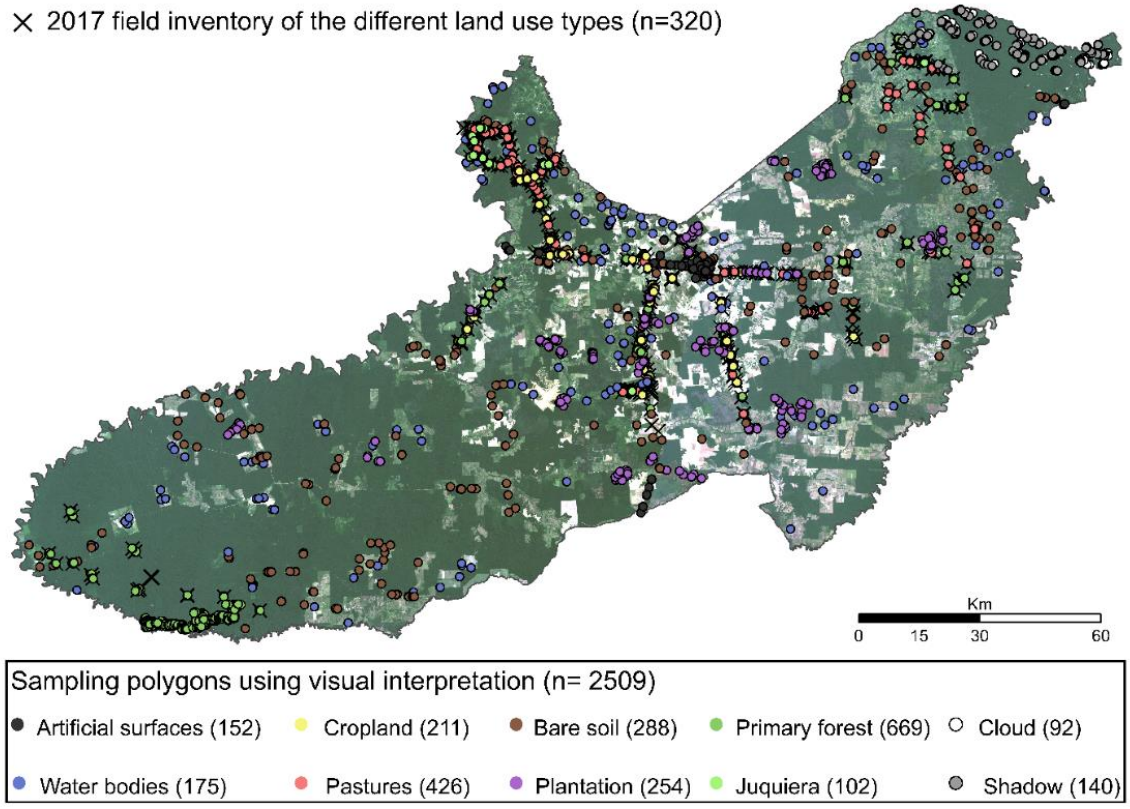

Appendix 4.4 Vegetation indices derived from Landsat images (G = Green band, R = Red band, NIR = Near-infrared band, SWIR1-2 = Short wave infrared spectral range)

Vegetation Index	Formulation	Name	Reference
NDVI	(NIR-R)/(NIR+R)	Normalized Difference Vegetation Index	(Rouse and Haas 1974)
NDWI	(G-NIR)/(G+NIR)	Normalized Difference Water	(McFeeterts 1996)
EVI	2,5*(NIR-R)/(NIR+6*R-7,5*B)+1)	Enhanced Vegetation Index	(Huete et al. 2002)
SAVI	(NIR-R)*1,5/(NIR+R+0,5)	Soil-Adjusted Vegetation	(Huete 1988)
MSAVI	(NIR-R)*(1+L)/(NIR+R+L) L=1-((2*s*(NIR-R)*(NIR- s is the slope of the soil line from a	Modified Soil-Adjusted-Vegetation Index	(Qi et al. 1994)
NBR	(NIR-SWIR2)/(NIR+SWIR2)	Normalized Burn Index	(Miller and Thode 2007)
NBR2	(SWIR1-SWIR2)/(SWIR1+SWIR2)	Normalized Burn Index 2	(Storey et al. 2016)
NDMI	(NIR-SWIR1)/(NIR+SWIR1)	Normalized Difference Moisture Index	(Vogelmann and Rock 1988)

Appendix 4.5 Sampled regions, Shannon diversity index average profile and resulting grid units

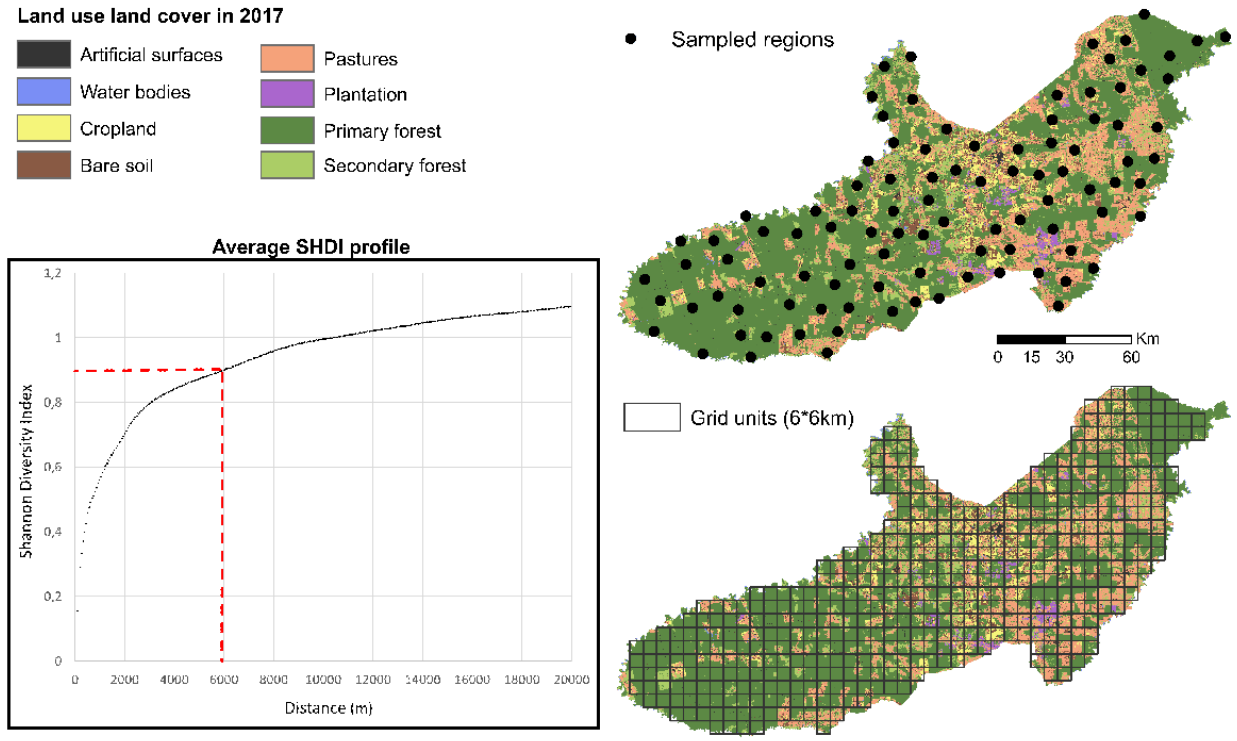

Appendix 4.6 Confusion matrix of Landsat-8 2017 based classification (user and producer accuracy, overall accuracy and kappa index)

Actual/Predicted	Artificial surfaces	Water bodies	Primary forest	Cropland	Pastures	Plantation	Bare soil	Juquiera	Cloud	Shadow	Total	User accuracy
Artificial surfaces	258,80	1,96	0,08	1,28	0,78	0,00	16,14	0,60	0,04	0,00	279,68	0,93
Water bodies	1,18	291,90	0,00	0,00	0,00	0,00	0,08	0,00	0,70	3,02	296,88	0,98
Primary forest	2,50	0,78	250,12	0,02	1,34	20,62	0,62	17,78	0,66	1,26	295,70	0,85
Cropland	7,44	0,02	0,00	256,68	22,34	0,76	25,82	0,74	0,00	0,00	313,80	0,82
Pastures	3,82	0,14	2,34	21,58	238,22	11,78	14,14	23,82	0,00	0,00	315,84	0,75
Plantation	0,34	0,06	19,68	0,10	3,82	254,58	1,42	9,54	0,52	0,00	290,06	0,88
Bare soil	23,58	1,00	0,20	19,46	10,60	0,60	233,80	3,80	1,24	0,00	294,28	0,79
Juquiera	2,34	0,02	26,28	0,88	22,86	11,66	7,20	243,72	0,00	0,00	314,96	0,77
Cloud	0,00	0,00	0,00	0,00	0,04	0,00	0,78	0,00	296,84	0,02	297,68	1,00
Shadow	0,00	4,12	1,30	0,00	0,00	0,00	0,00	0,00	0,00	295,70	301,12	0,98
Total	300,00	300,00	300,00	300,00	300,00	300,00	300,00	300,00	300,00	300,00	3000,00	
Producer accuracy	0,86	0,97	0,83	0,86	0,79	0,85	0,78	0,81	0,99	0,99		
Overall Accuracy	0,87											
Kappa	0,86											

Appendix 4.7 Forest non-forest classifications using historical Landsat images and overall accuracy (OA) and Kappa indexes. Cumulative deforestation (forest to non-forest transition), reforestation (non-forest to forest transition) and deforested regrowth.

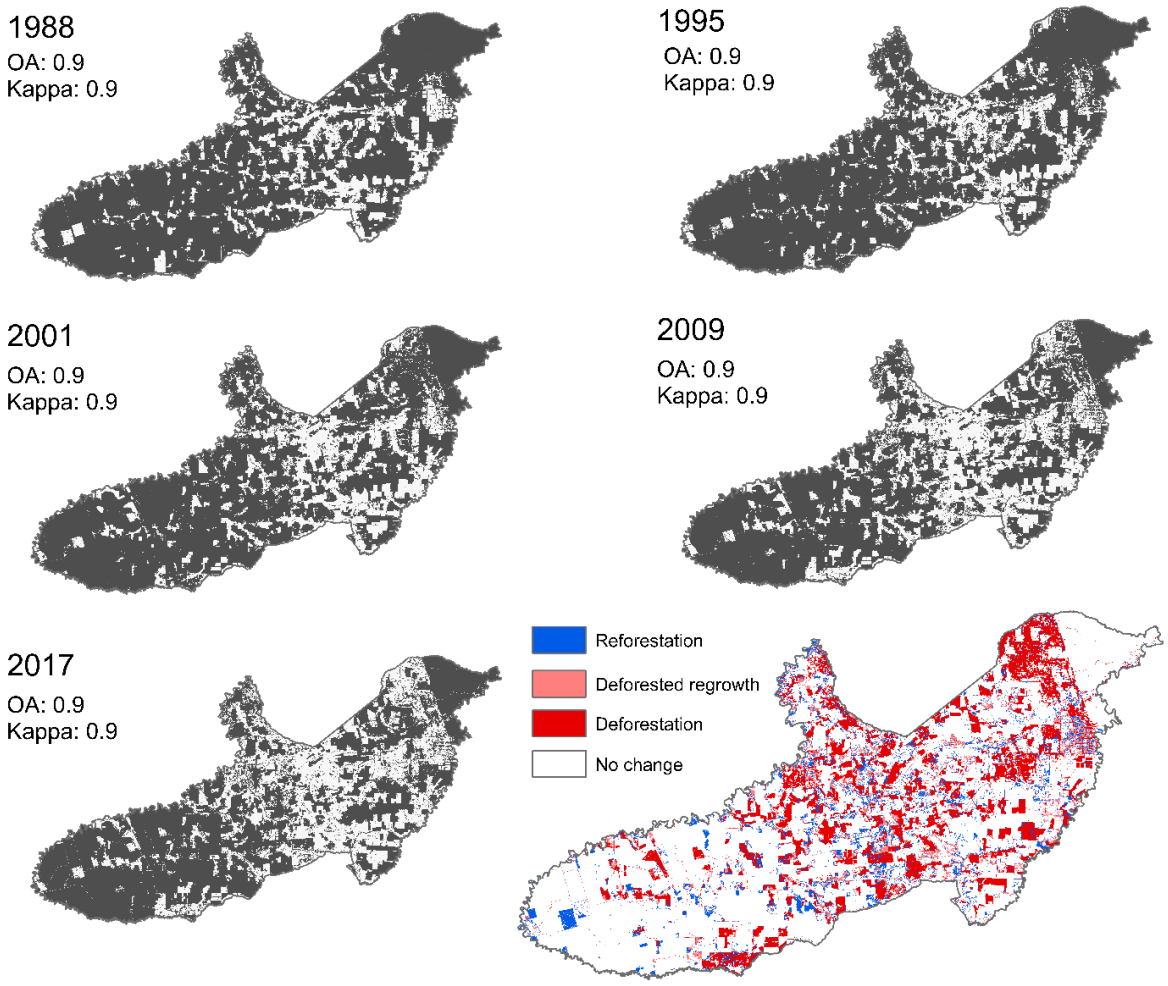

Appendix 4.8 Multiple linear regression models for the prediction of forest degradation proxies (mean/standard deviation of AGB, mean/standard deviation of NPVV) from landscape-level drivers.

	mean AGB R^2: 0.80, RMSE: 14.26 Mg.ha-1			Std AGB R^2: 0.31, RMSE: 5.49			mean NPVV R^2: 0.58, RMSE: 0.85 NPVV			Std NPVV R^2: 0.67, RMSE: 0.55		
	Estimate	Std. Error	pvalue	Estimate	Std. Error	pvalue	Estimate	Std. Error	pvalue	Estimate	Std. Error	pvalue
Intercept	219.73	0.63	< 2e-16	36.57	0.24	< 2e-16	5.36	0.04	< 2e-16	2.01	0.02	< 2e-16
Distance_Pgm	16.80	0.79	< 2e-16	3.37	0.28	< 2e-16	-0.33	0.05	1.54e-10			
DEM	-9.98	0.67	< 2e-16	-2.21	0.3	6.41e-13				0.15	0.03	7.55e-07
Slope	8.78	0.68	< 2e-16	2.16	0.26	1.70e-15						
Sand_p				-1.43	0.29	1.28e-06	0.43	0.04	< 2e-16	0.14	0.03	4.82e-06
Fire occurrence							0.25	0.05	1.54e-10			
pNV_Forest	11.33	0.95	< 2e-16				-0.73	0.09	2.99e-14	-0.64	0.07	< 2e-16
pNC_Forest_Pasture	-5.89	0.83	4.92e-12				0.32	0.05	2.12e-09			
pNC_Forest_BareSoil	3.62	0.64	2.16e-08	1.14	0.24	4.16e-06						
HET_agg							-0.68	0.09	5.60e-13			
HET_frag										0.79	0.09	< 2e-16
SHDI										-0.84	0.09	< 2e-16
CSHDI				1.42	0.29	1.30e-06				0.18	0.04	4.81e-06

Appendix 5.1 Sentinel-2 and Landsat characteristics (source ESA[1] and USGS[2])

	Sentinel-2	Landsat 5 and 8
Spatial resolution,	10 x 10 m	30 x 30 m
spectral (nm) and acquisition (Day-Month-	Blue (490), Green (560), Red (665) and 20 x 20 m Red edge (705), B6 (740), B7 (783), B8a (865), SWIR1 (1610) and SWIR2 12/02/2018 and 07/02/2018	Landsat 5: Blue (450-520), Green (520-600), Red NIR (760-900), SWIR1 (1550-1750), SWIR2 (2080- 07/02/2011, 18/12/2009, 26/12/2006, 05/01/2002, 10/01/1995, 22/03/1992, 09/01/1989 and Landsat 8: Ultra Blue (435-451), Blue (452-512), (533-590), Red (636-673), NIR (851-879), SWIR1 (1566-1651), SWIR2 (2107-2294) 25/01/2018, 20/01/2016 and 15/02/2014
Tile size	100 x 100 km	185 x 185 km
Tile number	48PZU and 48PZT	124/052

1 https://sentinel.esa.int/web/sentinel/user-guides/sentinel-2-msi (accessed on 7 March 2019).

2 https://earthexplorer.usgs.gov/ (accessed on 7 March 2019).

Appendix 5.2 Vegetation indices derived from Sentinel-2 (S2) and Landsat (L) images (G = Green band, R = Red band, NIR = Near-infrared band, SWIR1-2 = Short wave infrared spectral range)

Vegetation Index	Formulation	Name	Satellite/Sensor (S2/L)	Reference
NDVI	(NIR-R)/(NIR+R)	Normalized Difference	S2 and L	(Rouse et Haas 1974)
NDWI	(NIR-SWIR1)/(NIR+SWIR1)	Normalized Difference	S2	(Gao 1996)
EVI	2,5*(NIR-R)/(NIR+6*R-7,5*B)+1)	Enhanced Vegetation Index	S2 and L	(A. Huete et al. 2002)
NDSI	(SWIR-NIR)/(SWIR+NIR)	Normalized Difference Soil	S2	(Deng et al. 2015)
DWV	NDVI-NDWI	Difference Water Vegetation	S2	(Gond et al. 2004)
BSI	$\sqrt{R^2 + NIR^2}$	Bare Soil Index	S2	(Li et Chen 2014)
SAVI	(NIR-R)*1,5/(NIR+R+0,5)	Soil-Adjusted Vegetation	S2 and L	(Huete 1988)
MSAVI	(NIR-R)*(1+L)/(NIR+R+L) L=1-((2*s*(NIR-R)*(NIR- s is the slope of the soil line from a	Modified Soil-Adjusted-Vegetation Index	L	(Qi et al. 1994)
NBR	(NIR-SWIR2)/(NIR+SWIR2)	Normalized Burn Index	L	(Miller & Thode 2007)
NBR2	(SWIR1-SWIR2)/(SWIR1+SWIR2)	Normalized Burn Index 2	L	(Storey, Stow, &
NDMI	(NIR-SWIR1)/(NIR+SWIR1)	Normalized Difference	L	(J. E. Vogelmann &

Appendix 5.3 Landscape elements identified in Di Linh district and 2 levels of land use/cover typologies

Landscape components identified in the field	Detailed land use / land cover typology	Land use score following landscape intensification gradient [0-10]	Simplified land cover typology
Conserved, medium and poor evergreen forest: 2 to 4 vegetation layers. Basal area between 10 and 25 m3/ha. Diameter of the biggest trees >50 cm. Canopy between 15 to 30 m in height. Natural dead trees. No signs of human impacts (conserved) or old logging impacts.	Evergreen broadleaf forest	0	
Recent logging and/or burned forest: Located at the forest edge, signs of recent fire and logging. Low open canopy dominated by pioneer species.			Evergreen broadleaf forest
Bamboo forest: Evergreen broadleaf forest mixed with bamboo or pure bamboo forest. Between 5 to 25 m in height and 90% of tree cover, dense understory.	Degraded forest	3	
Bush: Composed of 2 layers: herbaceous <1 m and 1 layer <3 m in height.			
Young pine tree plantation: 4 m in height. 50% tree cover. No intermediate vegetation layers. Natural pine forest or old plantation: 30 years maximum. Trees spaced (5-10 m apart), tall (25 m in height), and regular height. Diameter between 30 and 60 cm. No intermediate vegetation layers.	Pine forest	6	Pine forest
Coffee plantation: From 50 cm to maximum 3 m in height. 50% tree cover. No understory.	Coffee	9	Cropland
Irrigated and rainfed rice.	Rice	9	
Banana plantations and/or maize: Height <3 m, mixed with a herbaceous layer. Sometimes intercropped with maize. Maize cultivated with coffee or banana. <1 m in height.	Cropland	9	
Bare soil: In both forest and agricultural habitats. Presence of stumps, dead trees, trunks and sometimes limited regeneration.	Bare soil	10	
Infrastructure: Buildings and paved roads and dirt tracks	Infrastructure	10	
Water bodies: Artificial lakes and rivers	Water bodies	10	Water bodies

Appendix 5.4 Land use/cover classification of Di Linh district using Sentinel-2 (10 m) and Landsat-8 (30 m) images

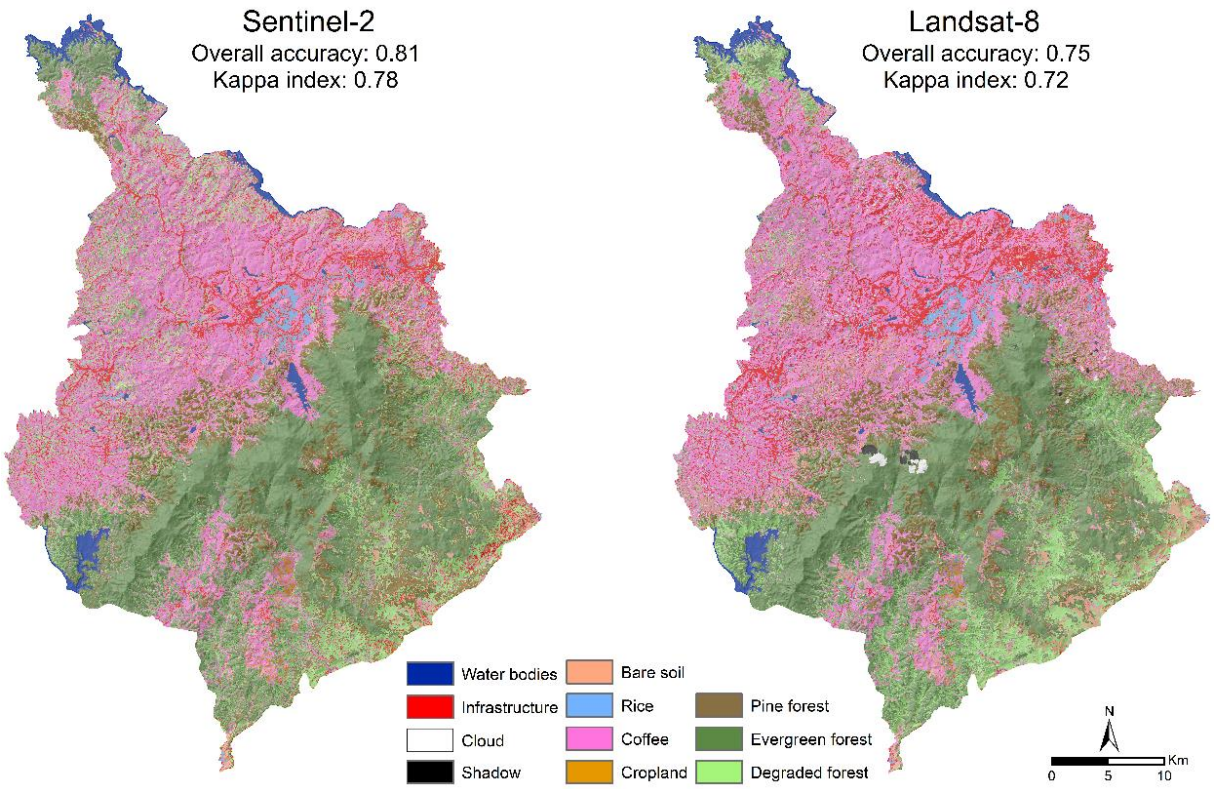

Appendix 5.5 Accuracy assessment of land use/cover classifications in 2018

	Sentinel-2		Landsat-8	
Overall accuracy	0.81		0.75	
Kappa index	0.78		0.72	
	User accuracy	Producer accuracy	User accuracy	Producer accuracy
Cloud (center)	0.91	0.93	0.95	0.98
Cloud (edge)	0.97	0.81	0.94	0.75
Water	0.89	1.00	0.86	0.99
Projected shadow	0.92	0.84	1.00	0.87
Buildings and roads	0.86	0.83	0.66	0.88
Young and mature coffee	0.74	0.76	0.68	0.61
Bare soil (agriculture and forestry areas)	0.59	0.84	0.56	0.75
Degraded forest	0.78	0.49	0.82	0.49
Young and mature pine forest	0.82	0.89	0.85	0.82
Irrigated rice field	0.95	0.82	0.81	0.81
Rainfed rice field	0.89	0.51	0.98	0.48
Evergreen forest (no shadow)	0.79	0.78	0.79	0.61
Evergreen forest (shadow)	0.93	0.61	0.84	0.59
Cropland	1.00	0.24	0.85	0.27

Appendix 5.6 Shannon diversity index profiles calculated using Landsat-8 based classification (2018) within 50 to 8000 m buffer zones at 15 sampled points in Di Linh district (Fig. 2). The bold line shows the mean of the 15 curves

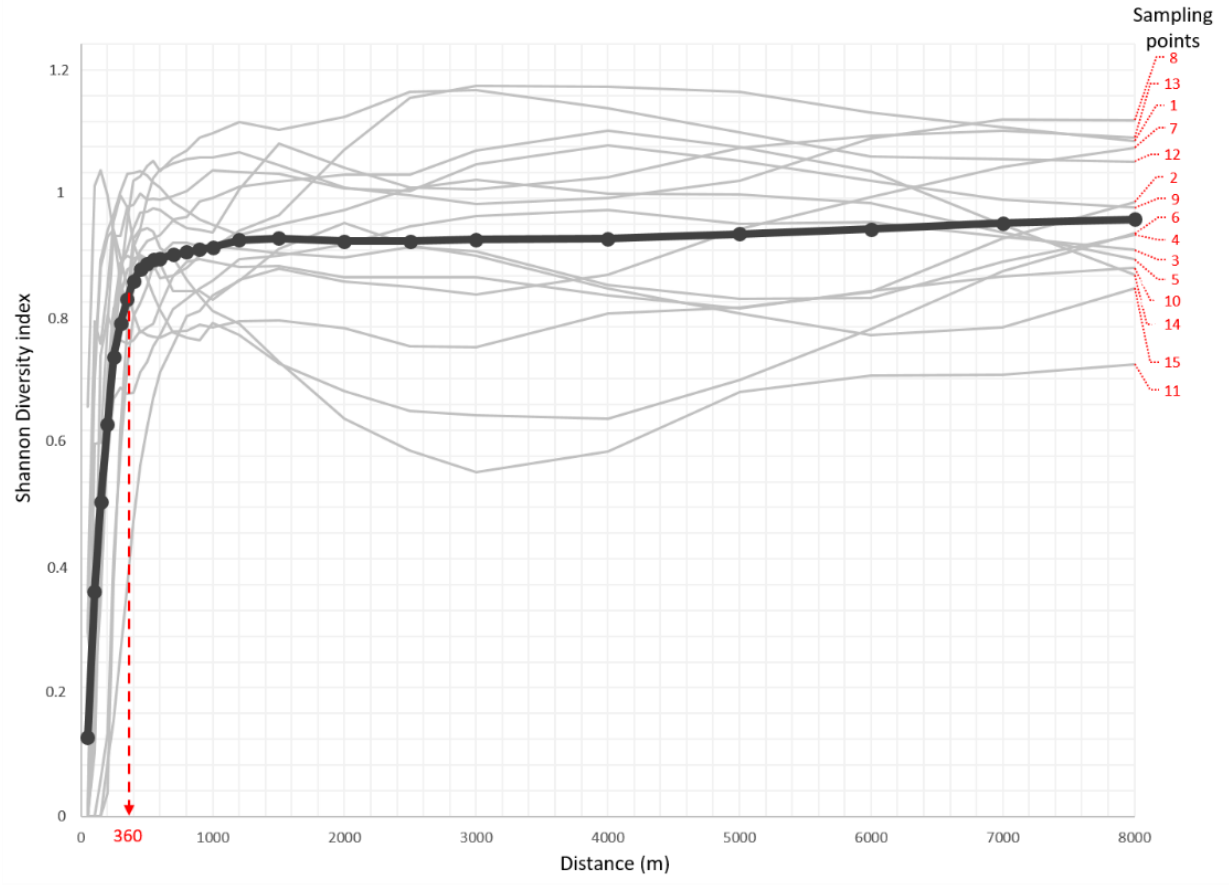

Appendix 5.7 Accuracy assessment (overall accuracy, kappa indexes, user and producer accuracy)

	User accuracy								Producer accuracy								OA	Kappa
	Pine forest	Evergreen forest	Forest shadow	Cropland	Urban	Cloud	Shadow	Water	Pine forest	Evergreen forest	Forest shadow	Cropland	Urban	Cloud	Shadow	Water		
2016	0.92	0.96	0.96	0.93	0.92	0.95	1.00	1.00	0.98	0.85	0.82	0.91	0.95	0.95	1.00	1.00	0.95	0.93
2014	0.93	0.93	0.85	0.89	0.90	1.00	1.00	1.00	0.95	0.86	0.83	0.89	0.92	1.00	1.00	1.00	0.93	0.91
2011	0.86	0.92	0.90	0.96	0.93	/	/	1.00	0.95	0.87	0.76	0.94	0.98	/	/	0.99	0.92	0.91
2009	0.89	0.94	0.93	0.94	0.93	1.00	0.99	0.89	0.97	0.91	0.76	0.92	0.88	0.99	0.92	1.00	0.93	0.92
2006	0.81	0.91	0.88	0.83	0.91	0.93	0.82	0.89	0.94	0.80	0.69	0.87	0.92	0.89	0.72	0.89	0.86	0.84
2002	0.87	0.89	0.90	0.87	0.92	1.00	/	0.96	0.86	0.90	0.724	0.92	0.94	1.00	/	0.97	0.89	0.86
1998	0.86	0.92	0.91	0.85	0.94	1.00	1.00	1.00	0.89	0.90	0.85	0.91	0.82	0.99	0.94	0.90	0.89	0.87
1995	0.83	0.89	0.90	0.84	0.88	/	/	0.98	0.81	0.91	0.79	0.92	0.75	/	/	0.98	0.87	0.83
1992	0.89	0.84	0.87	0.91	0.94	1.00	1.00	1.00	0.87	0.89	0.77	0.95	0.85	1.00	1.00	0.98	0.89	0.87
1989	0.83	0.85	0.82	0.84	0.95	1.00	/	0.96	0.79	0.88	0.69	0.95	0.74	1.00	/	0.83	0.85	0.80
1973	0.78	0.81	0.72	0.79	0.71	1.00	0.67	0.83	0.70	0.83	0.65	0.87	0.76	1.00	0.29	0.89	0.79	0.72

Appendix 5.8 Assessment of sensitivity and exposure scores derived from landscape trajectories

		Sensitivity										Exposure				
		Forest dynamics (green curve)					Fragmentation dynamics (grey dashed curve)					Agricultural expansion (yellow curve)				
Classes of landscape trajectory	Forest 2018	Average composition	Rate of change	Score of rate of change	Dynamic	Score of forest dynamic	Average value	Rate of change	Score of rate of change	Dynamic	Score of fragmentation dynamic	Sensitivity Score	Average composition	Rate of change	Score of rate of change	Dynamic	Exposition Score
T1	1	0.7	-0.08	6.0	4.4	8.6	0.6	0.3	10	5.7	5.9	7.2	0.2	0.0	2.9	0.5	1.0
T2	1	0.3	-0.09	6.7	2.1	4.2	1	-0.1	3.3	3.2	3.3	3.7	0.5	0.2	10	4.8	10.0
T3	1	0.5	-0.14	10.0	5.1	10.0	1.1	0.2	8.9	9.7	10	10	0.3	0.1	8.1	2.6	5.3
T4	1	0.6	0.00	0.0	0.0	0.0	0.7	-0.2	2.1	1.4	1.4	0.7	0.3	0.0	0.3	0.1	0.2
T5	1	0.5	-0.01	0.7	0.3	0.7	0.8	0.1	7.2	5.5	5.6	3.2	0.3	0.0	0.0	0.0	0.0
T6	1	0.6	0.00	0.0	0.0	0.0	1.1	0.0	5.5	6.1	6.3	3.2	0.2	0.0	1.9	0.3	0.7
T7	1	0.8	-0.03	2.1	1.7	3.3	0.7	0.1	7.6	5.2	5.4	4.3	0.1	0.0	1.9	0.2	0.5
T8	1	0.8	-0.01	0.8	0.6	1.2	0.4	0.1	6.4	2.6	2.7	1.9	0.2	0.0	0.7	0.1	0.3
T9	1	0.3	0.00	0.0	0.0	0.0	0.0	0.0	5.3	0.0	0.0	0.0	0.7	0.0	0.5	0.0	0.0
T10	1	0.3	0.00	0.0	0.0	0.0	0.2	0.0	5.1	1.3	1.3	0.6	0.6	0.0	0.8	0.5	1.1
T11	0	0.0	0.00	0.0	0.0	0.0	0.0	0.0	5.3	0.0	0.0	0.0	1.0	0.0	0.6	0.0	0.0
T12	0	0.0	0.00	0.1	0.0	0.0	0.0	0.0	5.1	0.0	0.0	0.0	1.0	0.0	0.7	0.0	0.0
T13	0	0.0	-0.01	0.7	0.0	0.0	0.1	-0.1	3.2	0.0	0.0	0.0	1.0	0.0	2.0	0.0	0.0
T14	0	0.0	-0.04	3.0	0.0	0.0	0.1	-0.2	2.6	0.0	0.0	0.0	1.0	0.1	3.9	0.0	0.0
T15	0	0.1	-0.11	7.6	0.0	0.0	0.4	-0.3	0.0	0.0	0.0	0.0	0.8	0.2	9.7	0.0	0.0

This table presents the average composition and rate of change for each class of landscape trajectory between 1998 and 2018, as well as the resulting dynamics for forest, fragmentation and agricultural expansion. Forest dynamic score clearly separates trajectory classes with a high proportion of forest that have experienced a sharp decrease in the last 20 years (values close to 10) from classes with a low proportion of forest and that have stabilized (values close to 0). We assigned a score of 0 to trajectory classes with no forest cover in 2018 or during the last 20 years. The fragmentation dynamic and agricultural expansion scores (i.e. exposition score) were obtained using the same method as for forest dynamics except that the higher the increase in the edge density (resp. cropland) indicator, the higher the score. The sensitivity score combines the two forest and fragmentation dynamics scores (and values resampled between 0 and 10).

Appendix 5.9 Assessment of adaptive capacity score derived from landscape mosaic composition (2018) and the agricultural intensification indicator (please refer to Fig. 3 for details on the calculation of landscape intensification scores)

Adaptive capacity separates homogeneous, low fragmented and evergreen forest dominated landscapes (values close to 10) from heterogeneous, highly fragmented forest mosaics associated with coffee, degraded and pine forests (values close to 0).

Classes of forest landscape mosaics	Landscape intensification score	Adaptive Capacity Score
L1	0.2	10.00
L2	1.4	7.78
L3	2.1	6.38
L5	4.3	2.07
L6	5.3	0.03
L7	5.4	0

agreenium
l'institut agronomique, vétérinaire & forestier de France

Ecole Doctorale ABIES

Title : A framework for evaluating forest ecological vulnerability in tropical deforestation fronts from the assessment of forest degradation in a landscape approach: Case studies from Brazil and Vietnam

Keywords : Ecological vulnerability, agricultural expansion, forest degradation, remote sensing

Abstract: The conservation of tropical forest cover is a key to ensuring sustainable provision of multiple ecosystem services. However, increasing demography, demand for agricultural products and changes in land uses are affecting forest sustainability through degradation processes. A first step to tailor effective forest management is to identify most vulnerable forests and to characterize their drivers. The objective of this thesis is to develop a multidimensional approach to assess forest degradation and the relations with the broader dynamics of land use/cover towards the evaluation of forest ecological vulnerability. The thesis was applied in Paragominas (Brazil) and Di Linh (Vietnam) where large-scale deforestation driven by commercial agriculture shaped the landscape into land use mosaics with increasing degradation pressures. In Paragominas, degradation is linked with selective logging and fire implying changes in forest structure. We estimated the potential of multisource remote sensing to map forest aboveground biomass from large-scale field assessment of carbon stock and investigated the consequences of degradation history on forest structures. We found that canopy textures correlated with forest structure variability and could be used as proxies to characterize degraded forests using very high resolution images. Based on environmental, geographical factors and landscape structure metrics, we demonstrated that 80% of forest degradation was mainly driven by accessibility, geomorphology, fire occurrence and fragmentation. The drivers of degradation acted together and in sequence. The combination of current forest state, landscape dynamics and information on degradation drivers would be at the basis of ecological vulnerability assessment. In Di Linh, degradation is driven by encroachment of coffee-based agriculture. Field inventory of the different forest types and other landscape elements combined with Sentinel-2 images allowed to map with high precision the current land cover. We constructed trajectories of landscape structure dynamics from which we characterized the expansion of the agricultural frontier and highlighted heterogeneous agricultural encroachment on forested areas. We also identified degradation and fragmentation trajectories that affect forest cover at different rates and intensity. Combined, these indicators pinpointed hotspots of forest ecological vulnerability. Through the developed remote sensing approaches and indicators at forest and landscape scales, we provided a holistic diagnosis of forests in human-modified landscapes This thesis aims to pave the way for tailored and prioritized management of degraded forests at the landscape scale.

Titre : Un cadre d'évaluation de la vulnérabilité écologique des forêts dans les fronts de déforestation tropicaux à partir de l'évaluation de la dégradation des forêts dans une approche paysagère: Etudes de cas au Brésil et Vietnam

Mots-clés : Vulnérabilité écologique, expansion agricole, dégradation des forêts, télédétection

Résumé : La conservation du couvert forestier tropical est essentielle pour assurer la fourniture durable de services écosystémiques. Cependant, l'accroissement de la démographie, la demande de produits agricoles et les changements dans l'utilisation des terres affectent leur durabilité. L'objectif de cette thèse est de développer une approche multidimensionnelle pour évaluer la dégradation des forêts et les relations avec la dynamique de l'utilisation des terres afin d'estimer leur vulnérabilité. La thèse a été appliquée à Paragominas (Brésil) et Di Linh (Vietnam), où la déforestation due à l'agriculture commerciale a façonné le paysage en mosaïques d'utilisation des terres. A Paragominas, la dégradation est liée à l'exploitation sélective du bois et au feu impliquant des changements dans la structure forestière. Nous avons estimé le potentiel de la télédétection multisource pour cartographier la biomasse forestière aérienne à partir de données de stock de carbone et avons étudié les conséquences de la dégradation sur les structures forestières. Nous avons constaté que les textures de la canopée étaient corrélées à la variabilité de la structure forestière et pouvaient être utilisés comme indicateurs pour caractériser les forêts dégradées grâce aux images à très haute résolution. En nous basant sur des facteurs environnementaux, géographiques et de structure du paysage, nous avons démontré que 80 % de la dégradation était principalement due à l'accessibilité, la géomorphologie, la fréquence des incendies et à la fragmentation et que ces facteurs agissaient en séquence. A Di Linh, la dégradation est due à l'empiètement de la culture de café. L'inventaire sur le terrain des différents types de forêts et d'autres éléments, combiné aux images Sentinel-2, a permis de cartographier avec une grande précision la couverture du sol actuelle. Nous avons construit des trajectoires de dynamique paysagère afin de caractériser l'expansion de la frontière agricole et mis en évidence l'empiétement agricole sur les zones forestières. Nous avons identifié des trajectoires de dégradation et de fragmentation qui affectent le couvert forestier à différentes intensités. Ensemble, ces indicateurs ont mis en évidence des points chauds de vulnérabilité. Grâce aux approches et aux indicateurs de télédétection développés à l'échelle de la forêt et du paysage, nous avons fourni un diagnostic holistique des forêts dans les paysages modifiés par l'homme. Cette thèse vise à ouvrir la voie à une gestion adaptée et prioritaire des forêts dégradées à l'échelle du paysage.